



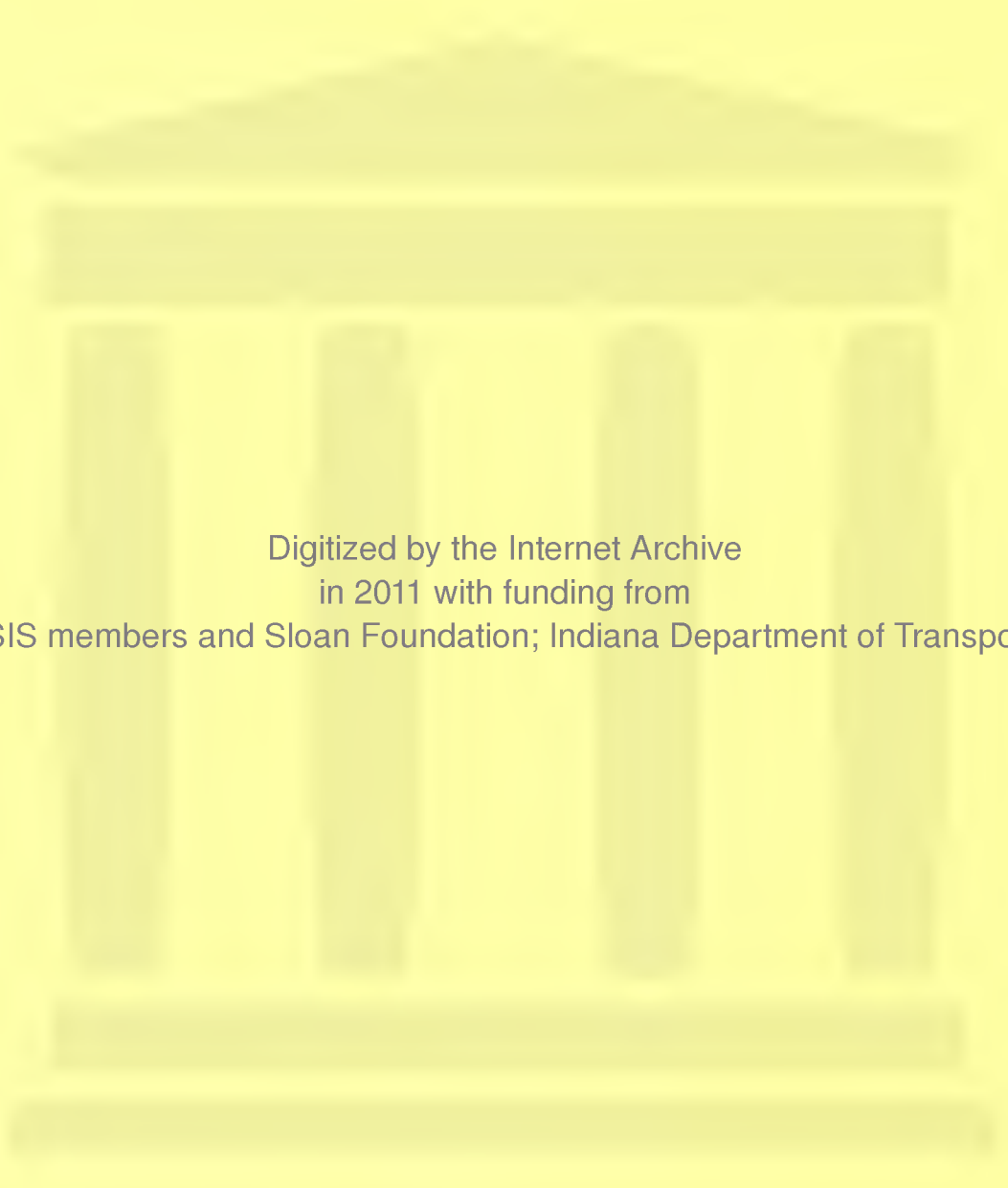
# JOINT HIGHWAY RESEARCH PROJECT

FHWA/IN/JHRP-81/3

## PREDICTING PERFORMANCE OF BURIED CONDUITS

G. A. Leonards  
Tzong-Hsin Wu  
Charng-Hsein Juang





Digitized by the Internet Archive  
in 2011 with funding from  
LYRASIS members and Sloan Foundation; Indiana Department of Transportation

## Final Report

## PREDICTING PERFORMANCE OF BURIED CONDUITS

TO: Harold L. Michael, Director  
Joint Highway Research Project

FROM: G. A. Leonards, Research Engineer  
Joint Highway Research Project

June 27, 1982

Project: C-36-62F

File: 9-8-6

Attached is the Final Report on the HPR Part II Study titled "Performance of Pipe Culverts Buried in Soil." The title of the Report is "Predicting Performance of Buried Conduits" and its authors are Dr. G. A. Leonards of the faculty and Drs. Tzong-Hsin Wu and Charng-Hsein Juang. Dr. Leonards served as principal investigator of the research.

The research has included determination of the capabilities of four finite element computer programs that predict the performance of buried conduits. Much work was also performed on characteristics and factors associated with performance of conduits and their evaluation by the several programs.

A draft Report was submitted for review on March 17, 1981 and was accepted by JHRP and FHWA without comment. However, on my own cognizance, a number of additional example problems were worked out in detail to provide a firmer basis for the conclusions that were drawn.

This Final Report is submitted as fulfillment of the objectives of Phase II of the research study.

Sincerely,



G. A. Leonards  
Research Engineer

GAL:ms

cc: A. G. Altschaeffl  
W. L. Dolch  
R. L. Eskew  
G. D. Gibson  
W. H. Goetz  
M. J. Gutzwiller  
G. K. Hallock

D. E. Hancher  
K. R. Hoover  
J. F. McLaughlin  
R. D. Miles  
P. L. Owens  
G. T. Satterly

C. F. Scholer  
K. C. Sinha  
C. A. Venable  
H. P. Wehrenberg  
L. E. Wood  
E. J. Yoder  
S. R. Yoder





Final Report  
PREDICTING PERFORMANCE OF BURIED CONDUITS

by  
G. A. Leonards  
Tzong-Hsin Wu  
and  
Charng-Hsein Juang

Joint Highway Research Project

Project No.: C-36-62F

File No.: 9-8-6

Prepared as Part of an Investigation

Conducted by

Joint Highway Research Project  
Engineering Experiment Station  
Purdue University

in cooperation with the  
Indiana State Highway Commission  
and the

U.S. Department of Transportation  
Federal Highway Administration

The contents of this report reflect the views of the authors who are responsible for the facts and the accuracy of the data presented herein. The contents do not necessarily reflect the official views or policies of the Federal Highway Administration. This report does not constitute a standard, specification, or regulation.

Purdue University  
West Lafayette, Indiana  
June 27, 1982



|   |  |  |           |
|---|--|--|-----------|
| 1. Report No.<br>FHWA/IN/JHRP-81/3  | 2. Government Accession No.                              | 3. Recipient's Catalog No.   |           |
| 4. Title and Subtitle<br><br>PREDICTING PERFORMANCE OF BURIED CONDUITS  |  | 5. Report Date<br>June 27, 1982  |           |
|   |  | 6. Performing Organization Code  |           |
| 7. Author(s)<br><br>G. A. Leonards, Tzong-Hsin Wu, and Charng-Hsein Juang   |  | 8. Performing Organization Report No.<br><br>JHRP-81-3   |           |
| 9. Performing Organization Name and Address<br>Joint Highway Research Project<br>Civil Engineering Building<br>Purdue University<br>West Lafayette, Indiana 47907   |  | 10. Work Unit No.  |           |
|   |  | 11. Contract or Grant No.<br>HPR-1(18) Part II   |           |
| 12. Sponsoring Agency Name and Address<br>Indiana State Highway Commission<br>State Office Building<br>100 North Senate Avenue<br>Indianapolis, Indiana 46204   |  | 13. Type of Report and Period Covered<br><br>Final Report  |           |
|   |  | 14. Sponsoring Agency Code   |           |
| 15. Supplementary Notes<br>Conducted in cooperation with the U.S. Department of Transportation, Federal Highway Administration under a research study titled "Performance of Pipe Culverts Buried in Soil."   |  |  |           |
| 16. Abstract<br>The capabilities of finite element computer codes FINLIN, CANDE, SSTIP and NLSSIP were evaluated. CANDE was judged to be the best over-all code for predicting performance of buried conduits. A number of improvements to this code were made.<br><br>Example solutions are given to illustrate the effects of conduit stiffness, interface slippage, and soil properties on conduit performance. It was found that conventional concepts of soil "arching" are misleading; that slippage at the soil-conduit interface strongly affect the response; and that soil behavior plays the most crucial role in controlling performance.<br><br>It was concluded that the Duncan-Chang hyperbolic model is a satisfactory representation of nonlinear soil behavior for routine studies of conduit response. Further use of equivalent elastic, overburden dependent, or default values in the extended Hardin soil models is not recommended. For prediction purposes, especially to investigate the effects of soil compaction and of localized shear failures, a plasticity model of soil behavior is needed.<br><br>Duncan's (1979) SCI procedure for design of long-span metal culverts with shallow cover was also investigated. The procedure provided good estimations of maximum thrust for the problems investigated in this study; however, agreement in both the magnitude of the bending moment and in the form of the bending moment equation was found to be poor, and the proposed safety factor to guard against plastic hinging in the conduit wall is considered to be overly conservative. |  |  |           |
| 17. Key Words<br><br>Culverts; performance prediction;<br>buckling; soil-structure interaction.   |  | 18. Distribution Statement<br><br>No restrictions. This document is available to the public through the National Technical Information Service, Springfield, Virginia 22161. |           |
| 19. Security Classif. (of this report)<br><br>Unclassified  | 20. Security Classif. (of this page)<br><br>Unclassified | 21. No. of Pages<br><br>213  | 22. Price |



## TABLE OF CONTENTS

|  |    |
|--|----|
| LIST OF TABLES . . . . .   | iv |
| LIST OF FIGURES . . . . .  | v  |
| HIGHLIGHT SUMMARY . . . . .  | ix |
| CHAPTER 1 INTRODUCTION . . . . .   | 1  |
| CHAPTER 2 ANALYTICAL MODELING OF SOIL-CONDUIT SYSTEM . . . . .                                 | 8  |
| 2.1 Characterization of Soil Response . . . . .  | 8  |
| 2.1.1 Linear Elastic Models . . . . .  | 9  |
| 2.1.2 Nonlinear Elastic Models . . . . .   | 11 |
| 2.1.2.1 Tabular Forms . . . . .  | 11 |
| 2.1.2.2 Functional Relationships . . . . .   | 12 |
| 2.1.3 Higher-Order Elasticity Models . . . . .   | 25 |
| 2.1.4 Plasticity Models . . . . .  | 27 |
| 2.1.5 Selection of a Soil Model for Analyses of<br>Soil-Conduit Interaction Problems . . . . . | 30 |
| 2.2 Characterization of Conduit Response . . . . .   | 30 |
| 2.3 Characterization of Interface Behavior . . . . .   | 33 |
| 2.3.1 Method of Stiffness . . . . .  | 33 |
| 2.3.2 Method of Constraints . . . . .  | 35 |
| 2.4 Other Factors . . . . .  | 36 |
| 2.4.1 Sequential Construction . . . . .  | 36 |
| 2.4.2 Compaction . . . . .   | 38 |
| 2.4.3 No-Tension Behavior of Soil Mass . . . . .   | 41 |
| 2.4.4 Buckling . . . . .   | 42 |
| 2.4.5 Live Loads . . . . .   | 44 |



|           |   |     |
|-----------|---|-----|
| CHAPTER 3 | FINITE ELEMENT COMPUTER CODES FOR ANALYZING<br>SOIL-CONDUIT INTERACTION . . . . . | 46  |
| 3.1       | FINLIN Code . . . . .   | 46  |
| 3.2       | CANDE Code . . . . .  | 48  |
| 3.3       | SSTIP Code . . . . .  | 53  |
| 3.4       | NLSSIP Code . . . . .   | 54  |
| CHAPTER 4 | COMPARISON OF COMPUTER CODES . . . . .  | 57  |
| 4.1       | Finite Element Discretization and Boundary Conditions . . .                       | 57  |
| 4.2       | Verification of the Computer Codes . . . . .                                      | 62  |
| 4.2.1     | Solution Levels of CANDE Code . . . . .   | 62  |
| 4.2.2     | Sequential Construction . . . . .   | 66  |
| 4.2.3     | The Constraint Element . . . . .  | 71  |
| 4.3       | Effect of Conduit Stiffness . . . . .   | 71  |
| 4.3.1     | Soil Arching . . . . .  | 73  |
| 4.3.2     | Rigid Vs. Flexible Conduit . . . . .  | 76  |
| 4.3.3     | Plastic Hinging of Conduit Wall . . . . .   | 86  |
| 4.4       | Effect of Interface Behavior . . . . .  | 95  |
| 4.4.1     | Group 1 Problems - Interface Slip - Circular Conduit                              | 95  |
| 4.4.2     | Group 2 Problems - Interface Slip -<br>Elliptical Conduit . . . . .               | 106 |
| 4.5       | Effect of Soil Response . . . . .   | 112 |
| 4.5.1     | Linear Elastic Soil Models . . . . .  | 112 |
| 4.5.2     | Nonlinear Soil Models . . . . .   | 113 |
| 4.5.2.1   | Soil Parameters (or Moduli) . . . . .   | 114 |
| 4.5.2.2   | Group 1 Problems - Soil Model -<br>Circular Concrete Pipe . . . . .               | 120 |
| 4.5.2.3   | Group 2 Problems - Soil Model -<br>Circular Steel Pipe . . . . .                  | 124 |





|             |   |     |
|-------------|---|-----|
| 4.5.2.4     | Group 3 Problems - Soil Model -<br>Long-Span Elliptical Pipe . . . . .                    | 132 |
| 4.5.3       | Sequence of Soil Layer Placement . . . . .  | 145 |
| CHAPTER 5   | EVALUATION OF PREDICTION CODES . . . . .  | 150 |
| 5.1         | Modifications to the CANDE Code . . . . .   | 155 |
| 5.1.1       | Calculation of Stress and Bending Moment in<br>the Conduit Wall Section . . . . .         | 155 |
| 5.1.2       | Duncan-Chang and Modified Duncan Soil Models . . . . .                                    | 156 |
| 5.1.3       | Automatic Mesh Generation . . . . .   | 159 |
| 5.1.4       | Iterative Scheme and Error Messages . . . . .   | 161 |
| CHAPTER 6   | CONCLUSIONS . . . . .   | 164 |
| CHAPTER 7   | RECOMMENDATIONS FOR FUTURE RESEARCH . . . . .   | 173 |
|             | ACKNOWLEDGEMENTS . . . . .  | 174 |
|             | REFERENCES . . . . .  | 175 |
|             | APPENDICES . . . . .  | 182 |
| APPENDIX A: | List of Symbols . . . . .   | 182 |
| APPENDIX B: | Calculating Bending Moment About the<br>Centroidal Axis Using the CANDE Code . . . . .    | 186 |
| APPENDIX C: | Incorporating the Duncan-Chang and Modified<br>Duncan Soil Models in CANDE Code . . . . . | 189 |
| APPENDIX D: | An Automated Mesh for Closed Pipe Arches . . . . .  | 198 |
| APPENDIX E: | Revised Iterative Scheme and Error Messages . . . . .                                     | 211 |



## LIST OF TABLES

| <u>Table</u> |   | <u>Page</u> |
|--------------|---|-------------|
| 2.1          | Components of the Constitutive Matrix for Isotropic, Linear Elastic Materials . . . . .           | 10          |
| 2.2          | Representative Parameter Values of the Duncan-Chang Model (after Wong and Duncan, 1974) . . . . . | 16          |
| 2.3          | Representative Parameter Values of the Modified Duncan Model (from Duncan, Feb. 1979). . . . .    | 20          |
| 2.4          | Decision Parameters for Various Assumed Interface States (after Katona, et al., 1976) . . . . .   | 37          |
| 4.1          | Conduit Responses Using Burns-Richard and Finite Element Solutions. . . . .                       | 65          |
| 4.2          | Responses of a Concrete Pipe Analyzed as Single Layer and Five Layers of Construction . . . . .   | 70          |
| 4.3          | Conduit Responses of Burns-Richard and Finite Element Solutions at Full Slip Condition. . . . .   | 72          |
| 4.4          | Responses of a Circular Conduit for Three Interface Conditions. . . . .                           | 97          |
| 4.5          | Responses of an Elliptical Conduit for Three Interface Conditions. . . . .                        | 107         |
| 4.6          | Young's Modulus Adopted for Overburden Dependent Soil Model. . . . .                              | 115         |
| 4.7          | Soil Model Parameters Derived from Lade's Triaxial Compression Test Results. . . . .              | 119         |
| 4.8          | Results from Group 1 Problems . . . . .   | 123         |
| 4.9          | Results from Group 2 Problems . . . . .   | 127         |
| 4.10         | Soil Parameters Employed in the Study of Group 3 Problems. . . . .                                | 134         |



## LIST OF FIGURES

| <u>Figure</u> |  | <u>Page</u> |
|---------------|--|-------------|
| 2.1           | Hyperbolic Functional Representation of a Stress-Strain Curve. . . . .   | 13          |
| 2.2           | Idealized Shear Stress-Shear Strain Relationship. . . .  | 18          |
| 2.3           | Spline Function Representation. . . . .  | 22          |
| 2.4           | Ramberg-Osgood Model. . . . .  | 24          |
| 2.5           | Analytical Simulation of Sequential Construction. . . .  | 39          |
| 3.1           | Idealized Stress-Strain Relationships incorporated in CANDE Code for Various Conduit Materials: (a) Steel, (b) Aluminum, (c) Concrete, and (d) Plastic . . . . . | 51          |
| 3.2           | Characterization of Conduit Behavior adopted in NLSSIP Code: (a) Stress-Strain Relationship; (b) Moment-Curvature Relation. . . . .                              | 55          |
| 4.1(a)        | Finite Element Mesh Used in Conjunction with FINLIN Code. . . . .  | 58          |
| 4.1(b)        | Finite Element Mesh Used in Conjunction with CANDE Code. . . . .   | 59          |
| 4.1(c)        | Finite Element Mesh Used in Conjunction with SSTIP and NLSSIP Codes. . . . .   | 60          |
| 4.2(a)        | Construction Layer Numbering Used Associated with the Finite Element Mesh Shown in Figure 4.1(a). . . . .  | 67          |
| 4.2(b)        | Construction Layer Numbering Used Associated with the Finite Element Mesh Shown in Figure 4.1(b). . . . .  | 68          |
| 4.3           | Schematic Diagrams of the Deformation of (a) a Flexible Pipe, and (b) a Rigid Pipe . . . . .   | 74          |
| 4.4           | Two Measures of Soil Arching. . . . .  | 75          |
| 4.5           | Distribution of Normal and Shear Stresses at the Soil-Conduit Interface, at 35 ft of Soil Cover Above the Springline. . . . .                                    | 77          |
| 4.6           | Distributions of Moment and Thrust in the Conduit Walls, at 35 ft of Soil Cover Above the Springline. . .  | 79          |
| 4.7           | Distributions of Normal and Shear Stresses at the Soil-Conduit Interface, at 20 ft of Soil Cover Above the Springline. . . . .                                   | 81          |



| <u>Figure</u> |   | <u>Page</u> |
|---------------|---|-------------|
| 4.8           | Distributions of Moment and Thrust in the Conduit Walls, at 20 ft of Soil Cover Above the Springline. . .   | 82          |
| 4.9           | Distribution of Horizontal Soil Pressure on Vertical Planes Above the Crown and the Springline (Soil Cover = 20 ft Above the Springline) . . . . .  | 84          |
| 4.10          | Shear Stress Distribution on a Vertical Plane Above the Springline (Soil Cover = 20 ft Above the Springline) . . . . .                              | 85          |
| 4.11          | Displacement Field of the Concrete Pipe with 20 ft of Soil Cover Above the Springline . . . . .   | 87          |
| 4.12          | Displacement Field of the Corrugated Steel Pipe with 20 ft of Soil Cover Above the Springline. . . . .  | 88          |
| 4.13          | Ground Surface Displacements and Deflections of the Concrete Pipe and the Steel Pipe. . . . .   | 89          |
| 4.14(a)       | Thrust and Moment at the Springline Versus Fill Height. . . . .   | 92          |
| 4.14(b)       | Effect of Soil Stiffness on Fill Height at which a Plastic Hinge is Formed . . . . .  | 94          |
| 4.15          | Effect of Interface Condition on Change in Vertical Diameter of a 10 ft Diameter Corrugated Steel Conduit, Overburden Dependent Soil Model. . . . . | 98          |
| 4.16          | Effect of Interface Condition on the Maximum Extreme Fiber Stress in a 10 ft Diameter Corrugated Steel Conduit . . . . .                            | 99          |
| 4.17          | Effect of Interface Condition on the Maximum Thrust in a 10 ft Diameter Corrugated Steel Conduit . . . . .  | 101         |
| 4.18          | Effect of Interface Condition on the Maximum Bending Moment in a 10 ft Diameter Corrugated Steel Conduit . .  | 102         |
| 4.19(a)       | History of Bending Moment at the Crown for the Three Interface Conditions. . . . .  | 103         |
| 4.19(b)       | History of Bending Moment near the Quarter-Point for the Three Interface Conditions. . . . .  | 104         |
| 4.19(c)       | History of Bending Moment at the Springline for the Three Interface Conditions. . . . .   | 105         |
| 4.20          | Effect of Interface Condition on the Change in Vertical Diameter of a 10 ft Span Elliptical Corrugated Steel Conduit . . . . .                      | 108         |





| <u>Figure</u> |   | <u>Page</u> |
|---------------|---|-------------|
| 4.21          | Effect of Interface Condition on the Maximum Moment in a 10 ft Span Elliptical Corrugated Steel Conduit . .                     | 109         |
| 4.22          | Effect of Interface Condition on the Maximum Thrust in a 10 ft Span Elliptical Corrugated Steel Conduit . .                     | 110         |
| 4.23          | Effect of Interface Condition on the Maximum Extreme Fiber Stress in a 10 ft Span Elliptical Corrugated Steel Conduit . . . . . | 111         |
| 4.24          | Results of Triaxial Compression Tests on Loose Specimens of Monterey No. 0 Sand (from Lade, 1972). . .                          | 117         |
| 4.25          | Results of Plane Strain Tests on Loose Specimens of Monterey No. 0 Sand (from Lade, 1972) . . . . .                             | 118         |
| 4.26          | Schematic Diagram for Shear Stress-Shear Strain Relationship. . . . .   | 121         |
| 4.27          | Poisson's Ratio Versus Shear Strain Ratio . . . . .   | 125         |
| 4.28(a)       | Change in Vertical Diameter Versus Fill Height, 10 ft Diameter Steel Pipe . . . . .   | 129         |
| 4.28(b)       | Change in Vertical Diameter Versus Fill Height, 10 ft Diameter Steel Pipe . . . . .   | 130         |
| 4.29          | Effect of Rise/Span Ratio on Maximum Thrust . . . . .   | 136         |
| 4.30(a)       | Moment Reduction Factor Versus Rise/Span Ratio Linear Soil Model . . . . .  | 138         |
| 4.30(b)       | Moment Reduction Factor Versus Rise/Span Ratio Duncan-Chang Soil Model . . . . .  | 139         |
| 4.31          | Maximum Moment Versus Flexibility Number, Rise to Span Ratio = 0.33 . . . . .   | 141         |
| 4.32          | Suggested Method for Examining Potential Consequences of Yielding and Plastic Hinge Formation in the Wall Section . . . . .     | 144         |
| 4.33(a)       | Favorable and Unfavorable Layer Sequences, Circular Conduits. . . . .   | 146         |
| 4.33(b)       | Favorable and Unfavorable Layer Sequences, Elliptical Conduits. . . . .   | 148         |
| 4.34          | Effect of Soil Layer Sequence on Relation between Maximum Bending Moment and Rise/Span Ratio. . . . .                           | 149         |



| <u>Figure</u> |  | <u>Page</u> |
|---------------|--|-------------|
| 5.1           | Comparison of Results Obtained Using Duncan-Chang<br>and Modified Duncan Soil Models . . . . . | 158         |
| 5.2           | Finite Element Mesh and Parameters Defining<br>Geometry of Pipe Arch . . . . .                 | 160         |



## HIGHLIGHT SUMMARY

A study was undertaken to evaluate existing computer codes for analyzing soil-conduit interaction, and to investigate the effects of conduit stiffness, soil-conduit interface behavior, and soil response on the performance of buried conduits.

Finite element computer codes FINLIN, CANDE, SSTIP, and NLSSIP were evaluated in detail with emphasis on advantages as well as their limitations. The analytical modeling features nonlinear behavior of soil masses, yielding and plastic hinging of conduit walls, slip at the soil-conduit interface, sequential construction, live loads, and no-tension behavior of soils. CANDE was judged to be the best over-all code currently available for predicting performance of buried conduits, and a number of improvements to this code were made: (a) CANDE obtained the strain distribution in the wall section correctly, but the bending stresses were calculated by dividing the summed incremental moments about different axes (once the wall section started to yield) by the section modulus. This was changed to obtain the stresses directly from the strain distribution and the stress-strain relation; (b) the stress distribution was utilized to calculate bending moments about the geometric axis of the section. This bending moment is the only one relevant for investigating the safety factor against formation of a plastic hinge; (c) the Duncan-Chang and modified Duncan soil models were incorporated in the CANDE code; (d) the criteria for adjusting soil moduli to accommodate failure (tension or shear) in a soil element was modified to reduce the incidence of convergence problems (for this latter purpose, reducing the magnitude of the load step or altering the loading sequence can also be effective); and (e) automated mesh generation was extended to pipe-arch shapes. FHWA has incorporated changes (a), (b), and the modified Duncan model of (c), into their current documentation of the CANDE program. The Duncan-Chang model and changes (d) and (e) are available [as of Nov. 1982] only in this report.



Example problems are given to illustrate the effects of conduit stiffness, interface slippage, and soil response. Conventional concepts of soil arching were found to be misleading. To characterize the effects of soil-conduit interaction fully, the following are needed: (1) distribution of normal and shear stresses at the soil-conduit interface, (2) distribution of moment and thrust in the conduit wall, (3) deformed shape of the conduit, and (4) distribution of stress and strain in the soil mass in the immediate vicinity of the conduit wall.

The response of buried conduits was found to be strongly affected by the interface behavior. Depending upon the geometry of a soil-conduit system, inducing interface slippage may not always be beneficial, especially for circular conduits with shallow burial.

Results obtained by using various soil models were very different. It was concluded that: (1) further use of equivalent elastic and overburden dependent soil models be abandoned, (2) the formulation in the extended-Hardin soil model to evaluate Poisson's ratio has inherent deficiencies and, because the results obtained can be unconservative at higher levels of shear strain, this model should be used with caution; the default values for the Hardin model presently in the CANDE code are defective and their use should also be abandoned, (3) spline function representation of plane strain test data is believed to be the best incrementally elastic soil model but the advantage gained in its use is too small to justify the additional inconvenience involved, and (4) the Duncan-Chang soil model gives a reasonable representation of soil response and is recommended for routine use until a more suitable soil model can be successfully implemented.

Duncan's (1979) SCI procedure for design of long-span metal culverts with shallow cover was also investigated. The procedure provided suitably





conservative estimations for the maximum thrusts in conduit walls for the problems investigated in this study; however, agreement between the magnitude of the bending moment and in the form of the bending moment equation was found to be poor, and the proposed safety factor to guard against plastic hinging is believed to be unduly conservative.

Recommendations for future research are proposed to extend the capability of the analytical model to predict performance, and to verify its applicability as a tool for developing more rational procedures for design of buried conduits.



## CHAPTER 1 INTRODUCTION

In January of 1973 a research program was initiated at Purdue University with the following objectives:

"I. Development of an analytical procedure valid for deformable culvert structures; that is, a procedure which would incorporate the essential characteristics of soil-structure interaction during the in-service functioning of the culvert.

II. Verification, by appropriate experiments, of the predictive capability of the analysis developed.

III. Establishment of a program for prototype measurements whereby the analysis can be developed into a rational design procedure."

Phase I of the program was funded in the amount of \$15,500 for a period of 2 1/2 years (to 6/30/75), and was to focus on a) development of an appropriate nonlinear representation of soil response, b) accommodation of slip at the soil-conduit interface, and c) examining the response of a range in pipe sizes and stiffness, and of varying depth of cover and construction sequences. In order to focus on these factors it was decided to limit the behavior of the culvert wall to a linear elastic response.

Considerable difficulties were encountered in developing the finite element code. Based on the literature survey, the pipe was initially represented by a series of triangular elements with two degrees of freedom at the nodes; later, this was found to be inapplicable for thin metal conduits and inappropriate for concrete pipes, unless a large number of pipe elements are introduced. Convergence problems and numerical instabilities were encountered with the interaction elements used to accommodate slip at the soil-pipe interface. When all features of the program were put together the storage capacity of the computer was exceeded, hence, more efficient ways



of organizing the program had to be sought. To overcome these difficulties, an increase in budget of \$13,500 and a time extension of 1 year (to 6/30/76) was granted.

A report covering Phase I of the study was submitted as scheduled (Leonards and Roy, 1976). The finite element computer code, dubbed FINLIN, had some unique features the most important of which was the procedure for fitting actual soil test data with spline functions and calculating incremental values of  $E$  and  $\mu$  in terms of octahedral normal and shear stress levels. Thus, the effects of intermediate principal stress and dilatancy due to shear stresses were fully accounted for. It was believed then -- and it is still believed -- that for monotonically increasing loads up to but not including failure, it is the most realistic representation of soil behavior currently available. It was also concluded that nonlinear models of soil behavior were essential to good predictions of culvert performance and that to account for the effects of soil compaction and of local failures in the soil mass, a plasticity model of soil behavior was required. It was acknowledged that convergence problems were encountered when interface slip was investigated using a nonlinear soil model, that the scheme for no-tension analysis needed further study, and that additional ways for achieving economy in computer time should be explored. It was also recognized that yielding of metal culverts (and some cracking in concrete pipes) was essential to their economic utilization. In the case of metal conduits, the capacity to yield without buckling was identified as a key design parameter.

The conclusions reached in the first phase of the study necessitated re-thinking the approach to be taken in Phase II. It was clear that the predictive capability of FINLIN, especially in terms of the behavior of the



conduit wall, was inadequate, and that there was no quantitative basis for comparing the relative advantages of the soil model incorporated in the code with other soil models then extant. Moreover, the key role that buckling plays in controlling culvert performance needed careful study and evaluation. Accordingly, the proposal for Phase II of the study was altered to include:

a) improving the predictive capabilities of FINLIN by accounting for yielding and plastic hinging in the culvert wall, and by developing a plasticity model of soil behavior,

b) an experimental study on half-sections of a 5 foot dia. flexible culvert with measurements of deflections, internal thrusts and bending moments in the pipe wall, and normal and shear stresses at the soil-pipe interface. Loading would be continued post-yielding or buckling to evaluate the loads at incipient collapse, and

c) comparisons between predicted and measured performance.

Approval to proceed with the revised Phase II of the project was received in September of 1977, and was budgeted for \$56,700 for a period of two years. However, it was requested that before updating FINLIN "the researchers will make an analysis which indicates it will be more beneficial to upgrade FINLIN than to use CANDE." Moreover, it was requested that the "researchers discuss the state-of-the-art of buckling theory in a progress report" before proceeding with the experimental portion of the study. At first "the researchers" were unhappy with these tasks because they were considered to be unduly restrictive. However, their chagrin proved to be short-lived. It was soon found that the state-of-the-art review of buckling theories for buried conduits was sterile in the absense of comparisons with observed results. Accordingly, the study was expanded to include all known experimental results. A vast majority of the latter investigations were on





scaled models; detailed performance data on full-scale culverts were not identified in the literature. Cooperation was solicited and generously given by the University of Utah, Armco Metal Products Division, the Bureau of Reclamation, Ohio State University, and the Prairie Farm Rehabilitation Administration in Canada. Study of the data thus made available revealed that local buckling and wall crushing could not be distinguished solely by observation. As these full-scale experiments were generally not instrumented to measure stresses in the conduit walls, it became necessary to distinguish between the two failure mechanisms by calculating the wall stresses when crimping was observed in the tests. As the CANDE code was suitable for this purpose, the two prerequisites previously cited meshed nicely and complimented each other in carrying out the stated tasks.

A report covering the detailed review of buckling theories and associated experimental data was completed about a year after Phase II of the study was authorized (Leonards and Stetkar, 1978). The following is a summary of the main findings:

"A. Wall crushing (yielding of the conduit section due to thrust forces only) has been observed experimentally in conventional-sized flexible conduits supported by very dense granular backfill. Deflections before failure were, consequently, small and bending contributed little to the wall stresses. If failure is by wall crushing, then the conduit is supporting its load in the most efficient manner possible.

B. Seam separation is the simplest failure mechanism to identify. Seam integrity is a function of the type of culvert, the construction technique, and the thrust load. Strength tests have shown that seam failure (either rivet shearing or weld rupture) is critical in corrugated steel culverts less than 2 feet in diameter. However, tests on culverts with larger diameters (up to 4 feet) showed that wall crushing is more critical. Although seam slippage occurs at loads less than the seam capacity, structural integrity of the culvert is not immediately affected and, generally, a more favorable distribution of interface soil pressure results. Research on seam design could be very rewarding: a seam that can continue to slip at thrust loads below those required to induce wall crushing, without impairing bending resistance, could result in more economic utilization of circular metal conduits.



C. Elastic buckling, the development of an instability before yielding is initiated in the conduit section, can occur in high modes if the interface pressures are reasonably uniform and if material or geometric imperfections or local residual stresses are insignificant. Otherwise, elastic buckling is initiated as a local buckle and may occur at the crown, invert, or at other locations, depending on where a critical combination of thrust, bending moment, imperfection and residual stress first develops. A snap-through buckle can be the initial sign of distress or it may develop at higher loads after yielding or local crimping has occurred.

Many high mode buckling theories assuming elastic soil support have been proposed. They are all similar, excluding the different approaches taken for formulating the modulus of soil support. Most expressions for the critical buckling pressure are lower-bound solutions. However, even lower-bound solutions generally overestimate the elastic buckling loads observed in controlled experiments. Imperfections and residual stresses lead to early local buckling. Several methods have been proposed to account for the accompanying reduction in critical pressure, but none of these methods has been verified by controlled experiments of sufficient scope and generality. Of the snap-through buckling theories, only Klöppel and Glock consider non-uniform boundary pressures and the deflected conduit shape. Their solution is probably the most satisfactory representation currently available, yet it may be overconservative in some situations and unsafe in others. Materials with high yield points are advantageous in overcoming the effects of imperfections and residual stresses on the load capacity.

Elliptical conduits are more susceptible to buckling than those of circular shape. For long-span metal conduits and backfill materials in current use, the critical buckling load would be approximately half that of an equivalent circular shape. Thus, buckling criteria adapted from experience with circular culverts are not applicable to long-span arches.

Critical buckling pressures for larger conduits cannot be evaluated from small-scale experiments because of the crucial role played by imperfections, residual stresses, and stress levels in the supporting soil mass. Larger-scale, controlled tests show that elastic local buckling can be the first sign of distress in flexible conduits with moderately good soil support and can occur at relatively small deflections. In some cases the development of a local buckle constitutes a performance limit, whereas in others the conduit can sustain considerable additional load before failure occurs (i.e., little resistance to further deflection). Studies are badly needed to define the conditions under which local buckling should be considered as a performance limit.

D. Excessive deflections have been observed in flexible conduits of conventional size supported by weak soil, and in long-span conduits supported by relatively strong soil. In the former case deflections may exceed 15% of the diameter before collapse is imminent, while in the latter case collapse may occur at deflections less than 5% of the



span. Failure by excessive deflection in long-span conduits with good backfill can be triggered by bending stress concentrations induced during construction. With increasing heights of cover catastrophic collapse in the form of a snap-through buckle can occur. Thus, careful monitoring of field installations are needed to advance the state-of-the-art.

Excessive deflections of typical culverts will not occur in granular backfill densified to (or above) 95% Std. AASHTO density: however, if a cohesive backfill compacted to this specification is used, more deflection is required to mobilize equivalent lateral soil resistance which, coupled with gradual loss of circumferential support due to time-dependent behavior, can lead to failure. More studies are needed on the behavior of conduits supported by cohesive backfills.

E. With less flexible conduits, yielding under combined bending and thrust stresses can develop a plastic hinge before excessive deflection at the crown occurs. If additional load is applied, redistribution of boundary pressures will occur and although a collapse mechanism may not develop, deflections will increase and inelastic buckling may occur prematurely. Consequently, bending moments can have important influences on buried conduit behavior. It has been verified experimentally that yielding of the pipe section can develop at small deflections, especially in large diameter culverts and pipe arches. Finite element analyses can estimate the contribution of bending to the total wall stress, but present formulations are not adapted to the analysis of post-hinging behavior. Analytical techniques need to be extended to permit prediction of collapse loads.

F. Many aspects of conduit-soil interaction, including stresses and deflections induced by compaction loads, cannot presently be modeled theoretically, hence controlled tests on large scale conduits are badly needed. These tests should be conducted with a sufficient range of conduit flexibility and soil support (granular and cohesive) to encompass all types of failure modes. Loading should be continued to collapse so that the relationship between initial wall disturbance and collapse load can be studied. In each test the stress-strain relations in the soil mass in the vicinity of the conduit wall should be measured directly and compared to results obtained from triaxial and plane-strain laboratory tests at comparable confining pressures.

Because imperfections and residual stresses can have a large effect on conduit behavior, tests on unsupported conduits should be conducted and the results compared with theoretical solutions to assess the influence of these factors on the load capacity.

Full-size conduits should be instrumented to measure their deflected shape, the distribution of strains in the conduit sections due to thrusts and bending moments, the distribution of interface soil pressures, and the stresses and strains in the soil mass near the culvert wall. The validity of simplifying assumptions used for design purposes can thus be examined. The ability of finite element computer techniques to predict behavior under a large variety of controlled conditions could also be



evaluated. These measurements will provide the basis for further developments in the design of all kinds of buried conduits, including that of long-span arches."

Although the CANDE code was helpful with the interpretation of field measurements for the state-of-the-art review of buckling, it was not possible to make a suitable comparison between CANDE and the potential of an up-graded FINLIN code. When a nonlinear model of soil behavior is considered, there is practically no overlap in the predictive capabilities of the two codes: the soil models used are very different in their formulation, the two codes utilized different solution techniques, CANDE could treat yielding in the conduit wall while FINLIN could not, and both had convergence problems for various combinations of nonlinear behavior. In addition, FINLIN exhibited numerical instabilities when the conduit stiffness was small compared to that of the soil. It seemed necessary to up-grade FINLIN as originally planned before a valid comparison could be made. However, it was decided that other existing codes might be used to bridge the gaps between CANDE and FINLIN. Two codes developed at the University of California at Berkeley, SSTIP and NLSSIP, seemed well-suited for this purpose and through the courtesy and generosity of Prof. J. M. Duncan they were made available. A detailed study and comparison of all four codes was then completed. This report presents the results of the entire study and concludes with recommendations for further research that, taking full advantage of the present state-of-the-art, could bring all these past efforts to fruition in the form of a generally reliable, rational design procedure.





## CHAPTER 2 ANALYTICAL MODELING OF SOIL-CONDUIT SYSTEM

### 2.1 CHARACTERIZATION OF SOIL RESPONSE

In general, soils are multiphase materials that consist of variable amounts of solid particles, water, and gas (air); the soil mass is often found to be inhomogeneous and anisotropic, thereby rendering the mechanical behavior dependent upon a number of factors such as mineralogical composition, dry density (or void ratio), stress level, stress path, stress history, temperature, time, degree of saturation, etc. If the result of an analysis is to be realistic, it is important that the stress-strain characteristics of the soil be represented in a proper way.

It is, however, very difficult to evolve a general constitutive (stress-strain) law which is valid for all soils under all placement and loading conditions. By necessity, simplified constitutive models based largely on phenomenological considerations have been employed to represent soil behavior in analyzing stresses and displacements of soil masses.

It is convenient to classify the various simplified models for defining time-independent behavior of soils into four categories: (1) linear elastic models, (2) nonlinear incrementally elastic models, (3) higher-order elasticity models, and (4) plasticity models.

Except for a few plasticity and higher-order elasticity models, most of the soil models employ the generalized Hooke's law as a deformation model; consequently, shear dilatancy is not explicitly accounted for. The effects of dilatancy are accommodated implicitly by attempting to model field conditions in the laboratory and relating the quasi-elastic response to the stress level. Attempts are also made to select a critical



set of soil moduli in lieu of accounting for the effects of time.

### 2.1.1 LINEAR ELASTIC MODELS

The assumption of linear elasticity constitutes the simplest approach to model the stress-strain behavior of soils.

The stress-strain relationship, which is governed by the generalized Hooke's law of elastic deformations, may be expressed as follows for conditions of plane strain:

$$\begin{Bmatrix} \sigma_x \\ \sigma_y \\ \tau_{xy} \end{Bmatrix} = \begin{bmatrix} C_{11} & C_{12} & 0 \\ C_{12} & C_{22} & 0 \\ 0 & 0 & C_{33} \end{bmatrix} \begin{Bmatrix} \epsilon_x \\ \epsilon_y \\ \gamma_{xy} \end{Bmatrix} \quad \text{Equation 2.1}$$

in which  $[\sigma_x, \sigma_y, \tau_{xy}]^T$  and  $[\epsilon_x, \epsilon_y, \gamma_{xy}]^T$  are stress and strain vectors, respectively.

Subject to the further assumption of material isotropy, only two independent elastic moduli are needed to completely define the coefficients  $C_{11}$ ,  $C_{12}$ ,  $C_{22}$  and  $C_{33}$ . Any two of the following elastic moduli may be selected: Young's modulus ( $E$ ), Poisson's ratio ( $\mu$ ), shear modulus ( $G$ ), bulk modulus ( $B$ ), constrained modulus ( $M$ ), Lamé's parameter ( $\lambda$ ), and principal stress ratio in uniaxial strain ( $K_0$ ). A summary of the relationships between the elastic moduli was given by Baladi (1979). Table 2.1 lists the components of the constitutive matrix (Equation 2.1) in terms of the elastic moduli pairs commonly used in stress-deformation studies.

For orthotropic or transversely isotropic materials, additional elastic moduli which reflect the directional dependency have to be incorporated to define the components  $C_{11}$ ,  $C_{12}$ ,  $C_{22}$ , and  $C_{33}$  (Lekhnitskii, 1963).



Table 2.1 Components of the Constitutive Matrix for Isotropic, Linear Elastic Materials

|                   | E = Young's Modulus<br>$\mu$ = Poisson's Ratio | B = Bulk Modulus<br>G = Shear Modulus | M = Constrained Modulus<br>G = Shear Modulus |
|-------------------|--|---------------------------------------|--|
| $C_{11} = C_{22}$ | $\frac{E(1 - \mu)}{(1 + \mu)(1 - 2\mu)}$       | $\frac{3B + 4G}{3}$                   | M  |
| $C_{12}$          | $\frac{E\mu}{(1 + \mu)(1 - 2\mu)}$             | $\frac{3B + 2G}{3}$                   | M - 2G                                       |
| $C_{33}$          | $\frac{E}{2(1 + \mu)}$                         | G                                     | G  |



## 2.1.2 NONLINEAR ELASTIC MODELS

Some field conditions can be approximated by a set of stress-strain curves determined from one or two loading conditions. In such cases, it is possible to describe the soil behavior by modeling the set of test data. Obviously, the soil model (nonlinear elastic model) is strictly valid for conditions where the stress paths are similar to those of the test loading configuration.

A number of simplified nonlinear elastic soil models have been proposed and used in analyzing stress-deformation of soil masses. The models are found to provide an expedient, and often satisfactory, means for solving many geotechnical engineering problems, as evidenced by the correlations that have been obtained with experimental and field observations (e.g., Clough and Woodward, 1967; Christian, 1968; Clough and Duncan, 1969; Lee and Shen, 1969; Nobari and Duncan, 1972; Desai, 1974).

Nonlinear elastic models differ among themselves in the way a given set of stress-strain curves are obtained and simulated. The schemes for representing stress-strain relations of soils involve either a tabular form or a functional relationship.

### 2.1.2.1 TABULAR FORMS

In the tabular scheme, points on a stress-strain curve are input in the computer in the form of number pairs denoting stress and strain at those points. The soil moduli required to relate stress and strain, as in Equation 2.1, are computed from the data by suitable numerical differentiation and interpolation (Clough and Woodward, 1967; Vallabhan and Reese, 1968; Desai, 1968).

A disadvantage in the use of these tabular-form schemes is that a large number of data points have to be input in the computer. The





procedure may become cumbersome and involve large computer storage and computation effort.

Alternatively, a set of soil moduli expressed as a function of stress level (e.g., overburden pressure) may be used directly as input data. The soil moduli may be evaluated by interpolation in accordance with selected combinations of the existing stresses.

#### 2.1.2.2 FUNCTIONAL RELATIONSHIPS

In functional-form relationships, a given set of stress-strain curves are represented by using mathematical functions such as a hyperbolic function, power function, parabolic function, Lagrangian (interpolation) formula, spline function, and others.

Some of the commonly used functional relationships are described in the following:

##### (1) Duncan-Chang Model

The most widely used functional relationship was developed by Duncan and Chang (1970). The model is based on Kondner's finding (1963) that stress-strain curves for a number of soils could be approximated by hyperbolas as shown in Figure 2.1(a). The hyperbola can be represented by an equation of the form:

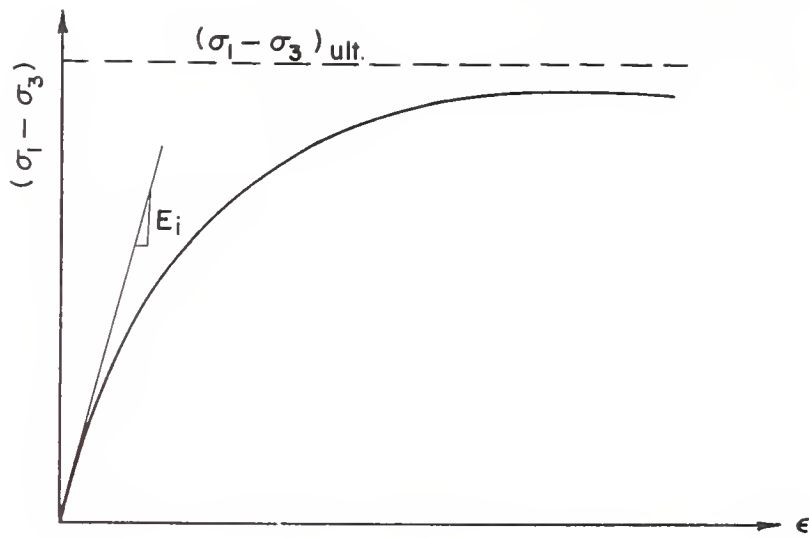
$$\sigma_1 - \sigma_3 = \frac{\epsilon}{\left(\frac{1}{E_i}\right) + \frac{1}{(\sigma_1 - \sigma_3)_{ult}}} \epsilon \quad \text{Equation 2.2}$$

While other types of curves could also be used, such as those proposed by Hansen (1963), hyperbolas have two characteristics which make their use convenient:

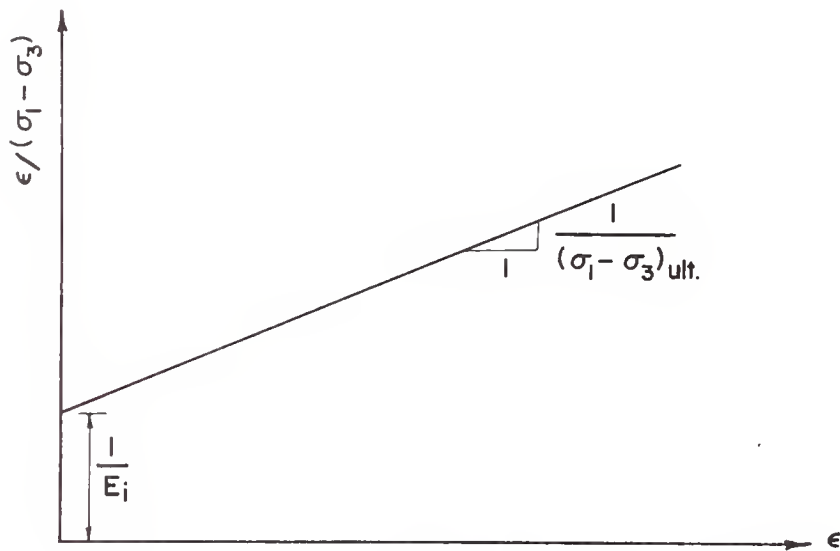
(1) The parameters in Equation 2.2 have physical significance.

$E_i$  is the initial tangent Young's modulus and  $(\sigma_1 - \sigma_3)_{ult}$





(a) REAL



(b) TRANSFORMED

FIGURE 2.1 HYPERBOLIC FUNCTIONAL REPRESENTATION  
OF A STRESS - STRAIN CURVE



is the asymptotic value of the stress difference which is related to the shear strength of the soil.

- (2) The values of  $E_i$  and  $(\sigma_1 - \sigma_3)_{ult}$  for a given stress-strain curve can be determined readily. The hyperbolic function can be transformed to a linear relationship between  $\epsilon/(\sigma_1 - \sigma_3)$  and  $\epsilon$  as shown in Figure 2.1(b).

Using the relationship between  $E_i$  and  $\sigma_3$ , as proposed by Janbu (1963), Mohr-Coulomb theory to obtain strength relationships, together with Equation 2.2, the expression for tangent Young's modulus,  $E_t$ , was given as:

$$E_t = \left[ 1 - \frac{R_f(1 - \sin\phi)(\sigma_1 - \sigma_3)}{2c \cos\phi + 2\sigma_3 \sin\phi} \right]^2 K P_a \left( \frac{\sigma_3}{P_a} \right)^n \quad \text{Equation 2.3}$$

Equation 2.3 involves five parameters:  $R_f$  is the failure ratio, which relates compressive strength of the soil to  $(\sigma_1 - \sigma_3)_{ult}$ ;  $c$  and  $\phi$  are the Mohr-Coulomb strength parameters; and  $K$  and  $n$  are experimentally determined constants.  $P_a$  is atmospheric pressure introduced into the equation to make the parameter "n" independent of the chosen system of units. To account for variation of  $\phi$  with confining pressure,  $\sigma_3$ , the following equation was used:

$$\phi = \phi_0 - \Delta\phi \log_{10} \left( \frac{\sigma_3}{P_a} \right) \quad \text{Equation 2.4}$$

in which  $\phi_0$  is the value of  $\phi$  for  $\sigma_3$  equal to  $P_a$ , and  $\Delta\phi$  is the reduction in  $\phi$  for a 10-fold increase in  $\sigma_3$ .

An expression for the tangent Poisson's ratio,  $\mu_t$ , was similarly obtained by Kulhawy, et al. (1969) as:



$$\mu_t = \frac{G - F \log\left(\frac{\sigma_3}{p_a}\right)}{\left\{ 1 - \frac{D(\sigma_1 - \sigma_3)}{Kp_a\left(\frac{\sigma_3}{p_a}\right)^n \left[ 1 - \frac{R_f(\sigma_1 - \sigma_3)(1 - \sin\phi)}{2c \cos\phi + 2\sigma_3 \sin\phi} \right]} \right\}^2} \quad \text{Equation 2.5}$$

in which parameters  $D$ ,  $F$  and  $G$  are constants to be determined experimentally.

Wong and Duncan (1974) listed the values of the hyperbolic parameters determined for more than one hundred different soils tested under drained and undrained conditions. This wide data base can be used to estimate reasonable values of the parameters in cases where the available information on the soil is restricted to descriptive classification. The data base is also useful for assessing whether parameter values derived from laboratory test results are consistent with past experience. Representative parameter values for granular soils tested under drained conditions are presented in Table 2.2. It is seen that the state of compaction alone does not define the Duncan-Chang parameters uniquely.

It should be noted that the parameter values were deduced from conventional triaxial compression tests. Consequently, for other than the triaxial test conditions (e.g., plane strain, uniaxial strain, etc.), use of these parameters may introduce serious errors. Moreover, for those soils in which the stress-strain-volume change relations deviate from the hyperbolic form, use of the model may also yield unsatisfactory results. Further discussion of the limitations of this model is given in section 4.5.2.

## (2) Extended-Hardin Model

The Hardin model (Hardin, 1970; Hardin and Drnevich, 1972) provides a relationship for the secant shear modulus of soils as a function of





Table 2.2 Representative Parameter Values of the Duncan-Chang Model,  
Drained Granular Soils (after Wong and Duncan, 1974)

| Soil<br>Description                           | Relative<br>Density<br>(%) | $\gamma_d$<br>(pcf) | $\phi$<br>(degree) | K                   | n                    | $R_f$                | G                    | F                     | D                  |
|---|----------------------------|---------------------|--------------------|---------------------|----------------------|----------------------|----------------------|-----------------------|--------------------|
| Very dense silty<br>sandy gravel<br>(GP-6)    | 100                        | 148                 | 53                 | 1300                | 0.40                 | 0.72                 | 0.33                 | 0.07                  | 7.1                |
| Mod. dense gravel<br>(GW-6)                   | 65                         | 132                 | 51                 | 690                 | 0.45                 | 0.59                 | 0.14                 | 0.10                  | 27.3               |
| Mod. loose sandy<br>gravel<br>(GP-2)          | 50                         | ---                 | 41                 | 420                 | 0.50                 | 0.76                 | 0.22                 | 0.06                  | 4.7                |
| Very dense sand<br>(SP-17C)<br>(SP-4D)        | 98<br>100                  | ---                 | 45<br>45           | 3100<br>1200        | 0.52<br>0.48         | 0.92<br>0.85         | 0.34<br>0.50         | 0.12<br>0.23          | 75.9<br>11.7       |
| Dense sand<br>(SP-16B)<br>(SP-4C)<br>(SP-3)   | ---                        | ---                 | 37<br>41<br>44     | 1400<br>1100<br>190 | 0.74<br>0.36<br>0.70 | 0.90<br>0.85<br>0.57 | 0.32<br>0.46<br>0.37 | -0.05<br>0.22<br>0.16 | 28.2<br>8.9<br>4.8 |
| Loose sand<br>(SP-5A)<br>(SP-17A)<br>(SP-16A) | ---                        | ---                 | 31<br>35<br>30     | 890<br>920<br>280   | 0.26<br>0.79<br>0.65 | 0.78<br>0.96<br>0.93 | 0.35<br>0.37<br>0.35 | 0.10<br>0.12<br>0.07  | 2.4<br>10.5<br>3.5 |
| Silty sand<br>(SM-13)                         | ---                        | 104                 | 36                 | 530                 | 0.28                 | 0.74                 | 0.38                 | 0.11                  | 3.9                |



accumulated shear strain and hydrostatic pressure. The secant shear modulus,  $G_s$ , which relates accumulated shear stress to accumulated shear strain, is expressed in a hyperbolic functional form:

$$G_s = \frac{G_{\max}}{1 + \frac{\gamma G_{\max}}{\tau_{\max}}} \left\{ 1 + \frac{a}{\exp\left[\left(\frac{\gamma G_{\max}}{\tau_{\max}}\right)^{0.4}\right]} \right\} \quad \text{Equation 2.6}$$

in which  $G_{\max}$  = maximum value of shear modulus;  $\tau_{\max}$  = maximum value of shear stress;  $\gamma$  = accumulated shear strain;  $a$  = parameter related to soil type and percent saturation (Figure 2.2).

The major advantage of the model lies in the extensive correlations (Hardin formula) between the parameters in Equation 2.6 and soil index properties (void ratio, percent saturation, and plasticity index) that have been established for a wide variety of soils.

Katona, et al. (1976) developed a hyperbolic Poisson's ratio function which provided the second elastic soil modulus for the Hardin model. Paralleling Hardin's work, the following relationship for secant Poisson's ratio,  $\mu_s$ , was proposed:

$$\mu_s = \frac{\mu_{\min} + q \frac{\gamma G_{\max}}{\tau_{\max}} \mu_{\max}}{1 + q \frac{\gamma G_{\max}}{\tau_{\max}}} \quad \text{Equation 2.7}$$

in which  $\mu_{\max}$  = Poisson's ratio at large shear strain (failure);  $\mu_{\min}$  = Poisson's ratio at zero strain;  $q$  = dimensionless parameter that defines the shape of the hyperbola. Eqns. 2.6 and 2.7 constitute the extended-Hardin model.



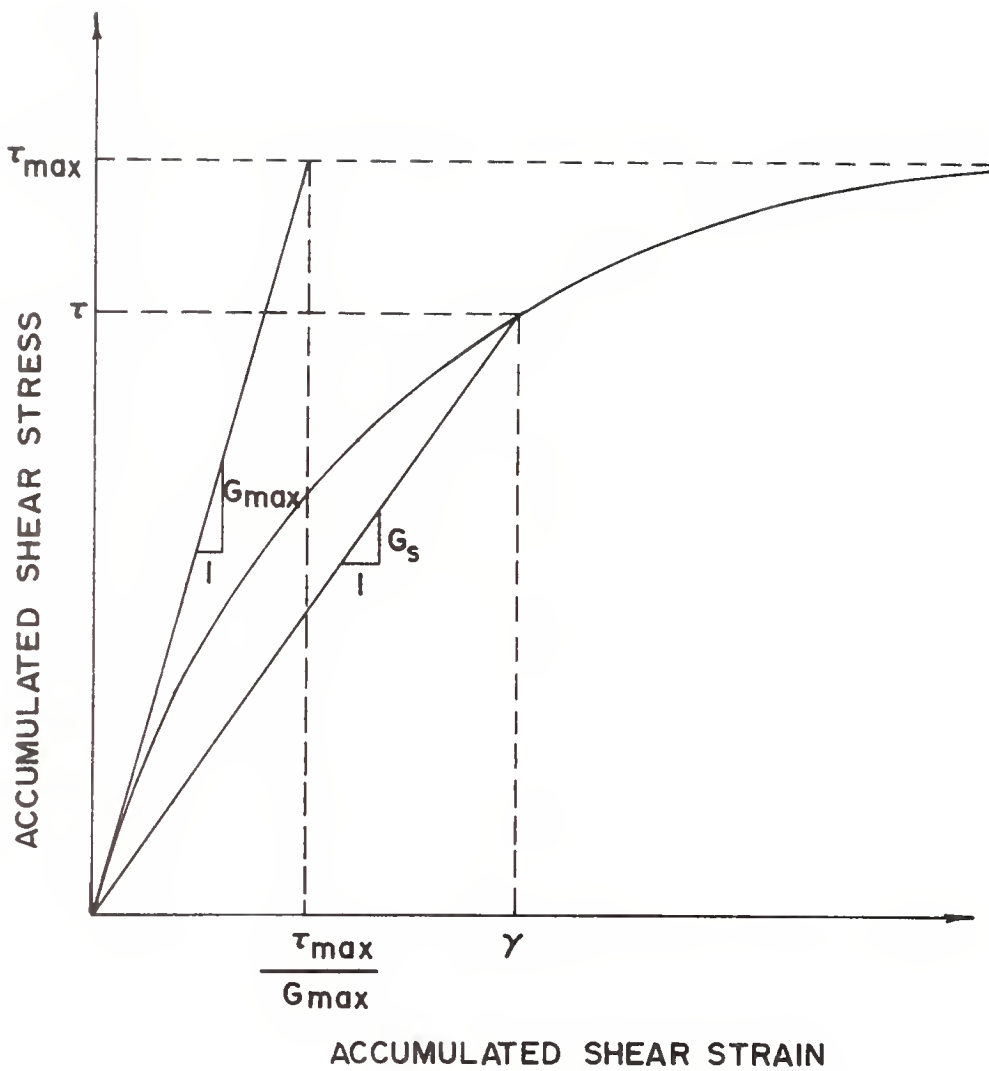


FIGURE 2.2 IDEALIZED SHEAR STRESS - SHEAR STRAIN RELATIONSHIP



It may be noted that, at present, the parameters  $\mu_{\max}$ ,  $\mu_{\min}$ , and  $q$  have to be determined from laboratory test data through curve fitting techniques. Empirical expressions for evaluation of the parameters are not currently available. Moreover, use of a simple curve (a hyperbola) fitted over the full range of Poisson's ratio, expressed as a function of  $\gamma G_{\max}/\tau_{\max}$ , may not be satisfactory. This will be illustrated in more detail in section 4.5.2.2.

### (3) Modified Duncan Model

Duncan, et al. (1978) proposed a modified hyperbolic model which employed bulk modulus in place of Poisson's ratio in the Duncan-Chang model. The model assumed that bulk modulus,  $B$ , is independent of stress difference ( $\sigma_1 - \sigma_3$ ), and that it varies with confining pressure,  $\sigma_3$ , in the following form:

$$B = k_b P_a \left( \frac{\sigma_3}{P_a} \right)^m \quad \text{Equation 2.8}$$

in which  $k_b$  and  $m$  are dimensionless parameters to be determined experimentally, and  $P_a$  is atmospheric pressure.

Duncan, et al. (1978) provided values of the bulk modulus parameters for a wide variety of soils, which later were revised and summarized by Duncan (Feb. 15, 1979). Table 2.3 lists representative parameter values taken from the latter report; they apply to soils tested under drained triaxial conditions.

### (4) Spline Function Representation

Desai (1971) proposed the use of cubic spline functions for simulation of a set of stress-strain data.

The cubic spline function approximates a given set of stress-strain data by a piecewise cubic polynomial such that the polynomial along with





Table 2.3 Representative Parameter Values of the Modified Duncan Model (from Duncan, Feb. 15, 1979)

| Unified Soil Classification | RC* Stand. AASHTO | $\gamma_m$ k/ft <sup>3</sup> | $\phi_o$ deg | $\Delta\phi$ deg | c k/ft <sup>2</sup> | K   | n    | $R_f$ | $k_b$ | m   |
|-----------------------------|-------------------|------------------------------|--------------|------------------|---------------------|-----|------|-------|-------|-----|
| GW, GP<br>SW, SP            | 105               | 0.150                        | 42           | 9                | 0                   | 600 | 0.4  | 0.7   | 175   | 0.2 |
|                             | 100               | 0.145                        | 39           | 7                | 0                   | 450 | 0.4  | 0.7   | 125   | 0.2 |
|                             | 95                | 0.140                        | 36           | 5                | 0                   | 300 | 0.4  | 0.7   | 75    | 0.2 |
|                             | 90                | 0.135                        | 33           | 3                | 0                   | 200 | 0.4  | 0.7   | 50    | 0.2 |
| SM                          | 100               | 0.135                        | 36           | 8                | 0                   | 600 | 0.25 | 0.7   | 450   | 0.0 |
|                             | 95                | 0.130                        | 34           | 6                | 0                   | 450 | 0.25 | 0.7   | 350   | 0.0 |
|                             | 90                | 0.125                        | 32           | 4                | 0                   | 300 | 0.25 | 0.7   | 250   | 0.0 |
|                             | 85                | 0.120                        | 30           | 2                | 0                   | 150 | 0.25 | 0.7   | 150   | 0.0 |
| SM-SC                       | 100               | 0.135                        | 33           | 0                | 0.5                 | 400 | 0.6  | 0.7   | 200   | 0.5 |
|                             | 95                | 0.130                        | 33           | 0                | 0.4                 | 200 | 0.6  | 0.7   | 100   | 0.5 |
|                             | 90                | 0.125                        | 33           | 0                | 0.3                 | 150 | 0.6  | 0.7   | 75    | 0.5 |
|                             | 85                | 0.120                        | 33           | 0                | 0.2                 | 100 | 0.6  | 0.7   | 50    | 0.5 |
| CL                          | 100               | 0.135                        | 30           | 0                | 0.4                 | 150 | 0.45 | 0.7   | 140   | 0.2 |
|                             | 95                | 0.130                        | 30           | 0                | 0.3                 | 120 | 0.45 | 0.7   | 110   | 0.2 |
|                             | 90                | 0.125                        | 30           | 0                | 0.2                 | 90  | 0.45 | 0.7   | 80    | 0.2 |
|                             | 85                | 0.120                        | 30           | 0                | 0.1                 | 60  | 0.45 | 0.7   | 50    | 0.2 |

\* RC = relative compaction, in percent



its first and second derivatives is continuous over the entire range of the data. This is accomplished by expressing a cubic polynomial,  $F(\epsilon)$ , (Figure 2.3) in each segment,  $(\epsilon_i, \epsilon_{i+1})$ , in terms of the known functional values,  $\sigma_i$  and  $\sigma_{i+1}$ , and second derivatives at the two ends,  $s_i$  and  $s_{i+1}$ , as:

$$F(\epsilon) = a_i(\epsilon - \epsilon_i)^3 + b_i(\epsilon - \epsilon_i)^2 + c_i(\epsilon - \epsilon_i) + d_i \quad \text{Equation 2.9}$$

where the coefficients  $a_i$ ,  $b_i$ ,  $c_i$ , and  $d_i$  can be written in the following form (Singh and Sandhu, 1975):

$$\begin{Bmatrix} a_i \\ b_i \\ c_i \\ d_i \end{Bmatrix} = \frac{1}{12h_i^2} \begin{bmatrix} -2h_i & 2h_i & 0 & 0 \\ 6h_i^2 & 0 & 0 & 0 \\ -4h_i^3 & -2h_i^3 & -12h_i & 12h_i \\ 0 & 2 & 12h_i & 0 \end{bmatrix} \begin{Bmatrix} s_i \\ s_{i+1} \\ \sigma_i \\ \sigma_{i+1} \end{Bmatrix} \quad \text{Equation 2.10}$$

in which  $h_i = \epsilon_{i+1} - \epsilon_i$  and the values of  $s_i$  and  $s_{i+1}$  can be obtained by requiring that the first derivative be continuous.

The derivative of the spline function,  $E(\epsilon)$ , for the segment  $(\epsilon_i, \epsilon_{i+1})$  can be evaluated simply by substituting  $a_i$ ,  $b_i$ , and  $c_i$  in the expression for  $F'(\epsilon)$ , namely:

$$E(\epsilon) = 3a_i(\epsilon - \epsilon_i)^2 + 2b_i(\epsilon - \epsilon_i) + c_i \quad \text{Equation 2.11}$$

Leonards and Roy (1976) employed the cubic spline function to represent the relationship between soil moduli (Young's modulus and Poisson's ratio) and octahedral normal stress at various values of failure stress ratio (octahedral shear stress/octahedral shear stress at failure).



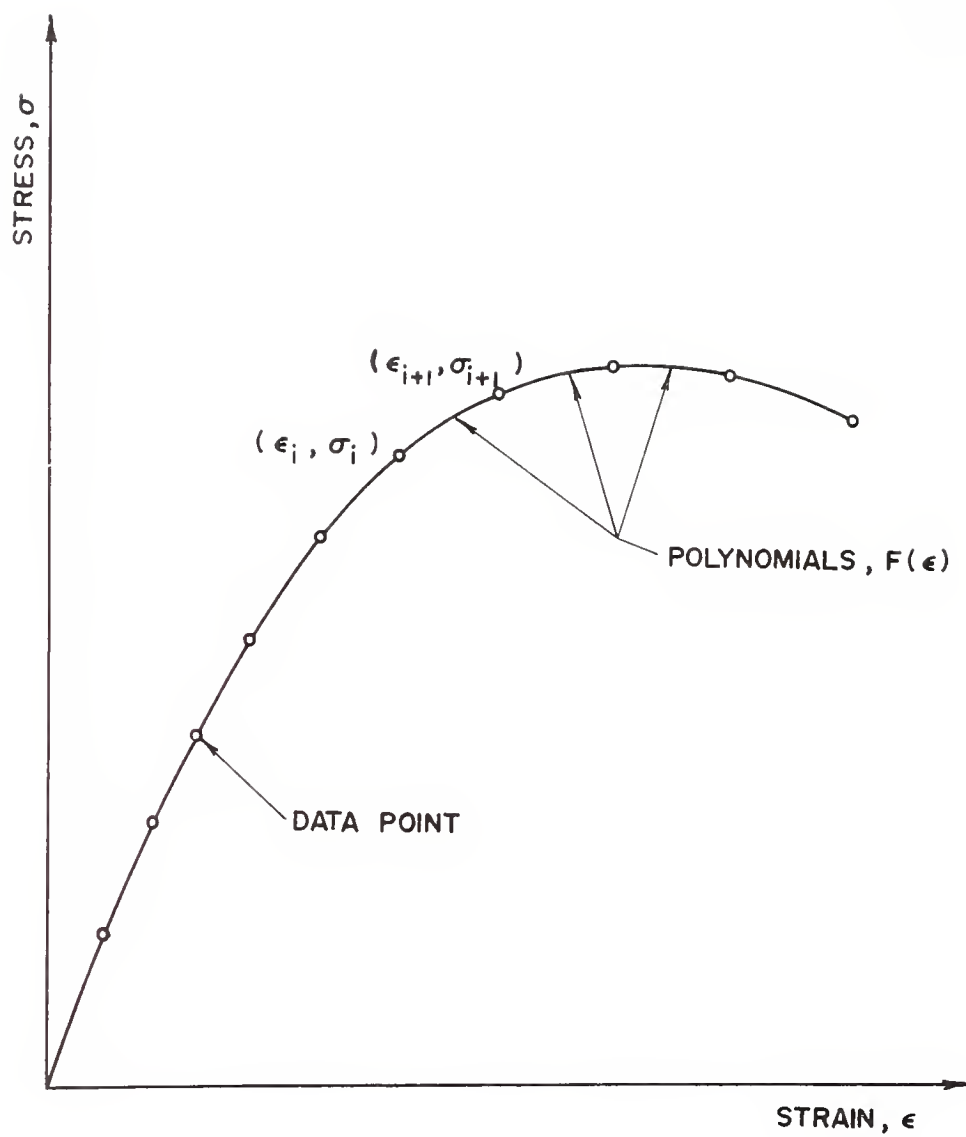


FIGURE 2.3 SPLINE FUNCTION REPRESENTATION



The cubic spline function representation was found to provide better simulation of stress-strain curves compared with that obtained by the hyperbolic function used in the Duncan-Chang model. Desai (1971) also found this representation to be superior, particularly in the initial range of the curves.

#### (5) Modified Ramberg-Osgood Model

The Ramberg-Osgood function (Ramberg and Osgood, 1943) is a three-parameter polynomial which can be written as

$$\epsilon = \frac{\sigma}{E_i} + k \left( \frac{\sigma}{E_i} \right)^p \quad \text{Equation 2.12}$$

in which  $k = \left( \frac{1}{m} - 1 \right) \left( \frac{\sigma_m}{E_i} \right)^{1-p}$  (as defined in Figure 2.4);  $E_i$  = initial Young's modulus; and  $p$  = a parameter defining the shape of the curve. Richard and Abbott (1975) proposed a similar three-parameter function which expressed stress explicitly in terms of strain:

$$\sigma = \frac{E_r \epsilon}{\left\{ 1 + \left| \frac{E_r \epsilon}{\sigma_y} \right|^p \right\}^{1/p}} + E_p \epsilon \quad \text{Equation 2.13}$$

in which  $E_r = E_i - E_p$ ;  $E_p$  = the plastic modulus; and  $\sigma_y$  = a reference yield stress (Figure 2.4).

Desai and Wu (1976) derived a numerical iterative scheme for evaluating the shape parameter,  $p$ , and proposed a procedure to incorporate effects of confining pressure and stress path.

It may be noted that for the conditions  $E_p = 0$  and  $p = 1$ , Equation 2.13 reduces to a hyperbolic function.

As the Ramberg-Osgood model includes a hyperbolic function as a special case, it is capable of representing a wider range of stress-





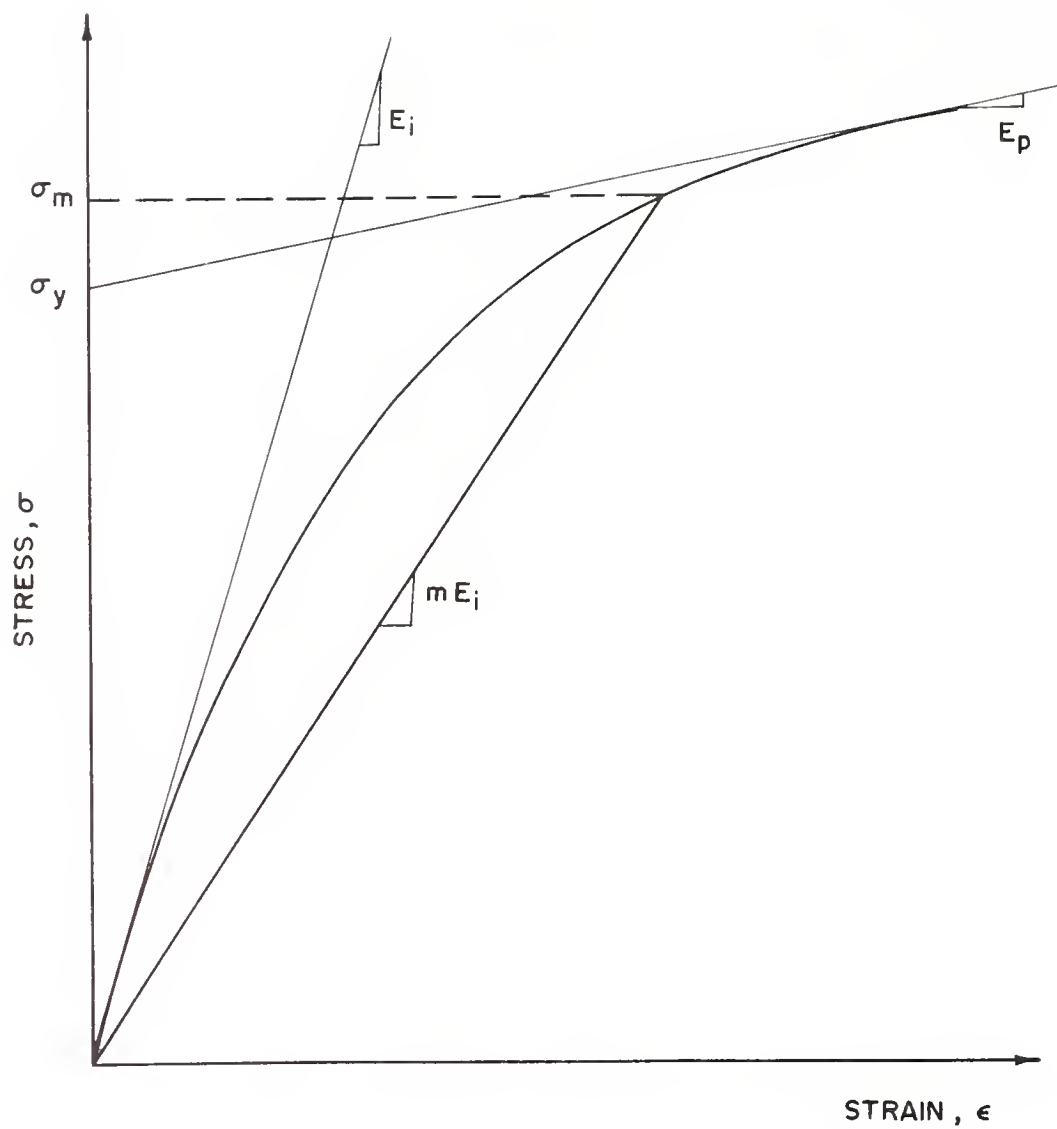


FIGURE 2.4 RAMBERG - OSGOOD MODEL



strain data than the hyperbolic models, including experimental curves exhibiting strain hardening.

### 2.1.3 HIGHER-ORDER ELASTICITY MODELS

Two higher-order elasticity models that have been investigated in geotechnical engineering are hyperelastic and hypoelastic models.

#### (1) Hyperelastic Models

The hyperelastic models rely on finding constitutive relations by differentiation of a strain energy function,  $U$ , with respect to invariants of strain,  $I_1$ ,  $I_2$  and  $I_3$ , as:

$$\begin{aligned}\sigma_{ij} &= \frac{\partial U}{\partial I_1} \frac{\partial I_1}{\partial \epsilon_{ij}} + \frac{\partial U}{\partial I_2} \frac{\partial I_2}{\partial \epsilon_{ij}} + \frac{\partial U}{\partial I_3} \frac{\partial I_3}{\partial \epsilon_{ij}} \\ &= A_1 \delta_{ij} + A_2 \epsilon_{ij} + A_3 \epsilon_{im} \epsilon_{mj}\end{aligned}\quad \text{Equation 2.14}$$

in which  $\sigma_{ij}$  = stress tensor;  $\epsilon_{ij}$  = strain tensor;  $\delta_{ij}$  = Kronecker delta; and  $A_i$  are response functions which satisfy the condition  $\frac{\partial A_i}{\partial I_j} = \frac{\partial A_j}{\partial I_i}$ .

Different orders of hyperelastic models can be obtained by retaining higher-order terms in Equation 2.14. Depending on the order, the model can account for various factors. Ko and Masson (1976) proposed a third-order hyperelastic soil model. The model can accommodate dilatancy and strain hardening of soils. The model was verified by examining its ability to predict the overall response and the strain distribution of a cuboidal sample of Ottawa sand tested under plane strain conditions.

It may be noted that in hyperelastic models, as in all the models discussed previously, the stresses are functions only of the strains. Consequently, the material behavior is assumed to be independent of the path followed during loading (Desai, 1972). Unfortunately, for most



soils, this assumption is valid only over a small stress range. Accordingly, laboratory tests must use stress paths that follow closely those anticipated in the field problem.

## (2) Hypoelastic Models

Truesdell (1955) proposed a rate theory which is known as the hypoelastic formulation:

$$\text{stress increment} = f(\text{strain increment})$$

in which the parameters in the function  $f$  depend on the state of stress.

The most general form of constitutive relation for an isotropic hypoelastic material involves twelve response parameters. Coon and Evans (1972) and Vagneron, et al. (1976) applied grade-one hypoelastic models, which retained only terms up to first order in the general hypoelastic relation (i.e.,  $f$  is only a linear function of stress tensor), to characterize behavior of cohesionless soils. Their models involve seven response parameters whose evaluation requires that several different types of laboratory tests (e.g., triaxial compression test, uniaxial strain test, isotropic compression test) be performed.

The incremental nature of hypoelastic models offers many advantages regarding their ability to characterize mechanical behavior of soils such as stress path dependence, work softening, and dilation. However, a number of difficulties are encountered in the use of the models: (1) the response parameters are not unique, their values being dependent on which types of tests are selected to be performed, (2) no relation has been found between the response parameters and other common soil properties, and (3) there is no explicit relationship that indicates the effect of varying any response parameter and the resulting change in stress-strain-volume change behavior of soils. Further research will be needed before



it can be readily applied in analyzing geotechnical engineering problems.

It may be noted that grade-zero hypoelastic models, which retain only zero-order terms in the function  $f$ , bear the same form as the incremental Hooke's law (e.g., Equation 2.1 in incremental form). Accordingly, all the models presented in sections 2.1.1 and 2.1.2 can be considered equivalent to grade-zero hypoelastic models.

#### 2.1.4 PLASTICITY MODELS

From an academic point of view, plasticity soil models (Roscoe, 1970; Lade, 1972; Frydman, et al., 1973; Prevost and Höeg, 1975) are attractive because they are inherently capable of accommodating such behavior of soils as:

- (1) inelastic strain components, even if the stress increment is small;
- (2) stress-strain relations that are stress path dependent;
- (3) coupling between volume changes and changes in shear stress;
- (4) the influence of all three principal stresses on the stress-strain and strength characteristics; and
- (5) the tendency to exhibit strain softening after a peak strength has been reached.

In incremental elastic-plastic models, the stress-strain relation is usually expressed as

$$\{d\sigma\} = [C^{ep}] \{d\epsilon\} \quad \text{Equation 2.15}$$

in which  $d$  denotes an increment, and  $[C^{ep}]$  is the elastic-plastic stress-strain matrix. Equation 2.15 may be used as a constitutive relation in finite element analysis in the same way as the generalized Hooke's law (Equation 2.1).





The elastic-plastic stress-strain matrix can be derived on the basis of the following concepts and assumptions from classical plasticity theory (Hill, 1950; Mendelson, 1968; Ozawa and Duncan, 1976; Chen and Atsuta, 1976:

(1) Incremental Elastic and Plastic Strains

During an infinitesimal change in stress, the total strain increments,  $\{d\epsilon\}$ , are assumed to be divisible into elastic components and plastic components.

(2) Yield Function

The yield function describes the yield surface which defines the boundary between states of stress causing only elastic strain and those causing both elastic and plastic strains.

(3) Hardening or Softening Rule

The rule redefines the yield function after plastic deformation continues to occur.

(4) Plastic Potential Function

It is assumed that there exists a plastic potential function from which the ratios of the components of plastic strain increments may be derived. It is usually assumed in classical plasticity theory that the plastic potential function takes the same form as the yield function (called associated plasticity).

(5) Flow Rule

The rule relates increments of plastic strain to increments of stress after the yield condition has been exceeded. The "normality rule" states that the plastic strain increments are directed outward normal to the plastic potential function.

(6) Relationship between Stress Increments and Elastic Strain Increments

The increments of stress are related to the increments of elastic



strain by means of an elastic constitutive law.

It has been shown experimentally (Barden and Khayatt, 1966; Ko and Scott, 1967; Roscoe and Burland, 1968; Smith and Kay, 1971; Lade, 1972) that the yield function and plastic potential function are not identical for most soils. This implies that the plastic strain increments of soils are generally not directed outward normal to the yield surface. Plasticity soil models which attempt to accommodate this experimental fact encounter two serious difficulties: (1) the elastic-plastic stress-strain matrix,  $[C^{ep}]$ , is not usually symmetrical, which results in a huge increase of computer storage and computation effort over the use of the soil models with associated plasticity, and (2) unlike associated plasticity soil models, the uniqueness and stability of the solutions is no longer guaranteed.

In recent years, many plasticity soil models have been proposed and some were incorporated in finite element analyses of stresses and deformations of soil masses, including the Drucker and Prager model (Drucker, and Prager, 1952; Drucker, et al., 1957), critical state models (Roscoe, et al., 1963; Roscoe and Burland, 1968; Schofield and Wroth, 1968), Lade's model (Lade, 1972; Ozawa and Duncan, 1976), and various modified cap models (Dimaggio and Sandler, 1971; Sandler, et al., 1976; Chen, 1980).

Aside from nonlinear behavior of soils, yielding of conduit walls and soil-conduit interface behavior are also of major concern. As the use of suitable plasticity soil models requires much greater computation effort than the nonlinear elastic models, plasticity models were not included in this investigation. For soil-conduit interaction problems in which a monotonically increasing load prevails, use of nonlinear elastic models provides a good (and, much simpler to use) representation of soil behavior. However, if the soil is approaching



failure, is in a post-peak stress-strain range, or if the effects of soil compaction are to be considered, nonlinear elastic soil models become invalid, because for these conditions plastic strains dominate the behavior.

#### 2.1.5 SELECTION OF A SOIL MODEL FOR ANALYSES OF SOIL-CONDUIT INTERACTION PROBLEMS

The stress-strain behavior of soils plays a very important part in analyzing soil-conduit interaction problems. Poor representation of the stress-strain characteristics can lead to calculated modes of behavior which are completely different from the actual ones. In spite of the considerable work which has been done in this area, a general and versatile way of representing the stress-strain characteristics of soils has not yet been established. The problem is very complex, and simplifications are essential for "practical" purposes. Accordingly, in selection of a soil model, a compromise between accuracy and simplicity is necessary.

Selection of a suitable soil model for analyses of soil-conduit interaction problems depends largely on the purpose of the analyses. For routine design or preliminary studies, it is desirable to select soil models which do not require soil sampling and laboratory testing. On the other hand, for prediction of soil-conduit system responses, development of new design methods, or extensive sensitivity studies, it is desirable to select the most realistic soil model possible - within the framework of computer storage space available, computation time, and prior investigations of validity - as discussed in Chapters 4 and 5.

### 2.2 CHARACTERIZATION OF CONDUIT RESPONSE

In soil-conduit interaction problems, the characterization of stress-strain relationships is somewhat easier for common conduit materials than for soil. Often the material is assumed to be linear elastic; however, if



the yield stress is exceeded, linear elastic models are not capable of characterizing the response of the conduit.

The stress-strain relations of steel and aluminum conduits are usually approximated by a bilinear curve to simulate behavior as yielding takes place.

Katona et al. (1976) presented an incremental procedure to account for the interaction of thrust and bending moment in metal conduit walls based on a nonlinear stress-strain relationship. The thrust increment,  $\Delta P$ , and the moment increment,  $\Delta M$ , were given by:

$$\Delta P = \Delta \epsilon_p E A^* \quad \text{Equation 2.16}$$

$$\Delta M = \Delta \phi E I^* \quad \text{Equation 2.17}$$

where

$$A^* = \int [1 - \alpha(\epsilon)] dA \quad \text{Equation 2.18}$$

$$I^* = \int [1 - \alpha(\epsilon)] (\bar{y} - y)^2 dA \quad \text{Equation 2.19}$$

and in which

$\Delta \epsilon_p$  = thrust strain increment;

$\Delta \phi$  = curvature increment;

$E$  = initial Young's modulus

$\alpha(\epsilon)$  = dimensionless function of strain, which relates stress increment to strain increment;

$\Delta \sigma = E[1 - \alpha(\epsilon)]\Delta \epsilon$ ;

$\bar{y}$  = distance to bending axis,  $\Delta \epsilon_M = 0$ ;

$y$  = spatial coordinate measuring depth of the section.

The location of the bending axis,  $\bar{y}$ , is determined by requiring that the thrust increment,  $\Delta P$ , not contribute to moment increment,  $\Delta M$ , and vice-





versa. The sectional properties of the conduit (i.e.,  $A^*$ ,  $I^*$ , and  $\bar{y}$ ) are updated in accordance with the strain distribution during a given load increment to reflect nonlinearity of the conduit material.

If the material is sufficiently ductile, the entire section may be in a state of yielding, hence, relatively large rotations are possible without a significant increase in bending moment; in other words, a plastic hinge will develop.

For a rectangular section subjected to the combined action of thrust,  $P$ , and bending,  $M$ , a plastic hinge will form if the following criterion is satisfied:

$$\frac{M}{M_p} + \left(\frac{P}{P_p}\right)^2 = 1 \quad \text{Equation 2.20}$$

in which  $M_p$  = fully plastic moment of the section, i.e., the limiting moment when the section is subjected to pure bending;

$P_p$  = squash load of the section in the absence of bending moment.

If the section is also subjected to shear force,  $V$ , an approximate criterion for the formation of a plastic hinge was given by Neal (1960):

$$\frac{M}{M_p} + \left(\frac{P}{P_p}\right)^2 + \frac{\left(\frac{V}{V_p}\right)^4}{\left[1 - \left(\frac{P}{P_p}\right)^2\right]} = 1 \quad \text{Equation 2.21}$$

where  $V_p$  = limiting shear force on the section under pure shear.

The plastic hinge thus formed permits redistribution of stresses in the conduit. Further increases of loads will be carried by other less heavily stressed sections of the conduit, until a sufficient number of plastic hinges are formed and the conduit starts to behave as a mechanism



(i.e., collapse occurs).

## 2.3 CHARACTERIZATION OF INTERFACE BEHAVIOR

Finite element analyses require compatibility not only at the nodes but also at element interfaces, even where the material types are dissimilar.

For conventional conduits buried in soils, the stiffness and the capability to resist bending of the soil and the conduit is very different. Under certain loading conditions, relative movements at the soil-conduit interface may occur due to the fact that the limiting interface friction has been reached and the tendency for the conduit to move inward and separate from the soil. In order to obtain a better simulation of soil-conduit interaction, it is desirable to incorporate techniques for accommodating this interface behavior.

The physical behavior of a soil-conduit interface may involve relative movements that are both normal and tangential to the interface surface. The term debonding describes the separation of the soil and the conduit, which were initially in contact, normal to the interface surface. Subsequent contact, termed rebonding, can develop by movement of the soil and the conduit towards each other. The term slip defines the relative movement along the surface of contact when the shear stress tangent to the interface exceeds the corresponding frictional resistance.

Attempts made to simulate the interface behavior, in the realm of finite element analysis, can be classified into (1) method of stiffness, and (2) method of constraints.

### 2.3.1 METHOD OF STIFFNESS

In this method, the stiffnesses of the elements representing the interface determine the extent of the bond between two bodies initially



in contact.

Zienkiewicz et al. (1970) advocated the use of continuous isoparametric elements with nonlinear material properties for interface normal and shear deformations, assuming uniform strain in the normal direction. Numerical difficulties can arise from ill-conditioning of the stiffness matrix due to very large off-diagonal terms or very small diagonal terms which are generated by these elements in certain cases.

Goodman, Taylor and Brekke (1968) developed a special type of interface element to account for relative movements between rock joints. The element consists of two lines each with two nodal points. The two lines occupy the same position before deformation and each node has two degrees-of-freedom, (horizontal and vertical displacements). If, for example, it is desired to simulate slippage across an interface as the frictional resistance is exceeded, an arbitrarily large normal stiffness would be specified to enforce near compatibility in normal direction, while the tangent (shear) stiffness is set equal to a small value (the residual interface shear stiffness) to allow independent movement in the tangent direction.

Clough and Duncan (1969) conducted (direct shear) interface tests in the laboratory to measure the interface shear stress-relative displacement relation between concrete and the backfill sand used for the Port Allen lock, and proposed a hyperbolic functional relationship for the interface shear stiffness. However, part of the measured displacements was due to shear strains in the soil, in addition to those at the interface.

Attempts have been made by a number of investigators to modify the Goodman-Taylor-Brekke interface model (Ghaboussi et al., 1973; Goodman



and St. John, 1977; Wong, 1977). However, there are certain inconsistencies with the elements that are very difficult to overcome. For example, in order to prevent the two contacting bodies from penetrating each other when subjected to compressive force, a very large interface normal stiffness has to be selected. On the other hand, penetration is required to recover the normal force at the interface. Due to the large normal stiffness, the significant digits of the penetration become truncated, hence the resulting interface normal force will be in error. On the other hand, if the normal stiffness is not large enough, significant penetration will occur which is kinematically inadmissible.

### 2.3.2 METHOD OF CONSTRAINTS

The concept of using constraint equations to represent the interface behavior in finite element analysis was introduced by Chan and Tuba (1971).

Katona et al. (1976) developed a general theory for treating constraint equations in the formulation of interface elements and devised an iterative procedure for characterizing the interface behavior.

The interface element is defined by a set of paired nodes joining two bodies. Prior to deformation, the paired nodes occupy the same location in space but are assigned to separate bodies (elements). In addition, a third node is assigned to the interior of the paired nodes. The spatial location of the interior node is immaterial; its sole purpose is to provide unique equation numbers for normal and tangential interface forces. Each of the paired nodes has two degrees-of-freedom (horizontal and vertical displacements). The element stiffness therefore is of the size  $6 \times 6$  in a mixed formulation.

By using the subscriptors "fixed" and "free" to describe the relative





movements of a contact point in normal and tangential directions, four kinematic states were defined to represent the interface behavior. For a given load increment, the choice of correct interface state is determined by a trial-and-error process. A particular state is first assumed and a set of trial responses are evaluated. The trial responses are then used to determine if the assumed state is correct, and if not, what is the new trial state. The trial responses which are used as decision parameters of the trial and error process for different assumed states are given in Table 2.4. The state which represents separation in the normal direction while retaining contact in the tangential direction was discarded because it had no physical significance in the interface model. Whenever separation occurs in normal direction, the state representing free movement in normal and tangential directions is automatically implied.

The constraint equations corresponding to the correct interface state are incorporated into the global stiffness matrix using standard finite element assembly techniques. In other words, the constraint equations are treated as interface element stiffness in the analysis.

## 2.4 OTHER FACTORS

### 2.4.1 SEQUENTIAL CONSTRUCTION

Soil backfilling in a soil-conduit system is usually carried out in a series of lifts. For a realistic analysis of stresses and deformations in the soil-conduit system, it is necessary to account for the effects introduced by sequential loading. The larger the conduit diameter, and the shallower the soil cover, the more the effects of sequential construction will dominate conduit performance.

A procedure for simulating sequential construction of soil masses commonly used in finite element analysis was derived from an idea proposed



Table 2.4 Decision Parameters for Various Assumed Interface States (after Katona, et al., 1976)

| Assumed Interface State | Fixed in both Normal and Tangential Directions (fixed-fixed state)  | Fixed in Normal Direction; Free in Tangential Direction (fixed-free state)  | Free in both Normal and Tangential Directions (free-free state)   |
|-------------------------|---|---|---|
|                         | <p>(1) if the total interface normal force <math>&gt;</math> the tensile breaking force, try free-free state;</p> <p>(2) if the total interface normal force <math>\leq</math> the tensile breaking force, and the absolute value of the total interface shear force <math>\geq</math> the frictional resistance, try fixed-free state; otherwise fixed-fixed state is correct.</p> | <p>(1) if the total interface normal force <math>&gt;</math> the tensile breaking force, try free-free state;</p> <p>(2) if the total interface normal force <math>\leq</math> the tensile breaking force, and the relative tangent displacement during the load increment bears an opposite sign to the imposed frictional resistance, try fixed-fixed state; otherwise fixed-free state is correct.</p> | <p>if the relative normal displacement <math>&lt; 0</math>, try fixed-fixed state; otherwise, free-free state is correct.</p> |

\*Compressive forces are assumed to be negative



by Goodman and Brown (1963). The procedure can be described by the following four steps:

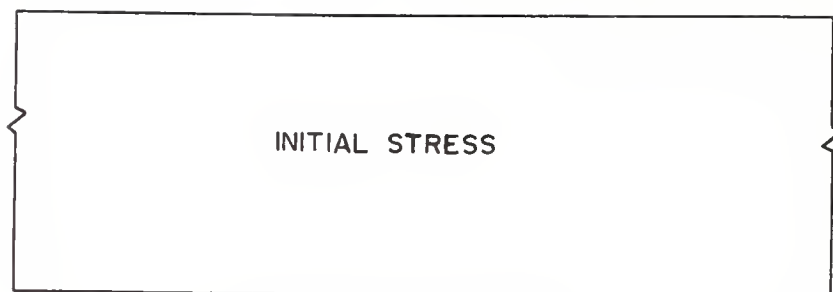
- (1) Introduce initial stresses in the foundation soil before construction starts (Figure 2.5(a)). The initial stresses can be obtained by performing one cycle of finite element analysis or simply by estimation.
- (2) Evaluate the stiffness matrix and the load vector associated with the configuration after the first soil lift was laid down, (Figure 2.5(b)). Solve for system responses. Add the stresses to the initial stresses. Store the results.
- (3) Compute combined stiffness matrix corresponding to the configuration after the second soil lift was laid down. Solve for the system responses due to the loads from the second soil lift. Add them to the results from step 2 and store the results.
- (4) Continue the same process for each soil lift as in step 3 (Figure 2.5(c)). The final state is the sum of all the responses.

Unfortunately, regardless of the accuracy of the technique for simulation of the basic construction process, there are many details in construction such as construction equipment loads and non-uniform back-filling which are very difficult to simulate rationally but which can strongly influence the system response. Knowledge of the effects of these details is essential to keep a reasonable perspective about possible perturbations due to factors not included in the analysis.

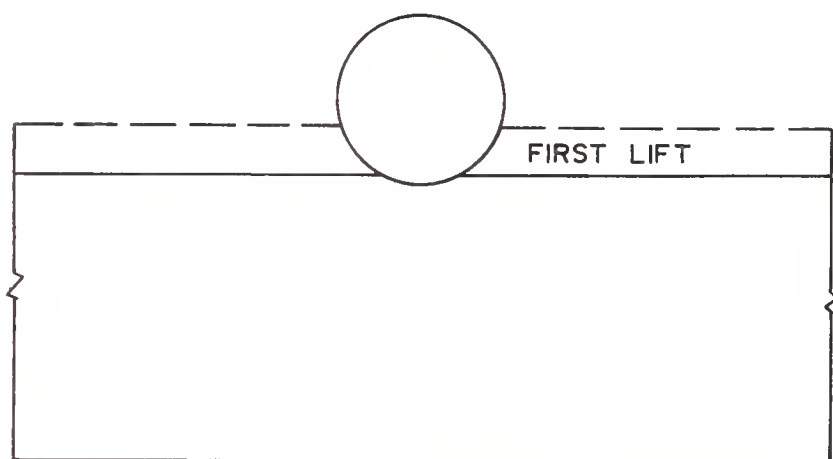
#### 2.4.2 COMPACTION

Compaction is the densification of soil by the application of

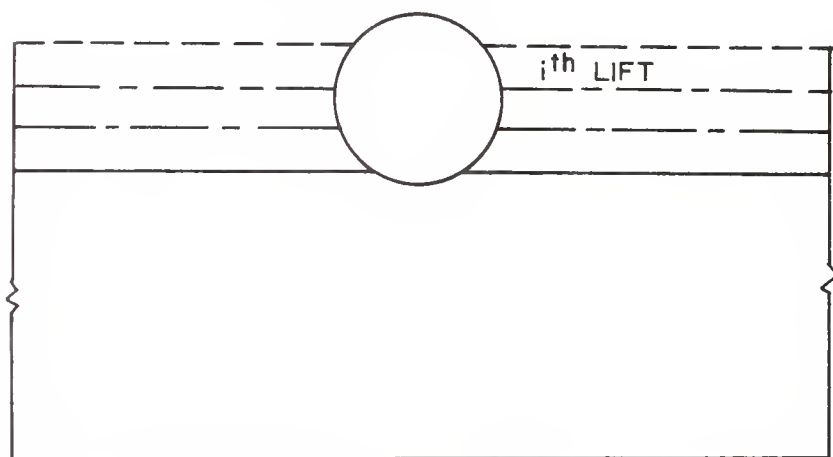




(a) INITIAL STATE



(b) LIFT 1



(c) LIFT  $i$

FIGURE 2.5 ANALYTICAL SIMULATION OF SEQUENTIAL CONSTRUCTION





mechanical energy.

It has long been realized that compaction plays an important role in the performance of soil-conduit systems. During the early stages of backfilling, inward lateral movement at the springline and "peaking" at the crown are important manifestations of the imposed compaction loads.

Compaction loads are temporary loads which are removed after compacting a construction lift. To simulate the effect of compaction on the response of a soil-conduit system, soil models, such as plasticity models, which are inherently capable of treating unloading and reloading effects, are preferable to other soil models. However, to-date only approximate methods of dealing with soil compaction have been considered.

Katona (1978) proposed a simplified procedure to simulate the effect of compaction by successively applying and removing a uniform surcharge along the surface of each compacted soil lift. The procedure is described as follows:

- (1) Apply a uniform pressure representing all compaction loads on the first compacted soil lift along the surface of the lift.
- (2) Apply the uniform pressure to the surface of the second compacted soil lift after it was laid ; in the meantime, remove the pressure on the surface in step 1 by imposing an equal but opposite pressure along the same surface.
- (3) Repeat the process for each soil lift subjected to compaction.
- (4) Terminate the process by removing the compaction pressure on the surface of the last soil lift so that no compaction loads remain in the soil-conduit system.



The procedure is simple, expedient, and can easily be incorporated in the solution scheme of existing computer codes. However, it suffers from two difficulties: (1) the process does not conform to the actual mechanism of compaction operations (compaction affects more than one soil lift), and (2) the proper magnitude of the "equivalent" uniform compaction pressure is very difficult to determine.

It may be noted that using soil modulus values different from those of loading to represent the influence on the soil stiffness of removal and reapplication of compaction loads is necessary to provide a better simulation of the compaction process. Unfortunately, the reloading moduli are strongly dependent upon stress path during unloading and the stress increment upon reloading (Lambrechts and Leonards, 1978); no methods for simulating these effects are currently available.

#### 2.4.3 NO-TENSION BEHAVIOR OF SOIL MASS

In soil-conduit interaction problems, tensile stress may develop in the soil mass as well as at the soil-conduit interface. A simple empirical approach often used for accommodating low (or zero) tensile strength of soil masses is to assign arbitrarily a small stiffness to those elements in which tensile stress is induced. This approach, however, depends on how "small" a stiffness is selected. If this stiffness is too low, convergence problems and artificially rapid propagation of failure zones may develop; if it is too large, the effects of local failures in the soil mass will be poorly simulated.

Zienkiewicz et al. (1968) developed a stress transfer (or relaxation) method to accommodate the no-tensile behavior of geologic media. When a particular soil element goes into tension during a load increment, the effect of the portion of the load increment that produced the tensile



stress is redistributed throughout the surrounding soil mass. The stress relaxation procedure involves four steps:

- (1) A standard finite element analysis is performed.
- (2) Soil elements with tensile stress are marked, and equivalent nodal forces are applied as self-equilibrating forces to nullify the tensile stresses. The equivalent nodal forces,  $\{Q_t\}$  are computed as:

$$\{Q_t\} = \int [B]^T \{\sigma_t\} d\bar{V} \quad \text{Equation 2.22}$$

in which  $\{\sigma_t\}$  are the element tensile stresses to be restrained by the nodal forces,  $\{Q_t\}$ , and  $[B]$  is the first derivative of shape functions which relate strains,  $\{\epsilon\}$ , to nodal displacements,  $\{q\}$ , as  $\{\epsilon\} = [B]\{q\}$ . The superscript T designates a transpose of the matrix  $[B]$ , and  $\bar{V}$  denotes the volume of the element.

- (3) Since the forces  $\{Q_t\}$  do not really exist, equal but opposite nodal forces are applied. An analysis is again performed. The resulting stresses are added to those computed in step 2.
- (4) The soil mass is searched for tensile stresses; and if they exist, steps 2 and 3 are repeated until the tensile stresses are negligibly small.

Chang and Nair (1973) and Leonards and Roy (1976) employed this procedure to account for the no-tension behavior of geologic material. The method was found to suffer from uncertainty of convergence.

#### 2.4.4 BUCKLING

Buckling of buried flexible conduits can occur at stress levels below yield or after yielding has initiated. The occurrence of buckling



in a given soil-conduit system depends on (1) the geometric configuration of the system, (2) the sectional properties of the conduit, (3) the material properties of the conduit, (4) the nature and stiffness of the surrounding soils, (5) the construction sequence and loading conditions, (6) the level of residual stresses in the conduit, due to cold forming, welding, etc., and (7) the inherent geometric imperfection of the conduit.

An extensive review on buckling failure of buried flexible conduits conducted by Leonards and Stetkar (1978) revealed that buckling is an important failure mode, especially for pipe arches, and can occur at deflections less than 5% of the pipe diameter. It is, therefore, necessary to take into account the possible occurrence of buckling in numerical modeling of soil-conduit systems.

In order to obtain realistic results for problems that involve buckling, large deformation theory is generally required in numerical models to accommodate geometric nonlinearity. However, this results in a far more complex formulation and much greater computational effort than those formulated on the basis of small displacement theory. A computer code written in terms of large deformation theory which can readily be used to investigate soil-conduit interaction problems including such important effects as construction sequence, interface slip, etc. is not currently available. In the realm of small displacement formulation, however, part of the effects of geometric nonlinearity can be accounted for by updating the geometry of the soil-conduit system after each load increment.

In most numerical methods developed on the basis of small displacement theory it is tacitly assumed that the structural capacity of the conduit can be reached before the occurrence of buckling. For design





purposes, it is mandatory to incorporate conservative buckling criteria to insure that the structural capacity of the conduit is not overestimated.

Buckling formulas based on theoretical and experimental studies have been incorporated in the numerical models to serve as buckling criteria. However, the general validity and applicability of the formulas has been questioned (Leonards and Stetkar, 1978). Most buckling theories are too simplistic to be of practical value and do not even consider snap-through buckling, which is generally found to be the most critical buckling mode for buried flexible conduits. Apart from the uncertainties in calculating the buckling load, the main difficulty with the use of buckling criteria in design is that buckling does not always constitute a performance limit (Leonards and Stetkar, 1978). As the conduit can often carry much larger loads without further distress, a rational design procedure that incorporates buckling must be able to estimate its effects on the collapse load. This is beyond the present state-of-the-art.

#### 2.4.5 LIVE LOADS

For conduits that can sustain relatively deep burial (say, depth of soil cover  $>$  one diameter), body forces due to soil weight generally overshadow the contributions from live loads. On the other hand, for conduits with shallower burial, the effect of live loads must be considered.

In plane strain finite element analysis, no additional problem arises in simulating live loads which are uniformly distributed in the longitudinal direction of the conduit. However, for live loads such as trucks and compaction equipment, which do not conform to plane strain conditions, equivalent line or strip loads that induce the same normal pressure at the crown have been used in the analysis. Classical stress distribution theories, such as the Boussinesq equation (Poulos and Davis,



1974; Jumikis, 1969), are usually adopted to evaluate this normal pressure. The validity of this technique has not been firmly established.



## CHAPTER 3    FINITE ELEMENT COMPUTER CODES FOR ANALYZING SOIL-CONDUIT INTERACTION

Four finite element computer codes for analyzing soil-conduit interaction problems were investigated in this study: (1) Finite element Isoparametric, NonLinear, with Interface interaction and No-tension program (FINLIN) - developed by Roy at Purdue University; (2) Culvert ANalysis and DEsign program (CANDE) - developed by Katona et al. at the U.S. Navy Civil Engineering Laboratory; (3) Soil-Structure Interaction Program (SSTIP) - developed by Duncan et al. at the University of California at Berkeley; and (4) NonLinear Soil-Structure Interaction Program (NLSSIP) - also developed by Duncan et al. at the University of California at Berkeley.

In all the four codes, small displacement formulation is adopted; time-independent response is assumed; the soil-conduit interaction is treated as a plane strain problem; and the technique for simulating sequential construction, described in section 2.4.1, is incorporated.

Detailed descriptions of the four codes are given in References 60, 50, 33 and 34, respectively. A brief summary of their main features is presented herein.

### 3.1 FINLIN CODE

Element Types. There are three basic element types employed in the FINLIN code:

- (1) curved beam-column element, with three degrees of freedom (horizontal and vertical displacements and a rotation) at each node, was used to model the conduit.
- (2) isoparametric linear strain triangular element (with intermediate nodes), with two degrees of freedom (horizontal and vertical displacements) at each node, was



used to represent the soil. A triangular element with one curved side to conform to the shape of the curved beam-column element is also provided.

- (3) Goodman-Taylor-Brekke type interface element (section 2.3.1), defined by four nodes with two degrees of freedom (horizontal and vertical displacements) at each node, was adopted to simulate soil-conduit interface behavior. A pair of the nodes were connected to the conduit element. The other pair of the nodes were connected to two consecutive nodes of an adjacent soil element. A linear variation of displacement along the two pairs of nodes was assumed.

Soil Models. FINLIN code incorporated a linear elastic and a nonlinear, incrementally elastic soil model. The nonlinear soil model uses a cubic spline function to represent actual test data (section 2.1.2.2). Plane strain soil test results were used directly as input data. The appropriate soil moduli for any soil element are interpolated using cubic spline function in accordance with the existing octahedral normal and shear stress conditions.

Conduit Model. The stress-strain relationship of conduit materials was assumed to be linear elastic.

Interface Model. The properties of the interface element were defined by a normal "stiffness,"  $k_n$ , and a shear "stiffness,"  $k_s$ , which are related to the corresponding normal stress,  $\sigma_n$ , and shearing stress,  $\tau$ , acting at the interface by the equations:

$$k_n \Delta_n = \sigma_n \quad \text{Equation 3.1}$$

$$k_s \Delta_s = \tau \quad \text{Equation 3.2}$$





in which  $\Delta_n$  is the average relative normal displacement across the element and  $\Delta_s$  is the average shear displacement along the element.

The value of  $k_n$  and  $k_s$  are assigned in accordance with interface stress condition to represent the interface behavior. Very high values of  $k_n$  and  $k_s$  are initially assigned to force near compatibility between the soil and the conduit. If, after application of a load increment, the interface normal stress is tensile,  $k_n$  and  $k_s$  are reduced to a very small number. If the interface normal stress is compressive but the ratio of shear stress to normal stress exceeds a limiting value, then  $k_s$  is reduced to a very small number while  $k_n$  remains unchanged, to simulate slip between the soil and the conduit.

No-tension Analysis. The stress-relaxation method proposed by Zienkiewicz et al. (section 2.4.3) was incorporated in the FINLIN code.

Nonlinear Solution Technique. FINLIN code adopted an incremental solution procedure for each soil layer. The loading (soil weight) is divided into a number of small increments. The soil is assumed to be a linear elastic material within each increment. The modulus values to be used for each soil element during an increment are determined in accordance with the stresses in the element prior to the increment.

### 3.2 CANDE CODE

Element Types. CANDE code incorporated three basic element types:

- (1) straight beam-column element, with three degrees of freedom (horizontal and vertical displacements and a rotation) at each node, was used to model the conduit.
- (2) incompatible (nonconforming) quadrilateral element, defined by four nodes with two degrees of freedom (horizontal and vertical displacements) at each node, was used to represent



the soil. The element, developed by Hermann (1973), is composed of two triangles with complete quadratic shape functions specified within each triangle. Upon applying appropriate constraints and static condensation (Felippa and Clough, 1970) the four-node quadrilateral element is formed.

- (3) constraint element, composed of two nodes with two degrees of freedom (horizontal and vertical displacements) at each node and an "interior" node representing normal and tangential interface forces, was used to simulate inter-face behavior. In fact, the element stiffness is a set of constraint equations with Lagrange multipliers. The constraint equations impose conditions on normal and tangential displacements, and the Lagrange multipliers are interface forces.

It may be noted that using the nonconforming elements to represent the soil, inter-element compatibility is not satisfied in general. Consequently, they are not consistent with the mathematical interpretation of displacement finite element methods which enables rigorous proof of an upper bound to the stiffness of the "system." Nevertheless, some nonconforming elements, which satisfy inter-element compatibility in the limit of mesh refinement as each element approaches a state of constant strain, were found to work better than closely related conforming elements. This is because the use of displacement finite element methods yields an approximate system that is stiffer than the actual system. By allowing separation, overlapping, or kinks between elements, the approximate system is "softened." However, this condition cannot be accepted a priori when new problems are tackled.



Soil Models. There are three soil models available in the CANDE code:

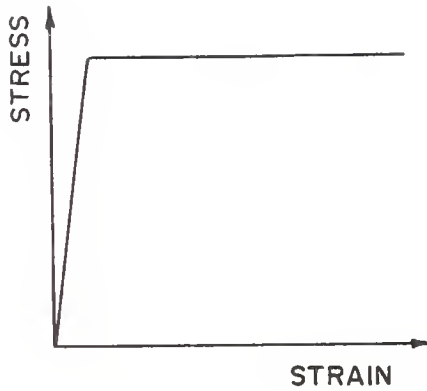
(1) linear elastic model, (2) overburden dependent model, in which elastic soil moduli are dependent upon current overburden pressure (section 2.1.2.1), and (3) extended-Hardin model, which employs a variable shear modulus and Poisson's ratio whose values are dependent on the maximum shear strain and the hydrostatic stress level (section 2.1.2.2).

Conduit Model. CANDE code employed a general multilinear model to represent the stress-strain characteristics of different conduit materials, including steel, aluminum, reinforced concrete, and plastic (Figure 3.1). The stress-strain relations of steel, aluminum, and plastic are approximated by an elastic-perfectly plastic bilinear curve, an elastic-linear strain hardening bilinear curve with a limiting (rupture) point, and an elastic curve with a rupture point, respectively, while a trilinear curve was used to simulate cracking, initial yielding, and crushing of concrete.

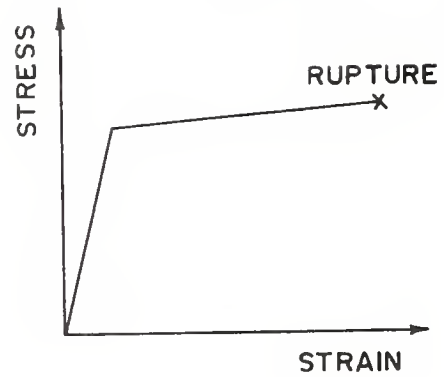
The nonlinear formulation takes into account moment-thrust interaction by determining the axis of bending in a consistent manner. For each load increment, the values of effective area, moment of inertia, and distance to bending axis are determined according to current stress-strain state of the conduit wall section through an iterative process. The basic formulation of the model was presented in section 2.2.

It should be pointed out that CANDE calculates bending moment at a conduit wall section by adding up the increments of moment at the wall section. The increment of moment for a given load increment is determined by integrating the first moment of the stress increment about the bending axis whose location varies once yielding at the wall section is initiated. Accordingly, at a conduit wall section where yielding has initiated, there is no physical significance to a moment which is the

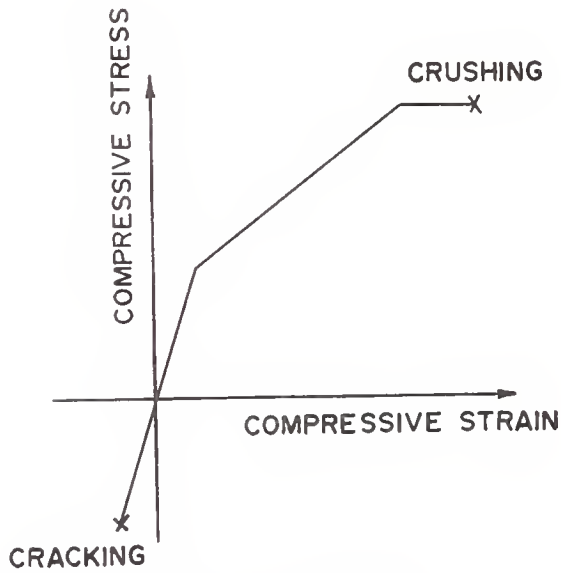




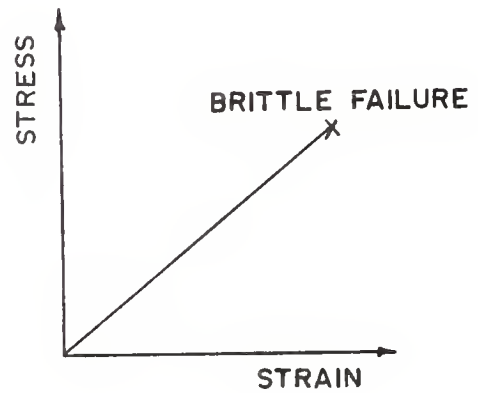
(a) STEEL



(b) ALUMINUM



(c) CONCRETE



(d) PLASTIC

FIGURE 3.1 IDEALIZED STRESS-STRAIN RELATIONSHIP FOR VARIOUS CONDUIT MATERIALS (a) STEEL (b) ALUMINUM, (c) CONCRETE, AND (d) PLASTIC INCORPORATED IN CANDE CODE





sum of increments about different axes; certainly, this moment cannot be used to calculate the stress distribution across the wall section.

Interface Model. The constraint elements described in section 2.3.2 were incorporated in CANDE code. Three possible interface states are defined by using the subscriptors "fixed" and "free" for describing the relative movements of soil-conduit interface in normal and tangential directions. For a given load increment, the choice of correct interface state is determined by a trial-and-error process. The decision parameters involved in the process are: limiting tensile force in normal direction, limiting shear resistance, relative tangential movement, and relative normal movement.

Nonlinear Solution Technique. CANDE code adopted an iterative solution procedure for each construction layer. The procedure consists of successive corrections of soil and conduit moduli until equilibrium, under the load from a newly added layer, is approximated to some acceptable degree.

Other Features. CANDE code provides an "automated" finite element mesh, which expresses the nodal coordinates of the soil-conduit system in terms of vertical and horizontal diameters of the conduit. The mesh will be further described in section 4.1.

In addition, CANDE code employed a direct search design algorithm for finding the required conduit wall geometric section properties based upon potential failure mode(s). That is, a series of analyses are performed such that an initial trial section is successively modified until specified safety factors with respect to potential failure modes (e.g., wall crushing, excessive deflections, buckling, etc.) are achieved. The buckling criterion incorporated in CANDE code is the critical buckling pressure derived by Chelapati and Allgood (1972) for deeply buried conduits buckled in high modes. According to Leonards and Stetkar (1978),



this is not a valid criterion for design purposes.

### 3.3 SSTIP CODE

Element Types. Two basic element types were employed in SSTIP code for simulation of soil-conduit systems:

- (1) straight beam-column element, with three degrees of freedom (horizontal and vertical displacements and a rotation) at each node, was used to simulate the conduit.
- (2) subparametric element (triangular or quadrilateral) developed by Wilson et al. (1971), with two degrees of freedom (horizontal and vertical displacements) at each node, was used to represent the soil. The element uses a higher order approximation for the element displacement field than for the element geometry which produces a parabolic incompatibility along the element boundaries.

Soil Model. SSTIP code employed Duncan-Chang model (section 2.1.2.2) for simulation of stress-strain characteristics of the soil. The values of tangent Young's modulus and tangent Poisson's ratio of a soil element during each increment of loading are determined on the basis of the calculated shear stress level ( $\sigma_1 - \sigma_3$ ) and confining pressure ( $\sigma_3$ ) in the element.

Conduit Model. The stress-strain relationship of conduit materials was assumed to be linear elastic.

Nonlinear Solution Technique. SSTIP code employed a 'one-iteration' solution procedure for each construction layer. Each layer is analyzed twice; the first time using soil moduli values based on the stresses before the placement of the layer, and the second time using soil moduli values based on the average stresses during the placement of the



layer. No direct check for convergence is made.

### 3.4 NLSSIP CODE

NLSSIP code is essentially the same as SSTIP code, except:

- (1) NLSSIP code incorporated modified-Duncan soil model (section 2.1.2.2) in place of Duncan-Chang soil model. The soil properties are characterized by a tangent Young's modulus and a tangent bulk modulus.
- (2) the stress-strain relationship of conduit materials is assumed to be bilinear (Figure 3.2(a)). A moment-curvature relationship was derived on the basis of the bilinear stress-strain relationship.

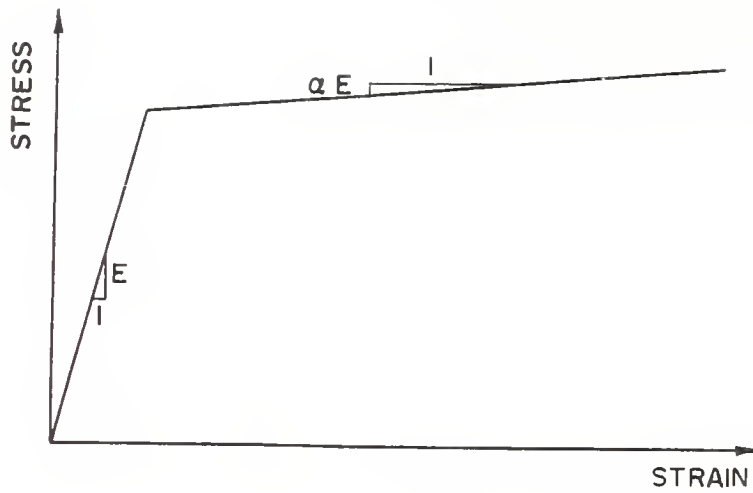
The moment-curvature relationship is approximated by an initial straight line portion representing the linear response and a hyperbola representing the nonlinear response (Figure 3.2(b)). Both the moment at which yielding first occurs,  $M_y^*$ , and the moment at which the conduit section becomes fully yielded,  $M_p^*$ , depend upon the magnitude of the thrust in the section,  $P$ , and are given by:

$$M_y^* = M_y \left( 1 - \frac{P}{P_p} \right) \quad \text{Equation 3.3}$$

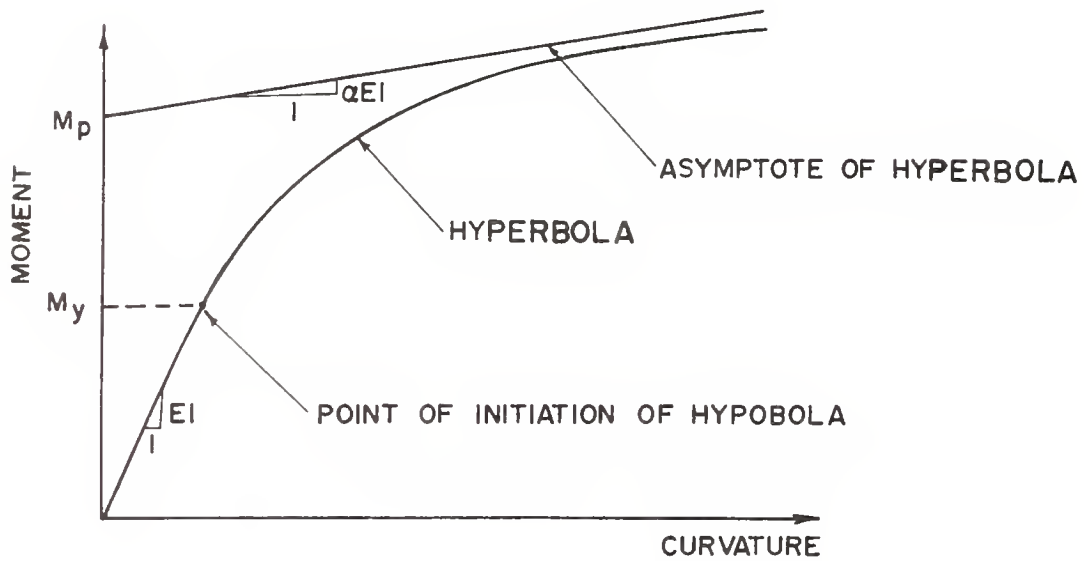
$$M_p^* = M_p \left[ 1 - \left( \frac{P}{P_p} \right)^2 \right] \quad \text{Equation 3.4}$$

in which  $M_y$  and  $M_p$  are the initial yield moment and fully plastic moment of the section, respectively, in the absence of thrust, and  $P_p$  is the squash load of the section in the absence of bending moment.





(a) STRESS - STRAIN RELATIONSHIP



(b) MOMENT - CURVATURE RELATIONSHIP

FIGURE 3.2 CHARACTERIZATION OF CONDUIT BEHAVIOR :  
 (a) STRESS - STRAIN RELATIONSHIP; (b) MOMENT-  
 CURVATURE RELATION, ADOPTED IN NLSSIP CODE





The terms in the incremental stiffness matrix that arise from flexure are derived from the slope of the moment-curvature relationship, while the axial stiffness is assumed to be independent of the bending moment.

- (3) NLSSIP code provided an option to account for part of the geometric nonlinearity by upgrading the nodal coordinates of the beam-column elements after each construction layer. Otherwise, the non-linear solution technique is the same as SSTIP.
- (4) Neither SSTIP nor NLSSIP provide for slip or no-tensile conditions at the soil-conduit interface.



## CHAPTER 4 COMPARISON OF COMPUTER CODES

### 4.1 FINITE ELEMENT DISCRETIZATION AND BOUNDARY CONDITIONS

To analyze a problem by finite element methods, a set of geometric boundaries and the conditions at these boundaries have to be properly defined. However, many geotechnical engineering problems involve soil masses that extend large distances beyond the locale that is of interest and approximations have to be made to establish the boundary conditions.

In soil-conduit interaction problems, the effects of loading (or disturbance) decrease with increasing distance from the conduit. It is thus possible to determine the extent of the soil medium that need be included in the finite element mesh of a soil-conduit system through a series of sensitivity analyses. By varying the extent of the boundaries and studying resulting effects upon conduit responses, the significant mesh boundaries can be determined.

Alternatively, past experience gained by other investigators considering similar problems may be assimilated to establish the finite element mesh. Past experience revealed (Leonards and Roy, 1976; Corotis et al., 1974; Anand, 1974; Desai, 1972) that the influence on a conduit buried in a homogeneous soil mass became insignificant if the lateral boundaries of the mesh were located at a horizontal distance of six conduit radii from the centerline of the soil-conduit system. The bottom boundary of the mesh need be placed only three to four conduit radii vertically below the springline to simulate an infinite depth of homogeneous soil mass.

Figure 4.1 shows three configurations of finite element discretization of soil-conduit systems. Throughout this study the three meshes, Figure 4.1(a), (b), and (c), were used in conjunction with computer codes FINLIN, CANDE, and SSTIP (NLSSIP), respectively, unless otherwise



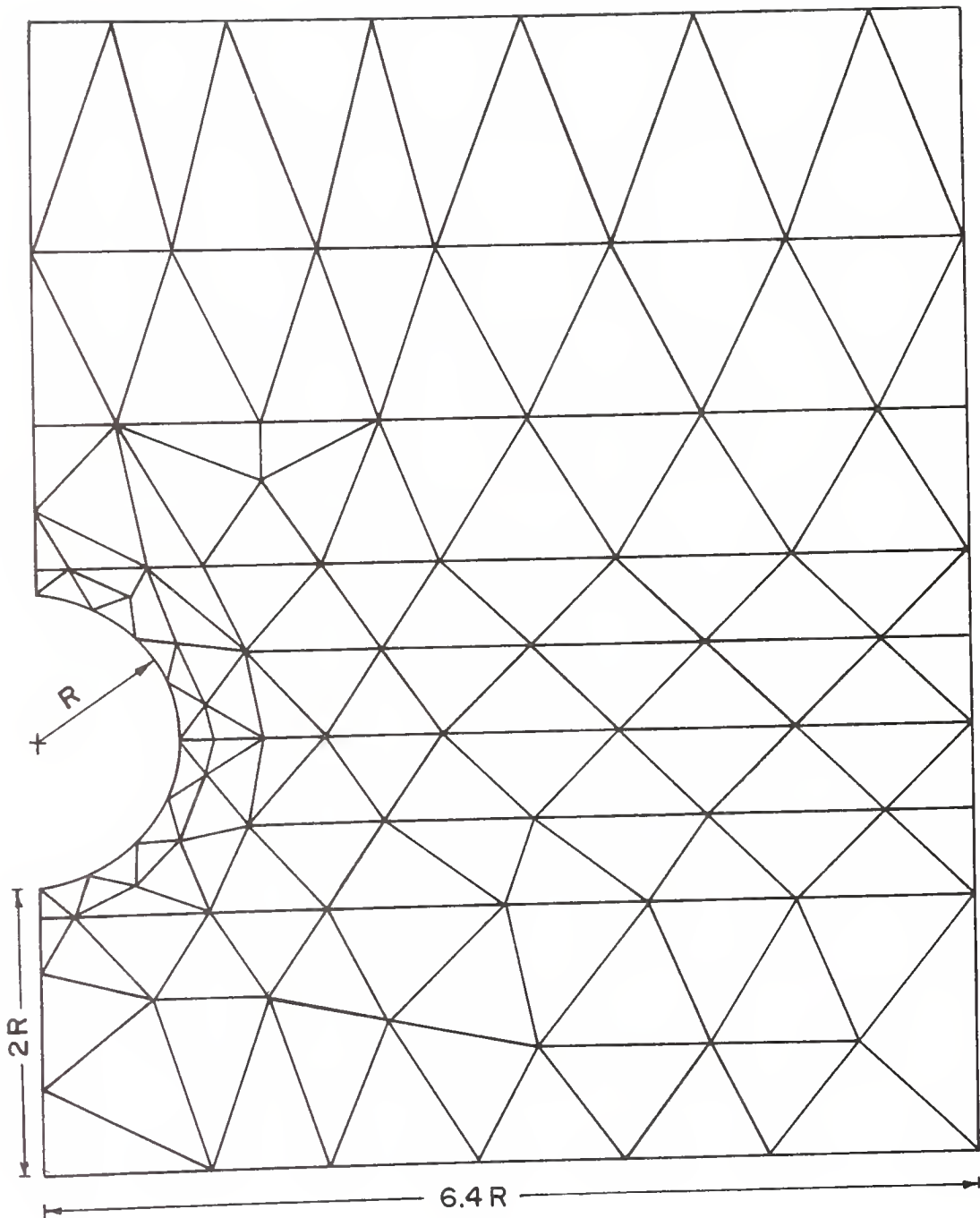


FIGURE 4.1(a) FINITE ELEMENT MESH USED IN CONJUNCTION WITH FINLIN CODE



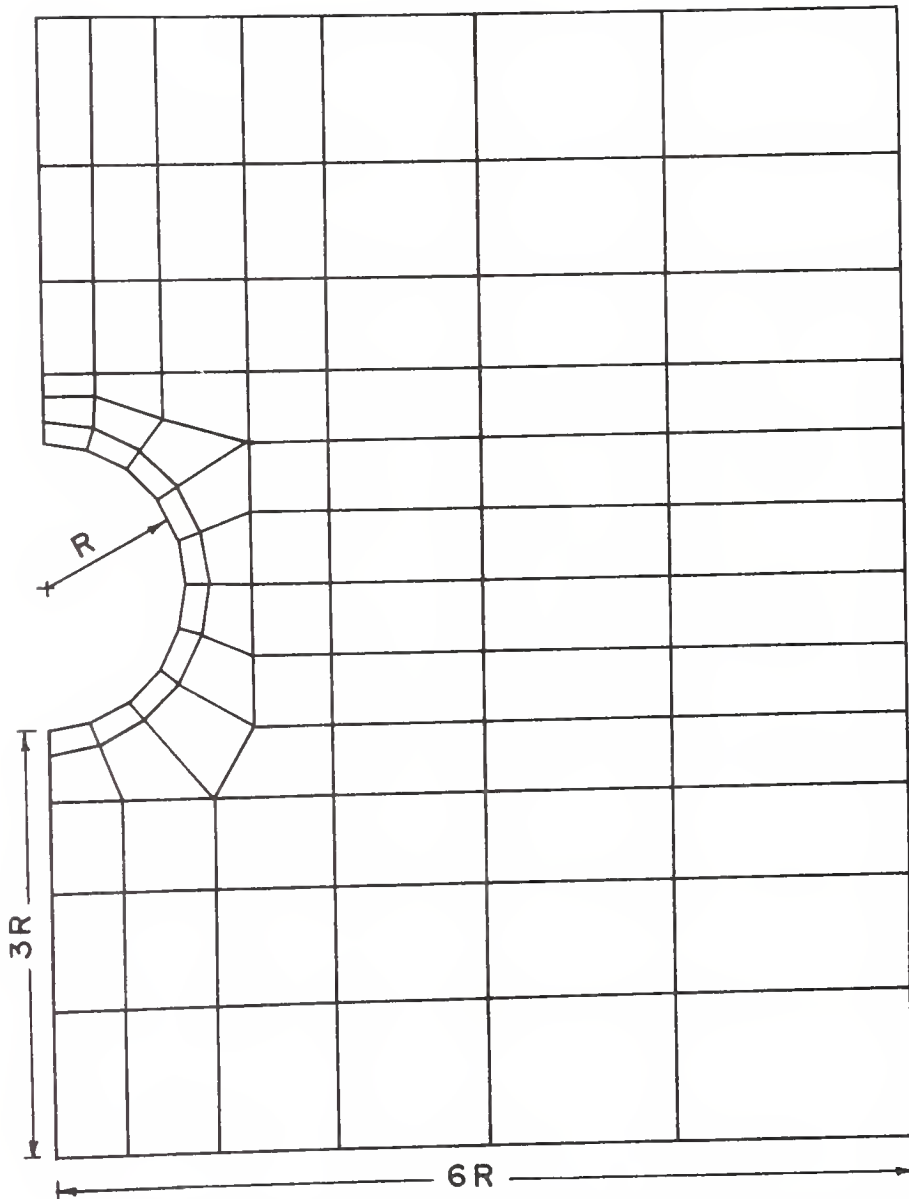


FIGURE 4.1 (b) FINITE ELEMENT MESH USED IN CONJUNCTION WITH CANDE CODE





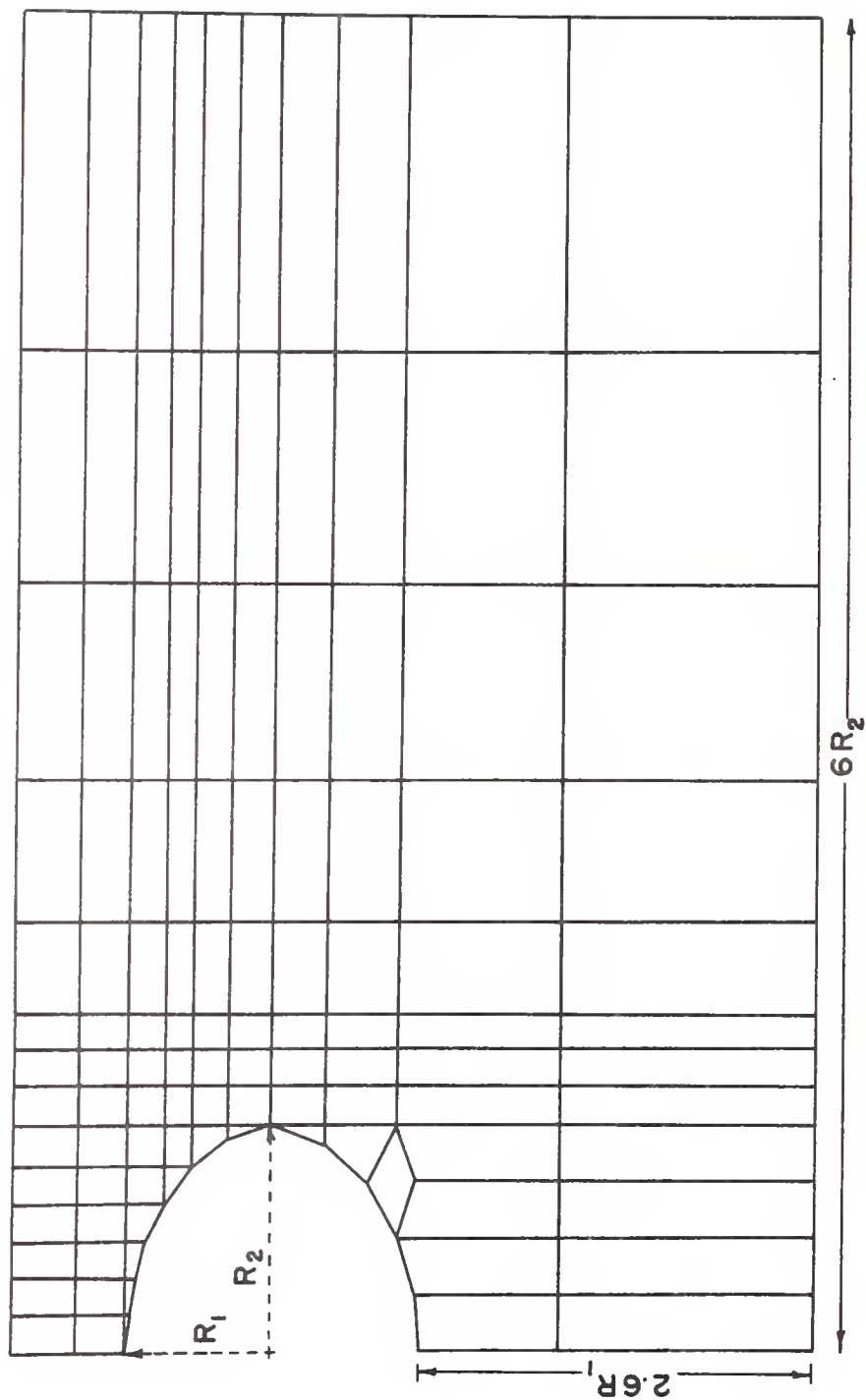


FIGURE 4.1(c) FINITE ELEMENT MESH USED IN CONJUNCTION  
WITH SSTIP AND NLSSIP CODES



specified. It is noted that finer mesh sizes were used for soil adjacent to the conduit due to the more pronounced variations in stresses in that region, and that the distance to the lower boundary in FINLIN is smaller than in the other codes.

The finite element mesh incorporated in the CANDE code (e.g., Figure 4.1(b)) is an "automated" mesh. The coordinates of the mesh are specified in terms of the vertical and horizontal diameters of the conduit. Therefore, once the diameters of a conduit are specified, the finite element mesh of the soil-conduit system will be readily established, including the meshes for elliptical conduits. If the fill height above the springline is greater than two vertical diameters, the mesh surface will be truncated at two vertical diameters above the springline. The remaining soil weight will be applied to the mesh surface as overburden pressure. On the other hand, if the fill height above the springline is less than two vertical diameters of the conduit, the mesh surface will coincide with the fill surface. The mesh below the level of  $0.75 \times$  vertical diameter above the springline is formulated in relation to the pipe diameter regardless of the fill height; above this height the elements are "flattened" to match the specified fill height. The validity of this procedure will be investigated in section 4.2.1.

For circular conduits, if the fill height is less than  $0.825$  diameter above the springline, an element mesh  $0.825 D$  above the springline will automatically be generated. Various ways of dealing with this condition will be treated later.

Once the significant extent of a soil mass is ascertained, the conditions along the boundaries must be idealized. Lateral boundaries are usually restrained against horizontal movement, and are free to



displace vertically. If both the geometry and the loading of a soil-conduit system is symmetric, it is only necessary to discretize the system on one side of the centerline. In this case, the centerline should also be restrained against horizontal displacement and be free to move vertically. The bottom boundary can be either completely fixed, or constrained only against vertical movement. Total restraint is often used if the bottom boundary is taken at the known elevation of a relatively stiff stratum.

## 4.2 VERIFICATION OF THE COMPUTER CODES

Verification of finite element computer codes may be made through comparison of the results obtained with one of the following four conditions: (1) controlled test results; (2) available closed-form solutions; (3) results obtained from other finite element codes; and (4) results obtained by other numerical methods.

For soil-conduit interaction problems, only the comparison with controlled test results can provide ultimate verification of a computer code. However, controlled test results with detailed measurements of soil properties and soil-conduit responses are not currently available.

In this section, preliminary verification of the computer codes described in Chapter 3 is attempted by comparing results obtained from the four different computer codes and, for simple cases, with available closed-form solutions.

### 4.2.1 SOLUTION LEVELS OF CANDE CODE

CANDE code provides three solution levels: (1) Burns-Richard elasticity solution (level 1 solution), (2) finite element solution with the automated mesh generation discussed in section 4.1 (level 2 solution) and (3) finite element solution in which the user provides his own representative mesh (level 3 solution).



The elasticity solution given by Burns and Richard (1964) is an exact solution for the interaction of an elastic cylindrical shell embedded in an elastic medium which is loaded by a uniformly distributed surface pressure at an infinite distance. The solution provides conduit responses, including radial and tangential displacements of the conduit, circumferential thrusts, and bending moments in the conduit wall, along with the stresses and deformations throughout the elastic medium. The soil conduit interface behavior is represented by a choice of two boundary conditions: (1) bonded interface, where compatibility conditions of zero relative displacements between the soil and the conduit is enforced; and (2) full slippage interface, where the condition of zero shear stress at the interface is employed. The solution is recommended for use only for deeply buried conduits under conditions where both the soil and the conduit may be assumed to behave linear-elastically.

Comparison of the closed-form Burns-Richard elasticity solution and the CANDE code, with and without the automated mesh generation was carried out by performing analyses of a 10 ft diameter, relatively stiff conduit buried under soil heights of 35 ft, 47.5 ft, and 70 ft above the springline. At each soil height, five solutions were examined:

- (1) Solution 1: Burns-Richard elasticity solution with the bonded interface condition;
- (2) Solution 2: A finite element solution in which the mesh surface coincides with the soil surface;
- (3) Solution 3: A finite element solution with the height of mesh surface above the springline equal to 20 ft (two diameters). The remaining soil weight was applied to the mesh surface in the form of overburden pressure (cf. section 4.1);





(4) Solution 4: A finite element solution in which the height of mesh surface above the springline equals 10 ft (one diameter), using CANDE extended level 2 to avoid "flattening" of soil elements. The remaining soil weight was applied to the mesh surface as overburden pressure.

(5) Solution 5: The same as Solution 4, except the mesh was obtained by the automated mesh generation procedure.

As shown in Table 4.1, Solution 2 and Solution 3 are in good agreement. The largest differences in the conduit responses of the two solutions are within 10% at all three soil heights. The differences between Solution 1 and Solution 3 are slightly larger (the largest difference is 18% in the maximum moment). They are mainly due to differences in the boundary conditions; note that the percent difference decreases with increasing fill height. Solutions 4 and 5 give essentially the same results, while the differences between Solution 4 and Solution 2 are much larger than those between Solution 3 and Solution 2.

It is concluded that, if the stresses in the conduit wall are below yield:

- (1) The "basic" logic of the CANDE code is correct.
- (2) In cases where the soil height is greater than two diameters above the springline, the automated finite element mesh (e.g., Figure 4.1(b)) provides an excellent approximation to the solutions which contain the total soil height in the finite element discretization.
- (3) If the mesh is truncated at fill heights less than two diameters above the springline, appreciable errors are introduced. Accordingly, truncating the mesh height at two diameters above the springline was a very good choice.



Table 4.1 Conduit Responses using Burns-Richard and Finite Element Solutions

Soil: linear elastic  $E_s = 107.6 \text{ lb/in}^2$ ,  $\mu_s = 0.4$ ,  $\gamma = 120 \text{ pcf}$   
 Conduit: 10 ft diameter  $EI = 1.36 \times 10^8 \text{ lb-in}^2/\text{in}$

SOLUTION No. 1: Burns-Richard solution

2: Mesh Ht. = Fill Height

3: Mesh Ht. = 2D above the springline (automated mesh)

4: Mesh Ht. = 1D above the springline

5: Mesh Ht. = 1D above the springline (automated mesh)

| SOIL COVER<br>ABOVE THE<br>SPRINGLINE              | 35'   |       |       |       |       | 47.5' |       |       |       |       | 70'   |       |       |       |       |
|--|-------|-------|-------|-------|-------|-------|-------|-------|-------|-------|-------|-------|-------|-------|-------|
| SOLUTION<br>NO.                                    | 1     | 2     | 3     | 4     | 5     | 1     | 2     | 3     | 4     | 5     | 1     | 2     | 3     | 4     | 5     |
| $P_{\max}$<br>(kip/in)                             | 1.93  | 2.20  | 2.13  | 2.02  | 2.01  | 2.73  | 3.00  | 2.92  | 2.75  | 2.75  | 4.17  | 4.45  | 4.34  | 4.14  | 4.11  |
| $M_{\max}$<br>(in-kip/in)                          | 12.7  | 15.5  | 14.4  | 12.4  | 12.2  | 17.9  | 21.3  | 19.8  | 16.7  | 17.0  | 27.5  | 31.6  | 29.5  | 25.7  | 25.6  |
| $\Delta Y$<br>(%)                                  | 0.164 | 0.103 | 0.175 | 0.142 | 0.142 | 0.232 | 0.258 | 0.233 | 0.192 | 0.200 | 0.355 | 0.383 | 0.358 | 0.300 | 0.300 |
| $P_c/\gamma H$                                     | 1.20  | 1.34  | 1.29  | 1.12  | 1.12  | 1.28  | 1.32  | 1.28  | 1.09  | 1.12  | 1.28  | 1.30  | 1.26  | 1.11  | 1.11  |
| $\sigma_{\theta_{\max}}$<br>(kip/in <sup>2</sup> ) | 1.20  | 1.54  | 1.41  | 1.21  | 1.20  | 1.81  | 2.12  | 1.94  | 1.64  | 1.66  | 2.76  | 3.15  | 2.91  | 2.54  | 2.50  |

Note:  $P_{\max}$  = maximum thrust in the conduit wall;  $M_{\max}$  = maximum moment in the conduit wall;

$\Delta Y\%$  = percent vertical diameter shortening;  $P_c/\gamma H$  = ratio of crown pressure to free-field stress at the crown;  $\sigma_{\theta_{\max}}$  = maximum extreme fiber stress in the conduit wall.



- (4) For conduits with fill heights less than two diameters above the springline, use of the automated mesh results in large aspect ratios of soil elements (between 0.75 diameter above the springline and the fill surface). For the case illustrated in Table 4.1, in which the fill height was one diameter above the springline, the error proved to be negligible. The effects of smaller fill heights and of nonlinear soil response remain to be investigated.

#### 4.2.2 SEQUENTIAL CONSTRUCTION

Past experience as well as results of analytical studies (e.g., Goodman and Brown, 1963; Clough and Woodward, 1967; Duncan, 1979) indicated that sequential construction had significant effects on the performance of earth structures.

All four computer codes described in Chapter 3 incorporate the analytical procedure illustrated in section 2.4.1 for simulation of sequential construction of a soil-conduit system. In this section, the coding of the sequential construction technique in the computer codes will be compared through analyses of a 10 ft diameter, 8 in thick concrete pipe with 25 ft of soil cover above the springline. It is recognized that the effects of sequential construction are less pronounced for this relatively stiff pipe; nevertheless, it was decided to use this stiff pipe because difficulties with numerical instabilities were encountered when the FINLIN code was used for more flexible conduits.

The construction layer numbering adopted to simulate multi-layer construction process for FINLIN and CANDE codes are shown in Figure 4.2(a) and Figure 4.2(b), respectively. SSTIP code adopts the same layer



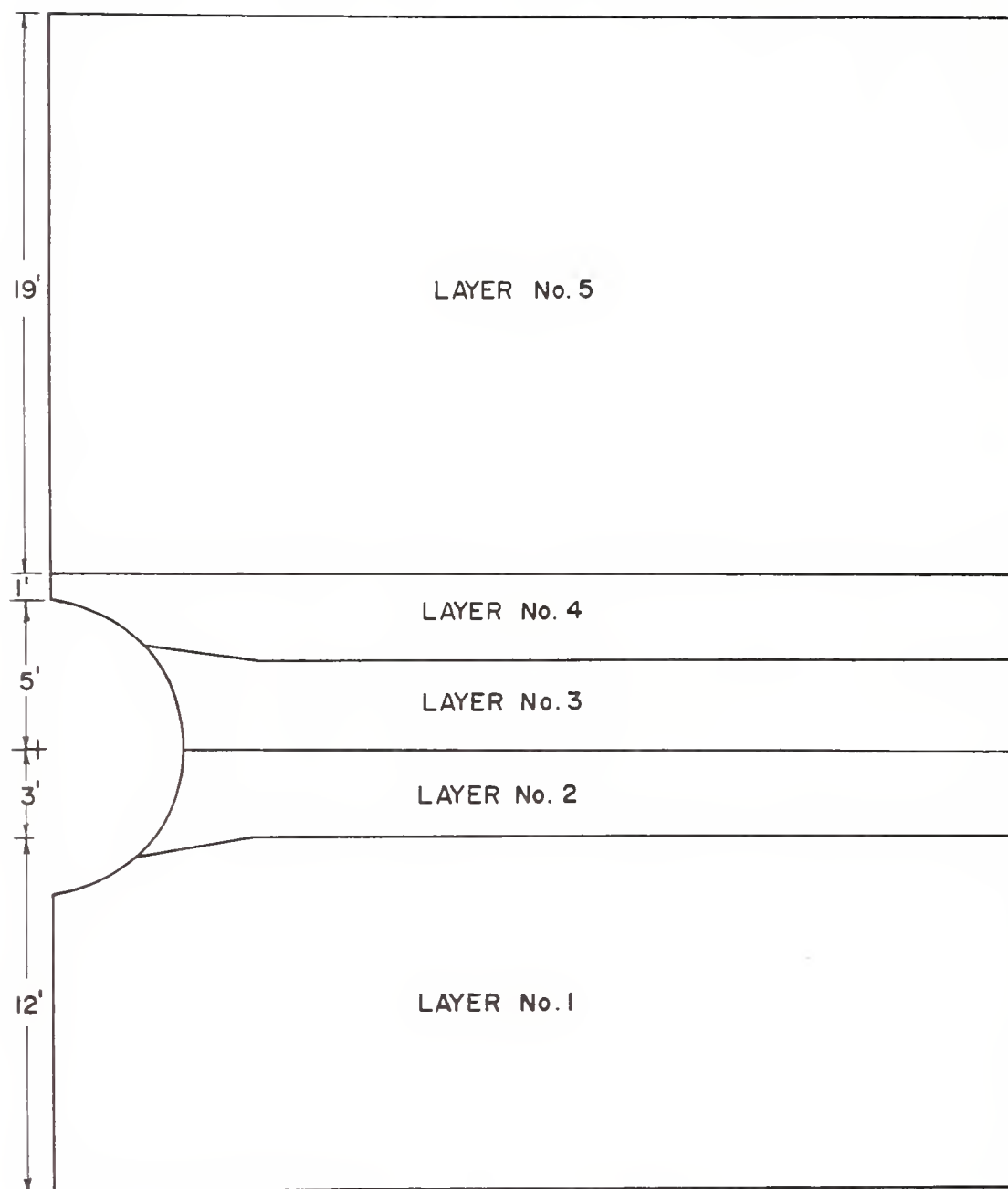


FIGURE 4.2(a) CONSTRUCTION LAYER NUMBERING  
ASSOCIATED WITH THE FINITE ELEMENT  
MESH SHOWN IN FIGURE 4.1(a)





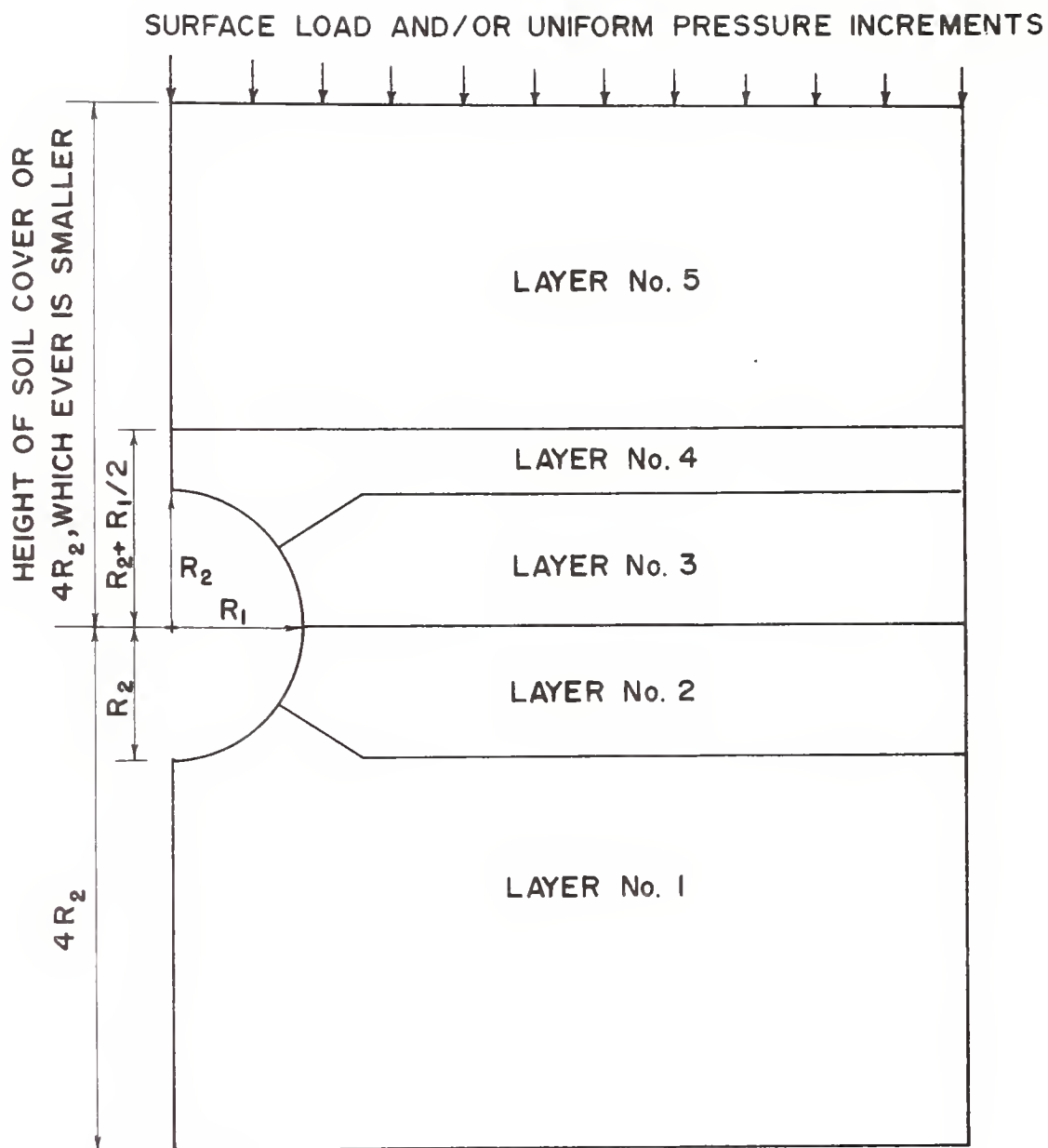


FIGURE 4.2(b) CONSTRUCTION LAYER NUMBERING  
ASSOCIATED WITH THE FINITE ELEMENT  
MESH SHOWN IN FIGURE 4.1(b)



numbering as that of CANDE code. It may be noted that when fill height is greater than the automated mesh height (two diameters above the springline, Figure 4.2(b)), a uniform pressure will be applied to the surface of the automated mesh in equal increments for construction layers that have passed the mesh surface. This procedure is employed throughout this study for analyses performed with CANDE code.

Two sets of linear elastic soil properties were employed: (1) Young's modulus = 2000 psi, Poisson's ratio = 0.3; and (2) Young's modulus = 10000 psi, Poisson's ratio = 0.3. The analyses were performed as single-layer construction and five-layers construction (Table 4.2). Results of single-layer analysis obtained from computer codes FINLIN, CANDE, and SSTIP are essentially the same, which indicates that the "basic" logic in all the three computer codes is correct. FINLIN code's results of the five-layers analysis are identical with those of the single-layer analysis, which reveals that FINLIN code does not accommodate the sequential construction procedure properly. This deficiency was found to be due to the fact that FINLIN code included the entire stiffness matrix (corresponding to a "completed" soil-conduit system) in the solution scheme throughout the analysis. Accordingly, stresses and displacements existed in the entire system including soil elements which had not yet been placed in the system. An attempt was made to correct this defect by setting all the terms in the stiffness matrix which correspond to the nodal points (of soil elements) not being included in the construction process equal to zero. However, the correction did not yield satisfactory results. This is believed to be due to numerical difficulties encountered during the solution procedure, which are in turn due to the nodal numbering associated with the mesh shown in Figure 4.1(a). In its present form, the use of FINLIN code to simulate



Table 4.2 Responses of a Concrete Pipe Analyzed as Single Layer and Five Layers Construction  
 Conduit = 10 ft diameter, 8 in thick concrete  
 Soil = 25 ft Soil Cover above the Springline,  $\gamma = 100$  pcf

|                           | Es = 2000 psi, $\mu_s = 0.3$ |       |       |          |       |       | Es = 10000 psi, $\mu_s = 0.3$ |       |       |          |       |       |
|---------------------------|------------------------------|-------|-------|----------|-------|-------|-------------------------------|-------|-------|----------|-------|-------|
|                           | Single Layer                 |       |       | 5 Layers |       |       | Single Layer                  |       |       | 5 Layers |       |       |
|                           | FINLIN                       | SSTIP | CANDE | FINLIN   | SSTIP | CANDE | FINLIN                        | SSTIP | CANDE | FINLIN   | SSTIP | CANDE |
| $P_{\max}$<br>(kip/ft)    | 17.1                         | 17.3  | 16.6  | 17.1     | 15.2  | 15.1  | 16.6                          | 16.7  | 16.0  | 16.6     | 15.0  | 14.6  |
| $M_{\max}$<br>(ft-kip/ft) | 11.8                         | 11.6  | 11.1  | 11.8     | 10.6  | 10.7  | 6.6                           | 6.8   | 6.5   | 6.6      | 6.9   | 6.3   |
| $\Delta Y\%$              | 0.14                         | 0.13  | 0.13  | 0.14     | 0.12  | 0.13  | 0.075                         | 0.079 | 0.076 | 0.075    | 0.081 | 0.076 |
| $p_c/\gamma H$            | 1.33                         | 1.40  | 1.34  | 1.33     | 1.12  | 1.23  | 1.10                          | 1.15  | 1.07  | 1.10     | 1.03  | 1.01  |

Note: The bottom boundary in CANDE and SSTIP codes is located at 1.5 diameter below the invert;  
 the bottom boundary in FINLIN code is located at 1 diameter below the invert.



sequential construction is not recommended. Whereas the results of the five-layer analyses by SSTIP and CANDE codes are fairly close, and based upon the additional fact that the procedure for simulation of sequential construction in SSTIP code (and NLSSIP code) had been verified through various geotechnical engineering problems (e.g., Ozawa and Duncan, 1976; Chirapuntu and Duncan, 1975; Quigley and Duncan, 1978), it was concluded that the sequential construction technique is working properly in computer codes CANDE, SSTIP, and NLSSIP.

#### 4.2.3 THE CONSTRAINT ELEMENT

The constraint element described in section 2.3.2 is incorporated in CANDE code for characterization of the relative movements of soil with respect to conduit at the soil-conduit interface or the relative movements between different soil zones at common interfaces.

For preliminary verification of the interface element, Burns and Richard's solution (1964) for full slippage condition was compared with finite element results using the constraint elements.

Table 4.3 lists the key responses of a 5 ft diameter, 18 gage, 2 2/3 x 1/2 in corrugated steel pipe with 30 ft soil cover above the springline, obtained from Burns-Richard full slip solution and finite element analysis with coefficient of friction at the soil-conduit interface equals to 0.0. Linear soil properties with Young's modulus = 1400 psi and Poisson's ratio = 0.32 were used. The results of the two solutions are in very good agreement. The minor differences between the results are mainly due to differences in the boundary conditions.

#### 4.3 EFFECT OF CONDUIT STIFFNESS

Buried conduits are historically classified as "rigid" (e.g., concrete) and "flexible" (e.g., corrugated metal) with separate design





Table 4.3 Conduit Responses of Burns-Richard and Finite Element Solutions at Full Slip Condition

Conduit = 5 ft diameter, 18 Gage 2 2/3" x 1/2" corrugated steel  
 Soil = 30 ft soil cover above the springline, single layer,  
 $E_s = 1400$  psi,  $\mu_s = 0.32$ ,  $\gamma = 120$  pcf

|                                | Burns & Richard's<br>Solution<br>(Full Slip) | Finite Element<br>Analysis<br>( $f = 0.0$ ) |
|--------------------------------|--|---|
| $P_{\max}$<br>(kip/in)         | 0.74   | 0.73  |
| $M_{\max}$<br>(in-kip/in)      | 0.083  | 0.079                                       |
| $\Delta Y\%$ **                | -1.71  | -1.55                                       |
| $p_c/\gamma H$                 | 1.19   | 1.19  |
| $\epsilon_{\max}/\epsilon_y$ * | 0.89   | 0.87  |

\*  $\epsilon_{\max}$  = max. strain in conduit wall

$\epsilon_y$  = yield strain of steel

\*\*  $\Delta Y\%$  = percent change in vertical diameter;  
 negative means shortening



procedures for each group. Rigid conduits are those for which the change in geometry prior to rupture is assumed to be too small to influence the resulting soil pressure distributions. Flexible conduits, on the other hand, are designed on the basis that sufficient deflection of the conduit will occur to mobilize additional lateral resistance from the surrounding soil mass.

Schematic diagrams of the deflections usually associated with rigid and flexible conduits are shown in Figure 4.3(a) and (b), respectively. The differences in deformation suggest that the stresses and strains in the soil mass will be different, hence the mechanism of interaction in the two soil-conduit systems will not be the same.

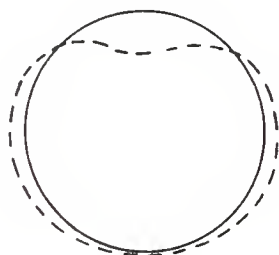
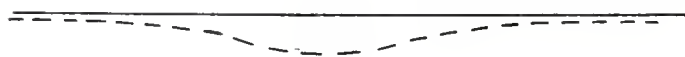
#### 4.3.1 SOIL ARCHING

Following Terzaghi (1943), the term "soil arching" has been used to describe the redistribution of normal and shear stresses within a soil mass as a result of different patterns of deformation at the soil-structure interface.

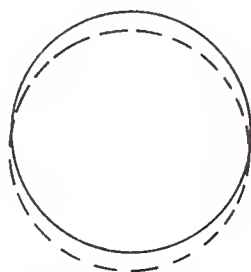
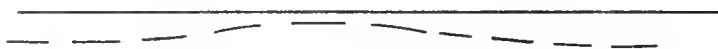
The extent of soil arching has been expressed as (1) the ratio of the normal soil pressure at the crown,  $p_c$ , to the free-field normal stress at the crown,  $\gamma H$ , in which  $\gamma$  is the unit weight of the soil and  $H$  is the soil height above the crown, or (2) the ratio of the maximum thrust in the conduit wall, which often occurs near the springline, to  $\bar{W} = \gamma HR$ , where  $R$  is the conduit radius (Figure 4.4).

In either measurement, if the ratio is less than one, positive arching is said to occur. The smaller the ratio the greater the positive arching. When positive arching occurs, the loads over the conduit are transferred to the soil around the two sides of the conduit. In the case of negative arching, the reverse is true; in other words, when negative





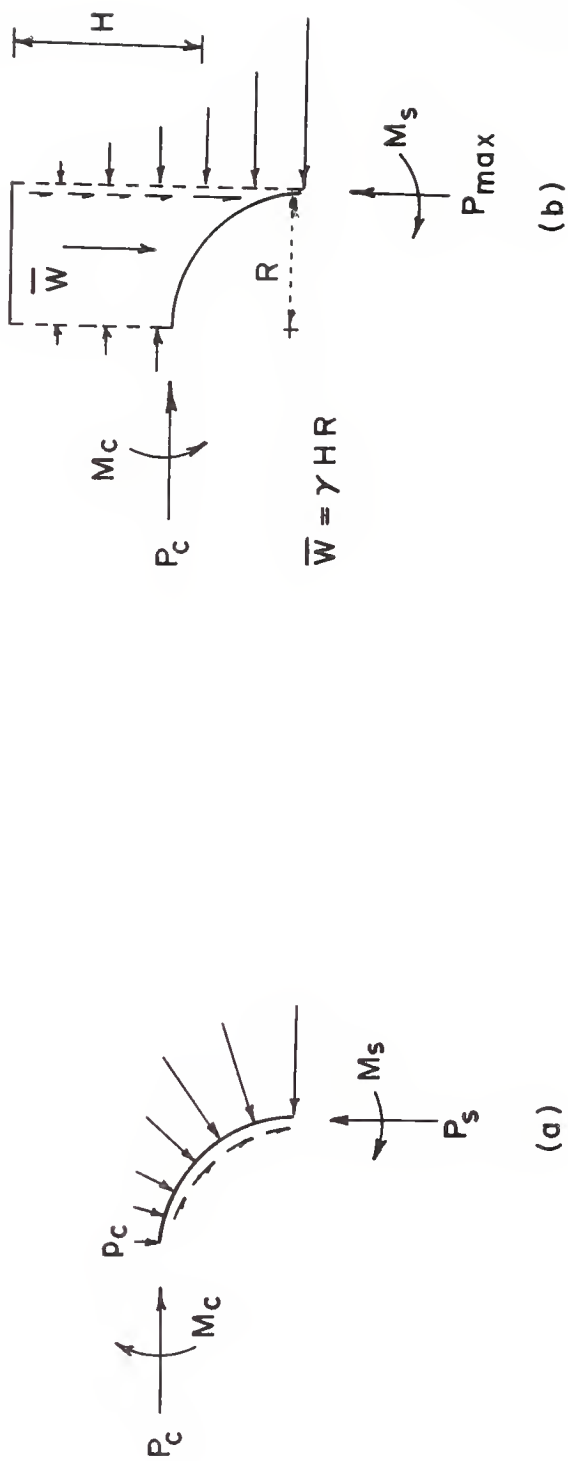
(a) FLEXIBLE PIPE



(b) RIGID PIPE

FIGURE 4.3 SCHEMATIC DIAGRAMS OF THE DEFORMATION OF (a) A FLEXIBLE PIPE AND (b) A RIGID PIPE





|                   |                      |    |                         |
|-------------------|----------------------|----|-------------------------|
| POSITIVE ARCHING: | $P_c / \gamma H < 1$ | OR | $P_{max} / \bar{W} < 1$ |
| NEGATIVE ARCHING: | $P_c / \gamma H > 1$ | OR | $P_{max} / \bar{W} > 1$ |

FIGURE 4.4 TWO MEASUREMENTS OF SOIL ARCHING





arching occurs, the stresses are concentrated on the conduit and correspondingly reduced in the surrounding soil. If, however, the ratios are equal to one, neutral arching is said to occur. Qualitatively, it is considered that positive arching is enhanced as the soil stiffness is increased relative to the conduit stiffness. The reverse is the case for negative arching.

#### 4.3.2 RIGID VS. FLEXIBLE CONDUIT

A 10 ft diameter, 8 in thick concrete pipe and a 10 ft diameter, 18 gage steel pipe with  $2 \frac{2}{3} \times \frac{1}{2}$  in corrugation were selected to represent "rigid" and "flexible" conduits, respectively, to investigate effects of conduit stiffness on soil-conduit interaction. CANDE code with nonlinear soil properties representing fairly compact granular soils and multi-layer construction procedure was employed.

The two pipes with 35 ft of soil cover above the springline and 8 construction layers were first investigated.

Figure 4.5 shows the normal stress and shear stress distributions at the soil-conduit interface of both pipes. Free-field states of stress at the soil-conduit interface are also shown in the figure. The shear stress distribution at the interface is shown on the left-hand side of the figure. It may be seen that the interface shear stresses of the two pipes are essentially the same, and the pattern is very similar to that of the free-field state. On the right hand side of Figure 4.5 is the normal stress distribution at the soil-conduit interface. For the steel pipe, the normal stress at the crown is smaller than the free-field stress. This can be explained by the fact that the vertical diameter is shortened under the soil weight over the crown. The reverse is true at the springline. Since the horizontal diameter elongates under the soil weight, the



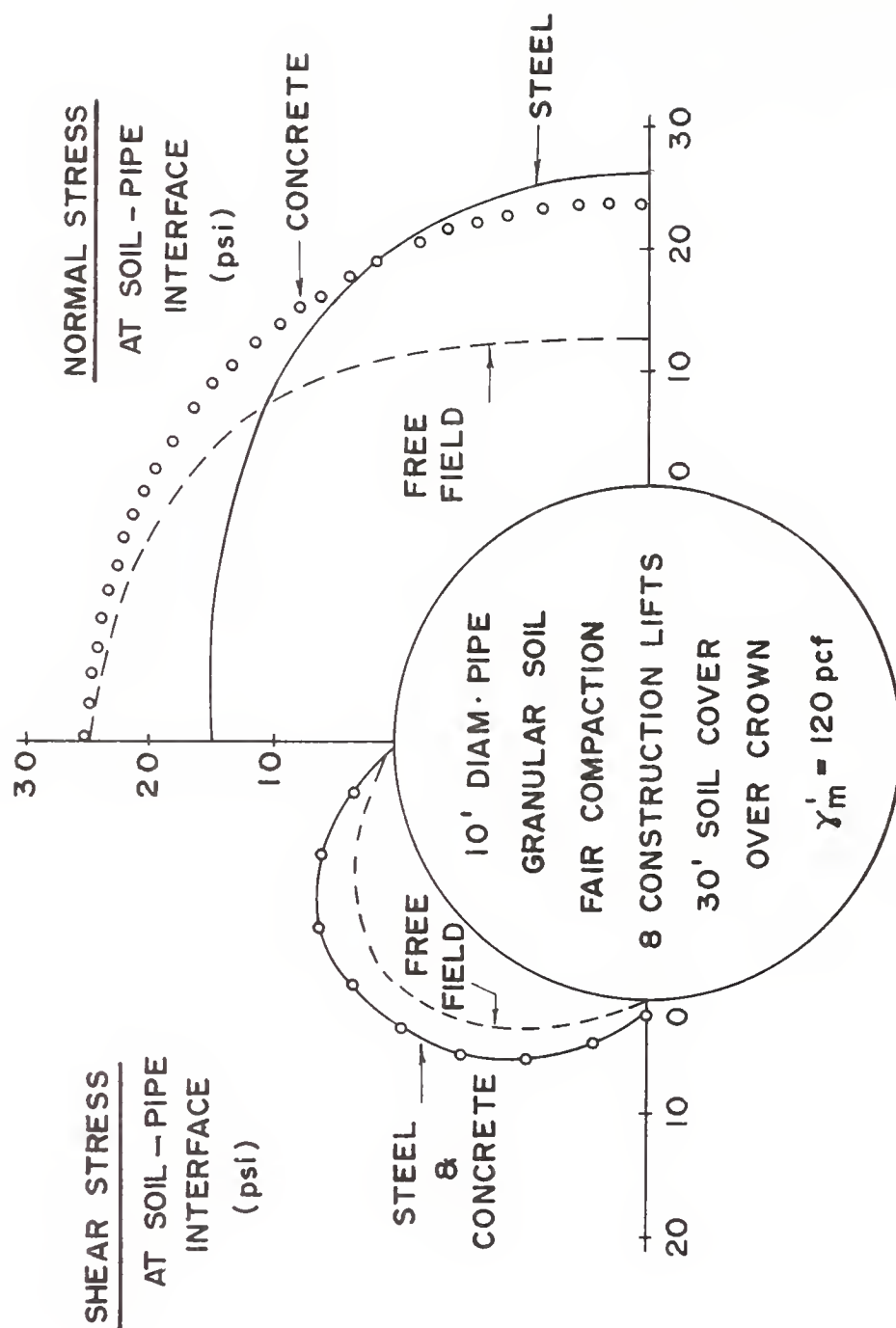


FIGURE 4.5 DISTRIBUTION OF NORMAL AND SHEAR STRESSES  
AT THE SOIL-CONDUIT INTERFACE, AT 30 ft OF SOIL COVER



normal pressure at the springline is greater than the free-field stress. For the concrete pipe, the interface normal stress distribution is nearly uniform, with the normal stress about equal to the free-field stress at the crown and greater than the free-field stress at the springline.

The distribution of the bending moment and thrust in the two conduit walls are shown in Figure 4.6. As may be expected, the rigid conduit induces greater thrusts and much greater bending moments than the flexible conduit. It should be noted that the bending moments in the steel pipe are not zero; however, when plotted on the same scale as those in the concrete pipe, the bending moments in the steel pipe become negligible.

The extent of soil arching for the two soil-conduit systems at 35 ft of soil cover are calculated as follows:

(a) concrete pipe:

$$P_{\max}/\gamma H R = 1.31 \text{ (large negative arching)}$$

$$p_c/\gamma H = 1.00 \text{ (neutral arching)}$$

(b) steel pipe:

$$P_{\max}/\gamma H R = 1.02 \text{ (essentially neutral arching)}$$

$$p_c/\gamma H = 0.62 \text{ (large positive arching)}$$

These values indicate that the two ratios used to quantify the extent of soil arching can be very different. Moreover, examining the interface soil pressure (Figure 4.5) and the thrust distributions (Figure 4.6) between the two pipes, it can be concluded that neither one of the two ratios is representative of soil-conduit interaction effects. In order to fully characterize the effects of soil-conduit interaction, the following are needed: (1) distribution of normal and shear stresses at the soil-conduit interface (to examine the soil model and the buckling criterion), (2) distribution of thrust in the conduit wall, and (3)



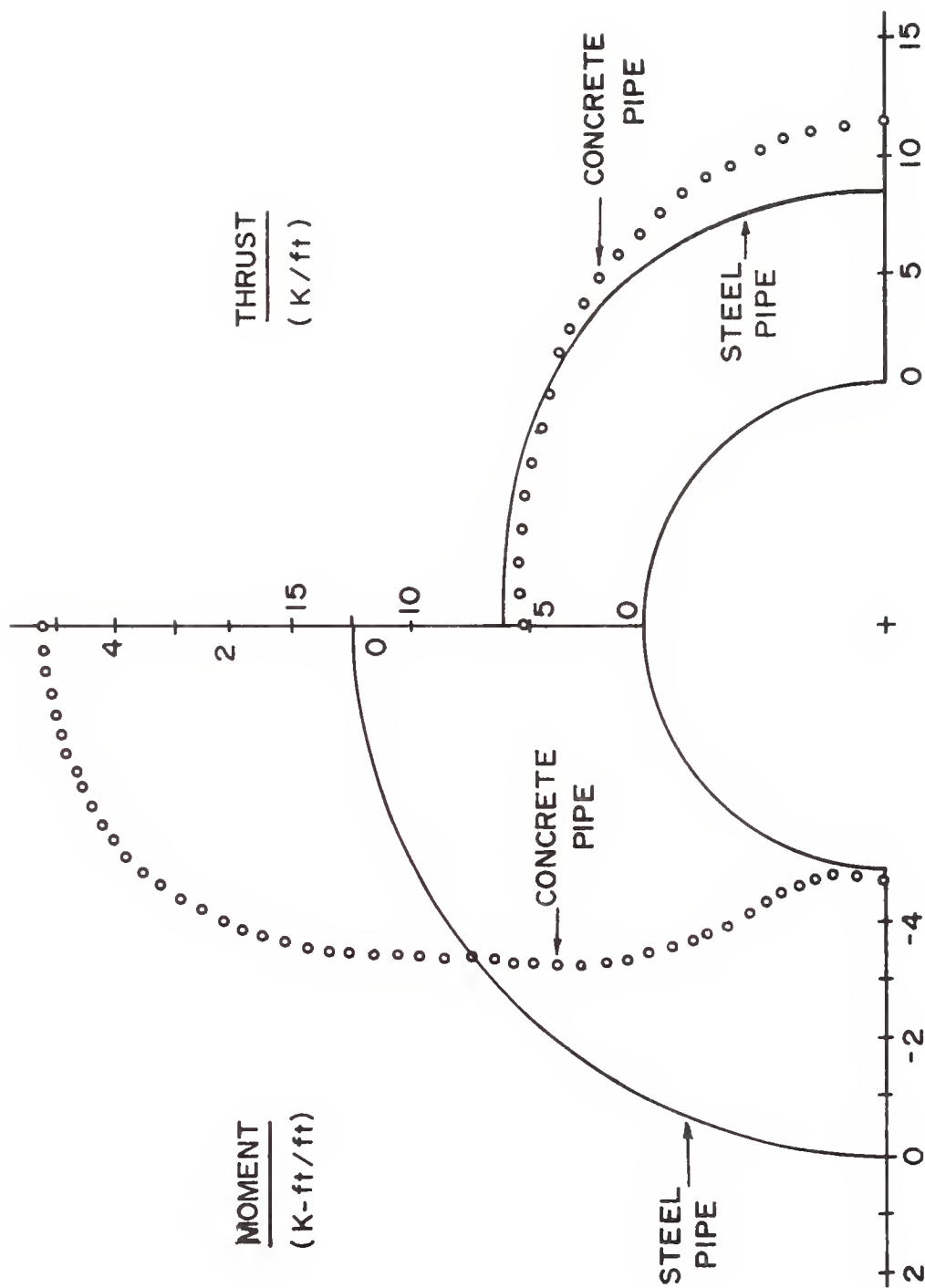


FIGURE 4.6 DISTRIBUTIONS OF MOMENT AND THRUST IN THE CONDUIT WALLS, AT 35 ft OF SOIL COVER ABOVE THE SPRINGLINE





distribution of moment in the conduit wall. Accordingly, the use of arching concepts is a tenuous basis for adjusting design procedures that are based on simplifying assumptions.

The two pipes with 20 ft of soil cover above the springline and five construction layers were next examined. Unlike those shown in Figure 4.5, the interface shear stress distributions of the two pipes are now different (Figure 4.7), the shear stresses on the concrete pipe being much greater, especially near the springline. The interface normal stress distributions of the two pipes, shown in the right-hand side of Figure 4.7, are striking: the steel pipe is now subjected to a much more uniform normal stress distribution than the concrete pipe. Except near the quarter point, the soil pressures around the concrete pipe are greater than those around the steel pipe.

Figure 4.8 shows the bending moment and thrust distributions in the two pipes. The bending moments in the concrete pipe wall are, again, found to be much greater than those in the steel pipe. However, in the vicinity of the crown, the thrusts in the steel pipe are now somewhat smaller than in the concrete.

The extent of soil arching for the two soil-conduit systems at 20 ft of soil cover are as follows:

(a) concrete pipe:

$$P_{\max}/\gamma H R = 1.32 \text{ (negative arching)}$$

$$p_c/\gamma H = 1.08 \text{ (negative arching)}$$

(b) steel pipe:

$$P_{\max}/\gamma H R = 0.96 \text{ (positive arching)}$$

$$p_c/\gamma H = 0.69 \text{ (positive arching)}$$

In this case, both ratios indicate negative arching for the concrete pipe



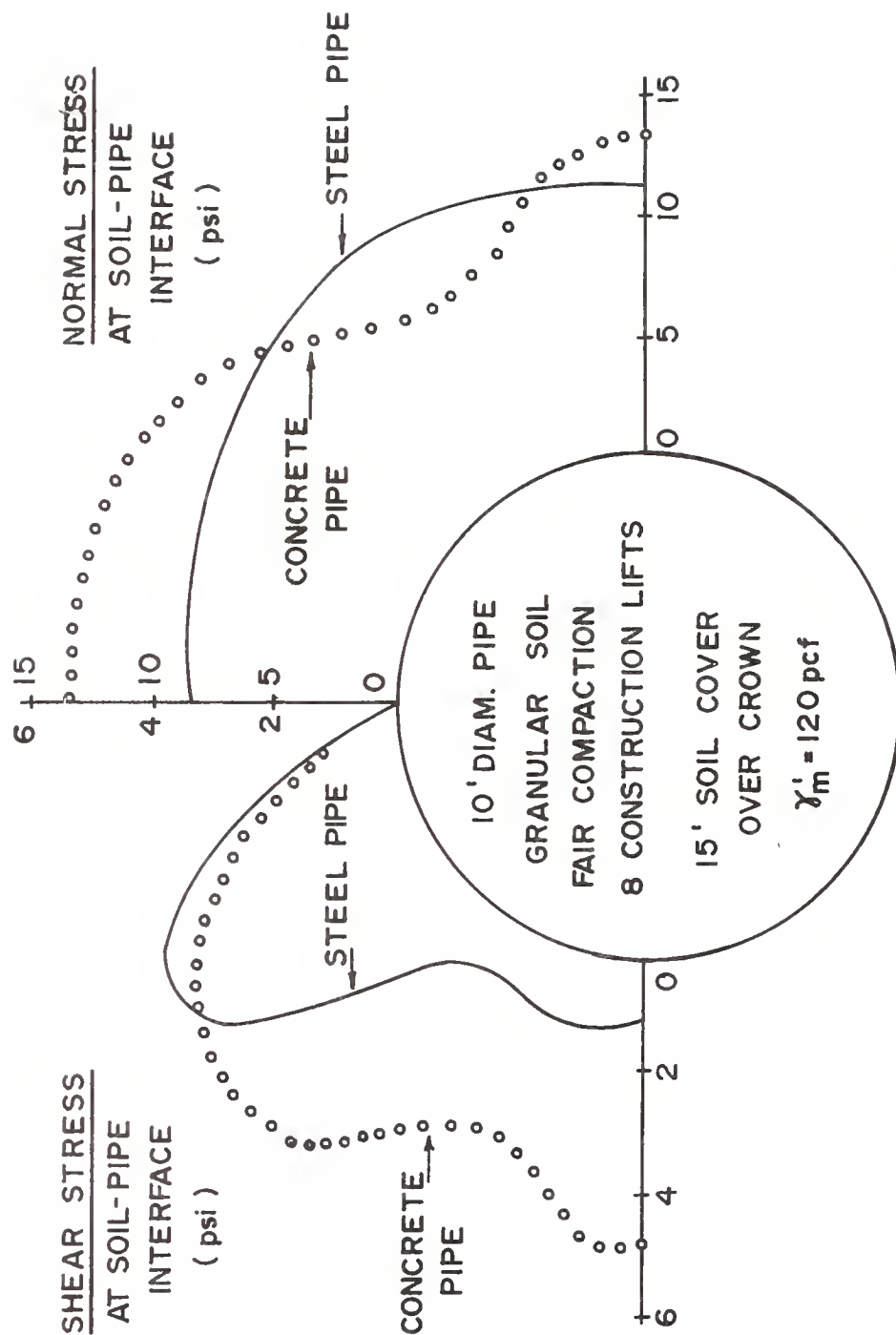


FIGURE 4.7 DISTRIBUTIONS OF NORMAL AND SHEAR STRESSES AT THE SOIL-CONDUIT INTERFACE, AT 20 ft OF SOIL COVER ABOVE THE SPRINGLINE



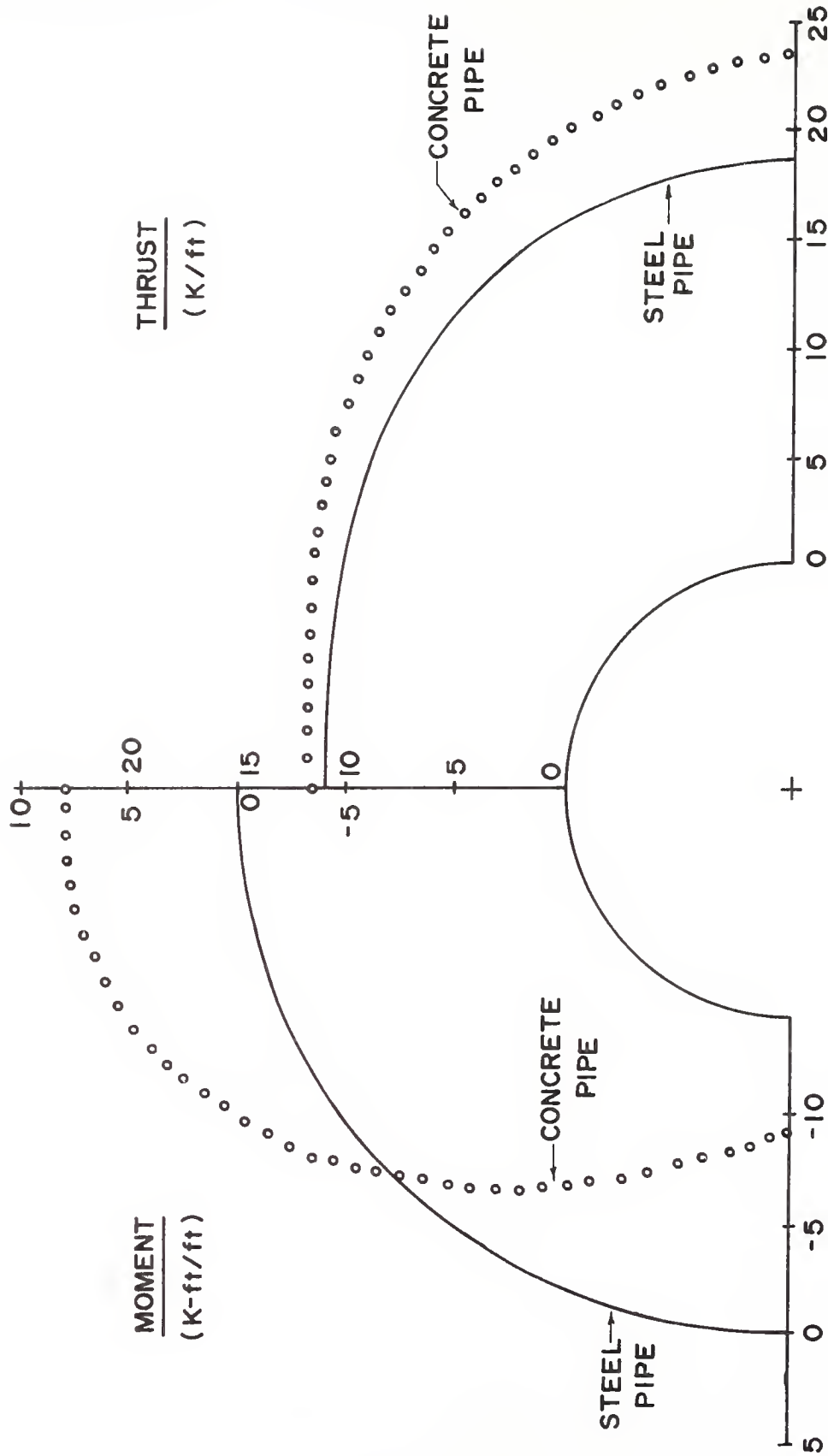


FIGURE 4.8 DISTRIBUTIONS OF MOMENT AND THRUST IN THE CONDUIT WALLS, AT 20 ft OF SOIL COVER ABOVE THE SPRINGLINE



and positive arching for the steel pipe. However, the extent of soil arching implied by the two ratios are very different. In addition, the differences in the distributions of the interface soil pressures and the thrust between the two pipes (Figures 4.7 and 4.8) confirm the fact that neither the relative crown pressure nor the maximum thrust can adequately characterize the effects of soil-conduit interaction.

Comparing the results of the conduits under the two depths of burial, it can be concluded that (1) the soil arching behavior at the two heights of cover is very different, and (2) characterizing soil-conduit interaction only in terms of the crown pressure or of the maximum thrust can be very misleading.

The horizontal pressures on vertical planes over the crown and the springline for the two pipes are shown in Figure 4.9. The free-field lateral stresses along the two planes, with coefficient of earth pressure at rest equals to 0.5, are also shown in the figure for reference. The differences in the horizontal pressures between the two pipes are found to be small. Along the plane over the crown, the horizontal pressures induced by the steel pipe are greater than those induced by the concrete pipe. However, along the plane above the springline, the reverse is true.

The shear stress along a vertical plane over the crown is zero since it is a plane of symmetry. The shear stresses along the plane over the springline of the two pipes are very different, as illustrated in Figure 4.10. For the steel pipe, the shear stresses act downwards between the springline and the crown, but reverse direction above the crown; for the concrete pipe, the shear stresses act in a downward direction all along the plane with a sharp change of slope in the stress distribution near the crown. This difference, again, confirms that the maximum thrust in





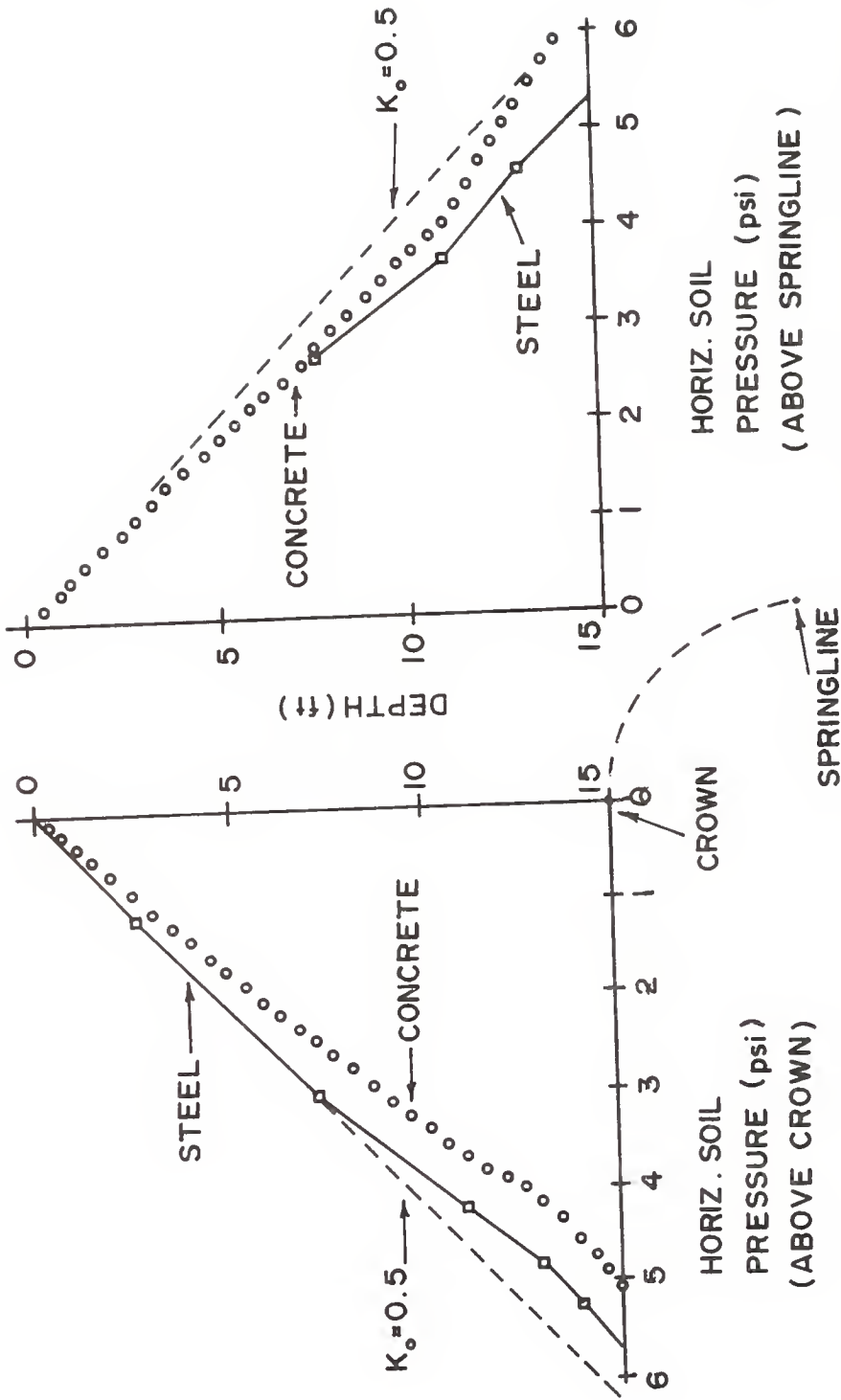


FIGURE 4.9 DISTRIBUTION OF HORIZONTAL SOIL PRESSURE ON VERTICAL PLANES ABOVE THE CROWN AND THE SPRINGLINE (SOIL COVER = 20 ft ABOVE THE SPRINGLINE)



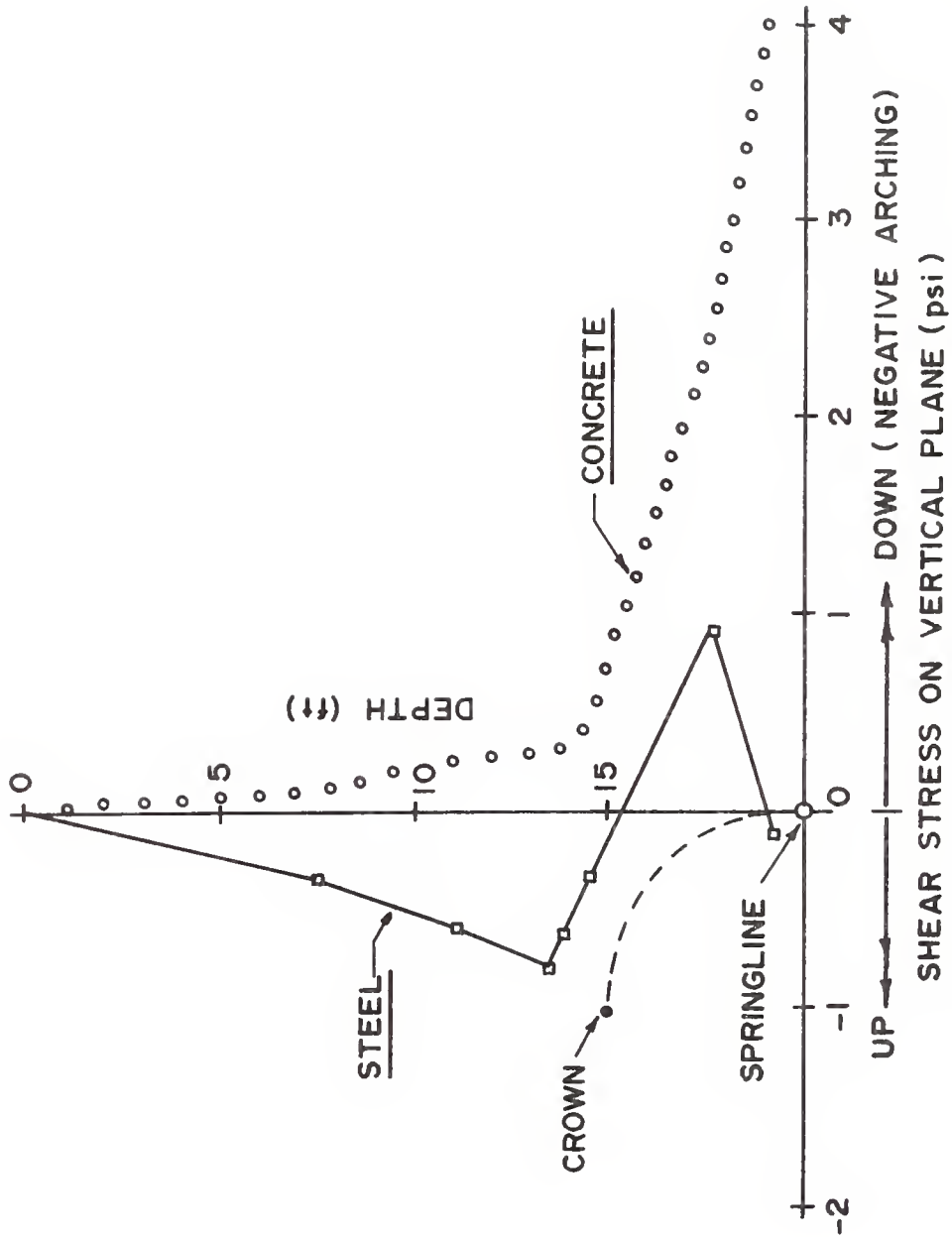


FIGURE 4.10 SHEAR STRESS DISTRIBUTION ON A VERTICAL PLANE ABOVE THE SPRINGLINE (SOIL COVER = 20 ft ABOVE THE SPRINGLINE)



the pipe wall, relative to the weight of overlying soil, cannot be used to characterize the soil arching behavior, since the magnitude of this ratio is the resultant of the shear forces along the vertical plane and cannot describe the nature of their distribution.

The displacement fields of the concrete pipe and the steel pipe at a soil height of 20 ft above the springline, illustrated by displacement vectors, are shown in Figures 4.11 and 4.12, respectively. For the steel pipe, the displacement vectors direct toward the pipe near the quarter point and away from the pipe near the springline. For the concrete pipe, most of the displacement vectors are directed downward nearly vertically. In addition, the change in shape of the steel pipe is much more significant than the concrete pipe, although the crown displacement is larger in the concrete pipe.

Figure 4.13 shows the displacements at the ground surface for the concrete pipe and the steel pipe. The ground displacements plotted in the figure are obtained by subtracting a constant value of 0.6 inch from the actual displacements for clear visualization of displacement patterns. Deformed shapes of the two conduits, which are drawn to scale (i.e., absolute rather than relative displacements are plotted) are also shown in Figure 4.13 for reference. It is seen that the ground displacement pattern of the steel pipe conforms well with the conventional concept of flexible pipe (Figure 4.3a). However, this is not true for the concrete pipe (cf., Figure 4.3b). Moreover, as mentioned previously, the crown displacement of the concrete pipe is actually greater than that of the steel pipe.

#### 4.3.3 PLASTIC HINGING OF CONDUIT WALL

To accommodate yielding and plastic hinging of a conduit wall, a nonlinear



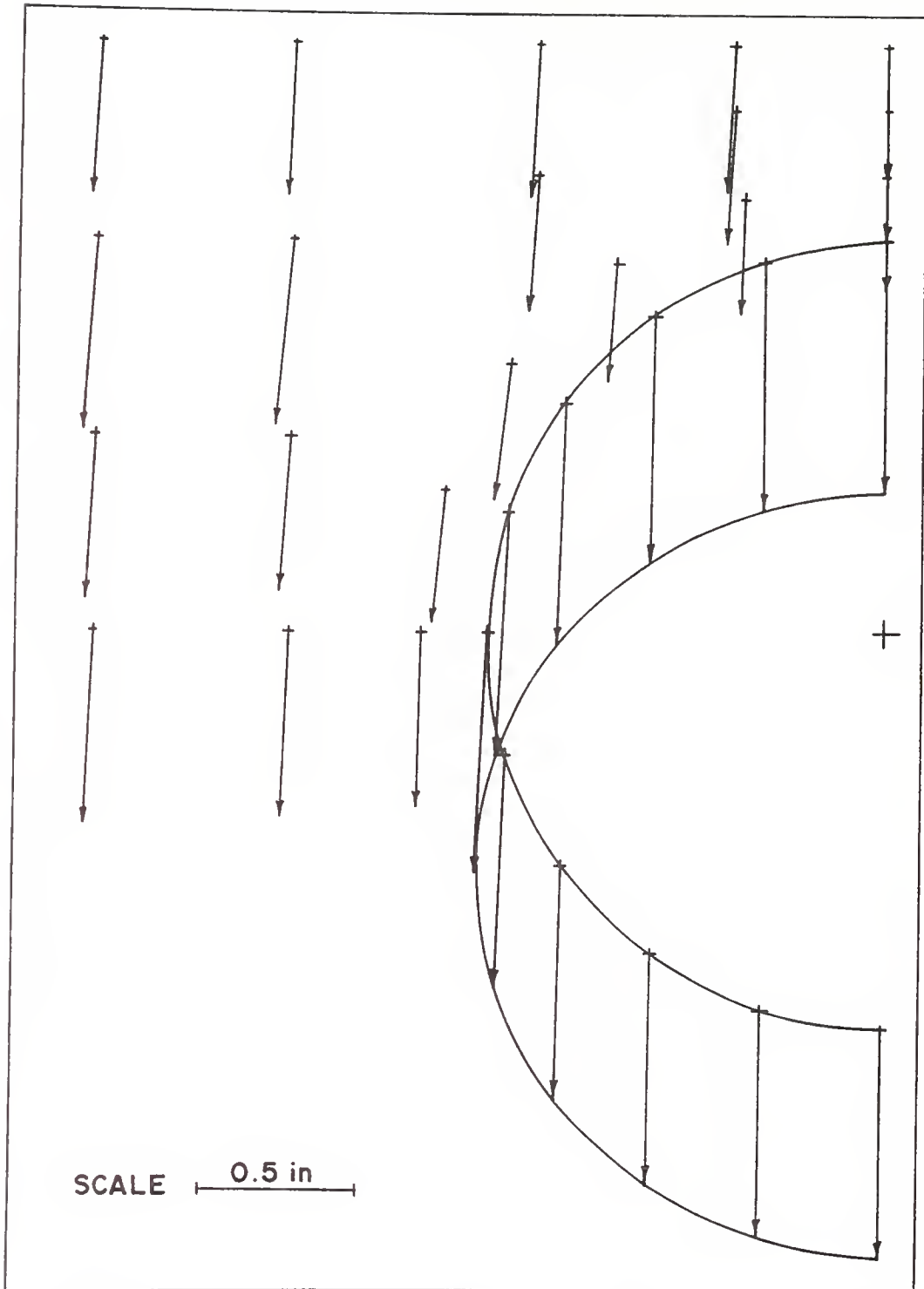


FIGURE 4.11 DISPLACEMENT FIELD OF THE CONCRETE PIPE WITH 20ft OF SOIL COVER ABOVE THE SPRINGLINE





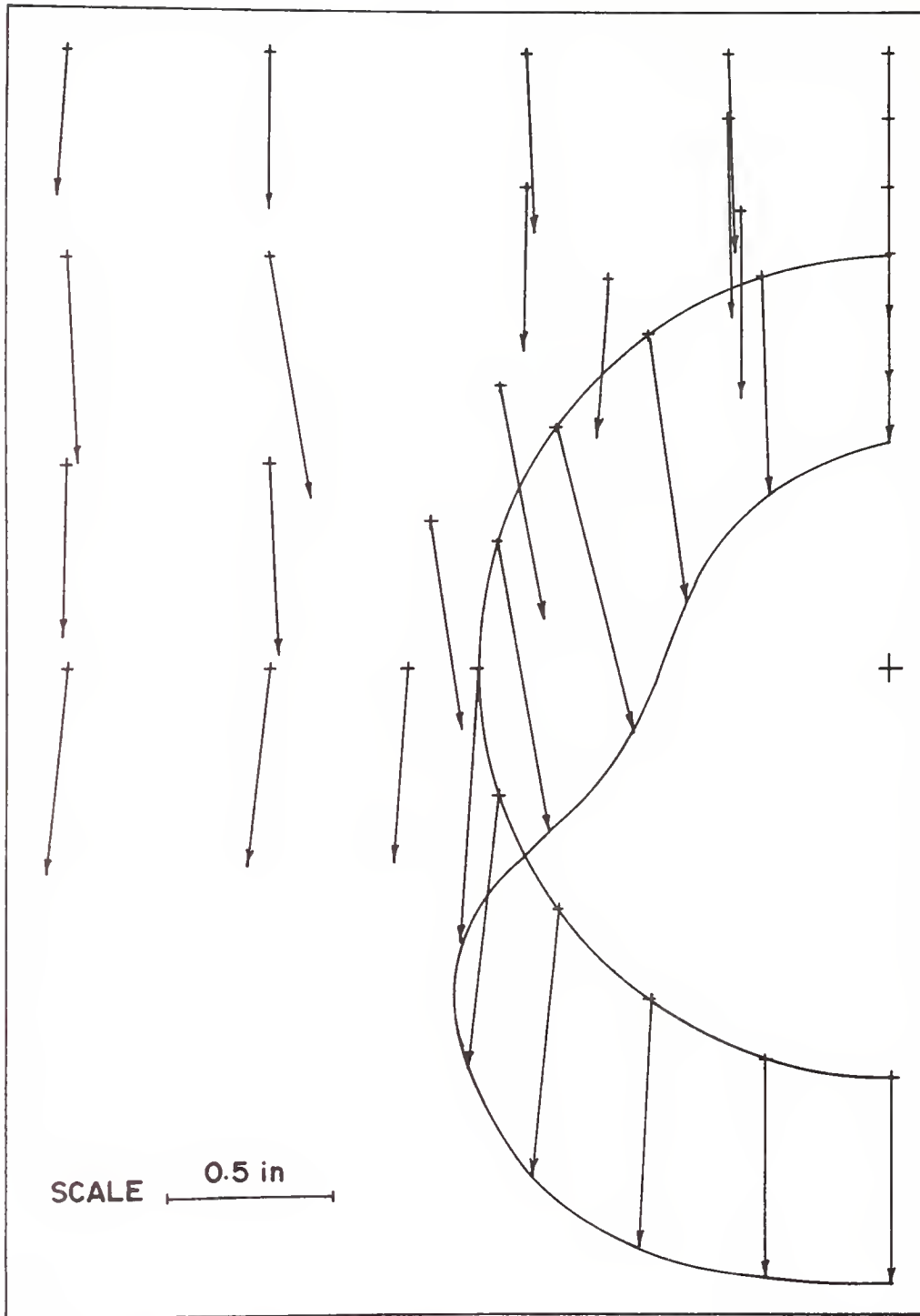


FIGURE 4.12 DISPLACEMENT FIELD OF THE CORRUGATED STEEL PIPE WITH 20ft OF SOIL COVER ABOVE THE SPRINGLINE



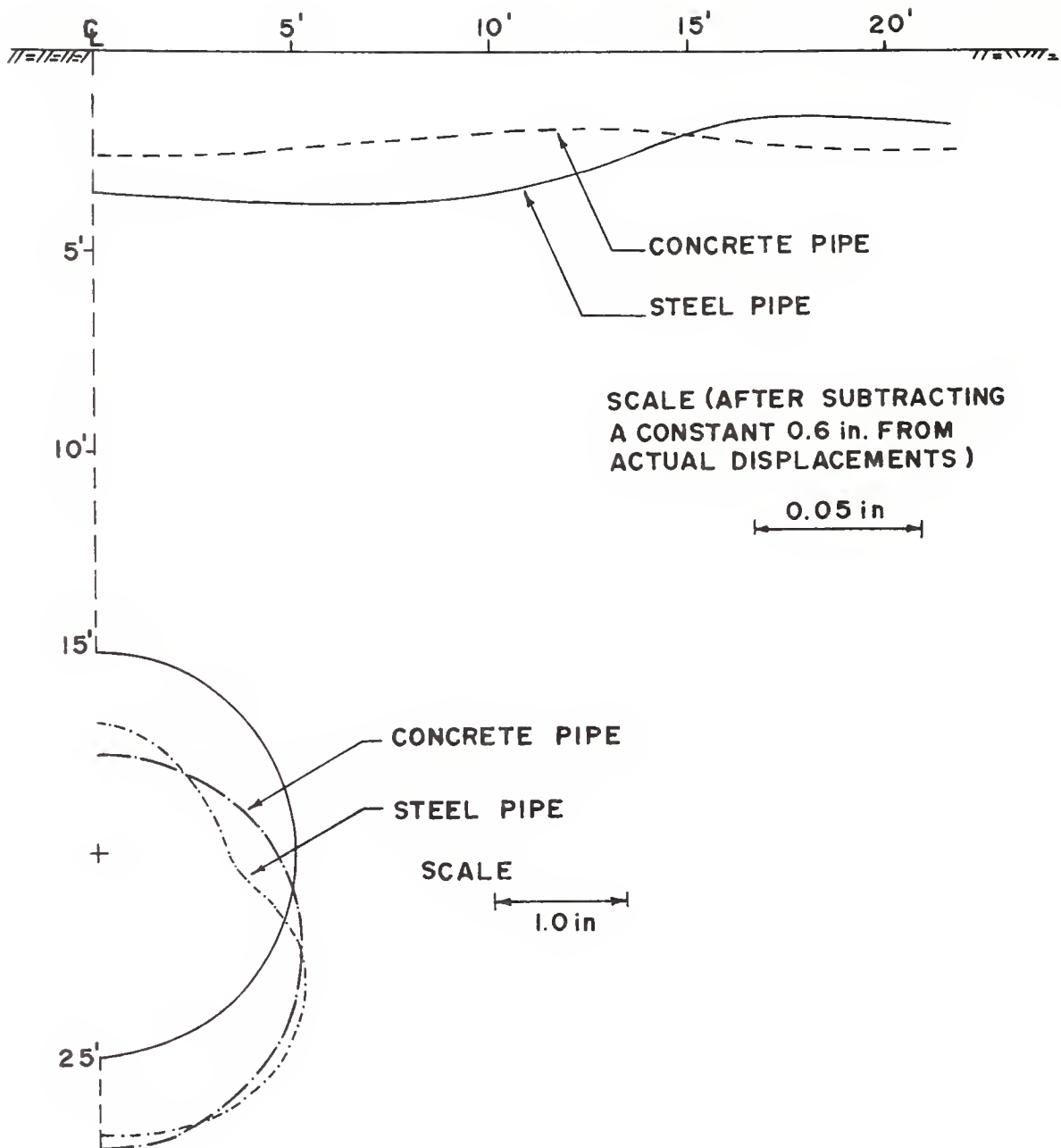


FIGURE 4.13 GROUND SURFACE DISPLACEMENTS AND DEFLECTIONS OF THE CONCRETE PIPE AND THE STEEL PIPE



constitutive relationship for the conduit material has to be employed. In this study, the behavior of plastic hinging of conduit walls was investigated by using NLSSIP and CANDE codes. This is because these are the only codes that address the problem of yielding in the conduit wall.

As described in Chapter 3, it can be misleading to calculate the bending moment at a wall section by summing increments of bending moments about different axes; for example, after yielding is initiated, CANDE prints out bending stresses calculated from the summed moments divided by the section modulus. Clearly, these calculated stresses are meaningless. Accordingly, CANDE code was modified to calculate the bending moment about the centroid of a wall section in accordance with the strain distribution and the stress-strain relation at the section. This modification, as well as a number of other changes in the CANDE code, is discussed more fully in Chapter 5.

In order to calculate bending moments from strain distributions, "equivalent" rectangular sections that provide approximate sectional properties of the full range of standard corrugated metal sections was investigated. Rectangular sections with cross-sectional areas and moment of inertias the same as corresponding corrugated sections were found to be the best choice. With this approximation, the maximum error in the section modulus is less than 7%.

Hand-calculations were carried out on an 18 gage steel plate section with  $2 \frac{2}{3} \times \frac{1}{2}$  in. corrugation to examine the error in bending moments that resulted from the rectangular approximation. With yield stress = 40 ksi, the initial yield bending moment,  $M_y$ , and the fully plastic bending moment,  $M_p$ , of the corrugated section were found to be 214.0 in-lb/in and 310.6 in-lb/in, respectively, while the corresponding



bending moments of the equivalent rectangular sections were  $M_y = 203.2$  in-lb/in and  $M_p = 304.9$  in-lb/in. The rectangular approximation is considered satisfactory.

A 5 ft diameter, 18 gage  $2 \frac{2}{3} \times \frac{1}{2}$  in. corrugated steel pipe with up to 70.0 ft of soil cover above the springline was selected to investigate plastic yielding of the conduit wall. Linear elastic soil properties with Young's modulus = 2500 psi and Poisson's ratio = 0.35, with a fully bonded interface, were employed.

The thrusts and bending moments at the springline versus fill height above the springline are shown in Figure 4.14a. The bending moments summed about successive incremental axes of bending (CANDE code's output before modification) are also shown in the figure. The thrust at the springline increases proportionally with fill height until it reaches the squash load of the section,  $P_p$ , whereas the bending moment at the springline increases at a constant rate with increasing fill height to a point at which wall yielding is initiated and then drops off rapidly as the fill height increases further. At a fill height of 65.5 ft above the springline, the wall section is fully yielded with thrust  $P_p = 2064$  lb/in and bending moment = 0; a plastic hinge is said to form at the section. If the fill height were increased further, additional plastic hinges would subsequently develop at other sections of the conduit.

The same problem was also analyzed by using NLSSIP code, and the thrusts and bending moments at the springline are depicted in Figure 4.14a. The thrusts calculated by NLSSIP code are close to those of CANDE code throughout the analysis. Before formation of the plastic hinge, the bending moments obtained from NLSSIP code do not differ appreciably from the bending moments of CANDE code which are obtained by summing increments





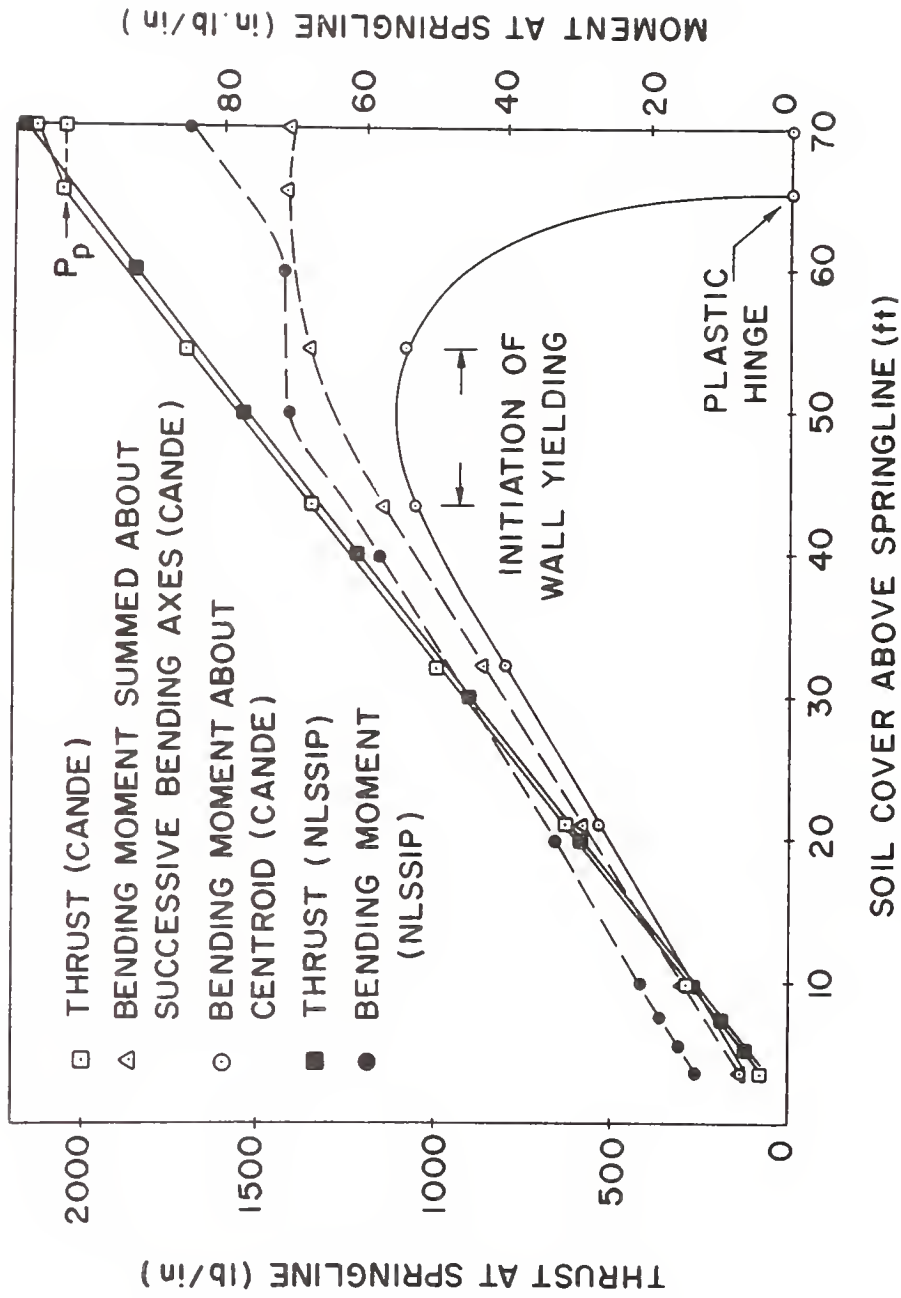


FIGURE 4-14a THRUST AND MOMENT AT THE SPRINGLINE VERSUS FILL HEIGHT



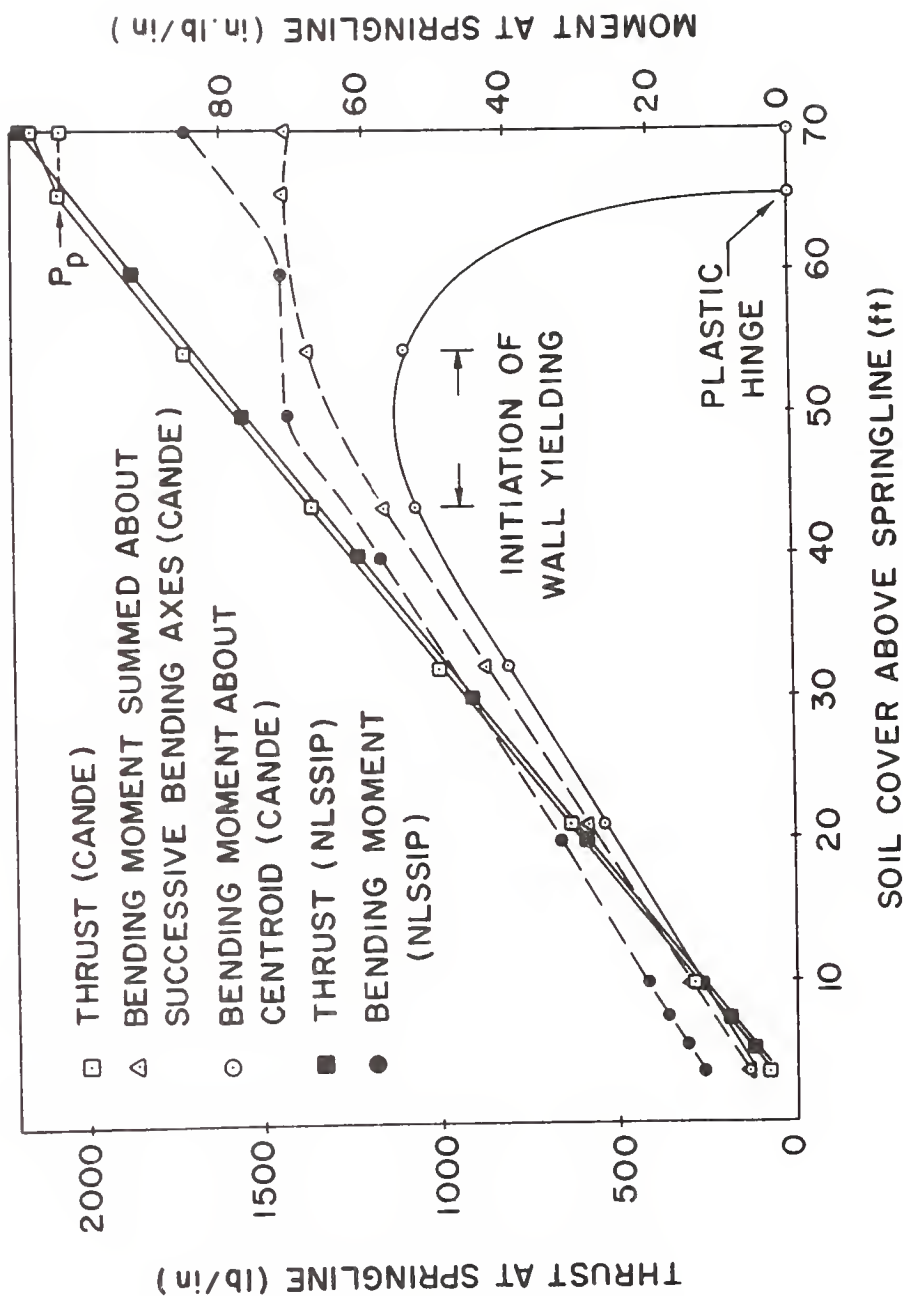


FIGURE 4.14a THRUST AND MOMENT AT THE SPRINGLINE VERSUS FILL HEIGHT



of moments about successive bending axes. The difference between the two is mainly due to the fact that the results of NLSSIP code are obtained by beginning the analysis at the springline. It may be noted that, as NLSSIP code employed a "one iteration" nonlinear solution procedure, after a large portion of the wall section is yielded, the results are less reliable than those of CANDE code which carried out iterations until convergence was secured (in cases where convergence was not obtained, a warning message would be given in the output). The fact that the combination of thrust and bending moment in the wall section do not satisfy the criterion for plastic hinge formation (Equation 2.20) indicates that the bending moments calculated by NLSSIP code are not taken about the centroidal axis of the wall section. Moreover, at a fill height of 70 ft above the springline, both the formulation in CANDE (before the modification) and NLSSIP codes give thrusts larger than  $P_p$ , the load at which wall crushing occurs in the absence of bending moments; this indicates that neither code gave correct values of strain distribution in the wall section once a fully plastic hinge was formed. The effect of soil stiffness on the fill height at which a fully plastic hinge is formed is illustrated in Figure 4.14b.

In the absence of stability problems due to buckling, plastic hinges can form long before the load capacity of a soil-conduit system has been reached. Therefore, it is mandatory to account for plastic hinging of the conduit wall in analyzing soil-conduit interaction problems. It is equally necessary to be able to deal with buckling problems if a full understanding of soil-conduit interaction is to be reached. CANDE appears to account for yielding in the conduit wall correctly, although convergence problems were encountered once a fully plastic hinge was formed. No code



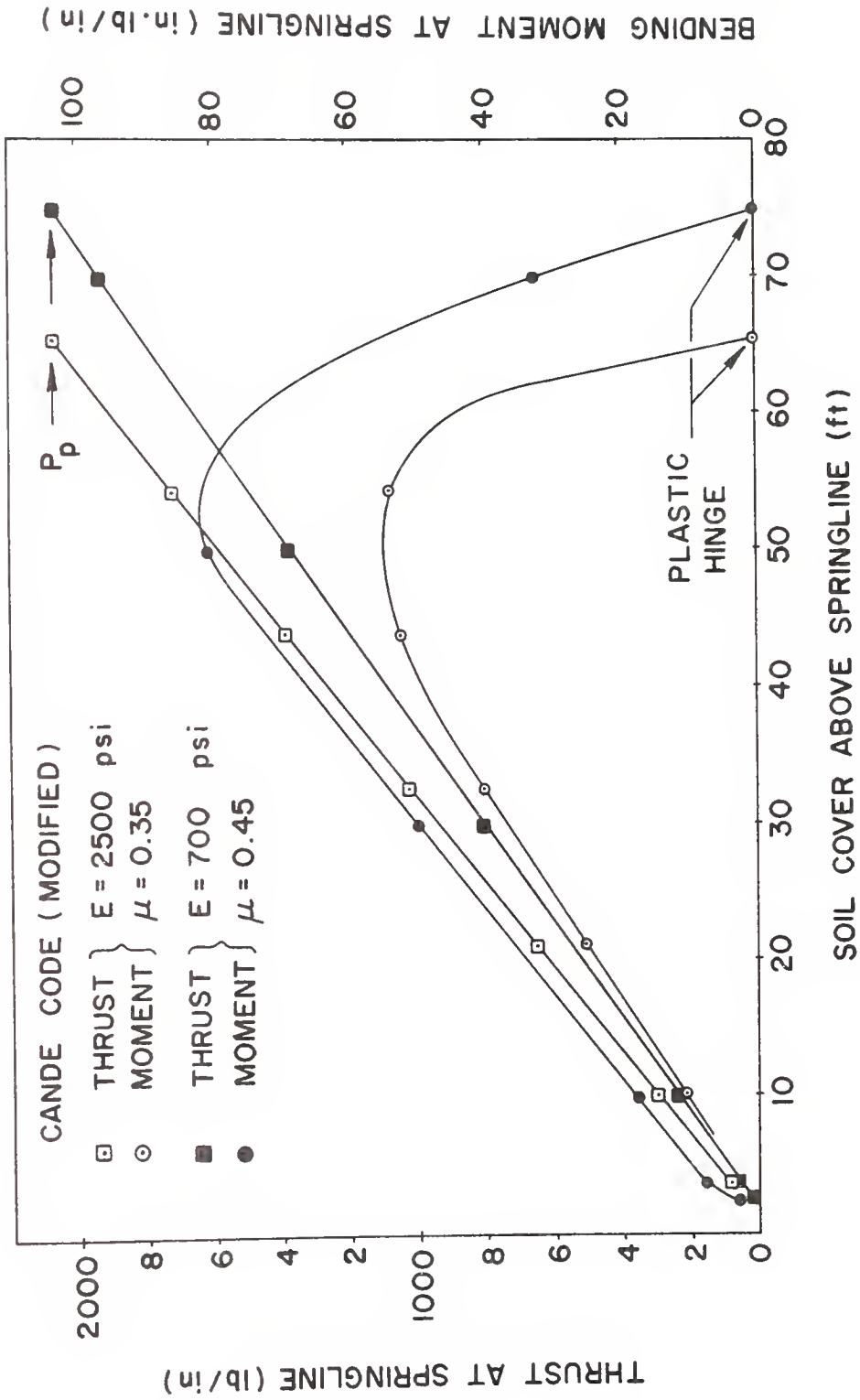


FIGURE 4.14 b EFFECT OF SOIL STIFFNESS ON FILL HEIGHT AT WHICH A PLASTIC HINGE IS FORMED





is currently available that can deal with buckling in a rational manner.

#### 4.4 EFFECT OF INTERFACE BEHAVIOR

Leonards and Roy (1976) and Duncan (1979) adopted Goodman-Taylor-Brekke type of bar elements for simulation of soil-conduit interface behavior. Both studies indicated that the effects of slip between the soil and the conduit on the responses of the conduit were small. Due to the deficiencies of Goodman-Taylor-Brekke type interface elements described in section 2.3.1, the present study employed the constraint interface element incorporated in CANDE code to investigate the effects of slip at the soil-conduit interface.

Two groups of problems were analyzed to study the effect of interface behavior on the performance of soil-conduit systems. Both groups utilized an 18-gage structural steel conduit with  $2 \frac{2}{3} \times \frac{1}{2}$  in. corrugation; in the first group the pipe was circular while in the second it was elliptical. The overburden-dependent soil model (section 2.1.2.1)\* with Young's moduli representing granular soils with fair compaction and a constant Poisson's ratio of 0.32 was employed.

##### 4.4.1 GROUP 1 PROBLEMS - INTERFACE SLIP - CIRCULAR CONDUIT

In this group of problems, a 10 ft diameter circular conduit with 25 ft of soil cover above the springline was employed. Multi-layer analyses were performed. Three interface conditions were investigated: (1) fully bonded through all construction layers, (2) full slip through all construction layers, and (3) full slip when backfilling to the springline and fully bonded thereafter. By enforcing full slip conditions until the soil reaches the springline (slip to springline condition),

---

\*It is recognized that this is not a good soil model (Section 4.5); however, at this stage of the investigation, it was the only non-linear soil model for which slip could be investigated without inducing convergence problems.



the unrealistic effect of soil "hanging" from the conduit, when soil is placed between the invert and the springline, can be mitigated.

The results of the analyses are summarized in Table 4.4. The percent change in vertical diameter of the conduit plotted as a function of fill height for the three interface conditions are shown in Figure 4.15. The effect of interface slip on the deflection of the conduit is found to be significant. The fully bonded condition induces greater shortening in the vertical diameter than the other two conditions. For the full slip condition, the vertical diameter initially elongates; as the backfill reaches the crown there is a change from elongation to shortening, whereas both the fully bonded and the slip-to-springline conditions result in a continuous shortening of the vertical diameter at an increasing rate. It should be mentioned that at 5 ft of soil cover above the springline, the surface of the backfill does not coincide exactly with the crown level (cf. levels of construction layers shown in Figure 4.2(b)). At fill heights between 0.5 and 2.5 diameters above the springline, the deflection rate is more or less independent of the interface conditions.

For slip conditions, as the backfill comes from the invert to the springline, the computer code fails to simulate "peaking" of the conduit (elongation in the vertical diameter), a phenomenon generally observed in the field. This is a result of the inadequacy of the soil model and also because the effects of compaction are not being simulated.

Figure 4.16 illustrates the history of maximum extreme fiber stress in the conduit wall as a function of fill height above the springline for the three interface conditions. Before the fill reaches about 1.25 diameters above the springline, the full slip condition induces larger maximum extreme fiber stress than the fully bonded condition; however, at fill



Table 4.4 Responses of a Circular Conduit for Three Interface Conditions

Conduit = 10' diameter 18 gage 2 2/3" x 1/2" corrugated steel; yield stress,  $\sigma_y = 33$  ksi

Soil = Overburden-Dependent Soil Model (Fair Compaction).  $\mu_{\text{soil}} = 0.32$ ,  $\gamma_{\text{soil}} = 120$  pcf

A = FULLY BONDED

B = SLIP-TO-SPRINGLINE

C = FULL SLIP

| FILL<br>HEIGHT<br>ABOVE<br>THE<br>SPRINGLINE<br>(ft) | PERCENT CHANGE IN<br>VERTICAL DIAMETER* |      |       | MAXIMUM EXTREME<br>FIBER STRESS (kip/in <sup>2</sup> ) |      |      | MAXIMUM THRUST<br>(kip/in) |      |       | MAXIMUM MOMENT<br>(lb-in/in) |      |      |
|--|---|------|-------|--|------|------|----------------------------|------|-------|------------------------------|------|------|
|  | A                                       | B    | C     | A  | B    | C    | A                          | B    | C     | A                            | B    | C    |
| 0  | 0.21                                    | 0    | 0     | 2.43   | ≈ 0  | ≈ 0  | 0.05                       | ≈ 0  | ≈ 0   | 6.9                          | ≈ 0  | ≈ 0  |
| 5  | 0.26                                    | 0.04 | -0.43 | 4.69   | 3.10 | 8.80 | 0.19                       | 0.14 | 0.003 | 15.6                         | 13.2 | 48.1 |
| 7.5  | 0.45                                    | 0.23 | -0.17 | 8.71   | 6.48 | 11.1 | 0.32                       | 0.29 | 0.15  | 18.3                         | 14.0 | 44.6 |
| 20   | 1.12                                    | 0.70 | 0.38  | 26.7   | 22.8 | 22.8 | 1.04                       | 1.03 | 0.76  | 36.2                         | 21.8 | 44.2 |
| 25   | 1.34                                    | 0.88 | 0.59  | 33.0   | 29.9 | 27.4 | 1.35                       | 1.33 | 1.00  | 47.0                         | 25.5 | 44.0 |

\*positive = shortening; negative = elongation.



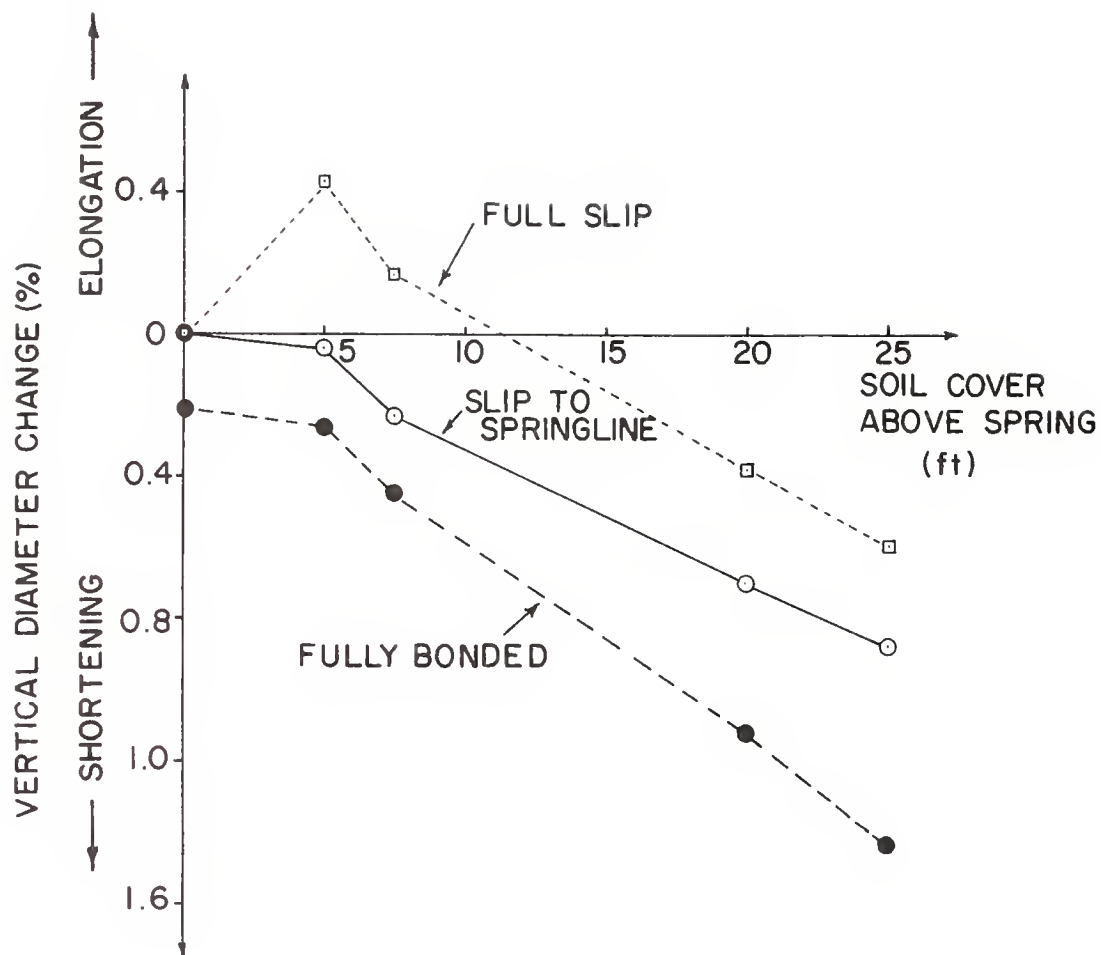
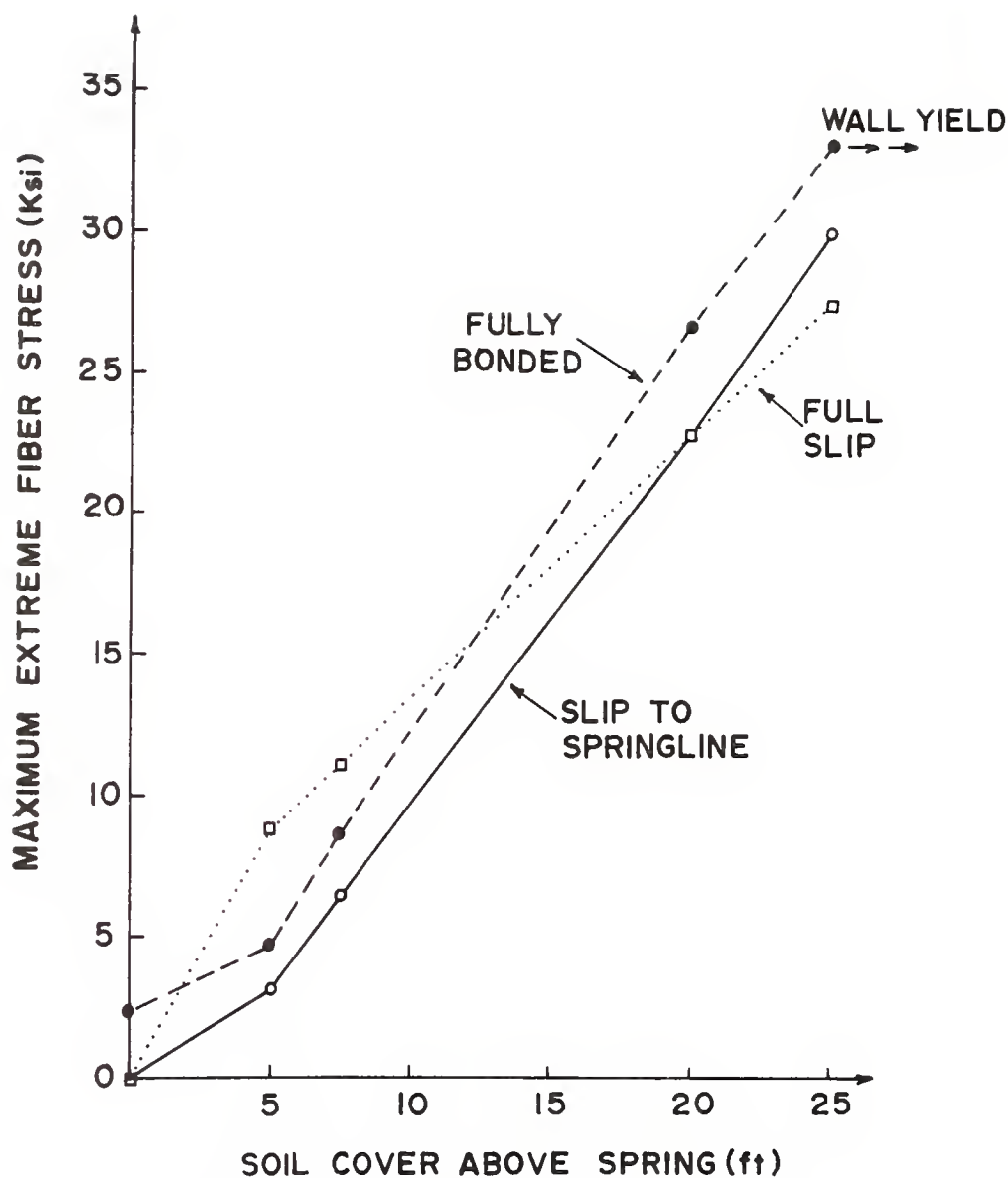


FIGURE 4.15 EFFECT OF INTERFACE CONDITION ON CHANGE IN VERTICAL DIAMETER OF A 10ft DIAMETER CORRUGATED STEEL CONDUIT, OVERBURDEN DEPENDENT SOIL MODEL.







**FIGURE 4.16 EFFECT OF INTERFACE CONDITION ON THE MAXIMUM EXTREME FIBER STRESS IN A 10ft DIAMETER CORRUGATED STEEL CONDUIT**



heights from 1.25 to 2.5 diameters above the springline, the reverse is true. The rate of increase of the maximum extreme fiber stresses in both slip-to-springline and fully bonded conditions are about the same, although wall yielding is initiated first in the fully bonded condition.

The maximum thrusts and the maximum bending moments in the conduit wall plotted as a function of fill height above the springline for the three interface conditions are shown in Figures 4.17 and 4.18, respectively.

The maximum thrusts in fully bonded and slip-to-springline conditions are very close and are greater than those in the full slip condition, which induces nearly uniform soil pressure around the conduit. This implies that if wall crushing is of main concern, reducing soil-conduit interface friction will be beneficial.

The effect of interface slip on the maximum bending moments in the conduit is found to be very significant. The maximum bending moments in full slip condition are greater than those in the other two conditions for fill heights less than about 2.3 diameters above the springline. Also, the effect of soil "hanging" from the lower half of the conduit is rather pronounced in terms of maximum bending moments. It should be noted that the locations where the maximum bending moments occurred were very different in the three interface conditions, as indicated in the parentheses in Figure 4.18. The history of bending moments at the crown, the quarter point, and the springline are depicted in Figure 4.19(a), (b), and (c), respectively. The bending moments are considered positive if tension is induced on the intrados (interior) of the conduit section. The large differences in bending moments for the three interface conditions reveal that the mode of soil-conduit system responses is greatly affected by the interface behavior. Analyses based upon results obtained by



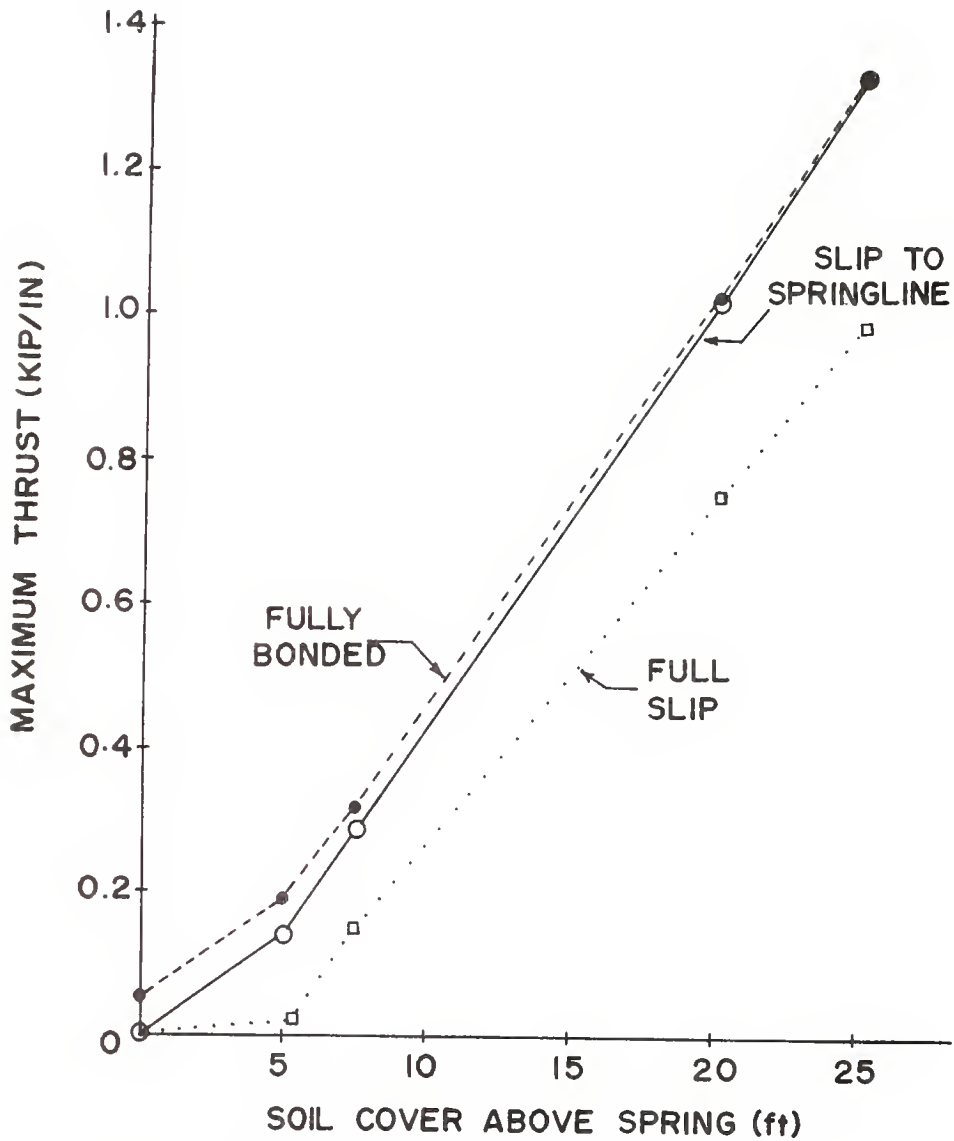


FIGURE 4-17 EFFECT OF INTERFACE CONDITION ON THE MAXIMUM THRUST IN A 10 ft DIAMETER CORRUGATED STEEL CONDUIT



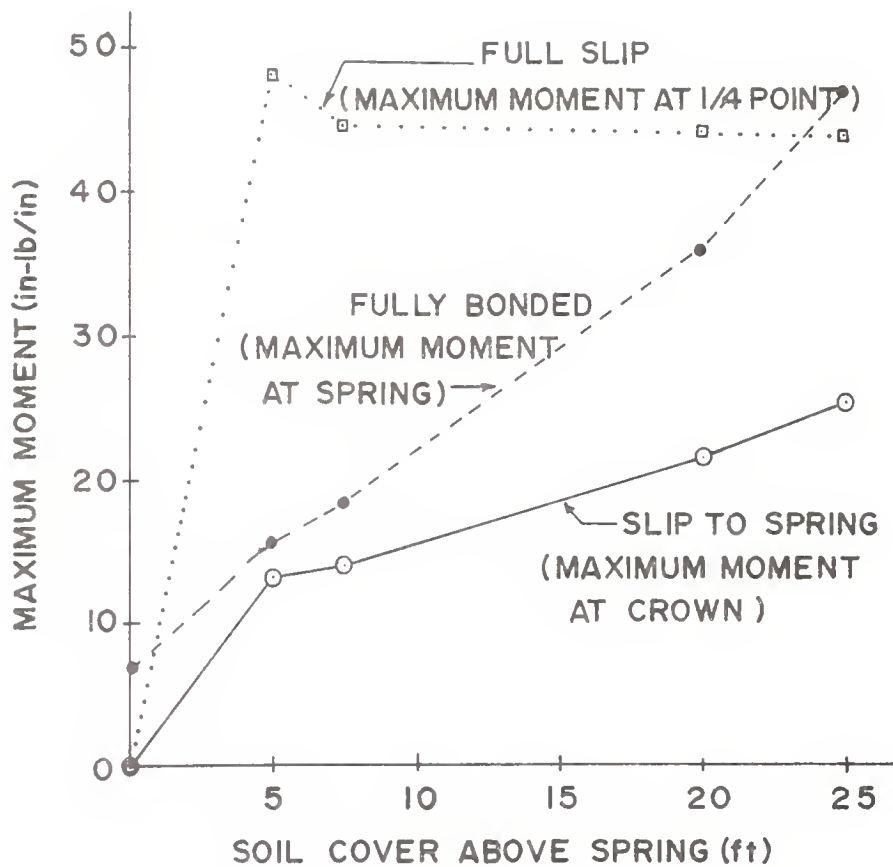


FIGURE 4-18 EFFECT OF INTERFACE CONDITION ON THE MAXIMUM BENDING MOMENT IN A 10 ft DIAMETER CORRUGATED STEEL CONDUIT





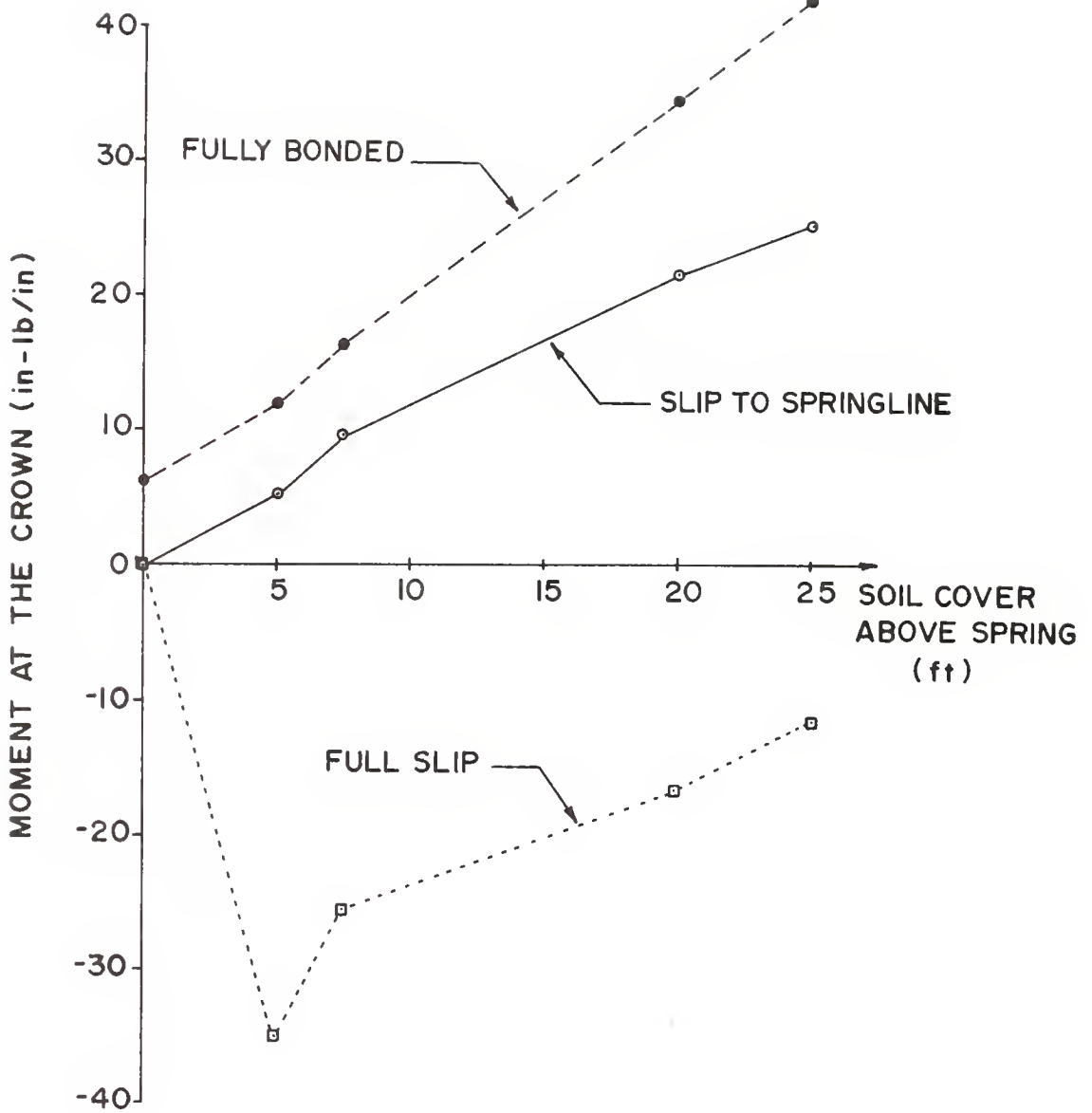


FIGURE 4.19(a) HISTORY OF BENDING MOMENT AT THE CROWN FOR THE THREE INTERFACE CONDITIONS



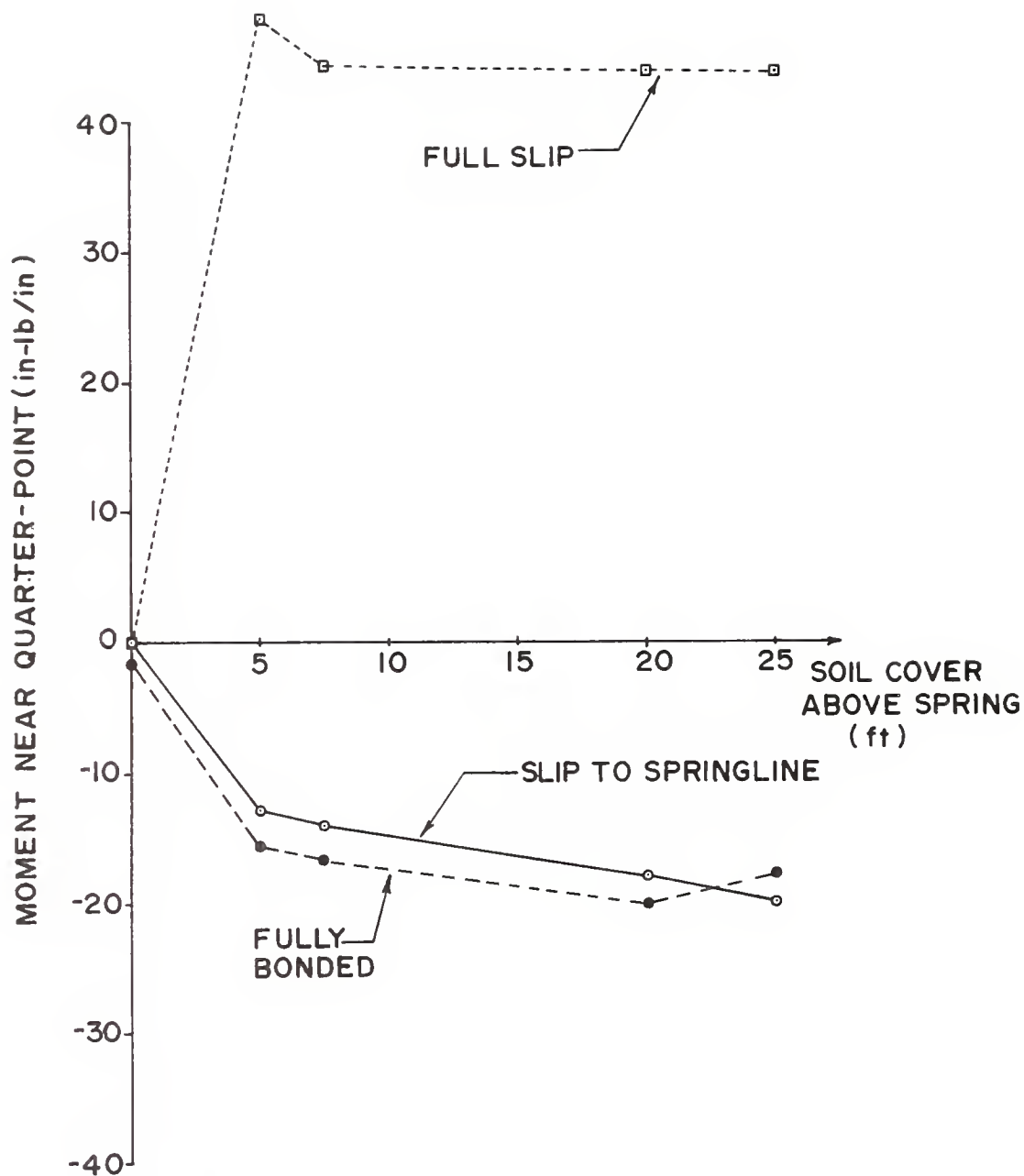


FIGURE 4.19(b) HISTORY OF BENDING MOMENT NEAR THE QUARTER-POINT FOR THE THREE INTERFACE CONDITIONS



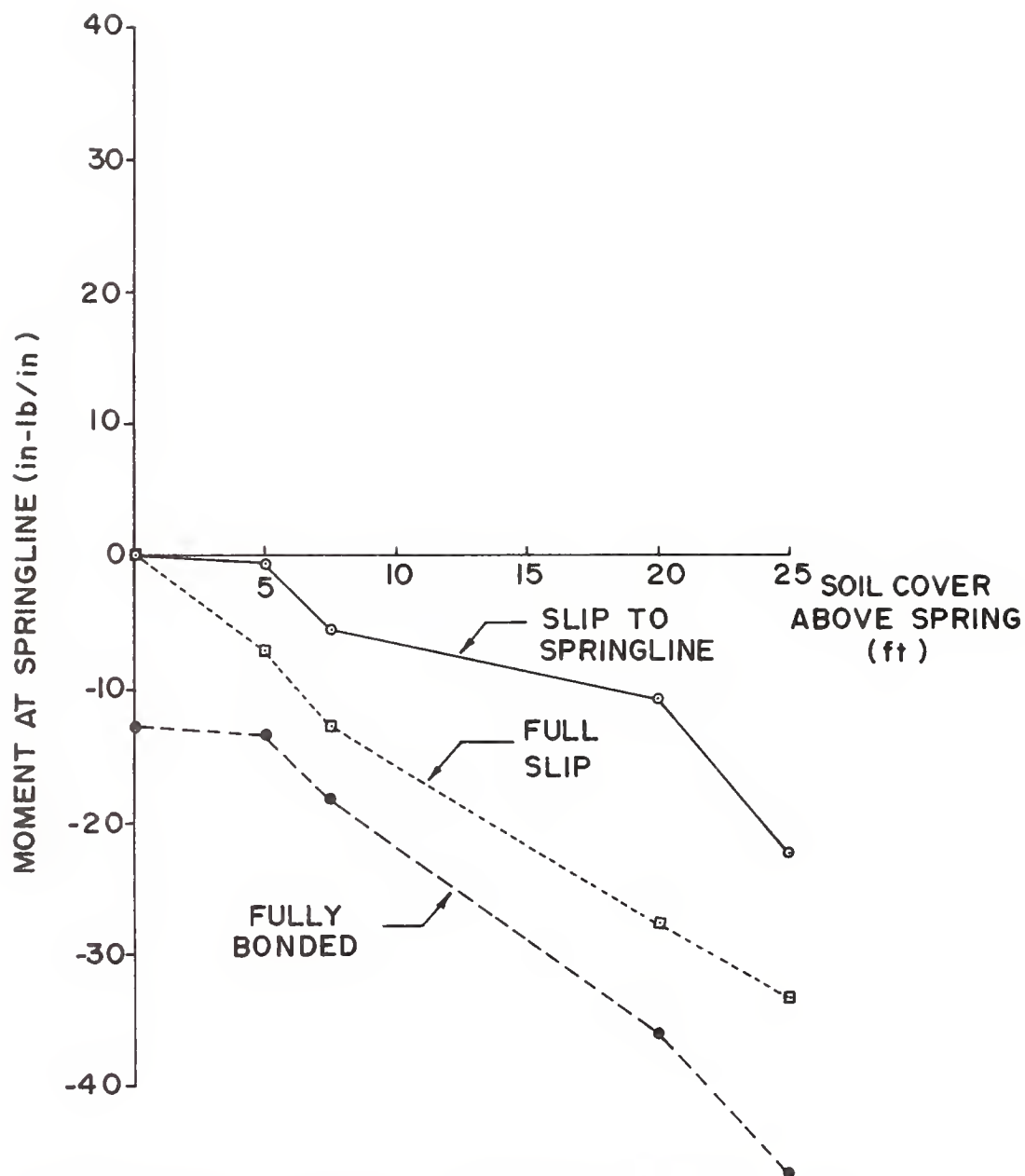


FIGURE 4.19(c) HISTORY OF BENDING MOMENT AT THE SPRINGLINE FOR THE THREE INTERFACE CONDITIONS



enforcing fully bonded interface conditions should be viewed with caution, especially for conduits with shallow burial.

#### 4.4.2 GROUP 2 PROBLEMS - INTERFACE SLIP - ELLIPTICAL CONDUIT

The conditions in this group of problems are essentially the same as those in the Group 1 problems, except that the shape of the conduit is elliptical. The elliptical conduit has a 10 ft span and a horizontal to vertical diameter ratio of 1.5. Multi-layer analyses were performed and, again, the three interface conditions were imposed.

The results of the analyses are summarized in Table 4.5. Figure 4.20 shows percent change in vertical diameter of the conduit versus fill height above the springline. The effect of interface slippage on the diameter change history is found to be less pronounced than that in the circular conduit, although the magnitudes of the vertical deflections are much greater.

The maximum bending moments are found to be influenced significantly by interface conditions (Figure 4.21) although, again, the effects are not as pronounced as for a circular conduit. Due to the elliptical shape, reducing interface friction does not produce as uniform thrust and normal pressure distributions as in the case of circular conduits, hence the effects of the full slip condition are not as striking. The maximum thrust history (Figure 4.22) is very similar to that of circular conduits.

Figure 4.23 shows the maximum extreme fiber stress history. It may be seen that the stress level induced by the full slip condition is lower than the other two conditions throughout the analyses. Initial yielding of the conduit wall for the fully bonded and the slip-to-springline conditions occurred at fill heights above the springline of about 16 ft and 18 ft, respectively, while for the full slip condition, yielding of





Table 4.5 Responses of an Elliptical Conduit for Three Interface Conditions

Conduit = Elliptical 10' span, R/S = 0.33, 18 gage 2 2/3" x 1/2" corrugated steel; yield stress,  $\sigma_y = 33$  ksi

Soil = Overburden-Dependent Soil Model (Fair Compaction),  $\mu_{\text{soil}} = 0.32$ ,  $\gamma_{\text{soil}} = 120$  pcf

A = FULLY BONDED  
 B = SLIP-TO-SPRINGLINE  
 C = FULL SLIP

| FILL<br>HEIGHT<br>ABOVE<br>THE<br>SPRINGLINE<br>(ft) | PERCENT CHANGE IN<br>VERTICAL DIAMETER* |      |       | MAXIMUM EXTREME<br>FIBER STRESS (kip/in <sup>2</sup> ) | MAXIMUM THRUST<br>(kip/in) |                 |             | MAXIMUM MOMENT<br>(in-lb/in) |
|--|---|------|-------|--|----------------------------|-----------------|-------------|------------------------------|
|  | A                                       | B    | C     |  | A                          | B               | C           |                              |
| 0  | 0.20                                    | 0    | 0     | 1.67 $\approx 0$                                       | 0.004 $\approx 0$          | $\approx 0$     | $\approx 0$ | 8.8 $\approx 0$              |
| 3.33   | 0.33                                    | 0.13 | -0.03 | 3.83 2.40 2.50   | 0.095 0.074 0.062          | 15.2 10.8 7.4   |             |                              |
| 5.83   | 0.84                                    | 0.63 | 0.71  | 10.5 8.75 7.10   | 0.20 0.19 0.15             | 36.9 27.7 22.3  |             |                              |
| 13.33  | 1.81                                    | 1.38 | 1.61  | 26.9 23.4 16.8   | 0.54 0.56 0.44             | 90.8 69.5 45.9  |             |                              |
| 23.33  | 2.73                                    | 2.30 | 2.68  | 33.0 33.0 29.3   | 0.99 1.02 0.80             | 104.4 97.5 76.0 |             |                              |

\*positive = shortening; negative = elongation.



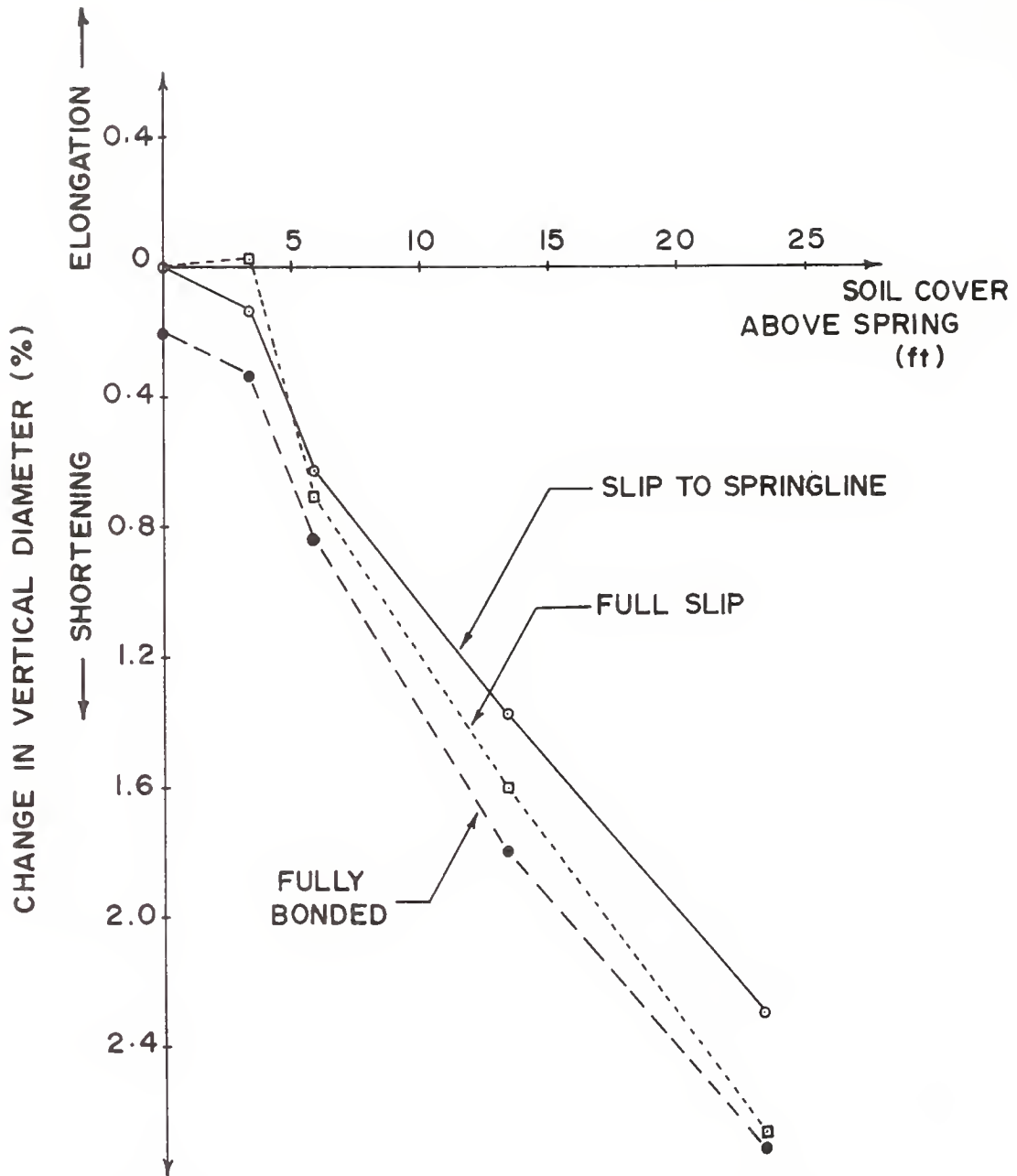


FIGURE 4.20 EFFECT OF INTERFACE CONDITION ON THE CHANGE IN VERTICAL DIAMETER OF A 10 ft SPAN ELLIPTICAL CORRUGATED STEEL CONDUIT



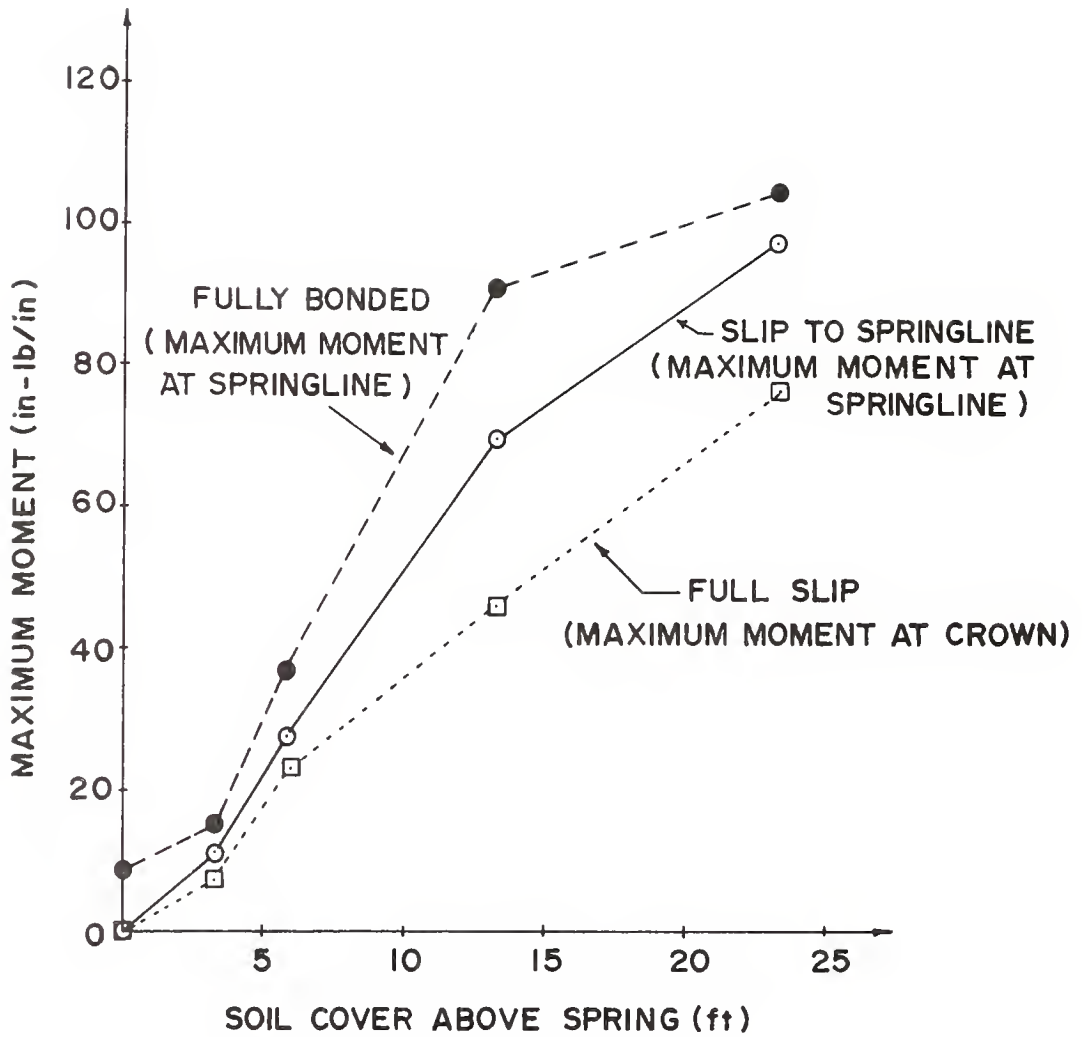


FIGURE 4.21 EFFECT OF INTERFACE CONDITION ON THE MAXIMUM MOMENT IN A 10ft SPAN ELLIPTICAL CORRUGATED STEEL CONDUIT



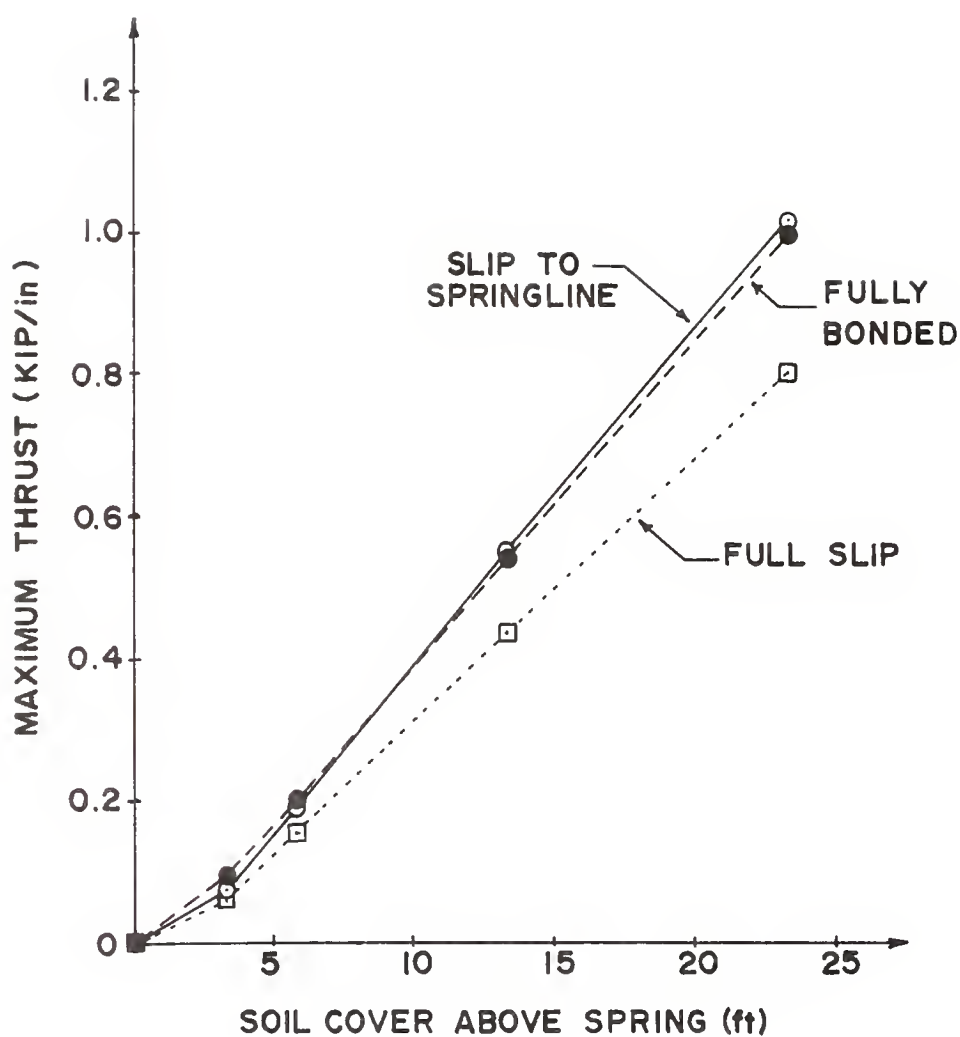


FIGURE 4.22 EFFECT OF INTERFACE CONDITION ON THE MAXIMUM THRUST IN A 10 ft SPAN ELLIPTICAL CORRUGATED STEEL CONDUIT





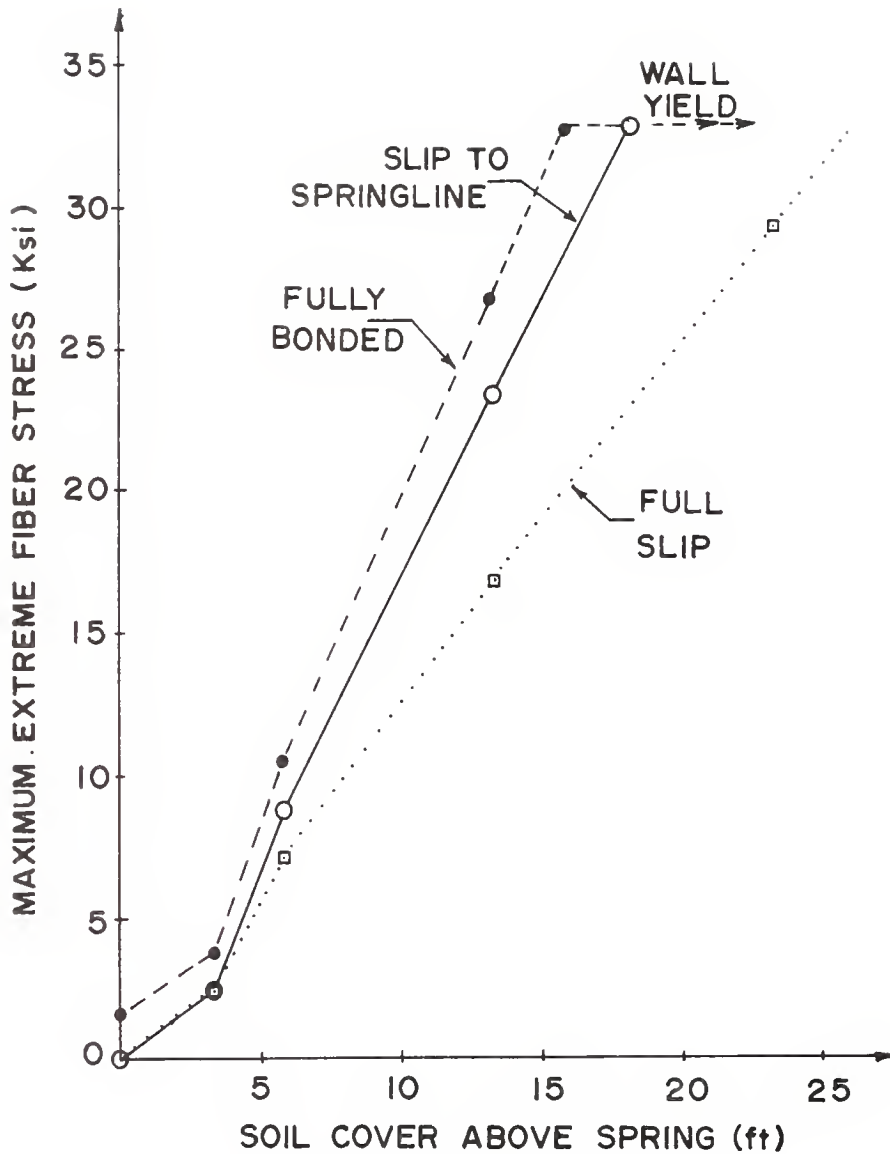


FIGURE 4.23 EFFECT OF INTERFACE CONDITION ON THE MAXIMUM EXTREME FIBER STRESS ON A 10ft SPAN ELLIPTICAL CORRUGATED STEEL CONDUIT



the conduit wall does not occur until fill height reaches 26 ft above the springline.

From the results illustrated in Figures 4.20 to 4.23, it can be concluded that promoting interface slippage for elliptical conduit is beneficial in all respects, especially from the standpoint of increasing the fill height required to induce yield in the conduit wall.

#### 4.5 EFFECT OF SOIL RESPONSE

The fundamental idea in design of buried conduits is to utilize soil as the principal load-carrying and load transmitting element of the system. With strong support from surrounding soil, a thin membrane of steel, 0.25 in thick with corrugations 6 x 2 in has been able to sustain safely a soil cover of 44 ft over a 51 ft span (Lafebvre et al., 1975). Accordingly, being able to simulate the behavior of the soil properly is essential in analyzing soil-conduit interaction problems. The more slender the conduit wall in relation to the curvature, the more critical it is to simulate soil behavior precisely.

##### 4.5.1 LINEAR ELASTIC SOIL MODELS

Soil seldom, if ever, behaves as a linear elastic material. However, the assumption of linear elasticity has the significant advantage of reducing considerably the computation effort required to analyze stresses and deformations in soil masses. Moreover, in parametric studies involving variables such as interface slip, plastic hinging, no tension considerations, etc., it is justifiable to assume linear elastic soil behavior in order to avoid computational difficulties due to the lack of convergence. The important question with respect to linear elastic soil models is what are the most suitable values of the elastic moduli for use in analyses.

Young's modulus and Poisson's ratio are the two most commonly used



elastic moduli in linear elastic soil models. The modulus of elasticity as determined from triaxial compression test data had been found to be a function of the soil density, confining pressure, and shearing stress level (Chen, 1948). Experimental studies of Poisson's ratio of sand had indicated that the value obtained was influenced considerably by the methods used to obtain it. Zero lateral strain tests yielded relatively constant values of Poisson's ratio in the range of 0.30 to 0.35 (Bishop and Henkel, 1962; Domaschuk and Wade, 1969). On the other hand, Jakobson (1957) found that the Poisson's ratio as determined by conventional triaxial compression tests varies with the magnitude of shear stress over a range of 0.1 to 0.6.

For analyses of stress and movements in dams during construction, Penman et al. (1971) described a procedure for selection of values of Young's modulus and Poisson's ratio for practical use of linear elastic analyses, using the results of oedometer tests on the embankment material.

For soil-conduit interaction problems, an equivalent elastic soil modulus which gives good agreement with all of the soil-conduit system responses does not exist. Generally speaking, elastic soil models can at best reproduce part of the key soil-conduit system responses (e.g., crown soil pressure, or maximum thrust or moment in the conduit wall, etc.) of interest in design. The more "flexible" the conduit, the more difficult it is to find a single set of "suitable" values of the elastic soil moduli. Examples of the difficulties associated with the concept of "equivalent" elastic soil moduli are given in section 4.5.2

#### 4.5.2 NONLINEAR SOIL MODELS

In general, soils are complicated, multiphase materials, and their mechanical behavior is governed by a number of factors, such as density,



water content, drainage conditions, stress history, stress path, etc.

To simulate the behavior of soils for use in analytical studies simplified soil models which describe the stress-strain relations of the soils derived from laboratory tests are often employed. The most common tests are uni-axial strain (consolidation) tests, triaxial tests, and plane strain tests.

In this study, five nonlinear incrementally elastic soil models were employed for simulation of the constitutive relation of soils: (1) overburden dependent model, (2) spline function representation of actual test data, and the functional-form soil models of (3) extended-Hardin, (4) Duncan-Chang, and (5) modified Duncan models. Detailed description of the soil models were presented in Chapter 2.

The problems selected to investigate the effects of using different soil models were divided into three groups: (1) Group 1 - problems solved with a 10 ft diameter, 8 in thick concrete pipe; (2) Group 2 - problems solved with a 10 ft diameter, 18 gage 2 2/3 x 1/2 in corrugated steel pipe; (3) Group 3 - problems solved with a 25 ft span steel pipe, using a range in section moduli and rise to span ratios.

The soil parameters (or moduli) for the five nonlinear soil models are presented in the following section. They were used throughout this study, unless otherwise specified.

#### 4.5.2.1 SOIL PARAMETERS (OR MODULI)

##### (1) Overburden Dependent Soil Model

Two sets of soil moduli representing granular soils with fair and good compaction, as recommended in CANDE User's Manual, are adopted for the overburden dependent model (Table 4.6). Poisson's ratio was assumed to be a constant value either in the narrow range of 0.30 to 0.35, or a value of 0.45.





Table 4.6 Young's Modulus Adopted for Overburden Dependent Soil Model

| Overburden Pressure (psi) | E(psi)          |                 |
|---------------------------|-----------------|-----------------|
|                           | Fair Compaction | Good Compaction |
| 5                         | 550             | 1100            |
| 10                        | 750             | 1300            |
| 15                        | 850             | 1500            |
| 20                        | 1000            | 1650            |
| 25                        | 1100            | 1800            |
| 30                        | 1150            | 1900            |
| 40                        | 1300            | 2100            |
| 50                        | 1400            | 2250            |



## (2) Functional-Form Nonlinear Soil Models

Lade's laboratory test results (Lade, 1972) were employed for the functional-form soil models. Triaxial compression and plane strain tests were performed by Lade on Monterey No. 0 sand. The stress-strain and volume change relationships obtained from these tests are shown in Figures 4.24 and 4.25, respectively. The sand was prepared with a void ratio of 0.78 and the corresponding relative density was  $D_r \approx 27\%$ .

Details of the procedures for evaluating the stress-strain-volume change parameters of extended Hardin model, Duncan-Chang model and modified Duncan model are described in References 50, 87, and 31, respectively. The parameters for the three nonlinear soil models thus derived using Lade's triaxial compression test results are listed in Table 4.7. It should be noted that the parameters are, to some extent, confining pressure dependent. Those listed in Table 4.7 are the average values for the confining pressures of 0.30, 0.60, and 1.20 kg/cm<sup>2</sup>, except the Poisson's ratio parameters of extended-Hardin model,  $\mu_{\min}$ ,  $\mu_{\max}$ ,  $q$ . Since the variation in the Poisson's ratio parameters at the three confining pressures was very large, the parameters were determined by fitting a hyperbola to the data in the entire range of confining pressure. This will be discussed further in section 4.5.2.2.

The shear modulus parameters in the extended-Hardin model can also be evaluated by the use of the Hardin formula (Hardin, 1970) which relates these parameters to index properties of soils.

With the index properties of the Monterey No. 0 sand (void ratio = 0.78 percent saturation = 0%, and plasticity index = 0), the shear modulus parameters derived from Hardin formula are:  $S_1 = 3320$ ,  $C_1 = 14720000$ , and  $a = 3.2$ . The values are very different from those interpreted from the triaxial test results (Table 4.7). For example, based on the parameters obtained from



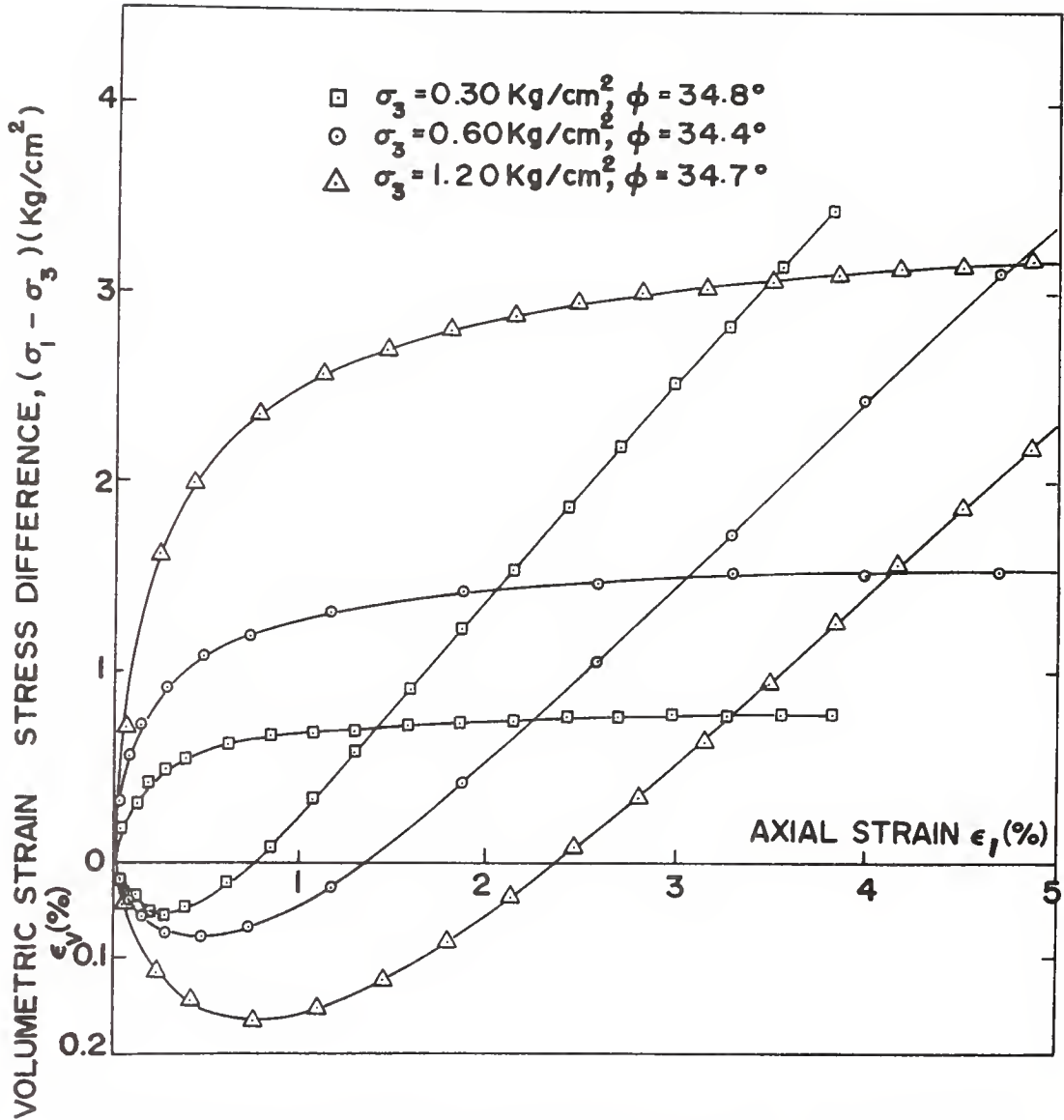


FIGURE 4.24 RESULTS OF TRIAXIAL COMPRESSION TESTS ON LOOSE SPECIMENS OF MONTEREY No. 0 SAND (FROM LADE, 1972)



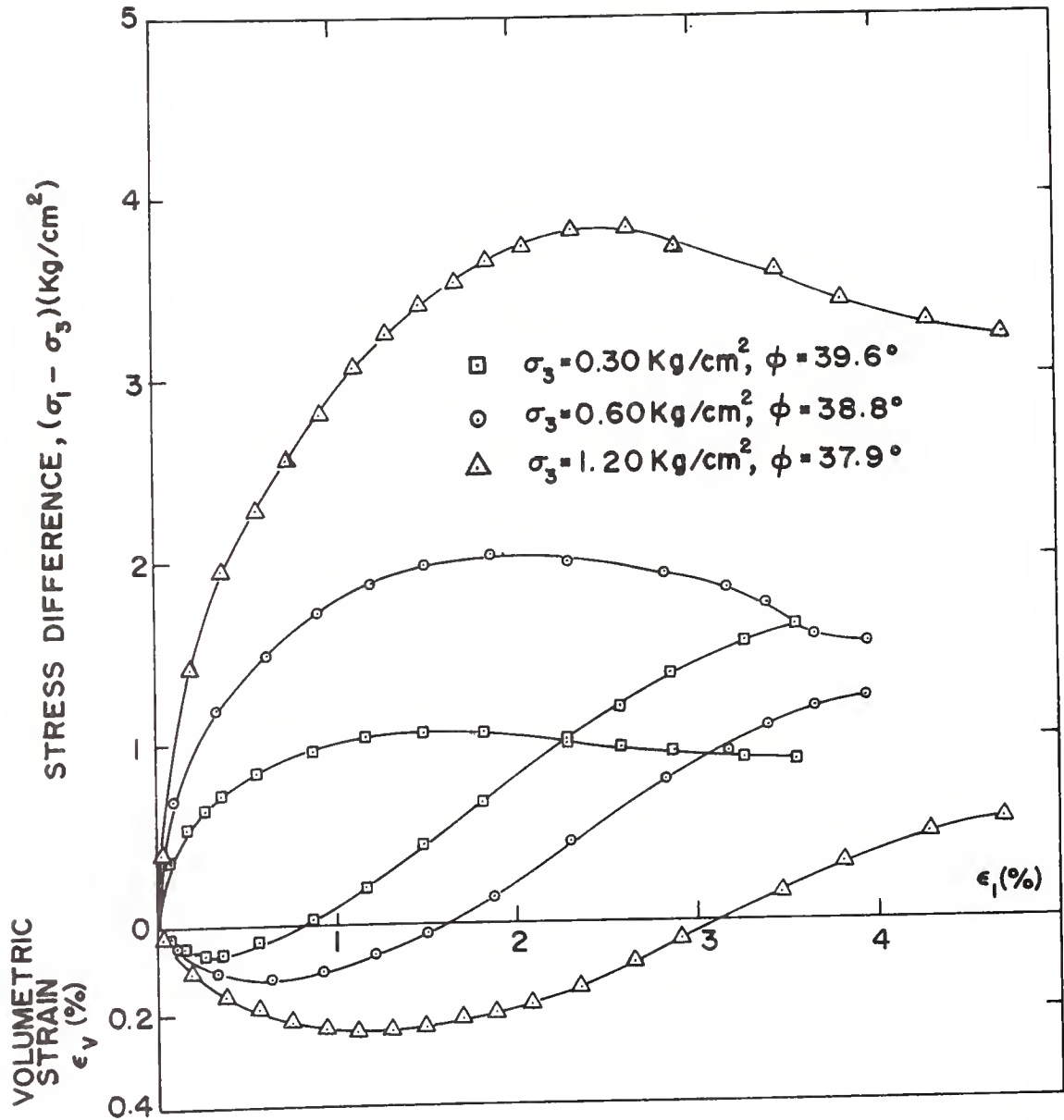


FIGURE 4.25 RESULTS OF PLANE STRAIN TESTS ON LOOSE SPECIMENS OF MONTEREY No. 0 SAND (FROM LADE, 1972)





Table 4.7 Soil Model Parameters Derived from Lade's Triaxial Compression Test Results (loose sand).

| Extended-Hardin model | Duncan-Chang model  | Modified-Duncan model    |
|-----------------------|---------------------|--------------------------|
| $\mu_{\min} = 0.20$   | $\phi = 35^{\circ}$ | $\phi_0 = 35^{\circ}$    |
| $\mu_{\max} = 0.495$  | $k = 920$           | $\Delta\phi = 0^{\circ}$ |
| $q = 3.75$            | $n = 0.79$          | $k = 920$                |
| $S_1 = 1038$          | $R_f = 0.96$        | $n = 0.79$               |
| $C_1 = 814000$        | $G = 0.37$          | $R_f = 0.96$             |
| $a = -1.75$           | $F = 0.12$          | $k_b = 465$              |
|                       | $D = 10.5$          | $m = 0.32$               |



Hardin formula, the maximum shear modulus,  $G_{\max}$ , and the maximum shear stress,  $\tau_{\max}$ , of the soil at  $\sigma_3 = 0.6 \text{ kg/cm}^2$  were found to be 9700 psi and 6.4 psi, respectively, whereas the test data indicated  $G_{\max} = 3000 \text{ psi}$  and  $\tau_{\max} = 11.3 \text{ psi}$ . A schematic diagram of the shear stress-shear strain relation of the soil derived from the Hardin formula as compared with those calculated from the test results is illustrated in Figure 4.26. It may be seen that in this particular case the Hardin formula, which is an option in the CANDE code, overestimates the shear modulus at low shear strains, but greatly underestimates the shear modulus at high shear strains.

### (3) Spline Function Representation

Lade's plane strain test results were fed directly into the computer using the FINLIN code (Leonards and Roy, 1976), which relates Young's modulus and Poisson's ratio to the octahedral normal and shear stress levels. For monotonic loading in the plane strain mode, it is believed that this model is the most realistic of the five soil models used in this study.

#### 4.5.2.2 GROUP 1 PROBLEMS - SOIL MODEL - CIRCULAR CONCRETE PIPE

In this group of problems, a 10 ft diameter, 8 in thick concrete pipe with 25 ft of soil cover above the springline was analyzed. Spline function representation (of the plane strain test data), overburden dependent soil model with Young's moduli representing granular soils with fair compaction and a constant Poisson's ratio of 0.30, Duncan-Chang soil model, and extended-Hardin soil model with the soil parameters obtained from the Hardin formula and from triaxial compression test results, were employed. The problems were solved by both single-layer and multi-layer analyses, except the one using the overburden dependent soil model in which only multi-layer analysis was performed (the overburden dependent model should



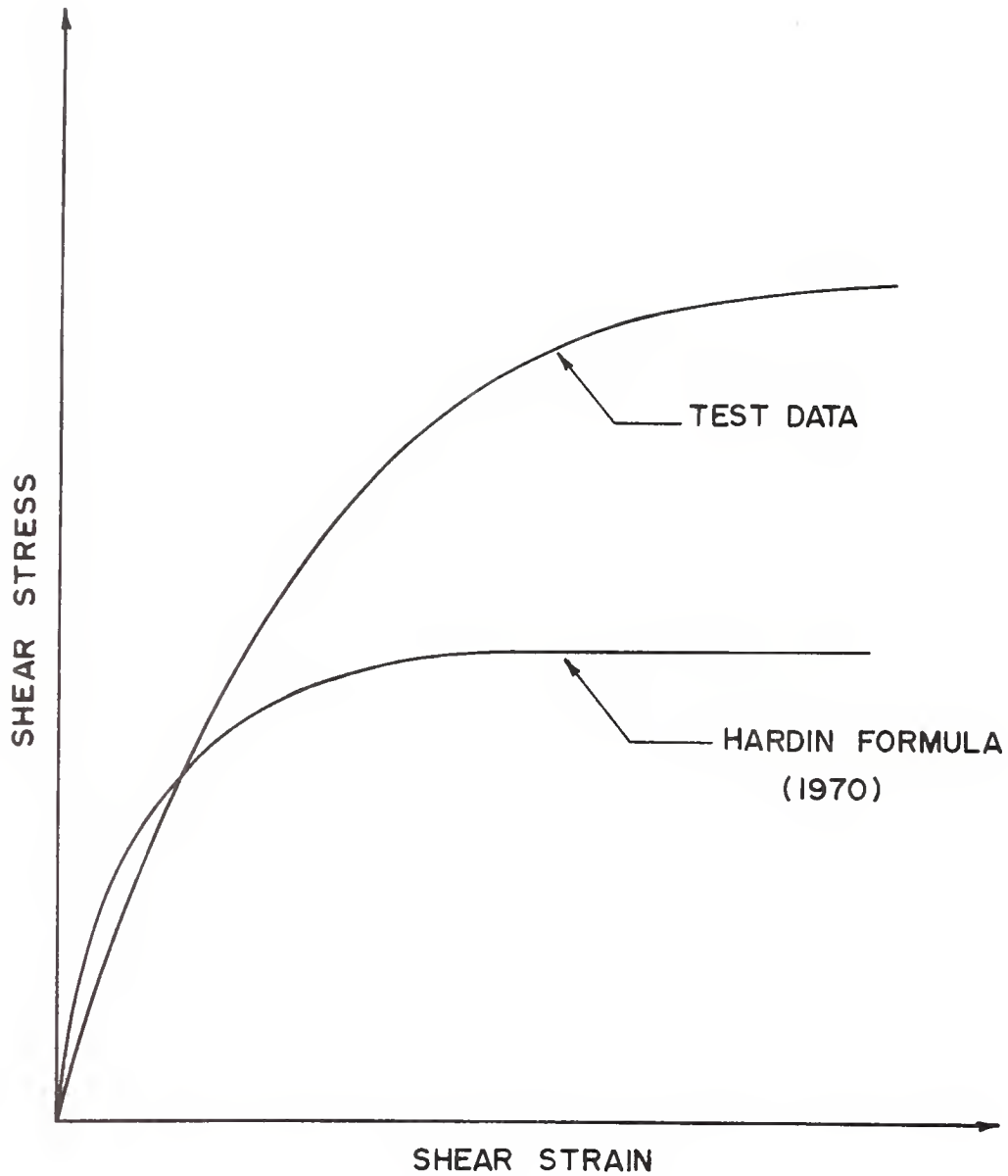


FIGURE 4.26 SCHEMATIC DIAGRAM FOR SHEAR STRESS -  
SHEAR STRAIN RELATIONSHIP



not be used in single layer analysis because the relative influence of soil weight on the applied loads and on the soil modulus may completely distort the over-all result). Results using the spline function representation were obtained from FINLIN code, while the others were obtained by using CANDE code (Table 4.8). Other than the results with overburden dependent soil model which employs much smaller Young's moduli and a constant Poisson's ratio, the maximum thrust in the conduit wall obtained by the nonlinear soil models do not differ very much, while the maximum bending moments and the vertical diameter changes that result from using the nonlinear soil models differ significantly, even for the case of a relatively "rigid" conduit.

A major source of the differences between the soil models comes from the different characterizations of the volume change behavior of the soil. Vagneron, et al. (1976) and Lucia and Duncan (1979) demonstrated that hyperbolic soil models cannot simulate dilatant volume changes resulting from shear stresses, and thus always indicate compressive volumetric strains under increasing values of stress, even though the test data may indicate dilation at larger values of axial strain. The Monterey No. 0 sand does exhibit dilation at axial strain greater than 0.25% - 0.75%, depending upon the confining pressure. Therefore, by using the hyperbolic soil models, the volume change characteristics of the soil are modeled properly only at very low strain levels.

The spline function representation, on the other hand, can accommodate the dilation effect since it defines piecewise polynomials in accordance with the test data which describe the volume change characteristics of the soil. However, it is necessary that the stress path used in the laboratory tests conform to those extant in the field.

In the extended-Hardin model, Poisson's ratio of the soil is expressed





Table 4.8 Results from Group 1 Problems

Conduit: Circular concrete pipe, 8" thick, 10' diameterSoil: Monterey No. 0 loose sand  $\gamma=100$  pcf  
25 ft soil cover above the springline  
Fully-bonded interface

|                             | SINGLE LAYER                                    |  |  |   | 5 LAYERS   |  |  |   |
|-----------------------------|---|--|--|---|--|--|--|---|
|                             | Spline Function (Lade's Plane Strain Test Data) | Duncan-Chang model (Lade's Triax. Test Data) | Extended-Hardin model (Hardin formula) | Extended-Hardin model (Lade's Triax. Test Data) | Overburden Dependent model (Fair Compaction) $\nu_{soil} = 0.30$ | Duncan-Chang model (Lade's Triax. Test Data) | Extended-Hardin model (Hardin formula) | Extended-Hardin model (Lade's Triax. Test Data) |
| $P_{max}$ (kip/ft)          | 14.3  | 14.5   | 14.5                                   | 15.6  | 15.1   | 12.4   | 11.2                                   | 13.1  |
| $M_{max}$ (ft-kip/ft)       | 4.79  | 5.62   | 8.81                                   | 6.09  | 11.63  | 2.32   | 6.95                                   | 4.05  |
| $\Delta\gamma$ (%)          | 0.054   | 0.066  | 0.103                                  | 0.070   | 0.135  | 0.028  | 0.074                                  | 0.047   |
| $P_c/\gamma H$              | 1.09  | 1.10   | 1.16                                   | 1.03  | 1.27   | 1.00   | 1.07                                   | 0.99  |
| $\sigma_{\theta max}$ (ksf) | 0.56  | 0.65   | 0.95                                   | 0.73  | 1.21   | 0.33   | 0.72                                   | 0.48  |



in terms of the ratio of shear strain to reference shear strain,  $\gamma/\gamma_r$ . The reference shear strain,  $\gamma_r$ , is defined as the ratio of maximum shear stress to maximum shear modulus. Figure 4.27 shows Poisson's ratio of the Monterey No. 0 sand plotted as a function of shear strain ratio,  $\gamma/\gamma_r$ . It is observed that the data do not collapse into a single curve. The hyperbola interpreted from the test data and from the default values in CANDE code are also shown in the figure. The very significant difference between the two curves is the major cause of the difference between the results of extended-Hardin model with the soil parameters obtained from Hardin formula and from the triaxial test results (Table 4.8).

From the results of Group 1 problems, it is seen that:

- (a) the overburden dependent model, using soil moduli as recommended in CANDE's users manual, predicts the thrust poorly and gives unrealistic values for bending moments,
- (b) the extended Hardin model, using either the Hardin formula and CANDE's default values for Poisson's ratio, is unreliable, and
- (c) both the extended Hardin and Duncan-Chang models, with parameters interpreted from triaxial test data, give consistent (and, it is believed, reasonably reliable) results in the case of a 10 ft diam. 8 in. thick concrete pipe.

#### 4.5.2.3 GROUP 2 PROBLEMS - SOIL MODEL - CIRCULAR STEEL PIPE

In this group of problems, a 10 ft diameter, 18 gage 2 2/3 x 1/2 in corrugated steel pipe with 30 ft of soil cover above the springline was analyzed. Results obtained by using "equivalent" elastic soil moduli; overburden dependent soil model (for granular soils with fair compaction), Duncan-Chang soil model, modified Duncan soil model, and extended-Hardin



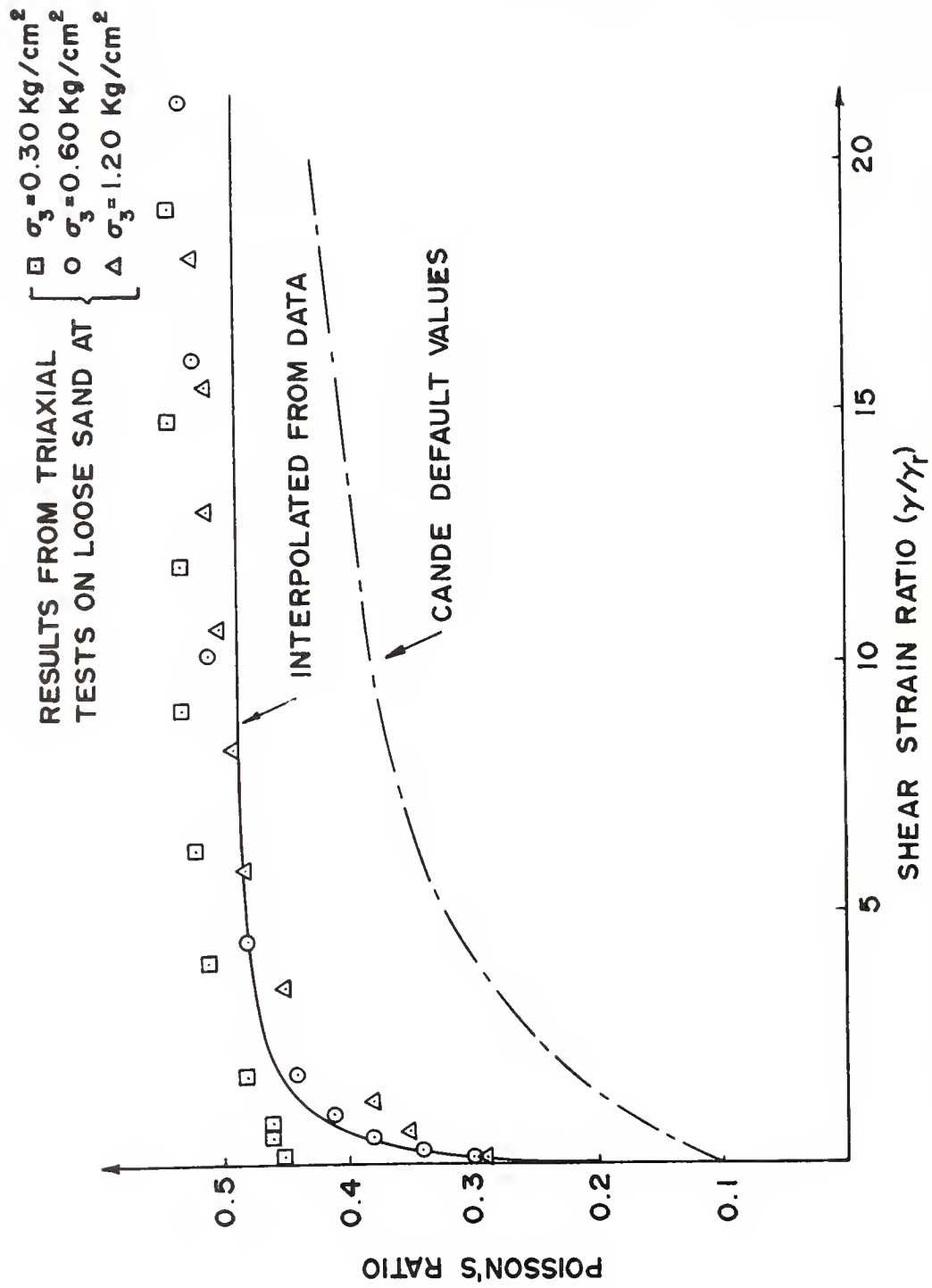


FIGURE 4.27 POISSON'S RATIO VERSUS SHEAR STRAIN RATIO



model with the soil parameters obtained from Lade's triaxial compression test results (Table 4.7) are listed in Table 4.9.

In order to examine the effects of "soil hanging" (section 4.4), the solutions using Duncan-Chang (SSTIP code) and the modified Duncan models (NLSSIP code) were obtained by beginning analyses at the springline. With the CANDE code analyses were made for the fully bonded and slip to the springline conditions. With the overburden dependent soil model results were obtained for both conditions, but for the other soil models the CANDE code suffered from soil modulus and interface element convergence problems. An investigation revealed that the convergence problems were related to local failure (tension or shear failure) in some of the soil elements adjacent to the conduit. This problem was solved partly by using less stringent criteria for reduction in soil moduli due to the incidence of failed elements (Chapter 5), and partly by reducing the magnitude of the load steps corresponding to each construction layer. As indicated in Table 4.9, with the modified Duncan model and NLSSIP code a moment of 278 ft-lb/ft is obtained, which is larger than the fully plastic moment ( $M_p = 256$  ft-lb/ft) in the absence of thrust. This anomaly results firstly from the fact that NLSSIP sums moments about different axes (after yielding in the conduit was initiated) and secondly because, using only one iteration, convergence in the nonlinear soil and pipe moduli was not achieved. Thus, it is suggested that for cases in which a large fraction of the conduit wall section has yielded, the NLSSIP code should be used with caution. The calculated moment using SSTIP is incorrect, because it is assumed that the pipe material remains elastic although the ratio  $\epsilon_{\max}/\epsilon_y \gg 1$ .

As may be seen from Table 4.9, maximum thrust using the overburden dependent soil model with  $\mu = 0.32$  is 35 to 45 percent greater than that obtained using either extended-Hardin or Duncan Chang soil models and





Table 4.9 Results from Group 2 Problems

Conduit: 18 Gage 2 2/3" x 1/2" corrugated steel pipe, 10' diameter,  
 $\sigma_y = 33 \text{ ksi}$

Soil: Monterey No. 0 loose sand,  $\gamma = 120 \text{ pcf}$   
30 ft soil cover above the springline; multi-layer analysis

|                                  | CANDE CODE                  |                               |                              |                       |            |                             |                               |                               |                      |                       |                 | SSTIP CODE | NLSSIP CODE |
|----------------------------------|-----------------------------|-------------------------------|------------------------------|-----------------------|------------|-----------------------------|-------------------------------|-------------------------------|----------------------|-----------------------|-----------------|------------|-------------|
|                                  | EQUIVALENT ELASTIC<br>MODEL | OVERBURDEN DEPENDENT<br>MODEL |                              |                       |            | EXTENDED-HARDIN<br>MODEL    |                               | DUNCAN-CHANG<br>MODEL         |                      | DUNCAN-CHANG<br>MODEL |                 |            |             |
|                                  |                             | SLIP TO<br>SPRINGLINE         | FULLY<br>BONDED<br>INTERFACE | SLIP TO<br>SPRINGLINE |            | HARDIN<br>FORMULA<br>e=0.78 | LADE'S<br>TRIAx.<br>TEST DATA | LADE'S<br>TRIAx.<br>TEST DATA |                      |                       |                 |            |             |
|                                  |                             |                               |                              | $\mu=0.32$            | $\mu=0.45$ |                             |                               | FULLY<br>BONDED               | SLIP<br>TO<br>SPRING |                       | FULLY<br>BONDED |            |             |
| $P_{max}$<br>(kip/ft)            | 17.9                        | 16.7                          | 19.7                         | 19.6                  | 16.4       | 14.4                        | 14.6                          | 13.4                          | 15.9                 | 14.7                  | 16.5            | 16.1       |             |
| $M_{max}$<br>(ft-lb/ft)          | 71                          | 21                            | 43                           | 27                    | 13         | 42                          | 9                             | 8                             | 21                   | 27                    | 162             | 278        |             |
| $\Delta Y\%^{*}$ at<br>H = 30 ft | -2.78                       | -0.55                         | -1.54                        | -1.08                 | -0.17      | -0.07                       | -0.10                         | -0.07                         | 0.00                 | +0.18                 | +1.06           | +2.43      |             |
| $p_c/\gamma H$                   | 0.67                        | 0.89                          | 0.72                         | 0.68                  | 0.86       | 0.63                        | 0.59                          | 0.70                          | 0.76                 | 0.73                  | 0.88            | 1.07       |             |
| $\epsilon_{max}/\epsilon_y$      | 1.37                        | 0.92                          | 1.35                         | 1.11                  | 0.84       | 0.94                        | 0.75                          | 0.67                          | 0.81                 | 0.80                  | 1.46            | >1.0       |             |

\* positive  $\Delta Y(\%)$  indicates elongation in vertical diameter

Note:  $\epsilon_{\max}$  = maximum strain in conduit wall,  $\epsilon_y$  = yield strain of steel



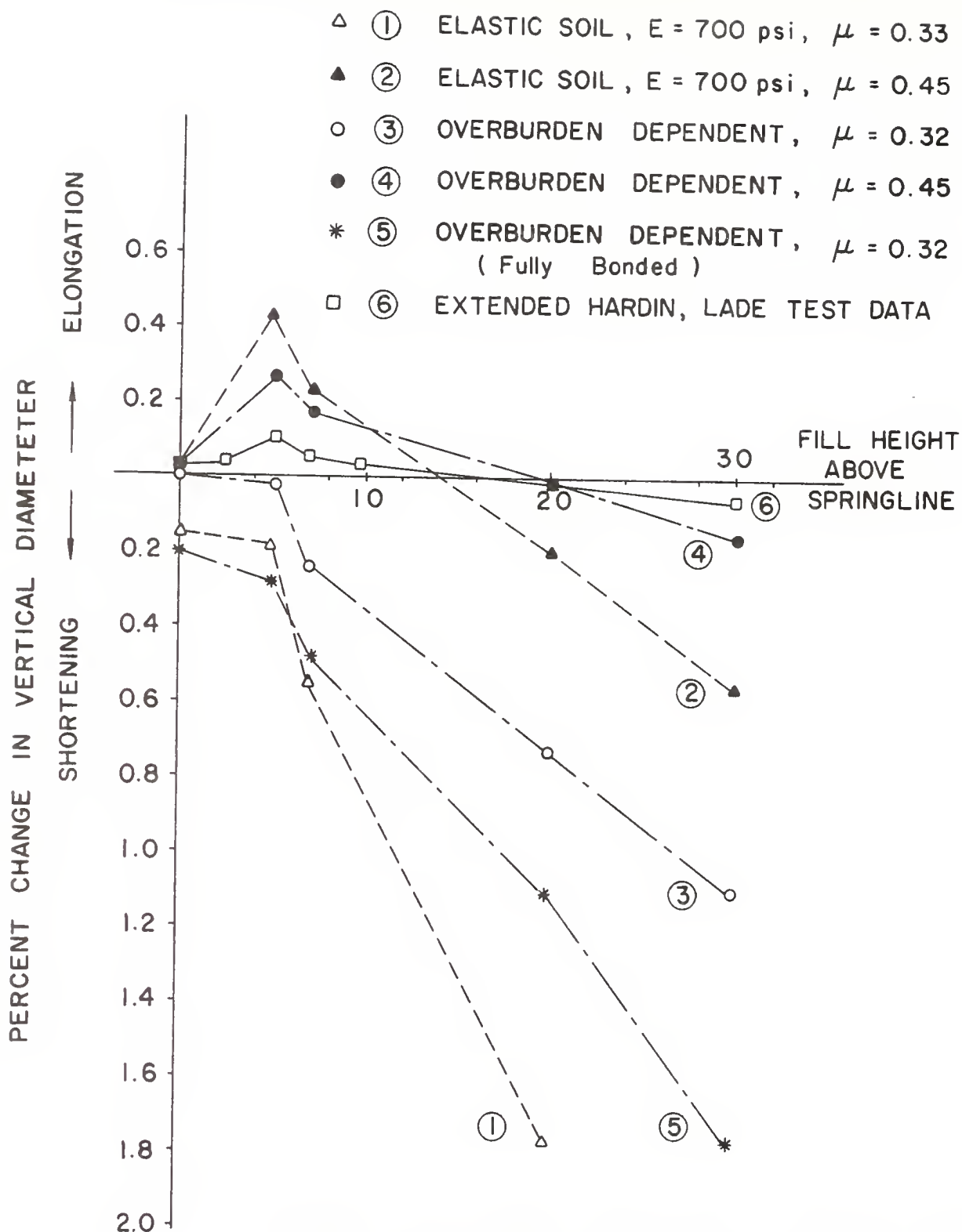
Lade's test data. The difference in the maximum moments and the vertical diameter changes are very significant in all cases yet, disregarding the results from the NLSSIP code, the differences in the amount of soil arching is very modest. This illustrates, again, that soil arching does not reflect large changes in the deformed shape of the conduit wall section.

The percent change in vertical diameter as a function of fill height is depicted in Figures 4.28a and 4.28b. Curves 3 and 5 show the difference between analyses using fully bonded vs. slip to springline conditions for the overburden dependent soil model, and curves 7 and 8 show this difference for the Duncan-Chang soil model. The fully bonded condition forces soil to "hang" from the portion of the pipe below the springline, unduly restricting its tendency to "peak" during construction. Although the effects of allowing slip to the springline are significant, they pale in relative importance compared to the effects of using different soil models and computer codes.

The use of equivalent elastic soil model with Poisson's ratio  $\mu = 0.33$  does not produce elongation of the vertical diameter during construction, which is an unrealistic result; on the other hand, with  $\mu = 0.45$ , the elastic model gives almost identical peaking effects during construction as the Duncan-Chang model with slip to the springline. However, the rate at which the diameter shortens after the fill height is above the crown is much more rapid for the elastic model than is the case for the Duncan-Chang model. This illustrates, again, that an elastic soil model that is "equivalent" for one aspect of the problem may not be equivalent for another aspect.

Curves 6 and 7 in Fig. 4.28b were obtained using the same computer logic and construction layer sequence: the difference in results stems solely from the difference between the extended Hardin and Duncan-Chang





NOTE : ALL CURVES , EXCEPT ⑤ , PROVIDE FOR FULL SLIP UP TO SPRINGLINE

FIGURE 4.28a CHANGE IN VERTICAL DIAMETER VERSUS FILL HEIGHT, 10ft DIAM. STEEL PIPE



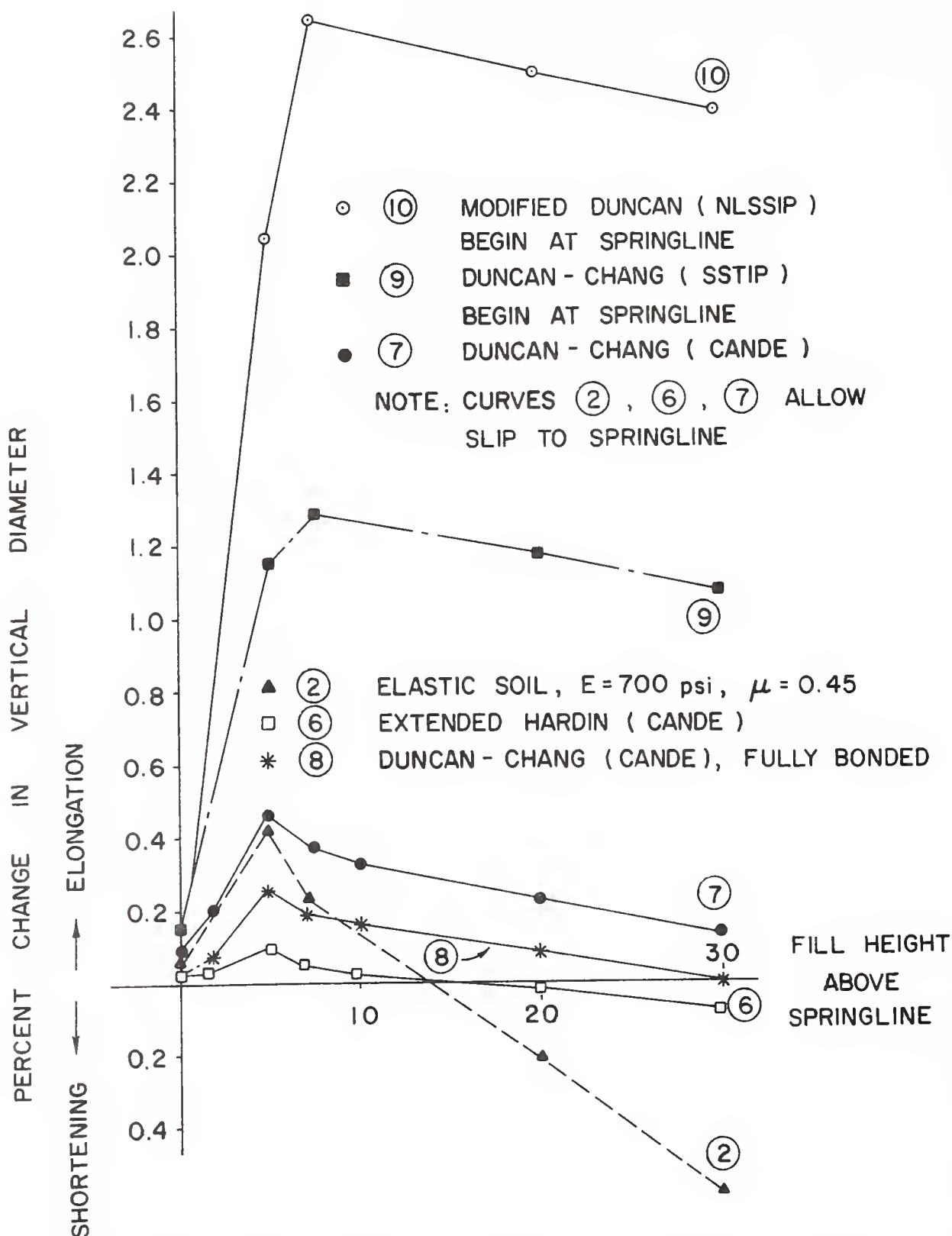


FIGURE 4.28b CHANGE IN VERTICAL DIAMETER VERSUS  
FILL HEIGHT, 10 ft. DIAM. STEEL PIPE





soil models. Noting that the soil parameters for these two models were obtained from the same set of triaxial test data, using procedures recommended by their authors, the observed differences reflect inherent differences in the models and not the errors associated with correlations between the soil parameters and the results of classification tests. It is felt that the response indicated by the extended Hardin model is too small for a 10 ft diam. conduit of 18 gage 2 2/3 x 1/2 in. corrugated steel pipe, even for a case where compaction loads are not applied.

The large differences between curves 7 and 9, which utilize the same soil model, is due to the differences between CANDE and SSTIP codes.

These differences include:

- (1) SSTIP begins the analysis at the springline while CANDE starts from the pipe invert
- (2) SSTIP iterates only once on the nonlinear soil modulus while CANDE iterates to convergence
- (3) SSTIP assumes the pipe wall is elastic throughout while CANDE permits yielding
- (4) SSTIP has a somewhat different sequence for placement of soil layers than CANDE.

It is not possible to determine what portion of the differences between curves 7 and 9 is due to the separate effects enumerated above; however, CANDE's treatment of the first three items is superior to that of SSTIP. The opportunity to vary the fourth item is available in both codes, and the effects of different sequences in placing soil layers around the pipe will be examined in section 4.5.2.4.

The discrepancy between curves 9 and 10 can be attributed to the differences in the modified Duncan and Duncan-Chang soil models and to the effect of yielding in the pipe wall section on the need for



satisfying convergence in both the soil and pipe moduli. As the difference between the modified Duncan and Duncan-Chang soil models is believed to be similar to that between Duncan-Chang and extended Hardin (curves 6 and 7), the large difference between curves 9 and 10 emphasizes the need to satisfy convergence requirements more strictly after yielding in the pipe wall is initiated.

From the results of Group 2 problems, it is seen that:

- (a) the overburden dependent model, with  $\mu = 0.32$ , predicts the thrust poorly and gives unrealistic trends in the conduit deflections; with  $\mu = 0.45$  the maximum bending moment seems to be underpredicted,
- (b) analyses using fully bonded interface conditions are unreliable,
- (c) the equivalent elastic soil model with  $\mu = 0.33$  is unrealistic; with  $\mu = 0.45$ , the results agree with those obtained from Duncan-Chang, except for the higher values of soil cover,
- (d) the Hardin model seems to simulate a stiffer soil than that corresponding to a loose sand, and
- (e) the modified Duncan soil model in the NLSSIP code appears to give excessively high deflections and moments.

Additional insight on the relative merits of the different soil models will be derived from the discussion in sections 4.5.2.4 and 5.1.2; however a precise assessment of their merits and limitations will require controlled tests on full-scale buried conduits, with and without compaction loadings.

#### 4.5.2.4 GROUP 3 PROBLEMS - SOIL MODEL - LONG-SPAN ELLIPTICAL PIPE

Duncan (1978, 1979) proposed a Soil Conduit Interaction procedure



(SCI procedure) for the design of flexible metal culverts based on results of finite element analyses using SSTIP and NLSSIP computer codes. Design for deep cover was based on consideration of maximum thrusts. Design for shallow cover was based on consideration of both maximum thrusts and maximum bending moments.

Group 3 problems were solved to compare the maximum thrusts and maximum bending moments in the conduit wall with those obtained from the formulae proposed in the SCI procedure. In this group of problems, elliptical steel pipes with 25 ft span and 6.25 ft of soil cover above the crown were analyzed. The pipe sections ranged from 1 gage 6 x 2 in. corrugation to 18 gage 3 x 1 in. corrugation with rise/span ratios varying from 0.2 to 0.7, (rise being defined as the distance from the springline to the crown). Both linear and nonlinear soil models and various interface slip conditions were used in the analyses; the soil models and corresponding parameters are listed in Table 4.10. The analyses with CANDE code were made in two ways: (1) using standard level 2 with automated mesh generation and specifying a soil height greater than 6.25 ft above the crown; however, the analysis was stopped when the sequential construction layers reached 6.25 ft above the crown, and (2) using extended level 2 with automated mesh generation but specifying different sequences in placement of soil layers.

The maximum thrust,  $P_{\max}$ , in the SCI procedure is evaluated by the following equation:

$$P_{\max} = \underbrace{K_{p1}\gamma S^2}_{(1)} + \underbrace{K_{p2}\gamma HS}_{(2)} \quad \text{Equation 4.1}$$



Table 4.10 Soil Parameters Employed in the Study of Group 3 Problems

| SOIL  |                                   | SOIL PARAMETERS   |
|---|-----------------------------------|---|
| Linear Soil   |                                   | $E = 700 \text{ psi}$ , $\mu = 0.30, 0.40 \text{ and } 0.45$  |
| Fine Sand,<br>Duncan-Chang<br>Model<br>(Wong and<br>Duncan, 1974)                       | SP-16A<br>soil<br>(loose<br>sand) | $\phi = 30^\circ$<br>$K = 280$ , $n = 0.65$ , $R_f = 0.93$<br>$G = 0.35$ , $F = 0.07$ , $D = 3.5$             |
|   | SP-16B<br>soil<br>(dense<br>sand) | $\phi = 37^\circ$<br>$K = 1400$ , $n = 0.74$ , $R_f = 0.90$<br>$G = 0.32$ , $F = -0.05$ , $D = 28.2$          |
| GW, GP, SW, SP<br>Soils with R.C. = 95%<br>Modified Duncan Model<br>(Duncan, Feb. 1979) |                                   | $\phi_o = 36^\circ$ , $\Delta\phi = 5^\circ$<br>$K = 300$ , $n = 0.4$ , $R_f = 0.7$<br>$k_b = 75$ , $m = 0.2$ |
| Overburden Dependent<br>Model, fair compaction  |                                   | Table 4.6 for $E$<br>$\mu = 0.45$   |





where

$\gamma$  = unit weight of soil

$S$  = span of conduit

$R$  = rise of conduit

$H$  = cover depth above the crown

$K_{p1}$ ,  $K_{p2}$  = thrust coefficients, dependent on the ratio  $R/S$

The (1) term corresponds to the maximum thrust due to backfill up to the crown, and the (2) term corresponds to the thrust due to fill above the crown.

Figure 4.29 shows the maximum thrusts versus the rise to span ratio ( $R/S$ ) for the Group 3 problems investigated in this study. The maximum thrusts calculated from the SCI procedure and from ring compression theory (White and Layer, 1960) are also shown in the figure (ring compression theory calculates the maximum thrust as  $P_{\max} = \gamma HS/2$ ). It may be seen that, for shallow cover, the calculated maximum thrusts are practically independent of the conduit sectional properties, the interface conditions or soil models used, or even of the sequence of soil layer placement.\* It is evident that ring compression theory underestimates, and the SCI procedure overestimates, the maximum thrusts in the conduit wall. Half the weight of the soil vertically above the springline gives a good approximation to the calculated maximum thrust.

The maximum bending moment in a conduit wall has been found to be related to the relative stiffnesses of the soil and the conduit defined

---

\*Although not shown in Figure 4.29, the maximum thrust is approximately proportional to the soil unit weight.



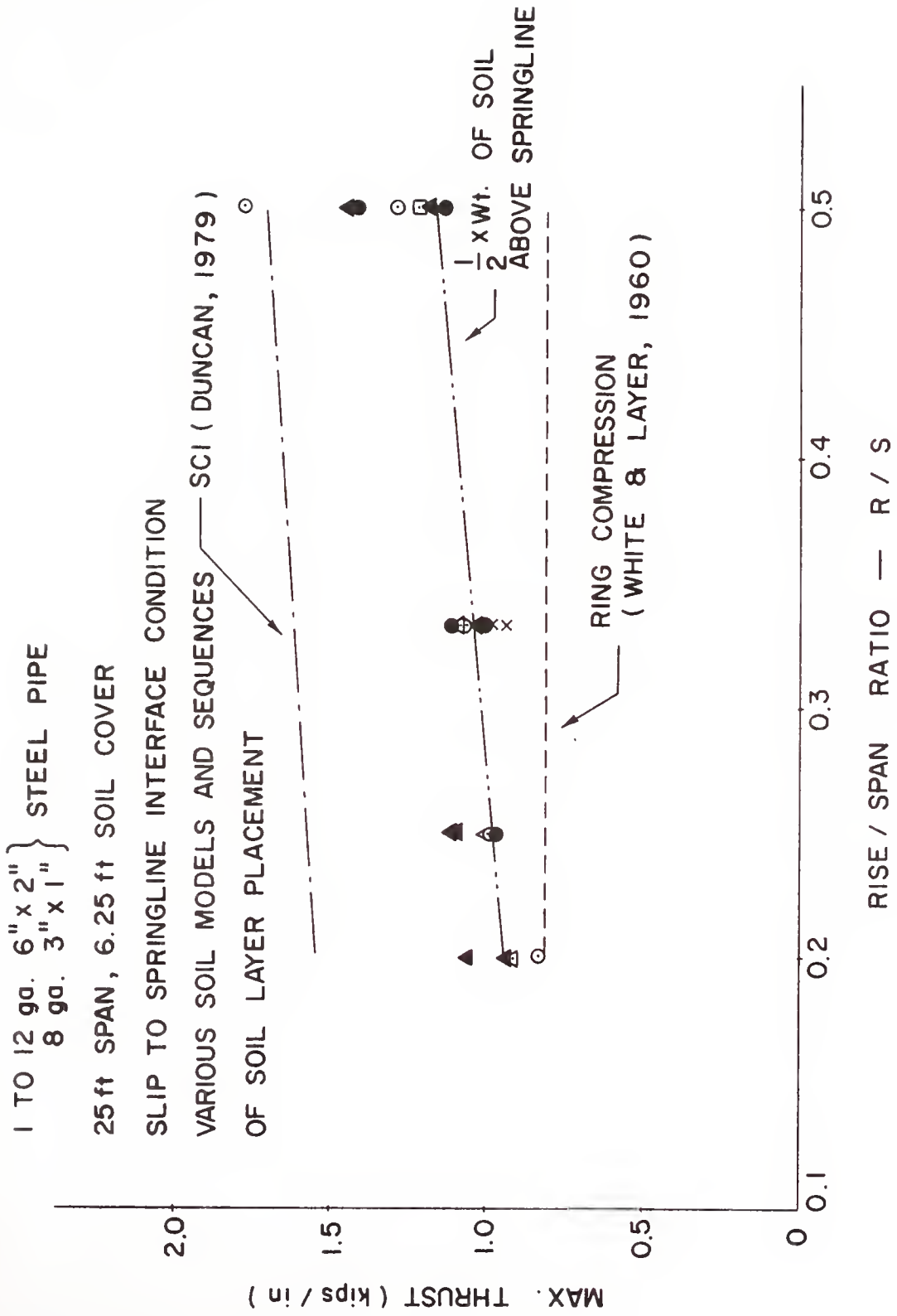


FIGURE 4.29 EFFECT OF RISE / SPAN RATIO ON MAXIMUM THRUST



as (Allgood and Takahashi, 1972):

$$N_f = \frac{E_s S^3}{EI} \quad \text{Equation 4.2}$$

where

$N_f$  = flexibility number (dimensionless)

$E_s$  = secant modulus of the soil

$E$  = Young's modulus of the conduit

$I$  = moment of inertia per unit length of  
the conduit section

$S$  = span of the conduit

In the SCI procedure, the maximum bending moment due to backfilling is evaluated by the following equation:

$$M_{\max} = R_B \left( \underbrace{k_{m1} \gamma S^3}_{(1)} - \underbrace{k_{m2} \gamma S^2 H}_{(2)} \right) \quad \text{Equation 4.3}$$

where

$H$  = height of soil cover above the crown

$R_B$  = moment reduction factor

$k_{m1}, k_{m2}$  = moment coefficients dependent on the flexibility  
number,  $N_f$  (Duncan, 1979)

The (1) term corresponds to the bending moment at  $H = 0$ ; the (2) term represents the bending moment due to fill above the crown. Equation 4.3 is valid for height of soil cover above the crown, from 0 to 0.25S only.

The factor  $R_B$ , which is intended to account for the shape of the ellipse, was investigated. In the SCI procedure,  $R_B$  was expressed as a function of the ratio of rise to span,  $R/S$ . A series of analyses was performed using different soil models and with  $R/S$  ranging from 0.2 to 0.7. The results are shown in Figures 4.30a and b.



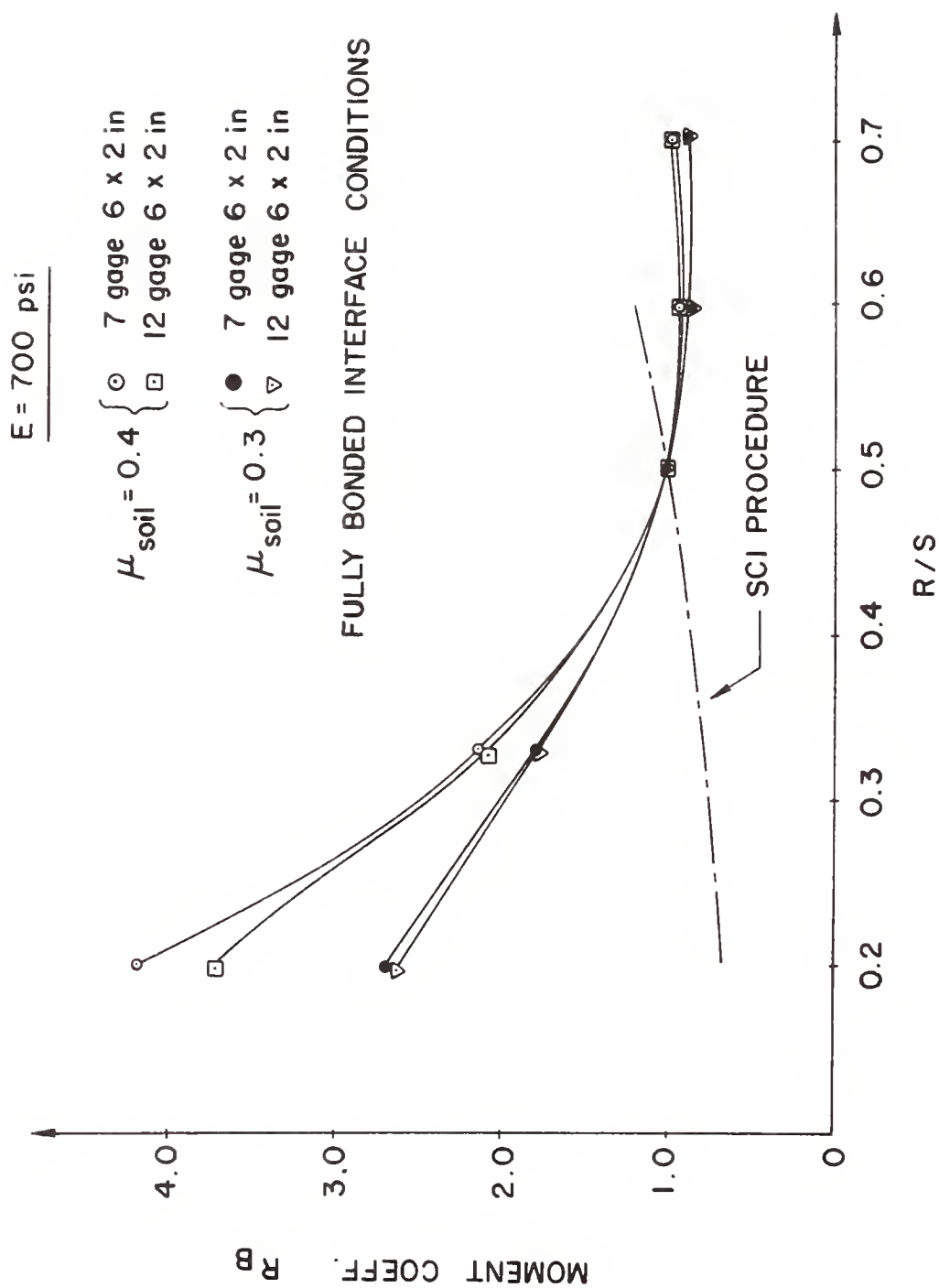


FIGURE 4.30a MOMENT REDUCTION FACTOR VERSUS RISE /SPAN RATIO ,  
LINEAR SOIL MODEL





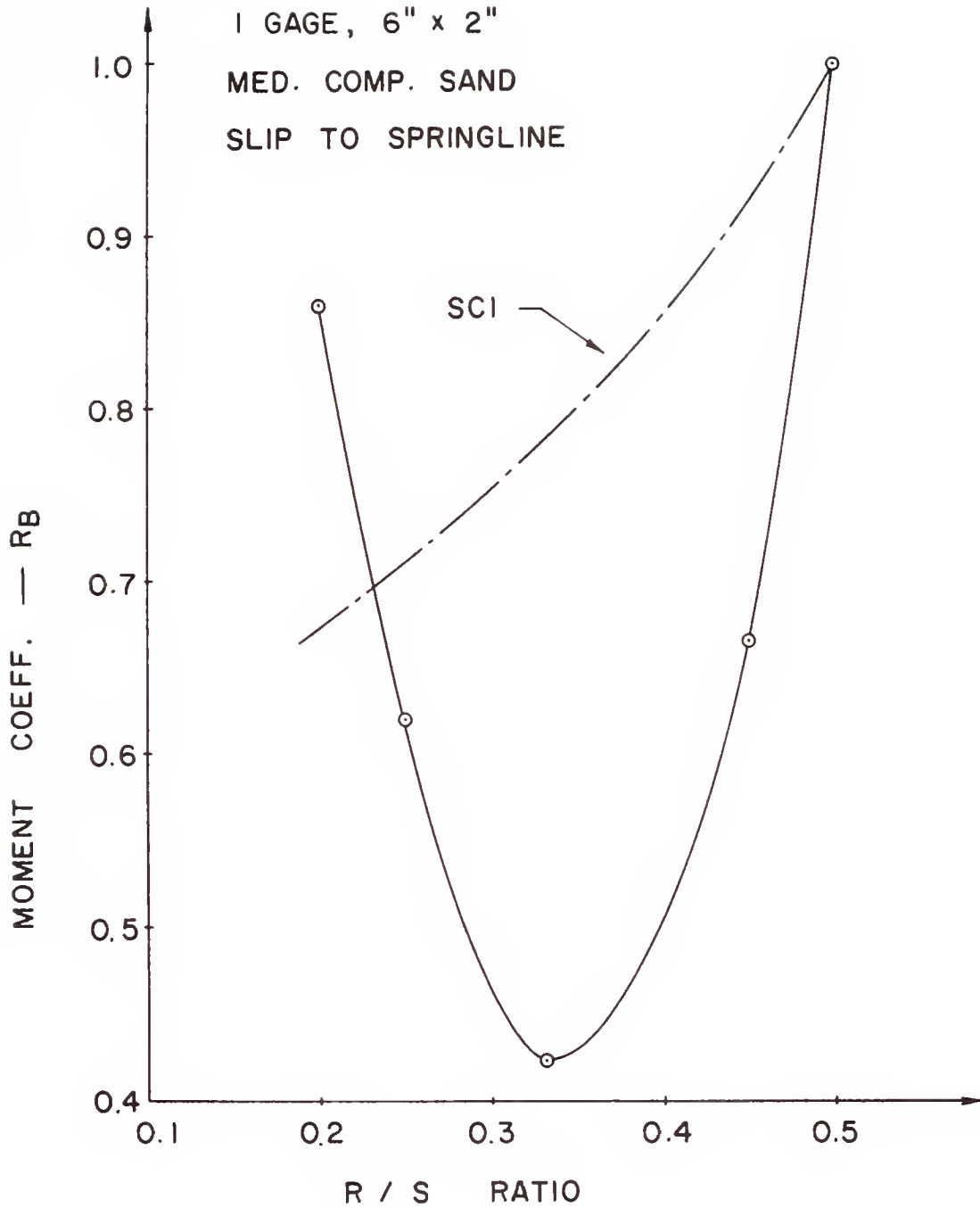


FIGURE 4.30b MOMENT REDUCTION FACTOR,  $R_B$ , VS. RISE / SPAN RATIO,  $R/S$ , DUNCAN-CHANG SOIL MODEL



The trend of  $R_B$  variation with the rise/span ratio differs significantly from that proposed in the SCI procedure and is highly dependent on the soil model used in the analysis. Comparing Fig. 4.30a with 4.30b, the difficulties associated with choosing an "equivalent" elastic soil model are, once again, apparent.

The discrepancy between the calculated values of  $R_B$  and those given by the SCI procedure is due in part to the fact that in the SCI procedure the magnitude of the factor  $R_B$  was determined at  $H = 0$  and was assumed to be applicable at other fill heights; however, in the case of the flat arches, the maximum bending moment occurs at  $H > 0$ . Accordingly, it appears that the formulation of Equation 4.3 is not generally valid.

The maximum moments in the conduit walls for the full range of corrugated metal conduits applicable to the conditions of the Group 3 problems (values of  $H = 6.25$  ft and  $R/S = 0.33$  remained constant) were plotted as a function of flexibility number  $N_f$  in Figure 4.31. The maximum moments computed by Equation 4.3 were also shown in the figure. Evaluation of  $E_s$  for soils with nonlinear properties is difficult since the modulus employed in each soil element in the system is not the same. Also, the modulus in a soil element varies with loading condition. To calculate  $N_f$ , values of  $E_s$  recommended by Duncan (1979) were adopted.

The results shown in Figure 4.31 show what has been found to be true in general: an increase in the relative stiffness of the soil to that of the conduit,  $N_f$ , results in a reduction in the maximum bending moment. The results obtained clearly show that soils with high Poisson's ratio effectively reduce the maximum bending moments, especially for the stiffer wall section. In the latter cases, the fully bonded condition has the effect of increasing the calculated bending moments by 40 to 50 percent.

As may be seen from Figure 4.31, Equation 4.3 does not provide



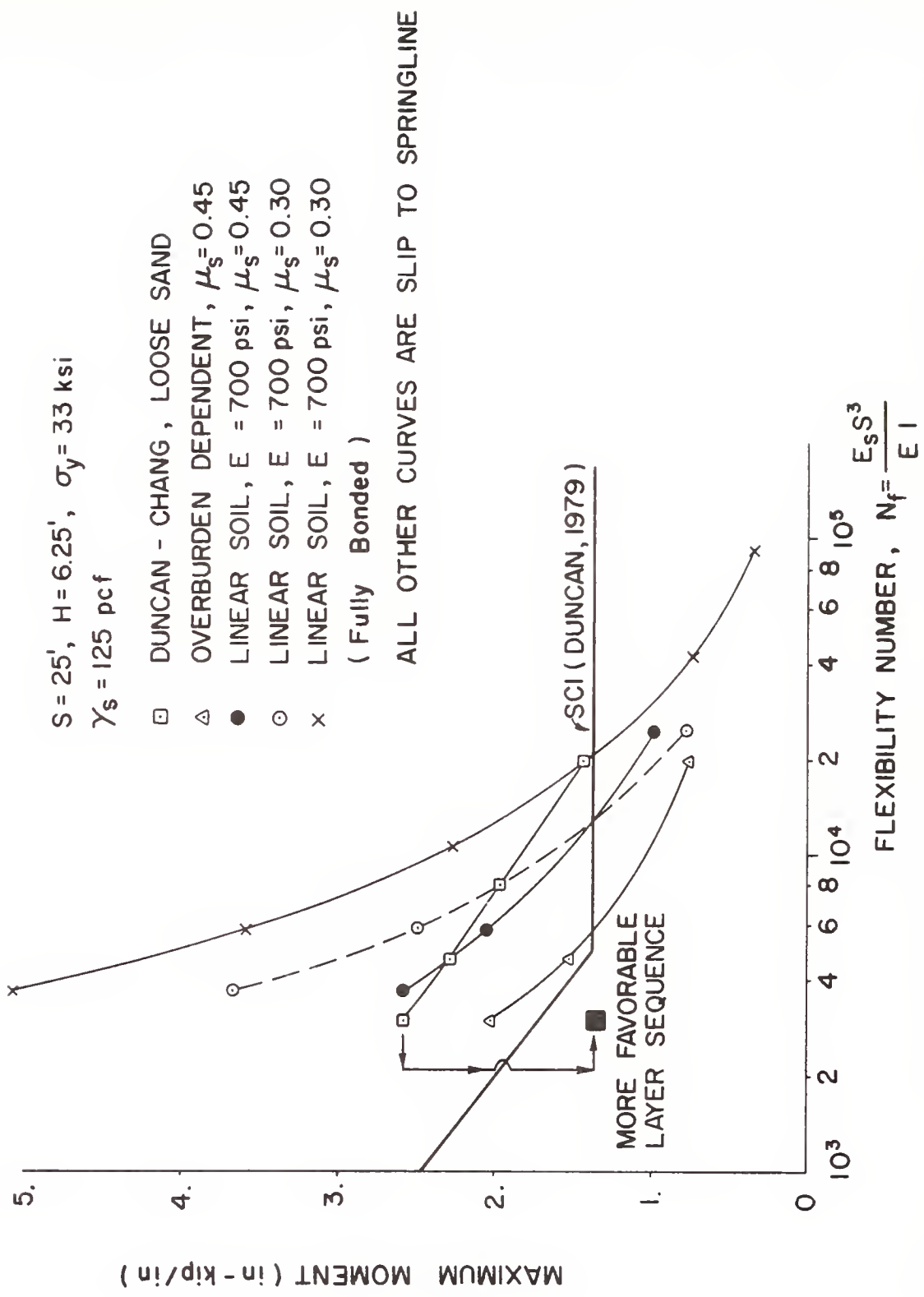


FIGURE 4.31 MAXIMUM BENDING MOMENT VS. FLEXIBILITY NUMBER,  $R/S = 0.33$



conservative estimations of the maximum moments in the conduit walls compared with those calculated using the soil models listed in the Figure, including the Duncan-Chang model. The explanation for this apparent anomaly is that the soil layering sequence used in CANDE differs from that in NLSSIP, as illustrated by the results shown in Figures 4.28a and b. This prompted a separate study of the effects due to different sequences in the placement of the soil layers, which will be described in Section 4.5.3.

It is to be noted that for design purposes the SCI procedure proposed the following formula for evaluation of a factor of safety,  $F_p$ , against development of a plastic hinge (considering both the thrust and moment in the section):

$$F_p = 0.5 \frac{P_p}{P} \sqrt{\left(\frac{M}{M_p}\right)^2 + \left(\frac{P}{P_p}\right)^2 + 4} - \left(\frac{M}{M_p}\right)\left(\frac{P}{P_p}\right) \quad \text{Equation 4.4}$$

in which  $P_p$  = squash load of the section in the absence of bending moment;  $M_p$  = fully plastic moment of the section in the absence of thrust;  $P$  = thrust in the section; and  $M$  = moment in the section. The formula was derived on the basis of the criterion for plastic hinge formation (Equation 2.20), in which the value of  $M$  is the moment about the centroidal axes of the wall section. Accordingly, it is inappropriate to use the moment about other axes (CANDE code before modification, and NLSSIP code, for example) for evaluation of this factor of safety. Moreover, the SCI procedure recommended use of a factor of safety of 1.65 or more against development of a plastic hinge. As bending moments exceeding those permitted using a safety factor of 1.65 often develop during the construction phase without adverse effects, it is felt that imposing this general requirement is unduly restrictive.





Insight into the consequences of approaching a plastic hinge in the wall section can be gained from a plot of  $M/M_p$  vs.  $P/P_p$  as defined in equation 2.20. An example of such a plot is shown in Figure 4.32 (for clarity, only one point in the wall section for each case has been plotted; in practice several key points can be followed on the same diagram). In this plot the ratio of the distances  $\overline{OA}/\overline{OB}$  is the factor of safety  $F_p$  given in equation 4.4.

Considering first the results from the conduit with a 25 ft span, the lowest safety factor against formation of a plastic hinge,  $F_p = 1.1$ , occurs during construction when the fill height is near the crown; at this time, a substantial fraction of the wall section has yielded. However, as long as care is exercised during construction, there is no danger from allowing  $F_p$  to be as low as 1.1. As the fill height is increased the thrust also increases, but the corresponding decrease in bending moment is such that  $F_p$  actually increases (to a value of 1.2 at  $H = 28.5$ ). Further increases in fill height cause  $F_p$  to decrease until at  $H = 50'$  it is again reduced to 1.1. Although  $F_p$  is only 1.1, there is no danger of collapse as the fill height could be increased at least to 80' before the squash load in the wall section is approached. The danger lies in the potential for snap through buckling, which is the reason why this mode of failure is such an important design consideration for large-span conduits. It also suggests that, in practice, stiffening ribs may need to function more as a guard against buckling than as additional resistance to bending.

In the case of the 10 ft diameter culvert, bending is not a significant factor provided the backfill is granular and reasonably well compacted. Increases in fill height manifest themselves largely as increases in thrust; thus, it is not the height of soil cover but the span of the conduit that plays the key role controlling the mode of soil-conduit interaction.



## CIRCULAR STEEL CONDUIT

SLIP TO SPRINGLINE, DUNCAN - CHANG SOIL MODEL

MODERATELY COMPACT SAND (16 - A)

○ 25' SPAN, 1 gage 6" x 2" CORRUGATION, NEAR 3/8-POINT

△ 10' SPAN, 18 gage 2 2/3" x 1/2" CORRUGATION, AT SPRINGLINE

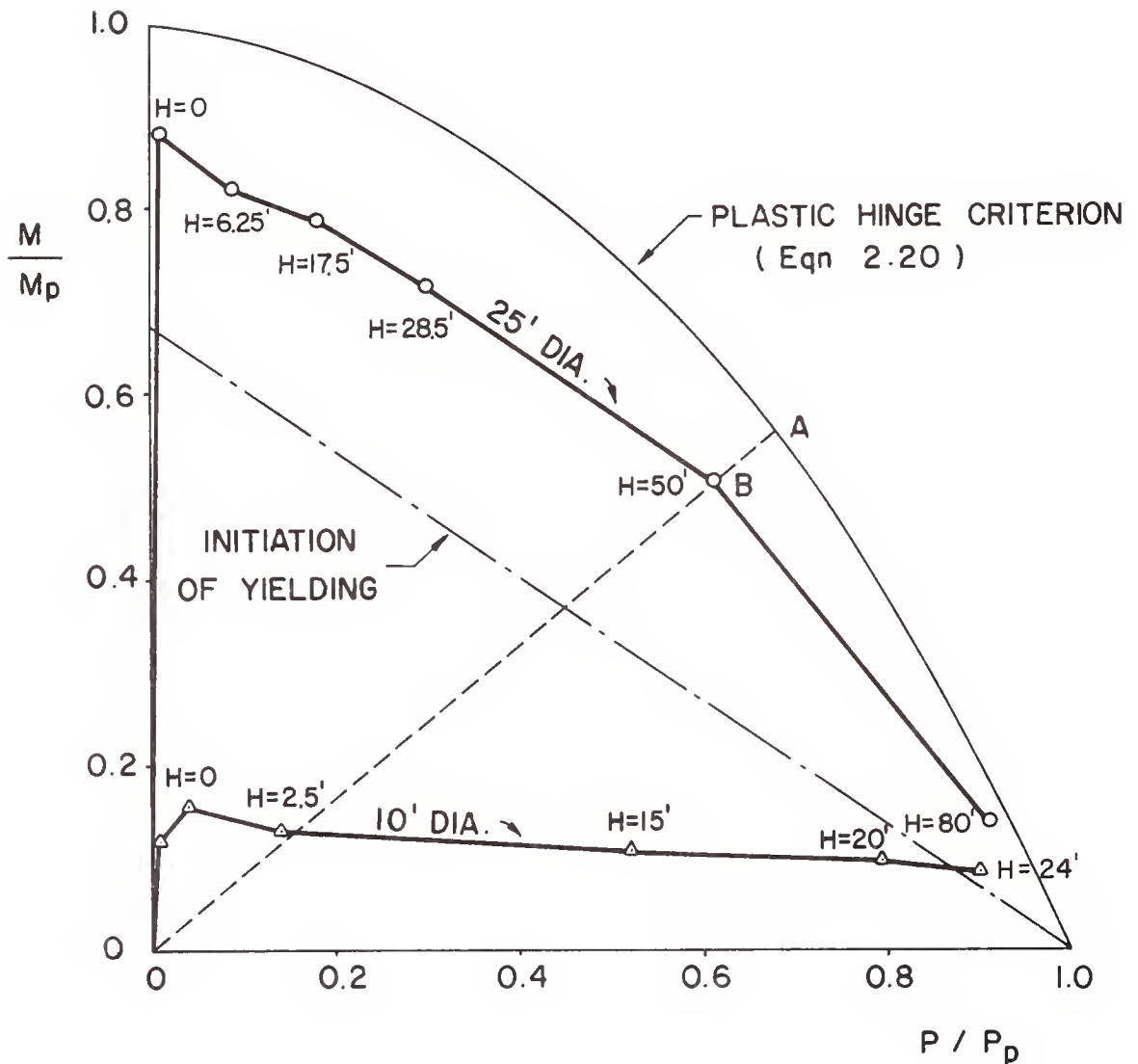


FIGURE 4.32 SUGGESTED METHOD FOR EXAMINING POTENTIAL CONSEQUENCES OF YIELDING AND PLASTIC HINGE FORMATION IN THE WALL SECTION



From the investigation of the SCI procedure (Group 3 problems) it is concluded that:

(a) the Duncan-Chang soil model in the CANDE code is the most generally useful model currently available for the purpose of predicting soil-conduit interaction behavior,

(b) the SCI equations usually overpredict the maximum thrust but may underpredict the maximum bending moments in long-span, corrugated steel culverts with shallow cover,

(c) the SCI formulation for bending moment, to account for the effects of varying the rise/span ratio, is not generally valid, and

(d) the unqualified requirement of a safety factor of 1.65 with respect to formation of a plastic hinge is considered to be unduly restrictive, particularly during the construction phase of a project.

#### 4.5.3 SEQUENCE OF SOIL LAYER PLACEMENT

As pointed out previously, the comparisons between CANDE and NLSSIP codes brought into focus the sensitivity of conduit response to modest variations in the sequence of placing soil in layers around and over the conduit. It became evident that, when comparing predictions with field measurements, failure to model the sequence of soil placement closely could invalidate the conclusions that were drawn---a fact that previously was not fully appreciated by the Authors. To illustrate the importance of this factor, comparisons were made between two loading sequences, "more favorable" and "less favorable" from the standpoint of inducing maximum bending moments in conduits with shallow cover. The layer sequences were chosen not to simulate actual construction practices but to provide a range that would bracket a majority of such procedures. Examples of the sequences adopted for this purpose are shown in Figure 4.33a for a circular conduit, and in



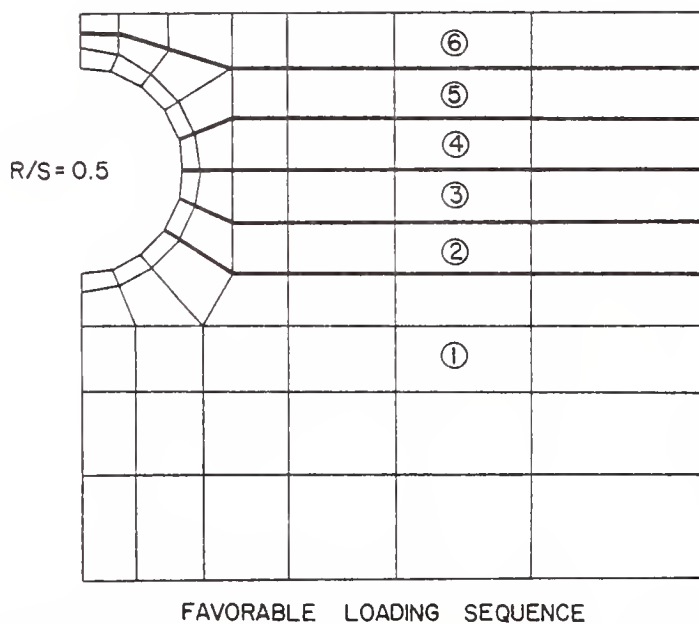
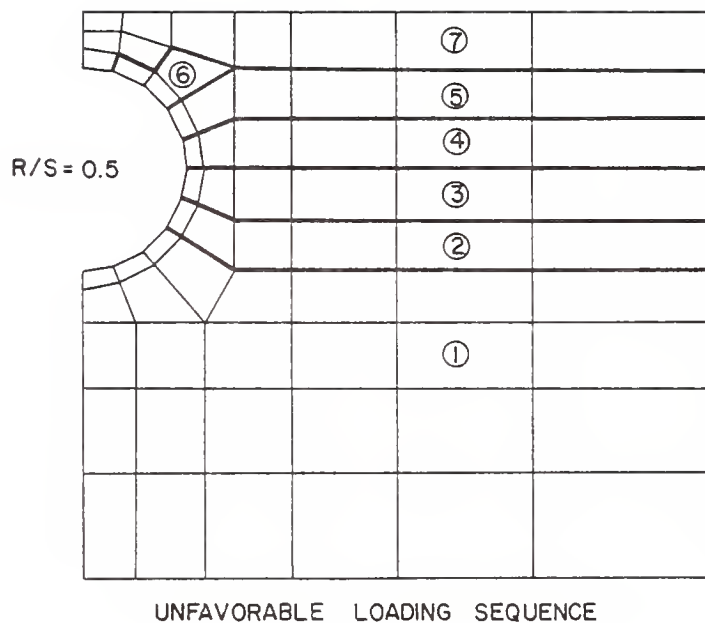


FIGURE 4.33  $\alpha$  FAVORABLE AND UNFAVORABLE LAYER SEQUENCE FOR CIRCULAR CONDUITS





Figure 4.33b for an elliptical conduit with  $R/S = 0.25$ . The corresponding effects on the maximum bending moments are illustrated in Figure 4.34. Even for the case of a dense sand backfill, the increase in bending moment is 75 percent when  $R/S = 0.25$  and 280 percent when  $R/S = 0.5$  (circular conduit). A similar phenomenon is observed from the standpoint of inducing maximum thrusts except that a layer sequence that is "unfavorable" for bending moments is usually "favorable" for thrust, and vice versa. These results clearly show the necessity of modeling the soil placement sequence as closely as possible to obtain meaningful comparisons between predicted and observed performance.



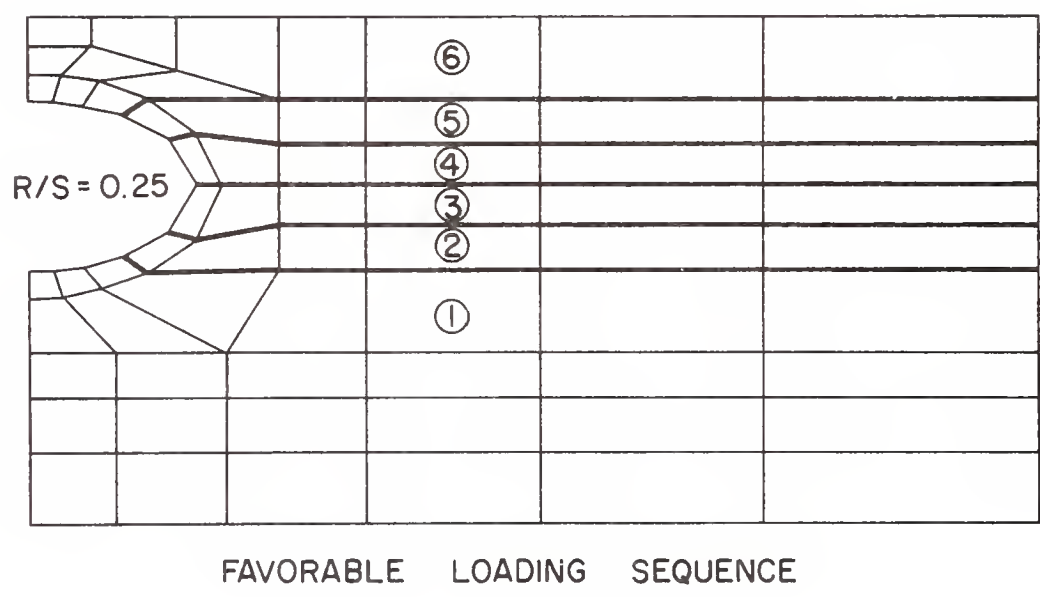
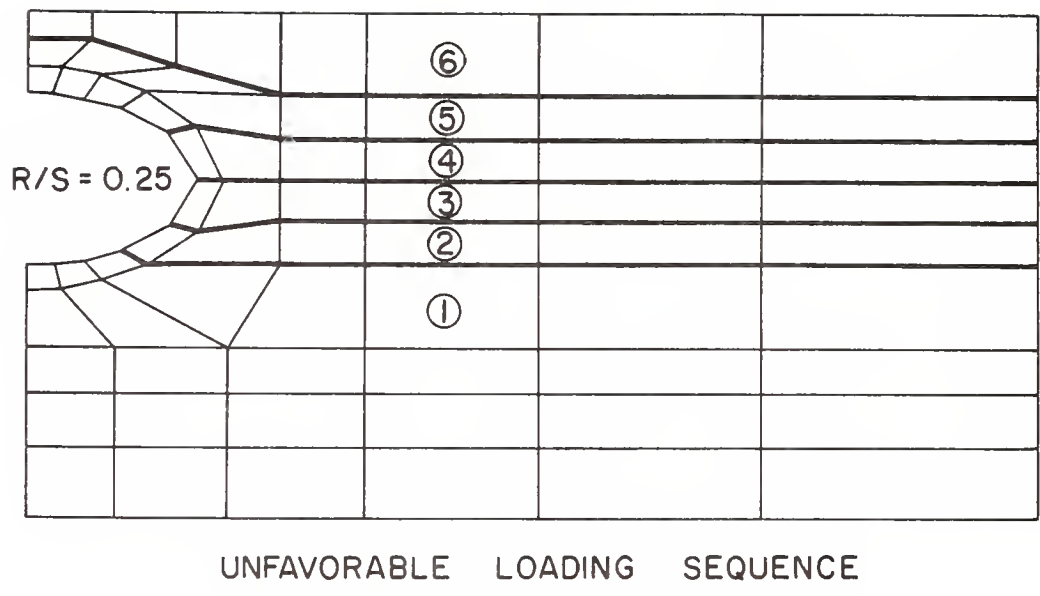


FIGURE 4.33b FAVORABLE AND UNFAVORABLE LAYER SEQUENCE FOR ELLIPTICAL CONDUITS



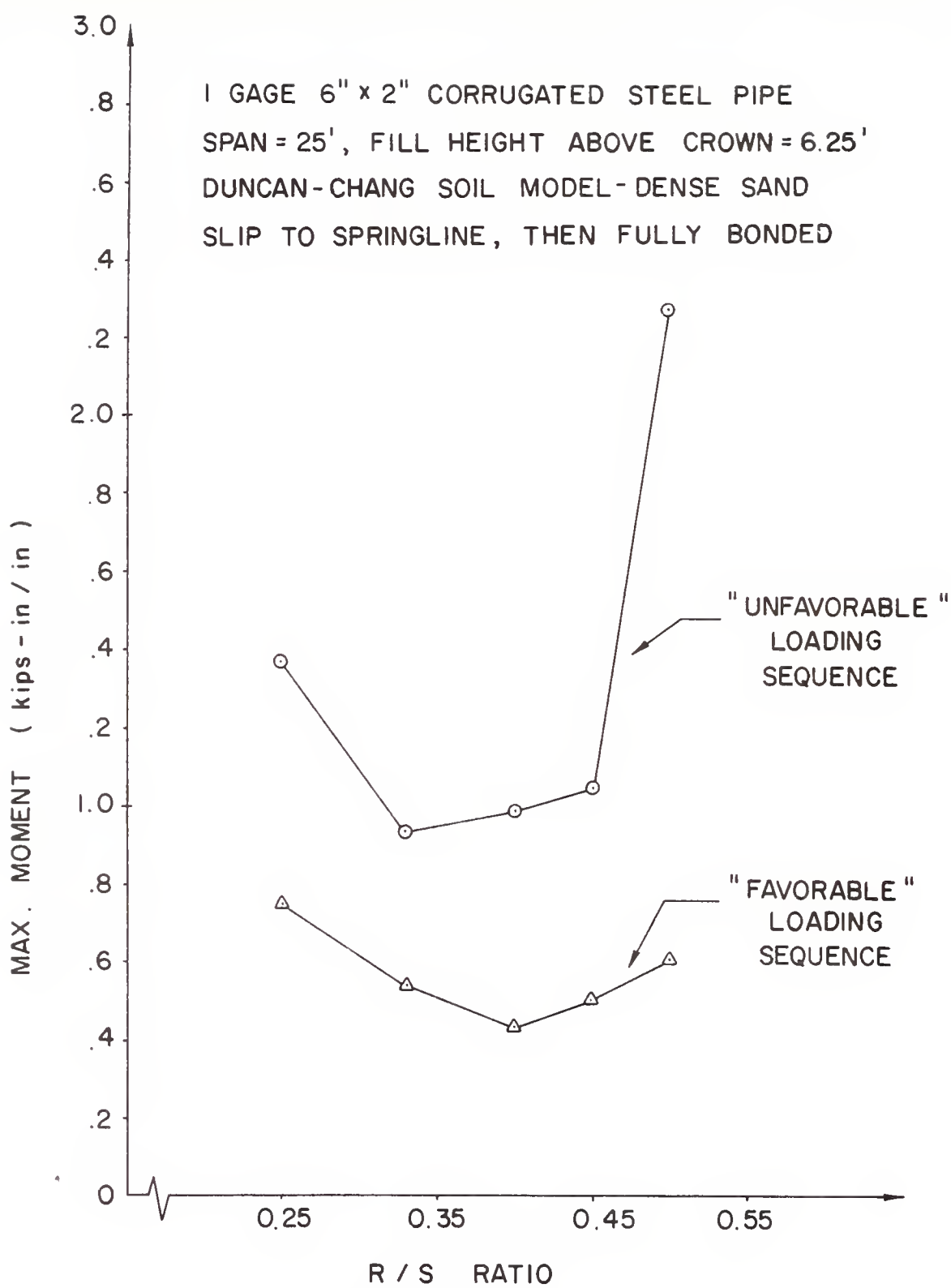


FIGURE 4.34 EFFECT OF SOIL LAYER SEQUENCE ON RELATION BETWEEN MAXIMUM BENDING MOMENT AND RISE / SPAN RATIO



## CHAPTER 5 EVALUATION OF PREDICTION CODES

In Chapter 3, the main features of the computer codes investigated in this study were presented, and in Chapter 4 the results of analyses on a variety of soil-conduit interaction problems were documented in detail. In this chapter, an evaluation of the computer codes is made with emphasis on their advantages and limitations for predicting performance of buried conduits.

There are five limitations common to all the four codes investigated in this study:

- (1) they are useful only for situations where a plane strain approximation is an adequate description of insitu behavior,
- (2) they can not be used to analyze problems involving large deformations (e.g., snap through buckling of the conduit),
- (3) only static loads are considered,
- (4) the soil-conduit system responses are assumed to be time-independent, and
- (5) the soil models incorporated in the codes are capable of representing soil behavior only if loading is monotonic in a relatively fixed stress path, and the soil is not stressed to a failure condition; thus, phenomena associated with soil compaction and propagation of local shear failures in the soil mass cannot be simulated adequately.

In the following, other advantages and limitations of each of the codes are presented.

### 1. FINLIN Code

FINLIN was designed to deal with the investigation of problems in which construction in layers is simulated, slip and no tension at the soil-conduit interface is accounted for, and allowance is made for the





possible development of tensile stresses in adjacent soil elements.

The investigations would be carried out using the most realistic non-linear elastic soil model that could be developed (fitting actual plane strain test data with cubic spline functions and calculating incremental values of  $E$  and  $\mu$  as function of octahedral normal and shear stress levels, accounting fully for dilatancy effects up to the development of shear failure). The soil weight of a construction layer was applied to the system in specified number of increments. At this stage yielding in the conduit wall was not accommodated.

It was found that:

(1) the procedure used to simulate sequential construction was defective,

(2) difficulties with convergence were frequently encountered when attempts were made to account for the development of tensile stresses in the soil mass, and

(3) numerical instabilities developed when the conduit stiffnesses were in a range normally encountered with corrugated metal conduits.

Because these limitations are severely restrictive, some effort was expended to eliminate them, but they were not entirely successful. In view of this, and the fact that FINLIN was not designed to account for yielding in the conduit wall, attempts to develop FINLIN further were abandoned. Further use of this code is not recommended, although the soil model used therein could be adopted in other codes.

## 2. CANDE Code

CANDE was designed to investigate problems in which sequential construction procedure is simulated, relative movements at the soil-conduit interface is accounted for, and nonlinear behavior in the conduit wall



(including the initiation of cracking in concrete) is accommodated. Four soil models (linear elastic, overburden dependent, and two forms of the extended Hardin model) are available for characterization of soil behavior. Different conduit materials, including steel, aluminum, reinforced concrete, and plastic, were accommodated. For each construction layer, iterative procedures were employed to deal with the nonlinear system responses. An automated mesh generation scheme (for circular and elliptical conduits) was incorporated.

It was found that:

(1) CANDE was more general and better documented than the other codes; the automated mesh generation provided a convenient and efficient tool for use of the code,

(2) the soil models incorporated in CANDE are less satisfactory than those in the other codes: the overburden dependent model is totally unsatisfactory; the Poisson's ratio function in the extended Hardin model does not always give a good representation of the volumetric change characteristics of the soil; and the Hardin formula for relating soil index properties to the parameters in the Hardin model (secant shear modulus formulation) was found to be defective,

(3) difficulties with convergence were encountered when attempts were made to account for relative movements at the soil-conduit interface; the difficulties increased in frequency and severity when nonlinear soil models were used, especially when local failure in the soil mass occurred. Convergence problems with the nonlinear conduit properties also frequently arose with non-linear soil models when plastic hinging of the conduit wall was approached, and

(4) the formulation to accommodate nonlinear behavior of the conduit



wall incorporated in CANDE satisfied equilibrium, kinematics, and stress-strain relationships at each load step; however, once yielding of a wall section was initiated, the method of calculating bending moment in the wall section, which was the sum of increments of moments about different axes, was misleading, as it was used incorrectly to calculate stress distributions in the conduit wall; moreover, the use of summed bending moments is not appropriate for defining conditions corresponding to a fully plastic hinge.

### 3. SSTIP Code

SSTIP was designed to deal with the investigation of problems in which in-situ stresses (pre-existing stresses) in the soil and the conduit are accommodated, and construction in layers is simulated. The Duncan-Chang model was employed to represent the behavior of the soil. A "one-iteration" procedure for accommodating nonlinear behavior was adopted. Relative movements at the soil-conduit interface were not allowed, and the stress-strain relationship of conduit materials was assumed to be linear elastic.

It was found that:

(1) As slip at the soil-conduit interface is not accommodated, beginning the analyses with soil up to the springline (the soil below the springline would be assigned initial stresses based upon assumed insitu states) is desirable,

(2) The Duncan-Chang soil model used in SSTIP was found to be the most generally suitable model for simulating behavior of soil around buried conduits, although in its present form it is incapable of dealing with unloading conditions and errors of unknown magnitude may develop when the state of stress approaches, or exceeds, a failure condition, and



(3) Since no direct check for convergence is made, load increments (soil weight of construction layers) must be carefully controlled, especially during backfilling between the springline and 0.75 times the vertical diameter above the springline.

Use of SSTIP is simple and economical in terms of computational effort; however, as it is unable to accommodate yielding in the conduit wall, it is considered inadequate for prediction purposes.

#### 4. NLSSIP Code

The basic "structure" of NLSSIP code is the same as SSTIP code. In NLSSIP, however, yielding of the conduit wall was accommodated (by deriving an approximate moment-curvature relationship on the basis of bilinear stress-strain relationships). A modified (Duncan) soil model (in place of Duncan-Chang model) was used to characterize the behavior of the soil (section 2.1.2.2).

It was found that:

(1) the load increments had to be very small when a large fraction of a conduit wall section had yielded,

(2) the calculated bending moments were the sum of moment increments taken about different axes, and the derived moment-curvature relationship may not always approximate the effects of plastic yielding with sufficient precision,

(3) NLSSIP does not accommodate slip at the soil conduit interface, and

(4) when local failure occurred in the soil mass, the bulk moduli of failed soil elements were unaffected, but the shear moduli were reduced to very small numbers---simulating the behavior of a liquid; the procedure is believed to be better than that of the other soil models





which reduce both bulk and shear moduli to very small numbers (simulating the behavior of air). When the above procedure for accommodating local failure in the soil mass is incorporated in iterative solution schemes, failure may propagate as the iterative process proceeds. As NLSSIP also adopts a "one iteration" scheme in dealing with nonlinear effects, errors of unknown magnitude are incorporated in the solution. Moreover, the output must be examined in detail to recognize that something may be amiss.

In view of its shortcomings in accommodating nonlinear conduit behavior, in its nonlinear solution technique, and its inability to allow for relative movements at the soil-conduit interface, the NLSSIP code is considered to be inferior to CANDE. Thus, it is concluded that CANDE is the best over-all code currently available for predicting performance of conduits buried in soil. Accordingly, a number of improvements were made in the code as described in the next section.

## 5.1 MODIFICATIONS TO THE CANDE CODE

As stated previously, CANDE was judged to be the best code, overall, for predicting performance of buried conduits. Accordingly, a number of modifications were made to this code to improve its capabilities. These improvements are documented in the following sections.

### 5.1.1 CALCULATION OF STRESS AND BENDING MOMENT IN THE CONDUIT WALL SECTION

Once yielding is initiated in the conduit wall section, each successive load increment induces increments of bending strain about a new bending axis. CANDE calculated the increment of bending moment associated with the increment of bending strains; at the end of any particular load step, the bending moment printed out was the sum of the moment increments about different axes. As the criterion for formation of a plastic hinge (eqns.



2.20 and 2.21, p. 32) is based on bending moments calculated about the centroidal axis of the section, the summed bending moments printed out by CANDE (or by NLSSIP) could not be used to calculate the safety factor against plastic hinging.

CANDE also printed out the stresses due to bending in the extreme fiber of the wall section as the summed bending moment divided by the section modulus of the X-section. This is a meaningless calculation; for example, in the case of steel, whose stress-strain curve was assumed to be elastic-perfectly plastic, total stresses exceeding the yield stress were printed out. Initially, this printout was very puzzling and prompted a careful review of the logic used in CANDE to deal with yielding in the wall section.

It was established that, provided convergence was reached in the 'nonlinear' pipe modulus, CANDE obtained the correct strain distribution in the wall section, i.e., kinematics, compatibility, and stress-strain relations were fully satisfied. To our knowledge, it is the only code available that satisfies all three requirements without approximation. Accordingly, CANDE was modified to calculate the stress distribution from the strain distribution and the stress-strain relation, and to integrate the first moment of the stress distribution to obtain the bending moment about the centroidal axis of the X-section. A listing for this modification is given in Appendix B.

#### 5.1.2 DUNCAN-CHANG AND MODIFIED DUNCAN SOIL MODELS

As explained in section 4.5, the nonlinear soil models used in CANDE--overburden dependent and extended Hardin--were judged to be less satisfactory than the Duncan-Chang model. Recently, the modified Duncan model has incurred favor because, it is claimed, convergence problems are less



severe than with Duncan-Chang. Accordingly, both soil models were incorporated in the CANDE code. A listing for this modification is given in Appendix C.

In section 4.5.2.3 (p. 124) the response of a 10 ft. diam., 18 gage 2 2/3 x 1/2 in. corrugated steel pipe with 30 ft of soil cover above the springline was analyzed using various soil models and computer codes. This problem was also solved using the modified Duncan soil model in the CANDE code and is compared with the previous results in Figure 5.1. Recalling that the same test data were used to obtain the parameters for the two soil models according to procedures recommended by their authors, the following conclusions can be drawn:

- 1) In the CANDE code, neither the Duncan-Chang nor the modified Duncan soil models caused any convergence problems.

- 2) The modified Duncan soil model gave a "softer" response for a 10 ft diam. steel pipe with 18 gage 2 2/3 x 1/2 in. corrugations than the Duncan-Chang soil model.

- 3) If the steel conduit wall is yielding, it is essential that the iterative scheme in the computer code be allowed to proceed until the interaction between nonlinear soil and pipe moduli reaches convergence at the end of each load step.

Detailed studies of convergence problems with the CANDE code revealed that they are most often associated with localized development of tension or shear failures in some of the soil elements. None of the incrementally elastic soil models can deal directly with this problem. The usual procedure is to set a lower bound to the incrementally elastic moduli so that the stiffnesses are reduced sufficiently to simulate failure conditions, but not to such low values that problems of compatibility



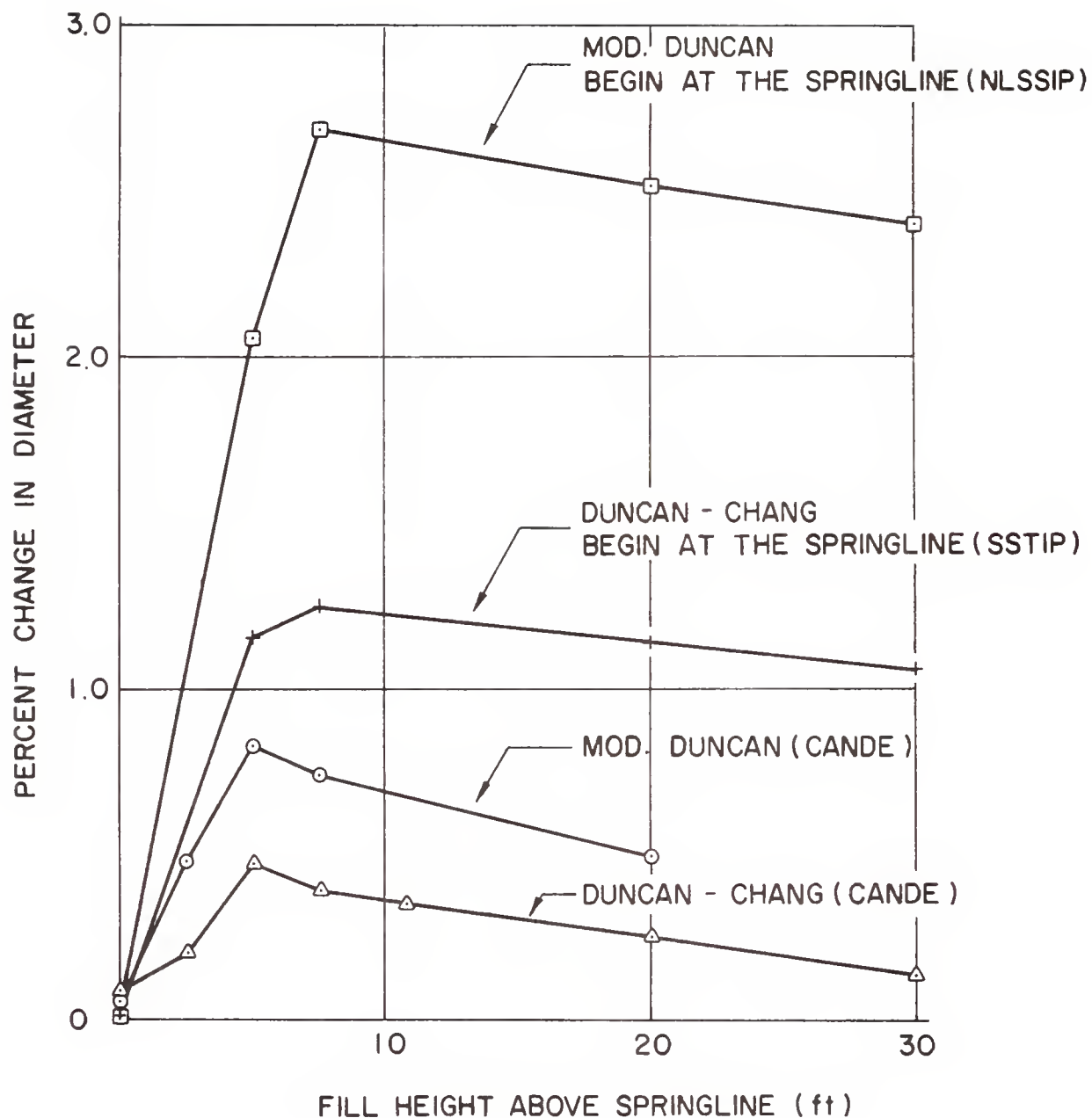


FIGURE 5.1 COMPARISON OF RESULTS OBTAINED USING  
DUNCAN - CHANG AND MODIFIED DUNCAN  
SOIL MODELS





with adjacent stiffer elements are created. For example, in the expression for tangent modulus,  $E_t$

$$E_t = K P_a \left\{ \frac{\sigma_3}{P_a} \right\}^n [1 - R_f \cdot SL]^2 \quad \text{Equation 6.1}$$

where

$K, n, R_f$  = parameters of Duncan-Chang model

$P_a$  = atmospheric pressure

$\sigma_3$  = minor principal stress

$SL$  = shear stress level

it was found that using  $\sigma_3 \geq 0.1 P_a$  and  $0 \leq SL \leq 0.95$  is generally a good compromise to minimize convergence problems on the one hand and to simulate failure conditions on the other. With this scheme, convergence (at the 5 percent level) may be reached although a number of soil elements have failed. Thus, it is important that the computer output be examined to identify the location of failed elements. As the soil models are inherently incapable of dealing with failure conditions, the results should be viewed with caution if more than two adjacent soil elements are found to have failed.

### 5.1.3 AUTOMATIC MESH GENERATION

An attractive feature of the CANDE code is the provision of automatic mesh generation for circular and elliptical conduits. Subroutines are provided in Appendix D to extend this convenience to closed pipe arches. The six basic parameters needed to define the geometry of the pipe arch and a sample of the mesh that is generated are shown in Figure 5.2.

Although there is no direct option for a fully bonded interface, a large



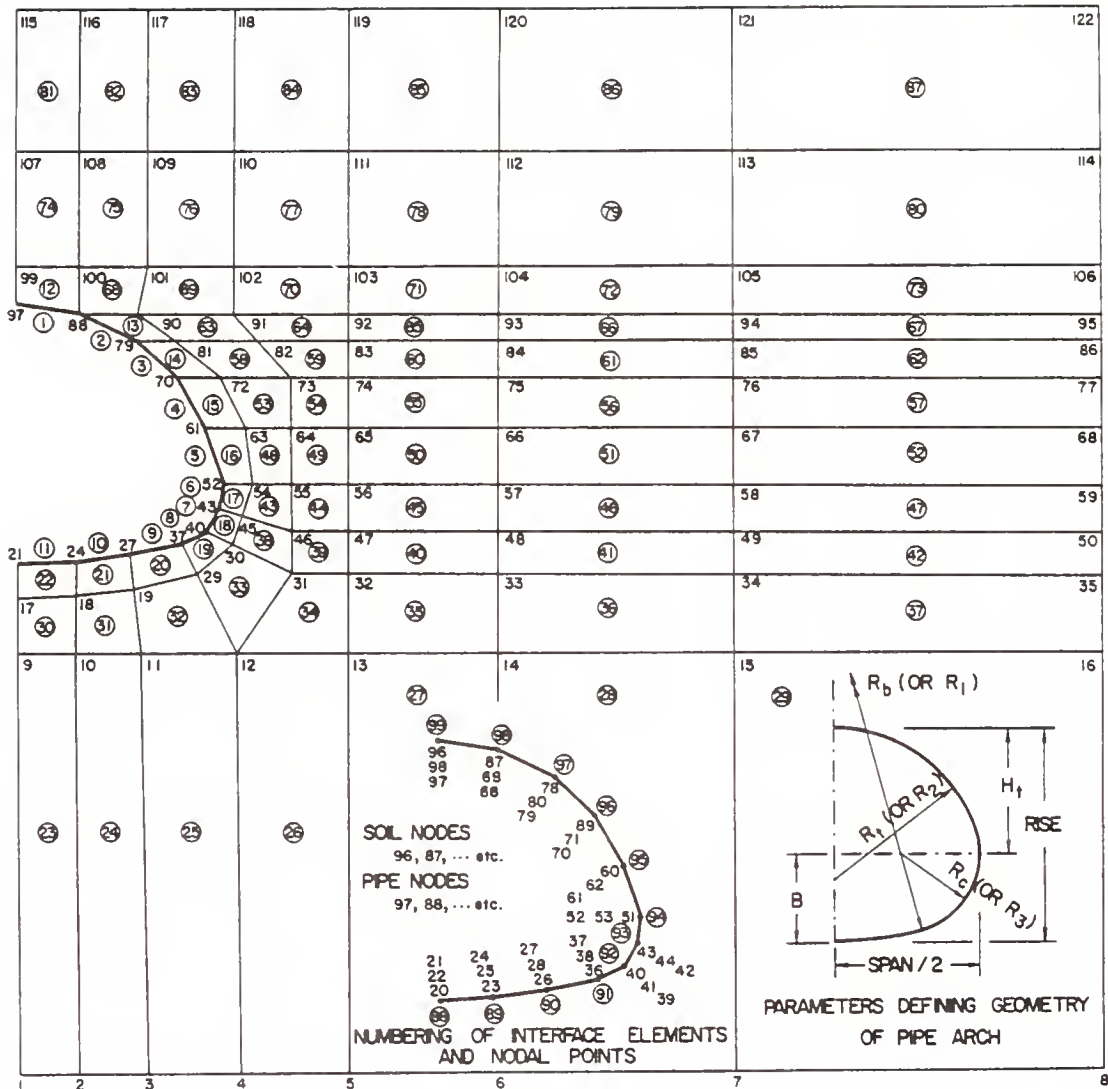


FIGURE 5.2 FINITE ELEMENT MESH AND PARAMETERS  
DEFINING GEOMETRY OF PIPE ARCH



coefficient of interface friction can be specified to simulate this condition. The extended level-2 feature in CANDE can be applied to alter the construction sequence, soil properties, boundary conditions, etc. This mesh has been compared with other proposed schemes and was found to be superior in all respects.

#### 5.1.4 ITERATION NUMBER AND ERROR MESSAGES

CANDE provided three opportunities to control the number of iterations that will be carried out to reach convergence in any particular load step; namely, in the subroutines for soil modulus, for the sectional properties of a yielding conduit wall, and for the selection of appropriate soil-conduit interface conditions. The user has a direct input on the number of iterations for convergence of the soil modulus while the other two were specified directly in the program. If convergence of the nonlinear sectional properties of the conduit was not reached in the specified number of iterations, the program automatically proceeded to the next load step and the following error message was printed out: "NONLINEAR MODULUS DID NOT CONVERGE. SOLUTION WILL CONTINUE WITH A PERCENT ERROR IN MODULUS OF \_\_\_\_."

There are three defects in this error message:

- 1) it is not stated specifically that the pipe modulus (not the soil modulus) is creating the problem,
- 2) the actual printout is in the form of an error RATIO, not as a percentage error, which is misleading by a factor of two orders of magnitude, and
- 3) in comparative studies, it was established that if the nonlinear pipe modulus does not converge the results for the next few load steps (and possibly the entire solution) can be very misleading.



To correct these deficiencies, the program was modified so that if the nonlinear sectional properties of the conduit did not converge after the specified number of iterations the program will automatically stop and the following error message printed out: NONLINEAR PIPE PROPERTIES DID NOT CONVERGE AT THE END OF \_\_\_\_\_ ITERATIONS. THE TOTAL ERROR (RATIO) OF PIPE MODULUS IS \_\_\_\_\_. PROGRAM STOP AT LOAD STEP \_\_\_\_\_. Due to the sensitivity of the solution to errors in the nonlinear sectional properties of the conduit, it is suggested that the iteration number for convergence of this feature be set at 12, and that the program be stopped if convergence is not reached. However, the original CANDE algorithm is retained; i.e., by introducing the word NOSTOP in the main control card the program will continue to the next load step. Although continuation is not recommended, the option is provided in the event the user has a special interest in proceeding with the computations.

If the interface state did not converge in the specified number of iterations CANDE printed out an appropriate warning message and proceeded to the next load step. This warning message was retained but, as in the case of the nonlinear pipe modulus, if convergence is not reached the program automatically stops and the following message printed out:

"WARNING, INTERFACE STATE DID NOT CONVERGE. PROGRAM STOP AT LOAD STEP \_\_\_\_\_. It is recommended that the iteration number for interface state also be set at 12. There is everything to gain if convergence is actually reached in 12 iterations and little to lose (as the program stops) if it does not. Of course, if convergence is reached at a lesser number of iterations, the program will automatically proceed to the next load step.

If the soil modulus did not converge in the specified number of iterations CANDE proceeded to the next load step WITHOUT PROVIDING AN ERROR MESSAGE. This deficiency was corrected by printing out the following





message: "WARNING, SOIL MODULUS IN ZONE \_\_\_\_\_ DID NOT CONVERGE AFTER \_\_\_\_\_ ITERATIONS. STRUCTURE RESPONSE WILL NOT BE CALCULATED. PROGRAM WILL STOP." For the same reason stated previously, it is recommended that the iteration number for soil modulus also be set at 12. However, if the user elects to use NOSTOP, he may wish to set the soil modulus iteration number at a smaller number, thereby significantly reducing costs.

Listings for all these modifications to the iterative scheme and error-message printouts are given in APPENDIX E.



## CHAPTER 6 CONCLUSIONS

This study was undertaken to investigate the behavior of buried conduits using the finite element method. Existing computer codes for analyzing soil-conduit interaction were examined in detail. Analytical simulation techniques for nonlinear, stress-dependent response of soils; yielding and plastic hinging of conduit walls; and buckling behavior were studied. Example problems are given to illustrate the effects of soil response, conduit stiffness, interface behavior, and sequential construction.

The findings and conclusions of these studies are summarized in the following:

1. Prediction of the performance of buried conduits is very sensitive to the manner in which the interaction process is modelled. For good predictions, proper account must be taken of at least the following:
  - (a) Nonlinear Behavior of Soils. The stress-strain-volume change behavior of soils is the most significant factor with regard to the responses of soil-conduit systems. This is especially true when the conduit is relatively flexible compared to the soil. Correct characterization of soils is, thus, crucial in analyzing soil-conduit interaction problems.
  - (b) Yielding of Conduit Walls. Allowance for initiation of yielding of steel (or cracking of concrete) in conduit walls is necessary if potential economies are to be fully realized. Yielding of conduit walls (or slip in the interlocks) will redistribute the soil pressures and maintain an adequate margin



against instability, as long as the associated deflections are not excessive.

- (c) Formation of Plastic Hinges. Plastic hinges can form in the conduit wall before the load capacity of a soil-conduit system has been reached; proper handling of their effects is essential if analytical procedures are to be used to formulate improved design methods.
- (d) Sequential Construction and Soil Compaction. For comparatively shallow cover (say, height of soil cover above the springline less than one diameter) and long-spans (say, greater than 20 feet), simulation of sequential construction is mandatory. At the present time, the influence of soil compaction on conduit response is not fully understood; to simulate the effects of compaction analytically, a plasticity model of soil behavior is needed.
- (e) Relative Movement at the Soil-Conduit Interface. Relative movements (slip, debonding, and rebonding) between the conduit and the surrounding soil occurs in practice; slip can have important effects on conduit performance, especially in the early stages of backfilling.
- (f) Buckling. Buckling of buried flexible conduits can occur at stress levels below yield or after yield has initiated; although buckling may occur at relatively small deflections, present methods of analysis are incapable of estimating its subsequent effects on the load capacity of the system.

2. The main features of the computer codes, FINLIN, CANDE, SSTIP, and NLSSIP are summarized in Chapter 3, and their rela-



tive merits were assessed in Chapter 5. The CANDE code was judged to be the best of the four, because:

- (a) its automated mesh generation procedure provides a convenient and efficient tool for analyzing the response of routine soil-conduit systems. Specifically, it could treat circular and elliptical-shaped conduits buried in soil; the conduit material may be corrugated steel or aluminum, reinforced concrete, or plastic; and sequential construction is accommodated. For very shallow cover (less than  $0.82D$  above the springline) CANDE will routinely place  $0.82 D$  of soil cover, which may introduce errors on the unsafe side if significant live loads are present. To avoid this imperfection, it is only necessary to apply the live loads when the sequential construction layer corresponding to the actual height of soil cover is reached, a procedure which may require the use of extended level-2 in the CANDE code.
- (b) CANDE uses an iteration scheme to treat non-linear behavior and prints out error messages if it fails to converge in a specified number of iterations. This procedure is preferred to the need for studying the entire output for "reasonableness" in codes where the program continues after only one iteration, and with no formal indication there may have been convergence problems.
- (c) the formulation in CANDE for accommodating yielding in the conduit wall is fundamentally correct, that is, equilibrium, kinematics, and stress-strain relationships are satisfied for each load step. Thus, a correct distribution of strains





in the wall section is obtained. However, it is considered undesirable to print out bending moments in a given wall section that is the sum of moment increments taken about different bending axes as yielding in the wall section propagates. The print-out of bending stresses calculated from these moments is incorrect and especially misleading.

- (d) among the methods available for accommodating slip at the soil-conduit interface, the "constraint equations approach" used in CANDE is the best. Unfortunately, it suffered from convergence problems when nonlinear soil models were used; these problems increased in severity and frequency of occurrence when yielding in the wall section was also initiated.

3. The following improvements in the CANDE code are documented in the body of the Report:

- (a) The stress distribution in the wall section is calculated from the strain distribution and the stress-strain relation; using this stress distribution, bending moments are calculated about the centroidal axis of the section. These latter moments are printed out (along with the thrusts and extreme fibre strains) as the structural response of the conduit wall section.
- (b) The Duncan-Chang and Modified Duncan soil models are incorporated in the code.
- (c) Convergence problems with the CANDE code are often associated with the localized development of tension or shear failures in some of the soil elements. None of the nonlinear incrementally elastic soil models can deal directly with these failure conditions. In the case of the Duncan-Chang and modified Duncan



soil models, it was found that using  $\sigma_3 \geq 0.1 P_a$  and  $0 \leq$  shear stress level  $\leq 0.95$  is usually a good compromise to minimize convergence problems on the one hand, and to simulate failure conditions on the other. It is emphasized that the results should be viewed with caution if more than two adjacent soil elements have failed. Convergence problems may also be mitigated by using smaller load steps and more "favorable" sequences in the placement of soil layers.

- (d) It was determined that if the solution fails to converge at any particular load step that the results for the next few load steps may be very misleading. The program was modified so that if the solution fails to converge at any load step in the specified number of iterations a comprehensive error message will be printed out identifying whether the problem is associated with the nonlinear soil modulus, the interface conditions, or the nonlinear pipe modulus after yielding in the conduit wall section is initiated. Then, to save time and money, the program will stop automatically. However, the original algorithm is retained so that, if desired, the user may elect to allow the program to continue its solution scheme even though the convergence check is not satisfied.
- (e) An attractive feature of the CANDE code is the provision for automatic mesh generation for circular and elliptical conduits. Subroutines are provided to extend this convenience to closed pipe arches.

4. Results obtained with the five soil models examined in this study are very different, especially with respect to deflections and bending moments in the conduit walls. An "equivalent



elastic" soil model capable of modelling various phases of soil-conduit interaction does not exist (different moduli would have to be selected when considering a given factor, say deflections, at different stages in the construction process; moreover, at any given construction stage different moduli are required to predict different response factors, say deflections, or moments, or the initiation of buckling). In many instances the errors associated with the use of a single set of elastic soil moduli are very large; accordingly, further use of this soil model should be abandoned.

The overburden dependent soil model gave unrealistic results so frequently that its use should also be abandoned.

The formulation of Poisson's ratio in the extended Hardin model is inappropriate and generally results in a stiffer response than that which would be expected from the level of soil compaction. The Hardin formula, which relates soil index properties to the shear modulus parameters, often yields poor representations of the shear stress-shear strain relations. Because these representations are generally unconservative at higher levels of shear strain (when conservative representations are preferred) the use of the Hardin formula is not recommended. The "default" option for the Hardin model in the CANDE code should be abandoned.

The Duncan-Chang soil model gives a good representation of soil response at stress levels where shear-dilatancy effects are such that the increments of volumetric strain are compressive. However, even when this is not the case, the results obtained are still reasonable. When the shear strength of the soil is approached the soil response is poorly modelled; arbitrary limitations on the soil moduli must be applied to avoid convergence problems. The modified Duncan model is very similar to the Duncan-Chang model; given comparable limita-



tions to simulate failed elements, the two models are equally resistant to convergence problems although the response of the modified Duncan model is somewhat "softer" than that of Duncan-Chang. Because it possesses a large data base, so that laboratory tests are not usually needed to select appropriate values of the soil parameters, and because it gives results that are reasonable at moderate stress levels, the Duncan-Chang model is recommended for routine use in studies of soil-conduit interaction.

Spline function representations of actual test data, as formulated in the FINLIN code, is believed to be the best available nonlinear, incrementally elastic soil model for predicting the response of soil-conduit systems. The more slender the conduit wall, in relation to the curvature, the more critical it is to characterize the soil behavior as precisely as possible. The need to obtain actual test data makes the use of this model inconvenient for routine studies.

To simulate the effects of local shear failures in the soil mass, as well as the important consequences of soil compaction procedures, the use of a plasticity model to represent soil behavior is mandatory.

5. The mode of soil-conduit interaction is strongly affected by the interface behavior. For circular conduits, if wall crushing is of main concern, reducing soil-conduit interface friction will be beneficial; however, from the point of view of bending and buckling, the reverse may be true. Predictions based upon results obtained by enforcing fully bonded interface conditions should be viewed with great caution, particularly for conduits with shallow burial. In the case of elliptical conduits, promoting interface slippage was found to be beneficial in all respects.

6. Soil arching can be examined in terms of the ratio:





(1) the maximum thrust in the conduit wall to the weight of soil immediately above the conduit,  $P_{\max}/\gamma H$ ; or (2) the normal pressure at the crown to the free-field normal stress at the crown,  $p_c/\gamma H$ . The ratio  $P_{\max}/\gamma H$  has implications largely with respect to wall crushing, while the potential for yielding and buckling of the conduit wall is more related to the ratio  $p_c/\gamma H$ . Unfortunately, it is possible for the ratio  $P_{\max}/\gamma H$  to indicate negative arching when the ratio  $p_c/\gamma H$  shows large positive arching. In any case, neither ratio--either separately or combined--gives a full indication of soil-conduit interaction. In order to characterize and check the response of soil-conduit systems, the deflected shape, the distributions of normal and shear stresses at the soil-conduit interface, the distributions of thrust and moment in the conduit wall, and the distribution of stresses and strains in the surrounding soil mass are needed.

Design procedures that utilize the above concepts of soil arching, whether explicitly or implicitly, should be used with great caution beyond the empirical data base from which they were derived.

7. The Soil-Conduit Interaction procedure proposed by Duncan (1979) provides reasonable approximations for the maximum thrusts in long-span flexible conduits with shallow cover. However, the predicted bending moments may be unconservative unless a favorable sequence of soil layer placement is adopted. Moreover, the form of the equation for maximum moment is not general, because the effects of rise to span ratio are not adequately simulated. A factor of safety of 1.65 against formation of a plastic hinge, as proposed in the SCI procedure,



is considered to be unduly restrictive, especially in the construction phase of a project.

8. The response of long-span buried conduits is very sensitive to the sequence of placing soil layers around the conduit. When comparing predictions with field measurements, far more attention should be given to the details of soil placement than has heretofore been the case. If strains in the conduit wall are being measured, it is essential that the yield strain at the location of the gages be ascertained; otherwise, it will not be possible to compare predicted vs. observed response on a rational basis.



## CHAPTER 7 RECOMMENDATIONS FOR FUTURE RESEARCH

Further research is recommended in the following areas:

1. In order to verify computer codes for predicting performance of buried conduits, controlled, full scaled laboratory tests are imperative. Through comparisons of predicted soil-conduit system responses and extensive test measurements under controlled conditions the predictive capability of the computer codes can be assessed beyond question.

It is also mandatory to establish buckling and ultimate load criteria for buried flexible conduits so that the applicability of computer codes as design tools can be determined. These criteria can best be established through controlled, full-scaled laboratory tests in which the conduits are loaded all the way to collapse.

2. More study with regard to analytical modelling of soil-conduit interaction is required in the following areas:

- (a) development of more generally applicable models to simulate soil behavior, including plasticity soil models;
- (b) analytical simulation of soil compaction;
- (c) improved procedures to deal with the limited capability of soils to resist tensile stresses;
- (d) provision for varying the stiffness of adjacent beam elements representing the conduit wall section;
- (e) an algorithm to calculate the normal and shear stresses at the soil-conduit interface more correctly; and
- (f) analytical simulation of buckling phenomena.



## ACKNOWLEDGEMENTS

The authors are indebted to Professor M. G. Katona, University of Notre Dame, for helpful discussions on the CANDE code and for assistance in incorporating the Duncan-Chang soil model in CANDE.

Special thanks are due Professor J. M. Duncan, University of California at Berkeley, for making available the SSTIP and NLSSIP codes, for instruction on their effective utilization, and for his constructive criticisms of the draft report.

We owe much to the earlier efforts on this project of M. B. Roy and R. E. Stetkar. Building on their experiences--both good and bad--contributed materially to our understanding of the soil-conduit interaction problem.

Financial support for this research was provided by the State of Indiana and the Federal Highway Administration through the Joint Highway Research Project at Purdue University.





## REFERENCES

1. Allgood, J. R. and Takahashi, S. K., "Balanced Design and Finite Element Analysis of Culverts," Highway Research Record, No. 413, 1972.
2. Anand, S. C., "Stress Distributions Around Shallow Buried Rigid Pipes," J. Struct. Div., ASCE, Vol. 100, No. ST 1, January, 1974.
3. Baladi, G. U., "Lecture Series on Constitutive Equations," U.S. Army Engineer Waterways Experiment Station, Corps of Engrs., November, 1979.
4. Barden, L. and Khayatt, A. J., "Incremental Strain Rate Ratio and Strength of Sand in the Triaxial Test," Geotechnique, Vol. 16, No. 4, December, 1966.
5. Bishop, A. W. and Henkel, D. J., "The Measurement of Soil Properties in the Triaxial Test," Edward Arnold Ltd., London, 1962.
6. Burns, J. A. and Richard, R. H., "Attenuation of Stresses for Buried Cylinders," "Proceedings of the Symposium on Soil-Structure Interaction, University of Alabama, September, 1964.
7. Chan, S. H. and Tuba, I. S., "A Finite Element Method for Contact Problems of Solid Bodies," Intl. J. of Mechanical Sciences, Vol. 13, 1971.
8. Chang, C.-Y. and Nair, K., "Development and Applications of Theoretical Methods for Evaluating Stability of Openings in Rock," Final Report, U.S. Bureau of Mines, Contract No. H0220038, December, 1973.
9. Chelapati, C. V. and Algood, J. R., "Buckling of Cylinders in a Confining Medium," Highway Research Record, No. 413, 1972.
10. Chen, L.-S., "An Investigation of Stress-Strain and Strength Characteristics of Cohesionless Soils by Triaxial Compression Tests," Proceedings, 2nd Intl. Conf. Soil Mech. Found. Engrg., Vol. V, 1948.
11. Chen, W. F., "Plasticity in Soil Mechanics and Landslides," J. of Engrg. Mech. Div., ASCE, Vol. 106, No. EM3, June, 1980.
12. Chen, W. F. and Atsuta, T., "Theory of Beam-Columns, Volume 1 - In-plane Behavior and Design," McGraw-Hill, New York, 1976.
13. Chirapuntu, S. and Duncan, J. M., "The Role of Fill Strength in the Stability of Embankments on Soft Clay Foundations," Report No. TE 75-3, Univ. of California, Berkeley, December, 1975.



14. Christian, J. T., "Undrained Stress Distribution by Numerical Methods," J. Soil Mech. Found. Div., ASCE, Vol. 94, No. SM6, November, 1968.
15. Clough, G. W. and Duncan, J. M., "Finite Element Analyses of Port Allen and Old River Locks," Report No. TE-69-13, Univ. of California, Berkeley, September, 1969.
16. Clough, R. W. and Woodward, R. J., "Analysis of Embankment Stresses and Deformations," J. Soil Mech. Found. Div., ASCE, Vol. 93, No. SM4, July, 1967.
17. Coon, M. D. and Evans, R. J., "Recoverable Deformation of Cohesionless Soils," J. Soil Mech. Found. Div., ASCE, Vol. 97, No. SM2, February, 1971.
18. Corotis, R. B., Farzin, M. H., and Krizek, R. J., "Nonlinear Stress-Strain Formulation for Soils," J. Geotech Engrg. Div., ASCE, Vol. 100, No. GT9, September, 1974.
19. Desai, C. S., "Solution of Stress-Deformation Problems in Soil and Rock Mechanics Using the Finite Element Method," Ph.D. Dissertation, University of Texas, Austin, August, 1968.
20. Desai, C. S., "Nonlinear Analyses Using Spline Functions," J. Soil Mech. Found. Div., ASCE, Vol. 97, No. SM10, October 1971.
21. Desai, C. S., "Overview, Trends, and Projections: Theory and Applications of the Finite Element Method in Geotechnical Engineering," Proc., Symp. Appl. Finite Element Method Geotech. Engrg., U.S. Army Engrg. Waterway Expt. Stn., 1972.
22. Desai, C. S., "Numerical Design-Analysis for Piles in Sands," J. Geotech. Engrg. Div., ASCE, Vol. 100, No. GT6, June, 1974.
23. Desai, C. S. and Wu, T. H., "A General Function for Stress-Strain Curves," Proceedings, 2nd Intl. Conf. on Numer. Methods in Geomechanics, June, 1976.
24. Dimaggio, F. L. and Sandler, I. S., "Material Model for Granular Soils," J. of Engrg. Mech. Div., ASCE, Vol. 97, No. EM3, June, 1971.
25. Domaschuk, L. and Wade, N. H., "A Study of the Bulk and Shear Moduli of a Sand," J. Soil Mech. Found. Div., ASCE, Vol. 95, No. SM2, March, 1969.
26. Drucker, D. C., Gibson, R. E., and Henkel, D. J., "Soil Mechanics and Work Hardening Theories of Plasticity," Transactions, ASCE Vol. 122, 1957.
27. Drucker, D. C. and Prager, "Soil Mechanics and Plastic Analysis or Limit Design," Quarterly of Applied Mathematics, Vol. 10, No. 2, 1952.



28. Duncan, J. M., "Soil-Culvert Interaction Method for Design of Metal Culverts." Transportation Research Record, 678, 1978.
29. Duncan, J. M., "Design Studies for Aluminum Structural Plate Box Culverts," Report to Kaiser Aluminum and Chemical Sales, Inc., Revised Section on Deflections, Feb. 15, 1979.
30. Duncan, J. M., "Behavior and Design of Long-Span Metal Culverts," J. Geotech. Engrg. Div. ASCE, Vol. 105, No. GT3, March, 1979.
31. Duncan, J. M., Byrne, P., Wong, K. S., and Mabry, P., "Strength, Stress-Strain and Bulk Modulus Parameters for Finite Element Analyses of Stresses and Movements in Soil Masses," Report No. UCB/GT/78-02, University of California, Berkeley, April, 1978.
32. Duncan, J. M. and Chang, C.-Y., "Nonlinear Analysis of Stress and Strain in Soils," J. Soil Mech. Found. Div., ASCE, Vol. 96, No. SM5, September, 1970.
33. Duncan, et al., "Soil-Structure Interaction Program," University of California, Berkeley.
34. Duncan, et al., "Nonlinear Soil-Structure Interaction Program," University of California, Berkeley.
35. Felippa, C. A. and Clough, R. W., "The Finite Element Method in Solid Mechanics," SIAM-AMS Proceedings, Vol. II, American Mathematical Society, 1970.
36. Frydman, S., Zeitlen, J. G., and Alpan, I., "The Yielding Behavior of Particulate Media," Can. Geotech. J., Vol. 10, 1973.
37. Ghaboussi, J., Wilson, E. L., and Isenberg, J., "Finite Element for Rock Joints and Interfaces," J. Soil Mech. Found. Div., ASCE, Vol. 99, No. SM10, October, 1973.
38. Goodman, L. E., and Brown, C. B., "Dead Load Stresses and the Instability of Slopes," J. Soil Mech. Found. Div., ASCE, Vol. 89, No. SM3, March, 1963.
39. Goodman, R. E. and St. John, C., "Finite Element Analysis for Discontinuous Rocks," Chapter 4, Numerical Methods in Geotechnical Engineering, Edited by Desai and Christian, McGraw-Hill, New York, 1977.
40. Goodman, R. E., Taylor, R. L., and Brekke, T., "A Model for the Mechanics of Jointed Rock," J. Soil Mech. Found. Div., ASCE, Vol. 94, No. SM3, March, 1968.
41. Hansen, J. B., discussion of "Hyperbolic Stress-Strain Response: Cohesive Soils," by R. L. Kondner, J. Soil Mech. Found. Div., ASCE Vol. 89, No. SM4, July, 1963.



42. Hardin, B. O., "Constitutive Relations for Air Field Subgrade and Base Course Materials," Technical Report UKY 32-71-CE5, Univ. of Kentucky, 1970.
- \* 43. Hardin, B. O. and Drnevich, V. P., "Shear Modulus and Damping in Soils: Measurement and Parameter Effects," J. Soil Mech. Found. Div., ASCE, Vol. 98, No. SM6, June, 1972.
44. Herrmann, L. R., "Efficiency Evaluation of a Two-Dimensional Incompatible Finite Element," Journal of Computers and Structures, Vol. 3, 1973.
45. Hill, R., "The Mathematical Theory of Plasticity," Oxford University Press, London, 1950.
46. Jakobson, B., "Some Fundamental Properties of Sand," Proceedings, 4th Intl. Conf. Soil Mech. Found. Engrg., Vol. I, 1957.
47. Janbu, N., "Soil Compressibility as Determined by Oedometer and Triaxial Tests," European Conf. on Soil Mechanics and Found. Engrg., Wiesbaden, Germany, Vol. 1, 1963.
48. Jumikis, A. R., "Theoretical Soil Mechanics," Van Nostrand Reinhold Co., New York, 1969.
49. Katona, M. G., "On the Analysis of Long Span Culverts by the Finite Element Method," Transportation Research Board, January, 1978.
50. Katona, M. G., Smith, J. M., Odello, R. S., and Allgood, J. R., "CANDE - A Modern Approach for Structural Design and Analysis of Buried Culverts," Report No. FHWA-RD-77-5, Naval Civil Engineering Laboratory, October, 1976.
51. Ko, H.-Y. and Masson, R. M., "Nonlinear Characterization and Analysis of Sand," Proceedings, 2nd International Conference on Numerical Methods in Geomechanics, June, 1976.
52. Ko, H.-Y. and Scott, R. F., "Deformation of Sand in Shear," J. Soil Mech. Found. Div., ASCE, Vol. 93, No. SM5, September, 1967.
53. Kondner, R. L., "Hyperbolic Stress-Strain Response: Cohesive Soils," J. Soil Mech. Found. Div., ASCE, Vol. 89, No. SM1, February, 1963.
54. Kulhawy, F. H., Duncan, J. M. and Seed, H. B., "Finite Element Analysis of Stresses and Movements in Embankments During Construction," Report No. TE-69-4, Univ. of California, Berkeley, 1969.
55. Lade, P. V., "The Stress-Strain and Strength Characteristics of Cohesionless Soils," Ph.D. Dissertation, Univ. of California, Berkeley, August, 1972.

---

\* See, also, Air Force Weapons Laboratory. Technical Report AFWL-TR-72-201: Effects of strain amplitude on the shear strength of soils, by B. O. Hardin, Kirtland Air Force Base, NM (March) 1973.





56. Lafebvre, G., Laliberte, M., Lafebvre, L. M., Lafleur, J., and Fisher, C. L., "Measurement of Soil Arching above a Large Diameter Flexible Culvert," Canadian Geotech, J., Vol. 13, No. 1, 1976.
57. Lambrechts, J. R. and Leonards, G. A., "Effects of Stress History on Deformation of Sand," J. Geotechn. Engrg. Div., ASCE, Vol. 104, No. GT11, pp. 1371-1387, November, 1978.
58. Lee, K. L. and Shen, C. K., "Horizontal Movements Related to Subsidence," J. Soil Mech. Found. Div., ASCE, Vol. 95, No. SM1, January 1969.
59. Lekhnitskii, S. G., "Theory of Elasticity of an Anisotropic Elastic Body," Holden Day, Inc., San Francisco, 1963.
60. Leonards, G. A. and Roy, M. B., "Predicting Performance of Pipe Culverts Buried in Soil," Joint Highway Research Project, Report No. JHRP-76-15, Purdue University, May, 1976.
61. Leonards, G. A. and Stetkar, R. E., "Performance of Buried Flexible Conduits," Joint Highway Research Project, Report No. JHRP-78-24, Purdue University, December, 1978.
62. Lucia, P. C. and Duncan, J. M., "Evaluation of Three Constitutive Models for Soils," Report No. UCB/GT/78-05, U.S. Army Engrg. Waterways Exp. Stn., March, 1979.
63. Mendelson, A., "Plasticity: Theory and Application," The MacMillan Company, New York, 1968.
64. Neal, B. G., "The Effect of Shear and Normal Forces on the Fully Plastic Moment of a Beam of Rectangular Cross Section," J. of Applied Mechanics, Vol. 60, December 1960.
65. Nobari, E. S. and Duncan, J. M., "Effect of Reservoir Filling on Stresses and Movements in Earth and Rockfill Dams," Report No. TE-72-1, Univ. of California, Berkeley, January, 1972.
66. Ozawa, Y. and Duncan, J. M., "Elasto-Plastic Finite Element Analysis of Sand Deformations," Proceedings, 2nd Intl. Conf. on Numer. Methods in Geomechanics, June 1976.
67. Penman, A. D. M., Burland, J. B., and Charles, J. A., "Observed and Predicted Deformations in a Large Embankment Dam During Construction," Proceedings of the Institution of Civil Engineers, Vol. 49, May 1971.
68. Poulos, H. G. and Davis, E. H., "Elastic Solutions for Soil and Rock Mechanics," John Wiley and Sons, New York, 1974.
69. Prevost, J.-H. and Höeg, K., "Effective Stress-Strain Strength Model for Soils," J. Geotechn. Engrgn. Div., ASCE, Vol. 101, No. GT3, March 1975.



70. Quigley, D. W. and Duncan, J. M., "Earth Pressures on Conduits and Retaining Walls," Report No. UCB/GT-78-06, Univ. of California, Berkeley, September 1978.
71. Ramberg, W. and Osgood, W. R., "Description of Stress-Strain Curves by Three Parameters," Technical Note, No. 902, National Advisory Committee for Aeronautics, Washington, D.C., 1943.
72. Richard, R. M. and Abbott, B. J., "Versatile Elastic-Plastic Stress-Strain Formula," J. of Engrg. Mech. Div., ASCE, Vol. 101, No. EM4, August 1975.
73. Roscoe, K. H., "The Influence of Strains in Soil Mechanics," 10th Rankine Lecture, Geotechnique, Vol. 20, No. 2, June 1970.
74. Roscoe, K. H., and Burland, J. B., "On the Generalized Stress-Strain Behavior of 'Wet Clay'," Engineering Plasticity, Edited by Heyman and Leckie, Cambridge University Press, 1968.
75. Roscoe, K. H., Schofield, A. N., and Thurairajah, A., "An Evaluation of Test Data for Selecting a Yield Criterion for Soils," ASTM Special Technical Publication No. 361, 1963.
76. Sandler, I. S., Dimaggio, F. L., and Baladi, G. Y., "Generalized Cap Model for Geological Materials," J. Geotechn. Engrg. Div., ASCE, Vol. 102, No. GT9, July 1976.
77. Schofield, A. and Wroth, P., "Critical State Soil Mechanics," McGraw-Hill, New York, 1968.
78. Singh, K. J. and Sandler, R. S., "A Computer Program for Finite Element Analysis of Nonlinear Elastic Incremental Soil System," Geotechnical Engrg. Report, No. 2, Ohio State Univ., November, 1975.
79. Smith, I. M. and Kay, S., "Stress Analysis of Contractive or Dilative Soil," J. Soil Mech. Found. Div., ASCE, Vol. 97, No. SM7, July 1971.
80. Terzaghi, K., "Theoretical Soil Mechanics," Wiley, New York, 1943.
81. Truesdell, C., "Hypo-elasticity," J. of Rational Mechanics and Analysis, Vol. 4, No. 1, 1955.
82. Vagneron, J., Lade, P. V., and Lee, K. L., "Evaluation of Three Stress-Strain Models for Soils," Proceedings, 2nd Intl. Conf. on Numer. Metds in Geomechanics, June 1976.
83. Vallabhan, C. V. G. and Reese, L. C., "Finite Element Method Applied to Some Problems in Soil Mechanics," J. Soil Mech. Found. Div., ASCE, Vol. 94, No. SM2, March 1968.



84. White, H. L. and Layer, J. P., "The Corrugated Metal Conduit as a Compression Ring," Proceedings, Highway Research Board, Vol. 39, 1960.
85. Wilson, E. L., Taylor, R. L., Doherty, W. P., and Ghaboussi, J., "Incompatible Displacement Modes," Proceedings of Naval Research Symposium, Univ. of Illinois, 1971.
86. Wong, K. S., "SSTIP - Soil STructure Interaction Program with Interface Elements," Univ. of California, Berkeley, 1977.
87. Wong, K. S. and Duncan, J. M., "Hyperbolic Stress-Strain Parameters for Nonlinear Finite Element Analyses and Movements in Soil Masses," Report No. TE-74-3, Univ. of California, Berkeley, July, 1974.
88. Zienkiewicz, O. C., Valliappan, S., Dullage, C., and Stagg, K. G., "Analysis of Nonlinear Problems in Rock Mechanics with Particular Reference to Jointed Rock Systems," Proc. of 2nd Conf. of Intl. Soc. for Rock Mech., Belgrade, 1970.
89. Zienkiewicz, O. C., Valliappan, S., King, I. P., "Stress Analysis of Rock as 'No-Tension' Material," Geotechnique, Vol. 18, No. 1, March 1968.



## APPENDIX A - LIST OF SYMBOLS

|                  |  |
|------------------|--|
| B                | Bulk modulus   |
| C                | Dimensionless coefficient                                |
| $C_1$            | Shear modulus parameter in the Hardin formula            |
| $[C^{ep}]$       | Elastic-plastic stress-strain matrix                     |
| D                | Parameter in Duncan-Chang soil model                     |
| $D_r$            | Relative density   |
| E                | Young's modulus  |
| $E_i$            | Initial tangent Young's modulus                          |
| $E_p$            | Plastic modulus  |
| $E_r$            | $E_i - E_p$  |
| $E_s$            | Young's modulus of soil                                  |
| $E_t$            | Tangent Young's modulus                                  |
| F                | Parameter in Duncan-Chang soil model                     |
| $F_p$            | Factor of safety against development of a plastic hinge  |
| G                | Shear modulus, also parameter in Duncan-Chang soil model |
| $G_{max}$        | Maximum value of shear modulus                           |
| $G_s$            | Secant shear modulus                                     |
| H                | Height of soil cover above crown                         |
| I                | Moment of Inertia  |
| $I_1, I_2, I_3$  | Invariants of strain                                     |
| K                | Parameter in Duncan-Chang soil model                     |
| $K_o$            | Principal stress ratio in uniaxial strain                |
| $K_{p1}, K_{p2}$ | Thrust coefficients in Duncan's SCI design procedure     |
| M                | Bending moment, or constrained modulus                   |
| $\Delta M$       | Bending moment increment                                 |
| $M_c$            | Moment at crown  |
| $M_{max}$        | Maximum bending moment in conduit wall                   |





|                                |   |
|--------------------------------|---|
| $M_p$                          | Fully plastic moment, in the absence of thrust load                     |
| $M_s$                          | Moment at springline  |
| $M_y$                          | Initial yield moment  |
| $N_f$                          | Dimensionless flexibility number = $\frac{E_s S^3}{EI}$                 |
| $\overline{OA}, \overline{OB}$ | Directed line lengths   |
| $P$                            | Thrust load   |
| $\Delta P$                     | Thrust increment  |
| $P_a$                          | Atmospheric pressure  |
| $P_c$                          | Thrust at crown   |
| $P_{max}$                      | Maximum thrust in conduit wall  |
| $P_p$                          | Fully plastic thrust (squash) load, in the absence of bending moment    |
| $P_s$                          | Thrust at springline  |
| $R$                            | Conduit radius, or conduit rise   |
| $RC$                           | Relative compaction (percent)   |
| $R_B$                          | Moment reduction factor in Duncan's SCI design procedure                |
| $R_f$                          | Failure ratio, ratio of shear strength to $(\sigma_1 - \sigma_3)_{ult}$ |
| $S$                            | Span  |
| $S_1$                          | Shear modulus parameter in the Hardin formula                           |
| $U$                            | Strain energy function  |
| $V$                            | Shear force   |
| $\overline{V}$                 | Volume  |
| $V_p$                          | Limiting shear force in pure shear                                      |
| $\overline{W}$                 | Weight of soil mass   |
| $\Delta Y\%$                   | Percent change in vertical diameter                                     |
| $a$                            | Parameter in the extended-Hardin soil model                             |
| $c$                            | Mohr-Coulomb strength parameter, cohesion                               |
| $e$                            | Void ratio  |



|                    |   |
|--------------------|---|
| $f$                | Coefficient of friction                                 |
| $k_b$              | Parameter in modified Duncan soil model                 |
| $k_{m1}, k_{m2}$   | Moment coefficients in Duncan's SCI design procedure    |
| $k_n$              | Normal "stiffness" of interface element                 |
| $k_s$              | Shear "stiffness" of interface element                  |
| $m$                | Parameter in modified Duncan soil model                 |
| $n$                | Parameter in Duncan-Chang soil model                    |
| $p$                | Parameter in Ramberg-Osgood soil model                  |
| $p_c$              | Soil contact pressure at the crown                      |
| $q$                | Parameter in the extended-Hardin soil model             |
| $y$                | Spatial coordinate                                      |
| $\bar{y}$          | Distance to the axis of bending                         |
| $\alpha$           | Dimensionless coefficient                               |
| $\alpha(\epsilon)$ | Dimensionless function of strain                        |
| $\gamma$           | Shear strain  |
| $\gamma_d$         | Dry unit weight   |
| $\gamma_m$         | Mass unit weight  |
| $\gamma_r$         | Reference shear strain = $\frac{\tau_{\max}}{G_{\max}}$ |
| $\delta_{ij}$      | Kronecker delta   |
| $\Delta\epsilon_p$ | Thrust strain increment                                 |
| $\Delta_n$         | Relative normal displacement                            |
| $\Delta_s$         | Relative shear displacement                             |
| $\Delta\phi$       | Curvature increment                                     |
| $\Delta\sigma$     | Normal stress increment                                 |
| $\epsilon$         | Normal strain   |
| $\epsilon_1$       | Principal normal strain                                 |
| $\epsilon_{ij}$    | Strain tensor   |



|                               |  |
|-------------------------------|--|
| $\epsilon(\max)$              | Maximum normal strain in the conduit wall        |
| $\epsilon_v$                  | Volumetric strain                                |
| $\epsilon_y$                  | Yield strain                                     |
| $\lambda$                     | Lame's parameter                                 |
| $\mu$                         | Poisson's ratio                                  |
| $\mu_{\max}$                  | Poisson's ratio at large shear strain (failure)  |
| $\mu_{\min}$                  | Poisson's ratio at zero shear strain             |
| $\mu_s$                       | Secant, or soil, Poisson's ratio                 |
| $\mu_t$                       | Tangent Poisson's ratio                          |
| $\sigma$                      | Normal stress                                    |
| $\sigma_1$                    | Major principal stress                           |
| $\sigma_3$                    | Minor principal stress                           |
| $(\sigma_1 - \sigma_3)_{ult}$ | Asymptotic value of stress difference            |
| $\sigma_{ij}$                 | Stress tensor                                    |
| $\sigma_t$                    | Tensile normal stress                            |
| $\sigma_y$                    | Yield stress                                     |
| $\sigma_\theta(\max)$         | Maximum extreme fiber stress in the conduit wall |
| $\tau$                        | Shear stress                                     |
| $\tau_{\max}$                 | Maximum value of shear stress                    |
| $\phi$                        | Mohr-Coulomb strength parameter, friction        |
| $\phi_o$                      | Value of $\phi$ for $\sigma_3$ equal to $P_a$    |
| $[ ]^T$                       | Transpose of a matrix                            |
| $\{ \}$                       | Vector   |



## APPENDIX B

CALCULATING BENDING MOMENT ABOUT THE CENTROIDAL AXIS  
USING THE CANDE CODE

1. Insert the following statements in Subroutine STEEL:

```

C      PRINT 8000,(RESULT(16,N),N=1,NPPT)
8000  FORMAT(//8X,7HYBAR = ,12F10.4)
      IF (NONLIN.EQ.2) WRITE(6,2990) 1A,(J,RESULT(19,J),RESULT(20,J),
      X RESULT(18,J),RESULT(13,J),J=1,NPPT)
C-----
C      CALCULATING BENDING MOMENT ABOUT THE CENTROID OF AN
C      EQUIVALENT RECTANGULAR SECTION - TZONG H. WU
C-----
C      DO 310 I=1,NPPT
C      XM(I)=RESULT(5,I)
310   XP(I)=RESULT(6,I)
C
334   PRINT 2830
      EEFF=PE/(1.-PNU*PNU)
      EPSY=PYIELD/EEFF
      DO 340 II=1,NPPT
      EINN=RESULT(19,II)
      EOUT=RESULT(20,II)
      H=SQRT(12.*PI/PA)
      B=PA/H
      IF (ABS(EINN).LE.EPSY.AND.ABS(EOUT).LT.EPSY) GO TO 335
      PIPP=RESULT(6,II)
      CALL MCENT(EINN,EOUT,PIPM,PIPP,EPSY,EEFF,PA,PYIELD,H,B)
      RESULT(5,II)=PIPM
      RESULT(6,II)=PIPP
      GO TO 340
335   ROUT=ABS(EOUT)/EPSY
      RINN=ABS(EINN)/EPSY
      IF ((EINN=EOUT).GT.0.) GO TO 337
      PM5=0.25*(ROUT+RINN)*PYIELD*B*H*H/3.
      IF (EOUT.GT.0.) GO TO 336
      RESULT(5,II)=PM5
      GO TO 340
336   RESULT(5,II)=-PM5
      GO TO 340
337   PM6=0.25*ABS(ROUT-RINN)*PYIELD*B*H*H/3.
      IF ((ABS(EOUT)-ABS(EINN))*EOUT.GT.0.) GO TO 338
      RESULT(5,II)=PM6
      GO TO 340
338   RESULT(5,II)=-PM6
340   PRINT 2850,RESULT(1,II),RESULT(2,II),RESULT(6,II),RESULT(5,II)
2830  FORMAT(/////5X,45HAXIAL FORCE AND BENDING MOMENT ABOUT CENTROID,
1      //12X,7HX-COORD,6X,7HY-COORD,8X,11HAXIAL FORCE,5X,
2      14HBENDING MOMENT)
2850  FORMAT(//10X,F9.2,F13.2,8X,E10.3,6X,E12.3)
      DO 348 I=1,NPPT
      RESULT(5,I)=XM(I)
      348  RESULT(6,I)=XP(I)
C

```





2. Add a new Subroutine MCENT:

```

SUBROUTINE MCENT(EINN,EOUT,PIPM,PIPP,EPSY,EEFF,PA,PYIELD,H,B)
*****
      MOMENTS ARE TAKEN ABOUT THE CENTROID
      --- BASED ON STRAIN DISTRIBUTION

      EQUIVALENT RECTANGULAR SECTION IS USED IN THE
      CALAULATION (I AND A ARE THE SAME AS THOSE OF
      CORRUGATED SECTION)
*****
      PPY=PA*PYIELD
      SGOUT=ABS(EOUT)*EEFF
      SGINN=ABS(EINN)*EEFF
      IF(EOUT*EINN.LT.0.) GO TO 200
      IF(ABS(EOUT).GE.EPSY.AND.ABS(EINN).GE.EPSY) GO TO 100
      IF(SGOUT.GE.SGINN) GO TO 50
      SGSM=SGOUT
      GO TO 60
50  SGSM=SGINN
60  SGA=ABS(PYIELD-SGSM)
      SGB=ABS(SGINN-SGOUT)
      HA=SGA*H/SGB
      PPI=PPY-0.5*HA*SGA*B
      IF(EINN.LE.0.) GO TO 65
      PIPB=PPI
      GO TO 70
65  PIPP=-PPI
70  PM1=0.5*(PYIELD-SGSM)*HA*(0.5*H-HA/3.)*B
      IF((ABS(EINN)-EPSY)*FINN).GT.0.) GO TO 75
      PIPM=-PM1
      RETURN
75  PIPM=PM1
      RETURN
100 PP=PYIELD*PA
      IF(EINN.GT.0.) GO TO 150
      PIPP=-PP
      PIPM=0.
      RETURN
150 PIPP=PP
      PIPM=0.
      RETURN
200 FLIMIT=10.*EPSY
      IF(ABS(EINN).GE.FLIMIT.AND.ABS(EOUT).GE.FLIMIT) GO TO 400
      IF(ABS(EINN).GE.EPSY.AND.ABS(EOUT).GE.EPSY) GO TO 300
      IF(ABS(EINN).GT.ABS(EOUT)) GO TO 250
      ELG=EOUT
      ESM=EINN
      SGSM=SGINN
      GO TO 260
250 ELG=EINN
      ESM=EOUT
      SGSM=SGOUT
260 H1=ABS(ELG)*H/(ABS(EINN)+ABS(EOUT))
      H2=0.5*H-(H1-H1*EPSY/ABS(ELG))
      SGC=(PYIELD+SGSM)*H2/(0.5*H+H2)
      PPS=0.5*((0.5*H+H1-H2)*PYIELD*B-(H-H1)*SGSM*B)

```



```

      IF((EINN*(ABS(EINN)-EPSY)).LT.0.) GO TO 265
      PIPP=PP3
      GO TO 270
265  PIPP=-PP3
270  PM3=H*H*3*(PYIELD+SGSM)/12.+B*SGC*(H*H/24.-H2*H2/6.)
      IF(EINN.GT.0.) GO TO 280
      PIPM=-PM3
      RETURN
280  PIPM=PM3
      RETURN
300  H1=ABS(EOUT)*H/(ABS(EINN)+ABS(EOUT))
      H2=0.5*H-(H1-H1*EPSY/ABS(EOUT))
      H3=0.5*H-(H-H1)*(ABS(EINN)-EPSY)/ABS(EINN)
      SGD=2.*PYIELD*H2/(H2+H3)
      PM4=(3.*H*H-4.*H3*H3)*(PYIELD*B)/12.+(H3*H3-H2*H2)*
1    (SGD*B)/6.
      PP4=0.5*(H-2.*H1+H2-H3)*PYIELD*B
      IF(EINN.GT.0.) GO TO 350
      PIPP=-PP4
      PIPM=-PM4
      RETURN
350  PIPM=PM4
      PIPP=PP4
      RETURN
400  X1=ABS(EOUT)*H/(ABS(EINN)+ABS(EOUT))
      PP5=2.*ABS(X1-0.5*H)*PYIELD*B
      PM5=(H-X1)*B*X1*PYIELD
      IF(EINN.GT.0.) GO TO 450
      PIPM=-PM5
      IF(ABS(EOUT).LT.ABS(EINN)) GO TO 420
      PIPP=PP5
      RETURN
420  PIPP=-PP5
      RETURN
450  PIPM=-PM5
      IF(ABS(EOUT).GT.ABS(EINN)) GO TO 480
      PIPP=PP5
      RETURN
480  PIPP=-PP5
      RETURN
      END

```



## APPENDIX C

INCORPORATING THE DUNCAN-CHANG AND MODIFIED DUNCAN SOIL MODELS  
IN CANDE CODE

1. Insert the following COMMON statement in Subroutines READM and HEROIC:

```

COMMON /HYPER/ C(10),PHIO(10),DPHI(10),ZK(10),ZN(10),RF(10),
1          UT(10),G(10),FF(10),D(10),RATIO(10),BK(10),BM(10)
2          ,S3PAGUS,S3PAINT,S3PADEL,S3PATEN,PGUESS
3          ,NAMEMOD(10),WORDTEN

```

2. Insert the following statement in Subroutine HEROIC:

```

C
C      *** INSERT NEW SOIL MODELS HERE ***
C
308 CALL DUNCAN(ST,STHARD,I,ICON,ITER,MN,NELEM,IA,JSOIL)

```



## 3. Insert the following statements in Subroutine READM:

```

70 H(I,L)=CP(J,K)                                04697000
GO TO 2                                            04698000
C*****
C
C      ITYP=3      THE DUNCAN-CHANG AND MODIFIED DUNCAN SOIL MODEL
C
C*****
C
80 READ(S,300) NON(I),ALPHA,RATIO(I),NAMEMOD(I),WORDTEN
C
CCC
C      NON(I) - MAXIMUM NUMBER OF ITERATIONS IN A SOIL LAYER
C                (IF NON(I) IS INPUT AS A NEGATIVE NUMBER, SOIL
C                MODULI VALUES WILL BE PRINTED OUT)
C      ALPHA - A SCALING FACTOR FOR TANGENT YOUNG'S MODULUS
C                (USUALLY USE ALPHA = 1.0)
C      RATIO(I) - A WEIGHTING RATIO APPLIED TO AN ELEMENT WHEN
C                IT FIRST ENTERS THE SYSTEM
C                (FOR SOIL LIFTS USE RATIO(I) = 0.5 ;
C                FOR INITIAL FOUNDATION SOIL, USE RATIO(I)=1.0)
C                --- M.G. KATONA ---
C
C      NAMEMOD= 1 FOR MODIFIED DUNCAN MODEL
C      (DEFAULT) FOR DUNCAN-CHANG MODEL
C
C      WORDTEN=TENSION: FOR CONSIDERATION OF TENSION-LOOP IN MOD. DUNCAN
C      MODEL, SEE SUBROUTINE DUNCAN; ONLY NEEDED WHEN NAMEMOD=1
C
C*****
C      S3PA FAMILY :
C      S3PAGUS= INITIAL GUESS OF S3PA
C      S3PAINT= MINIMUM S3PA IN CASE OF SHEAR FAILURE
C      S3PADEL= INCREMENT OF S3PA, IF NEEDED FOR CONVERGENCE
C      S3PATEN= MINIMUM OF S3PA IN CASE OF TENSION FAILURE
C
CCC
      READ(S,1111) S3PAGUS,S3PAINT,S3PADEL,S3PATEN,PGUESS
1111  FORMAT(SF10.0)
C
C      SET DEFAULTED VALUES
C
      IF(S3PAGUS.EQ.0.) THEN
        S3PAGUS=0.10
        S3PAINT=0.10
        S3PADEL=0.
        S3PATEN=0.10
        PGUESS =0.38
      ENDIF
      WRITE(6,1119) S3PAGUS,S3PAINT,S3PADEL,S3PATEN,PGUESS
1119  FORMAT(///5X,*,CRITERIA FOR ITERATION:*,3X,*,S3PAGUS=*,
X      F6.3,3X,*,S3PAINT=*,F6.3,3X,*,S3PADEL=*,F6.3,3X,
X      *,S3PATEN=*,F6.3,3X,*,PGUESS=*,F6.3///)

```





```

IF(NON(I).EQ.0) NON(I)=-12
IF(ALPHA.EQ.0.0) ALPHA=1.0
IF(RATIO(I).EQ.0.0) RATIO(I)=0.5
WRITE(6,305) NON(I),ALPHA,RATIO(I)

```

C  
C

```

READ(5,330) H1,H2A,H2B,H3,H4,H5,H6
C(I)=H1
PHIO(I)=H2A
DPHI(I)=H2B
ZK(I)=H3*ALPHA
ZN(I)=H4
RF(I)=H5
UT(I)=H6

```

C  
C  
C  
C

```

      UT(I) - ASSIGNED A CONSTANT POISSON RATIO IF DESIRED, OTHERWISE
              DEFAULT FOR VARIABLE POISSON RATIO OR BULK MODULUS

```

```

IF(H6.GT.0.) GO TO 86
IF(NAMEMOD(I).NE.1) READ(5,333) H7,H8,H9
IF(NAMEMOD(I).EQ.1) READ(5,333) H10,H11
G(I)=H7
FF(I)=H8
D(I)=H9
BK(I)=H10
BM(I)=H11

```

C  
C  
C

```

      PRINT OUT INPUT DATA FOR DUNCAN-CHANG OR MOD. DUNCAN MODEL

```

```

86 WRITE(6,310) (MATNAM(K),K=1,5),C(I),PHIO(I),DPHI(I),ZK(I),
1      ZN(I),RF(I)
IF(UT(I).GT.0.0) WRITE(6,325) UT(I)
IF(UT(I).LE.0. .AND. NAMEMOD(I).NE.1) WRITE(6,321) G(I),FF(I),D(I)
IF(UT(I).LE.0. .AND. NAMEMOD(I).EQ.1) WRITE(6,320) BK(I),BM(I)
PHIO(I)=H2A/57.29577951
DPHI(I)=H2B/57.29577951
GO TO 2

```

```

300 FORMAT(15,2F10.5,15,3X,A7)
305 FORMAT(//5X,31HCONTROLS FOR DUNCAN SOIL MODEL  ///
1 10X,30H MAXIMUM ITERATIONS..... IS//
2 10X,30H MODULUS REDUCTION, ALPHA..... F12.4//
3 10X,30H ENTERING ELEMENT RATIO..... F12.4/)
310 FORMAT(//5X,41HYPERBOLIC STRESS-STRAIN PARAMETERS///
1 10X,29H SOIL CLASSIFICATION..... SA4//
2 10X,29H COHESION INTERCEPT, C..... F12.4//
3 10X,29H FRICTION ANGLE,PHIO (DEG).. F12.4//
4 10X,29H 10-FOLD REDUCTION IN PHIO.. F12.4//
5 10X,29H SCALED MODULUS NUMBER, K.. F12.4//
6 10X,29H MODULUS EXPONENT, N..... F12.4//
7 10X,29H FAILURE RATIO, RF..... F12.4// )
321 FORMAT(10X,35H POISSON=S RATIO PARAMETER G ... F12.4/
1 10X,35H POISSON=S RATIO PARAMETER F ... F12.4/
2 10X,35H POISSON=S RATIO PARAMETER D ... F12.4/)
330 FORMAT(7F10.4)
320 FORMAT(10X,4 BULK MODULUS NUMBER BK...F12.4//
X      10X,4 BULK MODULUS EXPONENT BM..F12.4//)
325 FORMAT(10X,4 CONSTANT POISSON RATIO UT..F12.4//)
333 FORMAT(3F10.4)
END

```



## 4. Add a new Subroutine DUNCAN:

```

SUBROUTINE DUNCAN(ST,STHARD,NEL,ICON,ITER,MN,NELEM,IA,JSDIL)

DIMENSION ST(6,NELEM),STHARD(6,NELFM),DUN1(2),DUN(2),JSDIL(10)

COMMON /MATERL/ CP(3,3),DEN(10),E(10,10),GNU(10,10),H(10,10),
1             ITYPE(10),NON(10)
COMMON /HYPER/ C(10),PHIO(10),DPHI(10),ZK(10),ZN(10),RF(10),
1             UT(10),G(10),FF(10),D(10),RATIO(10),EK(10),BM(10)
2             ,S3PAGUS,S3PAINT,S3PADEL,S3PATEN,PGUESS
3             ,NAMEMOD(10),WORDTEN
DATA TOLER,PATM /0.05,14.7/
DATA DUN1/10HMOD.DUNCAN,10H MODEL /
DATA DUN/10HDUNCAN-CHA,10HNG MODEL /
DATA TENSION/7HTENSION/

C
C     RECOVER CURRENT STRESSES AND CONVERT TO PRINCIPAL VALUES
C
SXX=-ST(4,NEL)
SYY=-ST(5,NEL)
SXY=ST(6,NEL)
CENTER=(SXX+SYY)/2.
RADIUS=SQRT(SXY**2+((SXX-SYY)/2. )**2)
S1=CENTER+RADIUS
S3=CENTER-RADIUS

C
C     CALCULATE STRESS LEVEL
C     TENSION FAILURE - STRESS LEVEL < 0.0
C     SHEAR FAILURE - STRESS LEVEL > 1.0
C
IF(ITER.EQ.1) GO TO 2
IF(S3.LT.0.0) SLEV=-1.0+14.7*(S3/PATM)
IF(S3.LT.0.0) GO TO 2
S3P=S3/PATM
PHAI=PHIO(MN)-DPHI(MN)*ALCG10(S3P)
SHEARF=(2.*C(MN)*COS(PHAI)+2.*S3*SIN(PHAI))/(1.-SIN(PHAI))
DIFF=S1-S3
IF(C(MN).LT.0.000000001) THEN
    SLEV=DIFF*COS(PHAI)/SIN(PHAI)/(2.*SQRT(S1*S3))
ELSE IF(PHAI.LT.0.000000001) THEN
    SLEV=DIFF/(2.*C(MN))
ELSE
    SLEV=DIFF/SHEARF
ENDIF
2 CONTINUE

C
C     DECIDE WHICH MODEL TO USE... MOD. DUNCAN OR DUNCAN-CHANG
C
IF(NAMEMOD(MN).EQ.1) GO TO 9999

C
C     PART ONE.... TO GENERATE AN INCREMENTAL PLANE STRAIN
C     CONSTITUTIVE MATRIX BASED ON DUNCAN-CHANG MODEL
C
C
C     ON FIRST ITERATION OF EACH STEP, UPDATE PARAMETERS
C
IF(ITER.NE.1) GO TO 5
E2=STHARD(5,NEL)
E1=E2

```



```

      STHARD(1,NEL)=E1
      POIS2=STHARD(6,NEL)
      IF(UT(MN).NE.0.0) POIS2=UT(MN)
      POIS1=POIS2
      STHARD(2,NEL)=POIS1
C
C      FOR FIRST ITERATION OF NEW ELEMENT ENTERING SYSTEM,
C      ASSIGN INITIAL GUESS-VALUES
C
      IF(E1.NE.0.0) GO TO 5
      POIS1=UT(MN)
      IF(POIS1.EQ.0.0) POIS1=PGUESS
      S3=S3PAGUS*PATM
      S1=S3*(1.0-POIS1)/POIS1
C
C      RECALL PREVIOUSLY CONVERGED PARAMETERS ON SUBSEQUENT ITERATIONS
C
      5 IF(ITER.EQ.1) GO TO 10
      E1=STHARD(1,NEL)
      POIS1=STHARD(2,NEL)
      IF(UT(MN).NE.0.0) POIS1=UT(MN)
C
C      SET WEIGHING RATIOS FOR AVERAGING E(NEW) FROM E1 TO E2
C      AND P(NEW) FROM POIS1 TO POIS2
C
      10 WTE=0.5
      IF(E1.EQ.0.0) WTE=RATIO(MN)
      WTP=0.5
      IF(E1.EQ.0.0) WTP=1.0
C
C      SET MAXIMUM STRESS CUTOFF FOR S3, NOTE,
C      SHEAR=S1-S3 REMAIN THE SAME
C      DEFINITION OF S3PA-FAMILY CAN BE FOUND IN SUBROUTINE READM
C      IN ORDER TO GET CONVERGENCE SOMETIMES THE ITERATION CRITERIA
C      HAVE TO BE CHANGED. THIS ARRANGEMENT IS ONLY MEANINGFUL FOR
C      ANALYSIS OF CONDUIT-SOIL SYSTEM.
C
      S3PA=S3/PATM
      X3PA=S3PA
      IF(ITER.EQ.1 .AND. E1.EQ.0.0) GO TO 15
      IF(S3PA.LT.S3PAINT) S3PA=S3PAINT
      IF(IA.EQ.2 .AND. S3PA.LT.(S3PAINT+S3PADEL)) S3PA=S3PAINT+S3PADEL
      IF(IA.EQ.3 .AND. S3PA.LT.(S3PAINT+S3PADEL)) S3PA=S3PAINT+S3PADEL
      IF(IA.EQ.4 .AND. S3PA.LT.(S3PAINT+1.5*S3PADEL)) S3PA=S3PAINT+
X                                     1.5*S3PADEL
      IF(IA.GE.5 .AND. S3PA.LT.(S3PAINT+2.0*S3PADEL)) S3PA=S3PAINT+
X                                     2.0*S3PADEL
      IF(S3.LT.0.) S3PA=S3PATEN
C
C      COMPUTE YOUNG=S TANGENT MODULUS E2, THEN ET(NEW)
C
      15 IF(X3PA.LT.0.001) X3PA=0.001
      PHI=PHIO(MN)-D*PHI(MN)*ALOG10(X3PA)
      RFF=RF(MN)*(1.0-SIN(PHI))/
      1 (2.*C(MN)*COS(PHI)+2.*S3PA*PATM*SIN(PHI))
      DEU=RFF*(S1-S3)
      IF(DEU.LT.0.) DEU=0.
      IF(DEU.GT.0.65) DEU=0.65

```



```

C
C      THE VALUE OF 0.65 IS BASED ON RF=0.70
C
EINIT=ZK(MN)*PATM*S3PA**ZN(MN)
E2=(1.-DEU)**2*EINIT
C
C      USE UNDER-RELAXATION FOT E2 WHEN ITER.GT.2
C
E2P=STHARD(5,NEL)
IF(ITER.GT.2) E2=0.75*E2+0.25*E2P
ETNEW=(1.-UTE)*E1+UTE*E2
STHARD(5,NEL)=E2
ETCHEK=(E2-E2P)/E2
C
C      DETERMINE OPTIONAL VARIABLE POISSON RATIO, UT
C
IF(UT(MN).GT.0.) PNEW=UT(MN)
IF(UT(MN).GT.0.) GO TO 50
GF=G(MN)-FF(MN)*ALOG10(X3PA)
DKRF=D(MN)*(S1-S3)/(EINIT*(1.-DEU))
IF(DKRF.GT.0.99) DKRF=0.99
POIS2=GF/((1.-DKRF)**2)
IF(POIS2.GT.0.48) POIS2=0.48
IF(POIS2.LT.0.01) POIS2=0.01
C
C      CHECK CONVERGENCE OF POISSON RATIO, THEN GO TO LABEL 50
C
PNEW=(1.-WTP)*POIS1+WTP*POIS2
POIS2P=STHARD(6,NEL)
STHARD(6,NEL)=POIS2
PCHEK=(POIS2-POIS2P)/POIS2
IF(ABS(PCHEK).GT.TOLER) ICON=0
BNEW=ETNEW/(3.-S.*PNEW)
GO TO 50
C
C
C      PART TWO.... TO GENERATE CONSTITUTIVE MATRIX BASED ON
C      MODIFIED DUNCAN MODEL. THE BASIC ALGORITHM IS THE SAME
C      AS IN PART ONE.
C
C
9999 IF(ITER.NE.1) GO TO 51
E2 = STHARD(5,NEL)
E1 = E2
STHARD(1,NEL) = E1
B2 =STHARD(6,NEL)
B1=B2
STHARD(2,NEL)=B1
C
IF(E1.NE.0.) GO TO 51
POIS1 = UT(MN)
IF(POIS1.EQ.0.) POIS1 = PGUESS
S3 = S3PAGUS * PATM
S1 = S3*(1.0-POIS1)/POIS1
C
51 IF(ITER.EQ.1) GO TO 101
E1 = STHARD(1,NEL)
B1 = STHARD (2,NEL)

```





```

C
101 WTE = 0.5
    IF(E1.EQ.0.0) WTE = RATIO(MN)
    WTP=0.5
    IF(E1.EQ.0.0) WTP=1.0

C
    DECIDE IF A FIXED VALUE OF MODULUS OR A VARIED ONE IS PREFERRED
C
    IN CASE OF TENSION FAILURE.
C
    IF(S3.GT.0.) GO TO 201
    IF(WORDTEN.NE.TENSION) GO TO 201
    E2=300.
    POIS=0.40
    IF(UT(MN).GT.0.0)POIS=UT(MN)
    B2=E2/(3.0-6.0*POIS)
    E2P=STHARD(5,NEL)
    ETCHEK=(E2-E2P)/E2
    STHARD(5,NEL)=E2
    STHARD(6,NEL)=B2
    GO TO 301
201 CONTINUE
C
    S3PA=S3/PATM
    X3PA=S3PA
    IF(X3PA.LT. 0.001) X3PA=0.001
    IF(ITER.EQ.1 .AND. E1.EQ.0.) GO TO 1501
    IF(S3PA.LT.S3PAINT) S3PA=S3PAINT
    IF((IA.EQ.2 .OR. IA.EQ.3) .AND. S3PA.LT.(S3PAINT+S3PADEL))
X                                     S3PA=S3PAINT+S3PADEL
    IF(IA.EQ.4 .AND. S3PA.LT.(S3PAINT+1.5*S3PADEL)) S3PA=S3PAINT+
X                                     1.5*S3PADEL
    IF(IA.GE.5 .AND. S3PA.LT.(S3PAINT+2.0*S3PADEL)) S3PA=S3PAINT+
X                                     2.0*S3PADEL
    IF(S3.LT.0.) S3PA=S3PATEN

C
C
1501 PHI = PHIO(MN) - DPHI(MN)*ALOG10 (X3PA)
    RFF = RF(MN)* (1.0 - SIN(PHI))/
1      (2.0 * C(MN)*COS(PHI) + 2.0* S3PA*PATM*SIN(PHI))
    DEV = RFF * (S1 - S3)
    IF (DEV.GT.0.65) DEV = 0.65
    IF (DEV.LT.0.0) DEV=0.0
    EINIT = ZK(MN) * PATM* S3PA**ZN(MN)
    E2 = (1.0 - DEV)**2*EINIT
    E2A=0.34*E2
    E2B=0.*E2

C
    E2P = STHARD(5,NEL)
    IF(ITER.GT.2) E2 = 0.75*E2 + 0.25*E2P
    STHARD(5,NEL)= E2
    ETCHEK = (E2 -E2P)/E2

C
    IF(UT(MN).GT.0.0) GO TO 301
    B2=BK(MN)*PATM*S3PA**BM(MN)
    IF(B2.LT.E2A) B2=E2A
    IF(B2.GT.E2B) B2= E2B

C
    B2P = STHARD(6,NEL)

```



```

      IF(ITER.GT.2) B2 = 0.25*B2 + 0.75*B2P
      STHARD (6,NEL) = B2
C
301  ETNEW=(1.0-WTE)*E1+WTE*E2
      IF(UT(MN).GT.0.0) GO TO 401
      BNEW = (1.0-WTP)*B1+WTP*B2
C
      PNEW=(3.0*BNEW-ETNEW)/(6.0*BNEW)
      IF(PNEW.LT.0.01) PNEW=0.01
      IF(PNEW.GT.0.48) PNEW= 0.48
      GO TO 50
C
401  PNEW=UT(MN)
      BNEW=ETNEW/(3.0-6.0*PNEW)
C
C      THE FOLLOWING STATEMENTS( DOWN TO ≠END≠ ) ARE FOR BOTH
C      DUNCAN-CHANG AND MODIFIED DUNCAN MODEL
C
C      CHECK FOR CONVERGENCE
C      1) ICON IS CONVERGENCE INDEX
C      2) JSOIL IS AN INDEX FOR PRINTING ERROR MESSAGE,SEE
C      SUBROUTINE HEROIC.. RIGHT AFTER CALL DUNCAN
C
50   IF(ITER.EQ.1) ICON=0
      IF(ITER.EQ.1) SLEV=0.
      JSOIL(MN)=0
      IF(ABS(ETCHEK).GT.TOLER) ICON=0
      IF(ABS(ETCHEK).GT.TOLER) JSOIL(MN)=1
      IF(ITER.GE.IABS(NON(MN))) ICON=1
      NONABS3=IABS(NON(MN))-3
      IF(ITER.LT.NONABS3) JSOIL(MN)=0
C
C      CONVERT TO PLANE-STRAIN MATERIAL MATRIX
C
      CMOD=ETNEW
      CALL CONUT(CMOD,PNEW)
C
C      PRINT-OUT RECORD OF NONLINEAR MODULI (FOR NON(MN).LT.0 ONLY)
C
      IF(NON(MN).GT.0) GO TO 100
      IF(ITXX.EQ.ITER) GO TO 60
      IF(NAMEMOD(MN).EQ.1) WRITE(6,6030) DUN1
      IF(NAMEMOD(MN).NE.1) WRITE(6,6030) DUN
60   IF(ITXX.NE.ITER) WRITE(6,6000) IA,ITER
      ITXX=ITER
C
      IF(SLEV.LT.0.0) WRITE(6,6010) NEL,ICON,ETNEW,PNEW,
X      CMOD,ETCHEK,BNEW
      IF(SLEV.LT.0.0) WRITE(6,6020)
      IF(SLEV.LT.0.0) GO TO 100
C
      WRITE(6,6010) NEL,ICON,ETNEW,PNEW,CMOD,ETCHEK,BNEW,SLEV
100  CONTINUE
      RETURN
C
6000 FORMAT(1H+,5X,23HCONSTRUCTION INCREMENT ,I2,5X,10HITERATION ,I2///
15X,59HDUNCAN MODEL...ITERATION RECORD OF CONSTITUTIVE PROPERTIES.
2/5X,54HCONVERGENCE ERRORS ARE RATIOS GIVEN BY: (NEW-OLD)/NEW //

```



```

3 4X,≠      ELEMENT      ICON      YOUNGS-MOD.  POISSON-RATIO≠,5X,
458H  CONFINED-MOD.      ERROR-EMOD  BULK-MODULUS  STRESS LEVEL/)
6010  FORMAT(9X,2I7,3X,E15.7,E12.3,8X,E15.7,2X,F10.2,4X,E10.3
X      ,5X,F8.2)
6020  FORMAT(1H+,107X,≠TEN. FAIL≠)
6030  FORMAT(1H1,55X,≠***≠,2A10,≠***≠)
END

```



## APPENDIX D

## AN AUTOMATED MESH FOR CLOSED PIPE ARCHES

1. Insert or replace the following statements in the main program CANDE:

|     |   |          |
|-----|---|----------|
|     | DIMENSION HED(10),PLIST(10),PIPMAT(5,30),RESULT(20,30),SOLVE(6)       | 00009000 |
|     | X               , XSIZE(6)  |          |
|     | COMMON /CONTROL/ XNOSTOP  |          |
|     | DATA ARCH/4HARCH/   |          |
| 105 | RESULT(N,I) = 0.0   | 00020000 |
|     | READ(5,1000) XMODE,LEVEL,PTYPE,XWORD,HED,NPMAT,NPPT,XNOSTOP           | 00021000 |
|     | IF(LEVEL.NE.3) NPMAT = 10   | 00025000 |
|     | IF(LEVEL.NE.3) NPPT = 11  | 00026000 |
|     | IF(LEVEL.NE.3 .AND. XWORD.EQ.ARCH) NPMAT=11                           |          |
|     | IF(LEVEL.NE.3 .AND. XWORD.EQ.ARCH) NPPT=12                            |          |
| 301 | CALL STEEL (IA, ICOME, IEXIT, LEVEL, NINC, NPMAT, NPPT, PDIA, PIPMAT, | 00066000 |
| 1   | RESULT, SK, SM, XMODE, XSIZE, XWORD)                                  | 00067000 |
| 402 | CALL PRHERO(IA, ICOME, IEXIT, LEVEL, NINC, NPMAT, NPPT, PDIA, PIPMAT, | 00091000 |
| 1   | RESULT, SK, SM, XSIZE, XWORD)   | 00092000 |
| C   |   | 00105000 |
| C   | FORMATS   | 00106000 |
| C   |   | 00107000 |
|     | 1000 FORMAT (A4,3X,I1,1X,A4,2X,A4,1X,10A4,10X,2I2,A6)                 | 00108000 |





2. Insert or replace the following statements in Subroutine STEEL:

```

SUBROUTINE STEEL(IA, ICOME, IEXIT, LEVEL, NINC, NPMAT, NPPT, PDIA, PIPMAT, 00133000
1      RESULT, SK, SM, XMODE, XSIZE, XWORD)                                00134000

DIMENSION XM(30), XP(30), XX(30), YY(30), XSIZE(6)

DATA ARCH/4HARCH/

100  IF(XWORD.NE.ARCH) READ(5,1000) NONLIN, PDIA, PE, PNU, PYIELD, PDEN, PE2 00176000
    IF(XWORD.EQ.ARCH) READ(5,1001) NONLIN, PE, PNU, PYIELD, PDEN, PE2
X                                     , (XSIZE(I), I=1,6)

    IF(PIMIN.GT.FIMIN) PIMIN = PIMIN*FF(1)/FF(2)                                00182000
C                                     00183000
    IF(XWORD.NE.ARCH) WRITE(6,2000) PDIA, PE, PNU, PYIELD, PDEN, NONLIN 00184000
    IF(XWORD.EQ.ARCH) WRITE(6,2999) (XSIZE(I), I=1,6),
X                                     PE, PNU, PYIELD, PDEN, NONLIN

    CALL PRHERO(IA, ICOME, IEXIT, LEVEL, NINC, NPMAT, NPPT, PDIA, PIPMAT, 00361000
1      RESULT, SK, SM, XSIZE, XWORD)                                00362000

    IF(XWORD.NE.ARCH) WRITE(6,2900) IA, CIRCR, DISPR, BUCKR, BENDR, HANDR
350  CONTINUE                                                                00379000

1000  FORMAT(15,6F10.0)                                                    00390000
1001  FORMAT(15,5F10.0/6F10.0)

2999  FORMAT(///10X, PIPE PROPERTIES ARE AS FOLLOWS...//
X  15X, PIPE ARCH PARAMETERS (IN) .....//
X  18X, R1=, F7.2, 2X, R2=, F7.2, 2X, R=, F7.2, 2X, RISE=, F7.2, 2X,
X  SPAN=, F7.2, 2X, HT=, F7.2///
X  15X, YOUNG MODULUS OF PIPE (PSI)....., E15.5//
X  15X, POISSONS RATIO OF PIPE....., E15.5//
X  15X, YIELD STRESS OF PIPE(PSI) ..... , E15.5//
X  15X, DENSITY OF PIPE (PCI) ..... , E15.5//
X  15X, MATERIAL CHARACTER, NONLIN....., IS//

```



## 3. Replace the following statements in Subroutine PRHERO:

|   |  |              |
|---|--|--------------|
|   | SUBROUTINE PRHERO (IA, ICOME, IEXIT, LEVEL, NINC, NPMAT, NPPT, PDIA, | 02523000     |
| 1 | PIPMAT, RESULT, SK, SM, XSIZE, XWORD)                                | 02524000     |
| C |  | 02525000     |
|   | <br>DIMENSION PIPMAT(5, NPMAT), RESULT(20, NPPT), XSIZE(6)           | <br>02528000 |
|   | <br>REWIND LUPLOT  | <br>02542000 |
|   | CALL PREP (FEDATA, PIPMAT, DENSTY, ISIZE, KPUTCK, LEVEL, LUDATA,     | 02543000     |
| 1 | LUPLOT, MAXBC, MAXEL, MAXMAT, MAXNP, NPMAT, NPT, NSMAT,              | 02544000     |
| 2 | NXMAT, NBPTC, NELEM, PDIA, XSIZE, XWORD)                             | 02545000     |
| C |  | 02546000     |

## 4. Insert or replace the following statements in Subroutine PREP:

|      |   |          |
|------|---|----------|
|      | SUBROUTINE PREP(FEDATA, PIPMAT, DENSTY, ISIZE, KPUTCK, LEVEL, LUDATA, | 03480000 |
| 1    | LUPLOT, MAXBD, MAXEL, MAXMAT, MAXNP, NPMAT, NPT, NSMAT,               | 03481000 |
| 2    | NXMAT, NBPTC, NELEM, PDIA, XSIZE, XWORD)                              | 03482000 |
|      | DIMENSION FEDATA(ISIZE), PIPMAT(5, NPMAT), TITLE(17), XSIZE(6)        | 03483000 |
|      | DATA LSTOP, NUMLI /7, 200/  | 02484000 |
|      | DATA ARCH/4HARCH/   |          |
| C    |   | 03486000 |
| C**  | GENERATE THE CANNED MESH  | 03487000 |
| C    |   | 03490000 |
|      | KPUTCK = 0  | 02495000 |
|      | LUPREP = 5  | 03490000 |
|      | IF (LEVEL .EQ. 2) LUPREP = LUDATA                                     | 03491000 |
|      | IF(XWORD.NE.ARCH) GO TO 999   |          |
|      | IF(LEVEL.EQ.2) CALL CANJ1 (LUDATA, KPUTCK, XSIZE, WORDTB)             |          |
|      | GO TO 9999  |          |
| 999  | IF (LEVEL .EQ. 2) CALL CAN1 (LUDATA, KPUTCK, PDIA, DENSTY)            | 03492000 |
| C    |   | 03493000 |
| C**  | READ/WRITE MAIN CONTROL CARDS AND SET DEFAULT VALUES                  | 03494000 |
| C    |   | 03495000 |
| 9999 | READ (LUPREP, 5010) WORD, TITLE WORD2, NINC, MGENPR, NPUTCK, IPLOT,   | 03496000 |
| 1    | IWRT, NPT, NELEM, NBPTC   | 03497000 |



## 5. Add two new Subroutines SIZE and CANJ1.

```

SUBROUTINE SIZE (AX,AY,XSIZE)
C   THIS SUBROUTINE IS TO DEFINE GEOMETRY OF A PIPE ARCH
C   BASED ON PARAMETERS OF R1,R2,R3,RISE,SPAN,HT
  DIMENSION XSIZE(6),AX(12),AY(12),NADD(3),NP(3),XTEMP(4),YTEMP(4)
  DATA TOLER,XAIN,XBIN/0.005,0.2,0.5/

C
C   BEGIN TO SOLVE THE COORDINATES OF ARC-ENDS
C   BY TRIAL AND ERROR METHOD
C
  R1 = XSIZE(1)
  R2 = XSIZE(2)
  R = XSIZE(3)
  RISE = XSIZE(4)
  SPAN = XSIZE(5)
  HT = XSIZE(6)
  XA=XAIN*R1
  NXA=0
9   IF(XA.LE.0.) WRITE(6,5000)
  IF(XA.LE.0.) STOP
  IF(XA.GT.0.7*R1) WRITE(6,5000)
  IF(XA.GT.0.7*R1) STOP
  YA=R1-SQRT(R1**2-XA**2)
  XATEMP=(R1-YA)*(SPAN/2.-R)/(R1-RISE+HT)
  RATIOA1=ABS(XATEMP-XA)/XA
  RATIOA2=ABS(XATEMP-XA)/XATEMP
  XARATIO=AMAX1(RATIOA1,RATIOA2)
  IF(XARATIO.LT.TOLER) GO TO 10
  NXA=NXA+1
  IF(NXA.GT.50000) WRITE(6,1000)
  IF(NXA.GT.50000) STOP
  IF(XATEMP.GT.XA) XA=XA+0.00001*R1
  IF(XATEMP.LT.XA) XA=XA-0.00001*R1
  GO TO 9
10  CONTINUE
  XB=XBIN*R2
  NXB=0
19  IF(XB.LE.0.) WRITE(6,5000)
  IF(XB.LE.0.) STOP
  IF(XB.GT.R2) WRITE(6,5000)
  IF(XB.GT.R2) STOP
  YBX=SQRT(R2**2-XB**2)
  IF(R2.LT.HT) YB=(RISE-R2)-YBX
  IF(R2.GE.HT) YB=(RISE-R2)+YBX
  XBTEMP=(YB-RISE+R2)*(SPAN/2.-R)/(R2-HT)
  RATIOB1=ABS(XBTEMP-XB)/XB
  RATIOB2=ABS(XBTEMP-XB)/XBTEMP
  XBRATIO=AMAX1(RATIOB1,RATIOB2)
  IF(XBRATIO.LT.TOLER) GO TO 15
  NXB=NXB+1
  IF(NXB.GT.50000) WRITE(6,2000)
  IF(NXB.GT.50000) STOP
  IF(XBTEMP.GT.XB) XB=XB+0.00001*R2
  IF(XBTEMP.LT.XB) XB=XB-0.00001*R2
  GO TO 19
C
C   FORMATS
C
1000 FORMAT(////////#***STOP BECAUSE NO. OF ITERATION(NXA) GREATER THAN#/)

```



```

      X ≠      50000 --- DUE TO POOR DIMENSION OF PIPE ARCH#/////
2000 FORMAT(/////≠** STOP BECAUSE NO. OF ITERATION(NXB) GREATER THAN≠/
      X ≠      50000 --- DUE TO POOR DIMENSION OF PIPE ARCH#/////
C
5000 FORMAT(/////≠ **** POOR DESIGN OF PIPE ARCH---PROGRAM STOP≠/)
C
15  CONTINUE
C
C
C   BEGIN TO CALCULATE COORDINATES OF INTER-POINTS OF ARCS
C
      AX(1)=0.
      AX(6)=XB
      AX(9)=XA
      AX(12)=0.
      AY(1)=RISE
      AY(6)=YB
      AY(9)=YA
      AY(12)=0.
      NADD(1)=6
      NADD(2)=9
      NADD(3)=12
      NP(1)=4
      NP(2)=2
      NP(3)=2
C
C   GIVING COORDINATES OF ARC-ENDS
C
      DO 100 K=1,3
      GO TO (1,2,3) K
1    X2=AX(1)
      X1=AX(6)
      Y2=AY(1)
      Y1=AY(6)
      RADIUS=R2
      GO TO 20
2    X2=AX(6)
      X1=AX(9)
      Y2=AY(6)
      Y1=AY(9)
      RADIUS=R
      GO TO 20
3    X2=AX(9)
      X1=AX(12)
      Y2=AY(9)
      Y1=AY(12)
      RADIUS=R1
20   DX=X2-X1
      DY=Y2-Y1
      DL=SQRT(DX*DX+DY*DY)
      RSIGN=SIGN(1.0,RADIUS)
      RADIUS=ABS(RADIUS*1.000001)
      ASINFK=DL/RADIUS/2.0
      IF(ASINFK.GT.1.0 .OR. ASINFK.EQ.0.) WRITE(6,5000)
      IF(ASINFK.GT.1.0 .OR. ASINFK.EQ.0.) STOP
C
      THETA=2.0*ATAN(1.0)-ATAN(ASINFK/SQRT(ABS(1.0-ASINFK**2)))
      PHI=ATAN2(DY,DX)

```





```

ALPHA=PHI+RSIGN*THETA
XC=X1+COS(ALPHA)*RADIUS
YC=Y1+SIN(ALPHA)*RADIUS
FACTOR=1.0/FLOAT(NP(K)+1)
OMEGA=FACTOR*(4.0*ATAN(1.0)-2.0*THETA)
BETA=ATAN2(Y1-YC,X1-XC)
C
C   TO GENERATE COORDINATES OF INTER-POINTS
C
DO 140 NM=1,NP(K)
  BETA=BETA+RSIGN*OMEGA
  XTEMP(NM)=XC+COS(BETA)*RADIUS
  YTEMP(NM)=YC+SIN(BETA)*RADIUS
  JUANG=NADD(K)-NM
  AX(JUANG)=XTEMP(NM)
  AY(JUANG)=YTEMP(NM)
140 CONTINUE
100 CONTINUE
  RETURN
  END
C
SUBROUTINE CANJ1 (LUDATA,KPUTCK,XSIZE,WORDTB)
C   THIS SUBROUTINE IS TO PROVIDE CANNED MESH
C   FOR PIPE ARCH CONFIGURATION-----C.H. JUANG 3-20-1982
C
  DIMENSION NODMOD(2,84),LNOD(7,50),LNODX(7,23),NODBC(13),
X      PX(4,84),IPX(84),NNPX(13),INCRX(13),X(122),Y(122),
X      XA(12),YA(12),XSIZE(6),TITLE(17)
  DATA L1H,IBLANK,PREP/1HL,1H ,4HPREP/
  DATA HOMC/4HHOMO/
  DATA NUMNP,NUMEL,NBPTC,INCMAX,NUMINP,NUMIEL,NUMBC, NSIDBC,NINTER
X      /122,99,30,12,84,50,13,10,2/
  DATA IZERO,IONE,FZERO/0,1,0.0/
  DATA NODMOD/
1 1,0, 4,202, 5,200, 8,202, 9,0, 12,202, 13,200, 16,202,
2 17,0, 19,2, 20,0, 26,2, 21,0, 27,2, 22,0, 28,2,
3 39,0, 40,300, 41,300, 42,0, 43,300, 44,300, 51,0, 52,300,
4 53,300, 60,0, 61,300, 62,300, 69,0, 70,300, 71,300, 78,0,
5 79,300, 80,300, 87,0, 88,300, 89,300, 96,0, 97,300, 98,300,
6 30,0, 45,0, 54,0, 63,0, 72,0, 81,0, 90,0, 29,0,
7 31,0, 32,200, 35,202, 46,0, 47,200, 50,202, 55,0, 56,200,
8 59,202, 64,0, 65,200, 68,202, 73,0, 74,200, 77,202, 82,0,
A 83,200, 86,202, 91,0, 92,200, 95,202, 36,0,
B 37,0, 38,0, 99,0, 102,202, 103,200, 106,202,
C 107,0, 110,202, 111,200, 114,202,
D 115,0, 118,202, 119,200, 122,202/
  DATA LNOD/
1 1,88,97,0,0,1,1, 2,79,88,0,0,2,1, 3,70,79,0,0,3,1,
2 4,61,70,0,0,4,1, 5,52,61,0,0,5,1, 6,43,52,0,0,6,1,
3 7,40,43,0,0,7,1, 8,37,40,0,0,8,1, 9,27,37,0,0,9,1,
4 10,24,27,0,0,10,1, 11,21,24,0,0,11,1, 12,96,87,100,99,1,6,
5 13,87,78,81,90,1,5, 14,78,69,72,81,1,4, 15,69,60,63,72,1,3,
6 16,60,51,54,63,1,3, 17,51,42,45,54,1,2, 18,39,30,45,42,1,2,
7 19,36,29,30,39,1,1, 20,19,29,36,26,1,1, 21,18,19,26,23,1,1,
8 22,17,18,23,20,1,1, 23,1,2,10,9,1,1, 30,9,10,18,17,1,1,
X 32,11,12,29,19,1,1, 33,12,31,30,29,1,1, 34,12,13,32,31,1,1/
  DATA LNODX/
X 38,30,31,46,45,1,2,

```



```

1 43,45,46,55,54,1,2, 48,54,55,64,63,1,3, 53,63,64,73,72,1,3,
2 58,72,73,82,81,1,4, 63,81,82,91,90,1,5, 68,87,90,101,100,1,6,
3 69,90,91,102,101,1,6, 74,99,100,108,107,1,7,
4 81,107,108,116,115,1,8, 87,113,114,122,121,1,8,
5 88,21,20,22,0,1,1, 89,24,23,25,0,2,1, 90,27,26,28,0,3,1,
6 91,37,36,38,0,4,1, 92,40,39,41,0,5,1, 93,43,42,44,0,6,2,
7 94,52,51,53,0,7,2, 95,61,60,62,0,8,3, 96,70,69,71,0,9,3,
8 97,79,78,80,0,10,4, 98,88,87,89,0,11,5, 99,97,96,98,0,12,6/
DATA NODBC/9,20,21,96,97,99,16,35,50,106,1,22,98/
DATA INCRX/8,0,0,0,0,8,0,0,9,8,1,0,0/
DATA NNPX/17,0,0,0,0,115,0,0,95,122,8,0,0/

C
C
DO 111 I=1,23
DO 111 J=1,7
111 LNOD(J,27+I)=LNODX(J,I)
C
C
C MAIN CONTROL PARAMETERS, SEE MANUAL
READ(5,5010) WORD,TITLE,WORDTB,WORD2,IPL0T,IWRT,MGENPR,NINC
READ(5,5015) THIS,IS,JUNK,CARD
C
IF(WORD.NE.HOMO) WRITE(6,6005)
IF(WORD.NE.HOMO) STOP
KPUTCK=0
NOINCR=0
NPUTCK=0
IF(NINC.EQ.0) NPUTCK=1
IF(NINC.EQ.-1) NOINCR=1
IF(NINC.LT.0) NINC=1
WRITE(6,6010) TITLE,IPL0T,IWRT,MGENPR,NINC
DO 60 NP=1,NUMNP
X(NP)=0.
60 Y(NP)=0.
IF(NINC.GT.0 .AND. NINC.LE.INCMAX) GO TO 70
WRITE(6,6020)
KPUTCK=KPUTCK+1
C
70 R1=XSIZE(1)
R2=XSIZE(2)
R=XSIZE(3)
RISE=XSIZE(4)
SPAN=XSIZE(5)
HT=XSIZE(6)
C
C COMPUTE AND PREPARE COORDINATES OF NODES NEEDS
C TO GENERATE MESH
C
Y(1)=-2.80*R2
Y(9)=-0.45*R2
Y(17)=-0.18*R2
Y(99)=RISE+0.16*R2
Y(107)=RISE+0.8*R2
Y(115)=RISE+1.6*R2
X(4)=1.05*R2
X(5)=1.65*R2
X(8)=6.0*R2
X(31)=1.35*R2

```



```

      X(91)=1.05*R2
C
      CALL SIZE(XA,YA,XSIZE)
C
C      PX(1,N)=XCOORD
C      PX(2,N)=YCOORD
C      PX(3,N)=SPACNG
C      PX(4,N)=PADIUS
C      IPX(N)=NPINC
C
      GIVEN NODAL POINTS INFORMATION FOR DATA STATEMENT NODMOD
C
C LINE 1 IN DATA NODMOD
C
      PX(1,1)=XA(12)
      PX(2,1)=Y(1)
      PX(1,2)=X(4)
      PX(2,2)=1.
      PX(3,2)=1.158
      PX(1,3)=X(5)
      PX(2,3)=1.
      PX(1,4)=X(8)
      PX(2,4)=1.
      PX(3,4)=1.679
      PX(1,5)=XA(12)
      PX(2,5)=Y(9)
      PX(1,6)=X(4)
      PX(2,6)=9.
      PX(3,6)=1.158
      PX(1,7)=X(5)
      PX(2,7)=9.
      PX(1,8)=X(8)
      PX(2,8)=9.
      PX(3,8)=1.679
C
C LINE 2
C
      PX(1,9)=XA(12)
      PX(2,9)=Y(17)
      PX(1,10)=1.05*XA(10)
      PX(2,10)=-0.10*R2
      PX(4,10)=R1+0.15*R2
      PX(1,11)=XA(12)
      PX(2,11)=YA(12)
      PX(1,12)=XA(10)
      PX(2,12)=YA(10)
      PX(4,12)=R1
      IPX(12)=3
      PX(1,13)=XA(12)
      PX(2,13)=YA(12)
      PX(1,14)=XA(10)
      PX(2,14)=YA(10)
      PX(4,14)=R1
      IPX(14)=3
      PX(1,15)=XA(12)
      PX(2,15)=YA(12)
      PX(1,16)=XA(10)
      PX(2,16)=YA(10)

```



```
PX(4,16)=R1
IPX(16)=3
```

```
C
C LINE 3
C
```

```
PX(1,17)=XA(8)
PX(2,17)=YA(8)
PX(1,18)=39.
PX(2,18)=39.
PX(1,19)=39.
PX(2,19)=39.
PX(1,20)=XA(7)
PX(2,20)=YA(7)
PX(1,21)=42.
PX(2,21)=42.
PX(1,22)=42.
PX(2,22)=42.
PX(1,23)=XA(6)
PX(2,23)=YA(6)
PX(1,24)=51.
PX(2,24)=51.
```

```
C
C LINE 4
C
```

```
PX(1,25)=51.
PX(2,25)=51.
PX(1,26)=XA(5)
PX(2,26)=YA(5)
PX(1,27)=60.
PX(2,27)=60.
PX(1,28)=60.
PX(2,28)=60.
PX(1,29)=XA(4)
PX(2,29)=YA(4)
PX(1,30)=69.
PX(2,30)=69.
PX(1,31)=69.
PX(2,31)=69.
PX(1,32)=XA(3)
PX(2,32)=YA(3)
```

```
C
C LINE 5
C
```

```
PX(1,33)=78.
PX(2,33)=78.
PX(1,34)=78.
PX(2,34)=78.
PX(1,35)=XA(2)
PX(2,35)=YA(2)
PX(1,36)=87.
PX(2,36)=87.
PX(1,37)=87.
PX(2,37)=87.
PX(1,38)=XA(1)
PX(2,38)=YA(1)
PX(1,39)=96.
PX(2,39)=96.
PX(1,40)=96.
```





PX(2,40)=96.

C

C LINE 6

C

PX(1,41)=1.02\*R2  
 PX(2,41)=0.10\*R2  
 PX(1,42)=1.10\*R2  
 PX(2,42)=0.62\*YA(7)+0.38\*YA(8)  
 PX(1,43)=1.15\*R2  
 PX(2,43)=YA(6)  
 PX(1,44)=XA(5)+0.20\*R2  
 PX(2,44)=YA(5)  
 PX(1,45)=XA(4)+0.25\*R2  
 PX(2,45)=YA(4)  
 PX(1,46)=XA(4)  
 PX(2,46)=YA(3)  
 PX(1,47)=XA(2)+0.30\*R2  
 PX(2,47)=YA(2)  
 PX(1,48)=1.10\*XA(9)  
 PX(2,48)=-0.055\*R2

C

C LINE 7

C

PX(1,49)=X(31)  
 PX(2,49)=-0.07\*R2  
 PX(1,50)=X(5)  
 PX(2,50)=31.  
 PX(1,51)=X(8)  
 PX(2,51)=31.  
 PX(3,51)=1.679  
 PX(1,52)=X(31)  
 PX(2,52)=YA(8)-0.003\*R2  
 PX(1,53)=X(5)  
 PX(2,53)=46.  
 PX(1,54)=X(8)  
 PX(2,54)=46.  
 PX(3,54)=1.679  
 PX(1,55)=X(31)  
 PX(2,55)=YA(6)  
 PX(1,56)=X(5)  
 PX(2,56)=55.

C

C LINE 8

C

PX(1,57)=X(8)  
 PX(2,57)=55.  
 PX(3,57)=1.679  
 PX(1,58)=X(31)  
 PX(2,58)=YA(5)  
 PX(1,59)=X(5)  
 PX(2,59)=64.  
 PX(1,60)=X(8)  
 PX(2,60)=64.  
 PX(3,60)=1.679  
 PX(1,61)=X(31)  
 PX(2,61)=YA(4)  
 PX(1,62)=X(5)  
 PX(2,62)=73.



```

PX(1,63)=X(8)
PX(2,63)=73.
PX(3,63)=1.679
PX(1,64)=1.18*R2
PX(2,64)=YA(3)

```

```

C
C LINE A
C

```

```

PX(1,65)=X(5)
PX(2,65)=82.
PX(1,66)=X(8)
PX(2,66)=82.
PX(3,66)=1.679
PX(1,67)=X(91)
PX(2,67)=YA(2)
PX(1,68)=X(5)
PX(2,68)=91.
PX(1,69)=X(8)
PX(2,69)=91.
PX(3,69)=1.679
PX(1,70)=XA(9)
PX(2,70)=YA(9)

```

```

C
C LINE B
C

```

```

PX(1,71)=XA(9)
PX(2,71)=YA(9)
PX(1,72)=XA(9)
PX(2,72)=YA(9)
PX(1,73)=XA(1)
PX(2,73)=Y(99)
PX(1,74)=X(91)
PX(2,74)=99.
PX(3,74)=1.18
PX(1,75)=X(5)
PX(2,75)=99.
PX(1,76)=X(8)
PX(2,76)=99.
PX(3,76)=1.679

```

```

C
C LINE C
C

```

```

PX(1,77)=XA(1)
PX(2,77)=Y(107)
PX(1,78)=X(91)
PX(2,78)=107.
PX(3,78)=1.18
PX(1,79)=X(5)
PX(2,79)=107.
PX(1,80)=X(8)
PX(2,80)=107.
PX(3,80)=1.679

```

```

C
C LINE D
C

```

```

PX(1,81)=XA(1)
PX(2,81)=Y(115)
PX(1,82)=X(91)

```



```

PX(2,82)=115.
PX(3,82)=1.18
PX(1,83)=X(5)
PX(2,83)=115.
PX(1,84)=X(8)
PX(2,84)=115.
PX(3,84)=1.679
C
C
C   SAVE DATA FOR MAIN CONTROL CARDS
C
  WRITE(LUDATA,6105) PREP,TITLE,WORD2,NINC,MGENPR,NPUTCK,
X      IPLOT,IWRT,NUMNP,NUMEL,NBPTC
C
C   *****
C   SAVE DATA NEEDED FOR NODE GENERATION
C
  LIMIT= IBLANK
  DO 320 N=1,NUMINP
    NNP=NODMOD(1,N)
    NPINC=0
    SPACNG=0.
    RADIUS=0.
    XCOORD=X(NNP)
    YCOORD=Y(NNP)
C   CURRENT DATA STATEMENTS (INPUT)
    IF(PX(1,N).NE.0.0) XCOORD=PX(1,N)
    IF(PX(2,N).NE.0.0) YCOORD=PX(2,N)
    IF(PX(3,N).NE.0.0) SPACNG=PX(3,N)
    IF(PX(4,N).NE.0.0) RADIUS=PX(4,N)
    IF(IPX(N).NE.0) NPINC=IPX(N)
    IF(N.EQ.NUMINP) LIMIT=L1H
320  WRITE(LUDATA,6110) LIMIT,NNP,NODMOD(2,N),XCOORD,
X      YCOORD,NPINC,SPACNG,RADIUS
C
C
C   SAVE DATA NEEDED FOR ELEMENT GENERATION
C
  LIMIT=IBLANK
  DO 360 NE=1,NUMIEL
    INCR=LNOD(7,NE)
    IF(NOINCR.EQ.1) INCR=1
    INTERF=IZERO
    IF(LNOD(1,NE).GE.(NUMEL-11)) INTERF=IONE
    IF(NE.EQ.NUMIEL) LIMIT=L1H
    WRITE(LUDATA,6115) LIMIT,(LNOD(K,NE),K=1,6),
X      INCR,INTERF,IZERO,IZERO,IZERO
C   WRITE(6,6115) LIMIT,(LNOD(K,NE),K=1,6),
C   X      INCR,INTERF,IZERO,IZERO,IZERO
360  CONTINUE
C
C   SAVE DATA NEEDED FOR B.C.
C
  LIMIT=IBLANK
  DO 480 N=1,NUMBC
    INCR=IZERO
    NNP=IZERO
    J=IZERO

```



```

      IF(N.GT.NSIDBC .AND. N.LE.(NUMBC-NINTER)) J=IONE
      IF(N.EQ.NUMBC) LIMIT=L1H
      IF(NNPX(N).NE.0) NNP=NNPX(N)
      IF(INCRX(N).NE.0) INCR=INCRX(N)
      IF(N.GT.(NUMBC-NINTER)) GO TO 99
      WRITE(LUDATA,6120) LIMIT,NODBC(N),IONE,FZERO,J,FZERO,FZERO,
X      IONE,NNP,INCR,FZERO,FZERO
      GO TO 480
99    WRITE(LUDATA,6120) LIMIT,NODBC(N),IZERO,FZERO,IONE,FZERO,
X      FZERO,IONE,NNP,INCR,FZERO,FZERO
480   CONTINUE
C
C      *****
      REWIND LUDATA
      RETURN
C
C      *****
C
C      FORMATS
C
5010  FORMAT(A4,17A4,2X,A2,A4/4I5)
5015  FORMAT(F10.0,I5,I5,F10.0)
6010  FORMAT(1H1,//5X,≠ *** BEGIN GENERATION OF CANJ MESH≠//9X,17A4//
X      5X,≠ *** PLOTTING DATA SAVED-----≠,I5//
X      5X,≠ *** PRINT SOIL RESPONSE-----≠,I5//
X      5X,≠ *** PRINT CONTRCL FOR PREP (LEVEL 3) OUTPUT----≠,I5//
X      5X,≠ *** NO. OF CONSTRUCTION INCREMENTS-----≠,I5////)
6020  FORMAT(≠ FATAL DATA ERROR--- NO. OF CONSTRUCTION ≠)
6005  FORMAT(≠ MESH TYPE IS NOT HPMPGENEEOUS, PROGRAM STOP≠)
6105  FORMAT(A4,1X,17A4,3X,A4/8I5)
6110  FORMAT(A1,I4,I5,2F10.3,I5.5X,2F10.3)
6115  FORMAT(A1,I4,10I5)
6120  FORMAT(A1,I4,I5,F10.0,I5,2F10.0,3I5,2F10.0)
      END

```





## APPENDIX E

## REVISED ITERATIVE SCHEME AND ERROR MESSAGES

1. Insert or replace the following statements in Subroutine EMOD:

```

COMMON /CONTROL/ XNOSTOP
DATA LIMIT,TOLER/12,0.05/                                00462000

100  CONTINUE                                             00655000
C                                         00656000
C  CHECK ON OUTER LOOP CONVERGENCE                      00657000
C                                         00658000
      IF(NINC.LT.0) GO TO 125
      IF(ERRSUM.LE.TOLER) GO TO 1251
      IF(ICON.EQ.LIMIT .AND. XNOSTOP.EQ.≠NOSTOP≠) GO TO 125
      IF(ICON.EQ.LIMIT) WRITE(6,6501) LIMIT,ERRSUM,IA
      IF(ICON.EQ.LIMIT) STOP
      IF(ICON.GT.4) WRITE(6,6500) ICON,ERRSUM
      GO TO 125
6501  ICON=-1
      125 CONTINUE                                         00663000

6500  FORMAT(///≠ **** CAUTION : THE CURRENT (≠,I2,≠TH ITERATION) TOTAL
XERROR RATIO IN PIPE MODULI IS≠,      E12.4/)
6501  FORMAT(/////≠ *** NONLINEAR PIPE PROPERTIES DID NOT CONVERGE AT TH
XE END OF ≠,I2,≠ ITERATION≠//≠      THE FINAL TOTAL ERROR RATIO OF P
XIPE MODULUS IS≠,E12.4//≠ *** PROGRAM STOP AT LOAD STEP≠,I2,≠***≠)

```

2. Insert or replace the following statements in Subroutine STIFNS

```

COMMON /CONTROL/ XNOSTOP

95  IF(MNX.EQ.0) GO TO 97                                05628000
      CALL XFACES(MN,IAC,MNX,IX,ICON,ITER,NELEM,NPT,MNO,NOD,ST,U,V,IA
X      ,JFACE)
C
      IF(XNOSTOP.EQ. ≠NOSTOP≠) GO TO 313
      IF(JFACE.EQ.1) WRITE(6,6000) ITER,IA
6000  FORMAT(/////≠ *** WARNING, INTERFACE STATE DID NOT CONVERGE AFTER≠
1,I3, ≠ ITERATION.≠//≠      *** PROGRAM STOP AT LOAD STEP≠,I2,≠ ***≠)
      IF(JFACE.EQ.1) STOP
      GO TO 313                                           05630000

```



3. Insert or replace the following statements in Subroutine HEROIC:

```

      DIMENSION BIU(3,NBPTC),MNO(NELEM),NOD(4,NELEM),NODE(NBPTC),
1         NQ(NPT),PIPMAT(5,NPPT),RESULT(20,NPPT),ST(6,NELEM),
2         STHARD(4,NELEM),STPIPE(2,NPPT),U(NPT),U(NPT),X(NPT),
3         Y(NPT),JSOIL(10)
      COMMON /CONTROL/ XNOSTOP

```

04344000

04345000

04346000

(insert the following statements right after "CALL DUNCAN")

```

      NONABS=IABS(NON(MN))
C
C      USING JINDEX TO AVOID PRINTING NON-CONVERGENCE MESSAGE
C      FOR EACH ELEMENT.....JUANG
C
      IF(JINDEX.EQ.ITER) GO TO 349
      IF(ITER.LT.NONABS .AND. JSOIL(MN).EQ.1) THEN
        WRITE(6,6051) MN,ITER
        JINDEX=ITER
      ENDIF
      IF(ITER.EQ.NONABS .AND. JSOIL(MN).EQ.1) THEN
        IF(XNOSTOP.EQ. #NOSTOP#) GO TO 349
        WRITE(6,6050) MN,ITER
        STOP
      ENDIF
C
      GO TO 349
C
      CALL RESPIP (MNO,NOD,RESULT,ST,STPIPE,U,U,X,Y,NELEM,NPMAT,
1         NPPT,NPT,IEXIT,2)
C
      IF(ICON.NE.1) NINC = -NINCC
      IF(ITER.LE.15) RETURN
      NINC=NINCC
      IF(XNOSTOP.EQ. #NOSTOP#) RETURN
      WRITE(6,5000) IA,ITER
5000  FORMAT(////# ***WARNING,LOAD STEP#,I3,23H DID NOT CONVERGE AFTER,
X I3,12H ITERATIONS. /# *** PROGRAM STOP ***#
X/# *** PROGRAM STOP ***#)
6050  FORMAT(////# ***WARNING, SOIL MODULUS AT ZONE#,I2,# DIDNOT CONVER
1GE AFTER#,I3,# ITERATIONS#//# STRUCTURE RESPONSES WILL NOT BE
2CALCULATED. PROGRAM WILL STOP#//)
6051  FORMAT(//#*** CAUTION : SOIL MODULUS AT ZONE#,I2,# DID NOT CONVERG
XE AFTER#,I3,# ITERATIONS#//)
6000  FORMAT(///1X,#TURN TO NEXT PAGE FOR THE NEXT LOAD STEP#//)
6500  FORMAT(I7,17X,F8.2,16X,F8.2/)
      STOP
      END

```

04527000

04324000

04625000

04626000

04527000

04628000

04629000

04637000

04638000



4. Insert or replace the following statements in Subroutine XFACES:

```

SUBROUTINE XFACES(MN,IAC,MNX,NEL,ICON,ITER,NELEM,NPT,MNO,NOD,ST, 05634000
1 U,V,IA,JFACE)

DATA CON,ITMAX/0.0174533,12/ 0T20NG00

C 06011000
C STORE CURRENT STATE OF ELEMENT AND CHECK CONVERGENCE 06012000
C 06013000
C JFACE=1 : TO PRINT OUT MESSAGE OF NON-CONVERGENCE OF INTERFACE
C STATE AT END OF ITERATION, SEE SUBROUTINE STIFTN .. RIGHT AFTER
C CALL XFACE
C
MNO(NEL) = 1000*MN + 10*IAC + MNX 06014000
IF(LKCHNG.NE.0 .AND. ITER.GT.4) WRITE(6,6010)
JFACE=0
IF(LKCHNG.NE.0 .AND. ITER.EQ.ITMAX) JFACE=1
IF(ITER.EQ.1) ICON=0
IF(ITER.LT.ITMAX .AND. LKCHNG.NE.0) ICON=0
RETURN 05020000
6010 FORMAT (1H ,10X,≠ * * * CAUTION : INTERFACE ELEMENT(S) DID NOT 006021000
1NVERGE. PROGRAM WILL CONTINUE * * ≠ ////) 06022000
END 06023000

```





COVER DESIGN BY ALDO GIORGINI